



National Library
of Canada

Bibliothèque nationale
du Canada

Canadian Theses Service

Services des thèses canadiennes

Ottawa, Canada
K1A 0N4

CANADIAN THESES

THÈSES CANADIENNES

NOTICE

The quality of this microfiche is heavily dependent upon the quality of the original thesis submitted for microfilming. Every effort has been made to ensure the highest quality of reproduction possible.

If pages are missing, contact the university which granted the degree.

Some pages may have indistinct print especially if the original pages were typed with a poor typewriter ribbon or if the university sent us an inferior photocopy.

Previously copyrighted materials (journal articles, published tests, etc.) are not filmed.

Reproduction in full or in part of this film is governed by the Canadian Copyright Act, R.S.C. 1970, c. C-30.

**THIS DISSERTATION
HAS BEEN MICROFILMED
EXACTLY AS RECEIVED**

AVIS

La qualité de cette microfiche dépend grandement de la qualité de la thèse soumise au microfilmage. Nous avons tout fait pour assurer une qualité supérieure de reproduction.

S'il manque des pages, veuillez communiquer avec l'université qui a conféré le grade.

La qualité d'impression de certaines pages peut laisser à désirer, surtout si les pages originales ont été dactylographiées à l'aide d'un ruban usé ou si l'université nous a fait parvenir une photocopie de qualité inférieure.

Les documents qui font déjà l'objet d'un droit d'auteur (articles de revue, examens publiés, etc.) ne sont pas microfilmés.

La reproduction, même partielle, de ce microfilm est soumise à la Loi canadienne sur le droit d'auteur, SRC 1970, c. C-30.

**LA THÈSE A ÉTÉ
MICROFILMÉE TELLE QU'É
NOUS L'AVONS REÇUE**

THE UNIVERSITY OF ALBERTA

NMR STUDIES OF THE INTERACTION OF Cd(II) WITH LIGANDS
OF BIOLOGICAL INTEREST AND WITH RED BLOOD CELLS

by

C

WEBE CELINE KADIMA

A THESIS

SUBMITTED TO THE FACULTY OF GRADUATE STUDIES AND RESEARCH
IN PARTIAL FULFILMENT OF THE REQUIREMENTS FOR THE DEGREE
DOCTOR OF PHILOSOPHY

DEPARTMENT OF CHEMISTRY

EDMONTON, ALBERTA

FALL, 1986

Permission has been granted to the National Library of Canada to microfilm this thesis and to lend or sell copies of the film.

The author (copyright owner) has reserved other publication rights, and neither the thesis nor extensive extracts from it may be printed or otherwise reproduced without his/her written permission.

L'autorisation a été accordée à la Bibliothèque nationale du Canada de microfilmer cette thèse et de prêter ou de vendre des exemplaires du film.

L'auteur (titulaire du droit d'auteur) se réserve les autres droits de publication; ni la thèse ni de longs extraits de celle-ci ne doivent être imprimés ou autrement reproduits sans son autorisation écrite.

ISBN 0-315-32602-6

THE UNIVERSITY OF ALBERTA
FACULTY OF GRADUATE STUDIES AND RESEARCH

The undersigned certify that they have read, and recommend to the Faculty of Graduate Studies and Research, for acceptance, a thesis entitled NMR STUDIES OF THE INTERACTION OF Cd(II) WITH LIGANDS OF BIOLOGICAL INTEREST AND WITH RED BLOOD CELLS submitted by WEBE, CELINE KADIMA in partial fulfilment of the requirements for the degree of DOCTOR OF PHILOSOPHY

Delos Heberlein
Supervisor

Gary Kowalski

Ande Z. Bouz

Byron Kratochvil

Scott Korbach

Robert W. Hurst
External Examiner

Date *August 25th 1986*

DEDICATION

In loving memory of a passionate learner, my Father,

Gaston M.K. Kadima

who taught best:

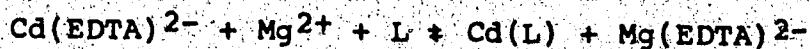
*Que ton cœur demeure constamment grand dans
la foi chrétienne et dans les actes de vie.*

*Courage Ton Père KAMHAKACHOE KANU-HAYI
Fokun*

ABSTRACT

The complexation of Cd^{2+} by ligands of biological interest has been studied by ^1H , ^{13}C and ^{113}Cd nuclear magnetic resonance (NMR) spectroscopic measurements. The aim of this study was to gain an understanding of the behavior of Cd^{2+} in biological systems in general and in red blood cells (RBC) in particular.

Blood transports Cd^{2+} to various tissues where it is ultimately accumulated; hence the importance of the interaction of Cd^{2+} with blood components in the toxicology of cadmium. Previous research has shown that glutathione (GSH) and hemoglobin (Hb) are the main binding sites for Cd^{2+} in red blood cells. The stability of the complexes formed in red blood cells was determined semi-quantitatively by ^1H -NMR spectroscopy in the present research. A competitive reaction was exploited whereby the ligands in red blood cells had to compete with ethylenediaminetetraacetic acid (EDTA) for the binding to cadmium:



where L is the reacting ligand(s) in hemolysed red blood cells (HRBC). This was accomplished by incorporating cadmium in HRBC in the form of its EDTA complex ($\text{Cd}(\text{EDTA})^{2-}$). The

displacement of EDTA from $\text{Cd}(\text{EDTA})^{2-}$ was monitored by measuring the intensity of the resonance due to the ethylenic protons of $\text{Mg}(\text{EDTA})^{2-}$ in the spin echo ^1H NMR spectra of HRBC to which $\text{Cd}(\text{EDTA})^{2-}$ was added. $\text{Mg}(\text{EDTA})^{2-}$ was formed by the magnesium present in red blood cells and the EDTA displaced upon reaction of the $\text{Cd}(\text{EDTA})^{2-}$ with ligands of the red blood cells. From the equilibrium constant estimated for this reaction, the stability constant for the complexes formed by Cd^{2+} with ligands of the HRBC was determined to be of the order 10^9 . It is suggested that in a first step GSH reacts with cadmium binding through its sulfhydryl group and then hemoglobin reacts with the complex $\text{Cd}(\text{GSH})$ to form the mixed complex $((\text{GS})\text{Cd}(\text{Hb}))$. Model systems were studied in D_2O by single pulse ^1H NMR to validate the results obtained with red blood cells. Equilibrium constants obtained for Cd^{2+} complexes of GSH, cysteine and N-acetylpenicillamine are comparable to those obtained with red blood cells.

To characterize the tendency of various biological ligands to react with a Cd-ligand complex to form mixed ligand complexes, a model system was studied in aqueous solutions. Nitriloacetic acid (NTA) was used as the primary ligand to form the $\text{Cd}(\text{NTA})^-$ complex. The secondary ligands were glutathione (GSH), penicillamine (PSH), N-acetylpenicillamine (N-PSH), cysteine (Cys), N-acetylcysteine

(N-Cys), mercaptosuccinic acid (MSA), S-methylglutathione (CH₃SG), glycine and glutamic acid. Glycine, glutamic acid and CH₃SG formed only mixed complexes Cd(NTA)L. Their formation constants were determined from chemical shift measurements made on the exchange averaged resonances of the secondary ligands. All thiols studied also form mixed complexes. Also, they form single ligand complexes (Cd(L)) by displacing NTA from its Cd(NTA)⁻ complex. The formation constants of the mixed ligand complexes as well as the single ligand complexes were determined from chemical shift and intensity measurements on the resonances due to free and bound NTA. Results of this study are discussed in terms of the basicity of the ligands, their ability to chelate, and steric factors. The exchange behavior among species in these systems was also discussed.

Given the importance of glutathione complexation in the toxicology of Cd²⁺, its reactions with glutathione were studied by ¹¹³Cd NMR. The pH as well as the concentration dependence of the ¹¹³Cd NMR spectra of Cd²⁺ and GSH mixtures were investigated. Two slow exchange resonances were observed at 320 ppm and 674 ppm for Cd(GSH) complexes formed in a mixture of Cd²⁺ and GSH in a 1 to 2 ratio at pH 9.5. The resonance at high frequency is in the region generally assigned to CdS₄ sites and where Cd²⁺ clusters formed with metallothionein occur. A calibration curve was established

to determine the percentage of the total cadmium represented by the resonances observed in the ^{113}Cd NMR spectra. This information and the chemical shift information obtained are discussed in terms of the nature of the complexes formed. Measurements were made on the Cd^{2+} complexes of a few other thiols for comparison and as an aid to interpretation of data on the glutathione- Cd^{2+} system. ^{13}C and ^1H NMR measurements were also made which were consistent with the ^{113}Cd NMR results. It is suggested that glutathione forms cluster compounds with Cd^{2+} similar to those formed by metallothionein.

The approach used to determine the concentration of species from ^{113}Cd NMR intensity measurements is discussed. It has the potential to reveal dynamics within Cd^{2+} systems and to provide information about the stoichiometry of complexes formed.

ACKNOWLEDGEMENTS

Direction of this thesis by Dr. Dallas Rabenstein is gratefully acknowledged as well as financial support from the Alberta Heritage Foundation for Medical Research, the University of Alberta and The Natural Sciences and Engineering Research Council.

It is my pleasure to acknowledge Dr. Bruce Cheeseman for his help with the ^{13}C and ^{113}Cd NMR measurements. Thanks go to him for many fruitful discussions and the constant interest he showed for my work.

I feel indebted to the academic staff at the Chemistry Department for their contribution to my scientific growth. However, I am even more obliged to the non-academic staff for their support with numerous services. Many thanks to the staff at the general office, machine shop, glass shop, electronic shop and stores.

My family has shown love, concern and support throughout all my education. I could never thank them enough.

As this thesis was being completed, my brother Faustin died on May 6, 1986. As in the past my friends were ever present, comforting and encouraging. I owe them much more than this acknowledgement.

I am especially grateful to Mike Clegg for his long distance constant and consistent care during my stay in Riverside.

For his unwavering support and for the gift of his love, here is an expression of my deepest appreciation to a special friend; my husband-to-be, Laurent Bona.

Finally, I would like to praise Ms. Nancy G. Clark for her competent effort in typing, retyping, retyping.... and editing this thesis. I could not have done it without her.

TABLE OF CONTENTS

CHAPTER	PAGE
I. INTRODUCTION	1
A. Toxicity of Cadmium.	1
B. The Coordination Chemistry of Cadmium.	2
C. Coordination Chemistry of Cd^{2+} with Biological Ligands	3
D. ^{113}Cd -NMR Spectroscopy	7
E. This Thesis.	12
II. EXPERIMENTAL	16
A. Chemicals.	16
B. Synthesis and Analysis of S-Methyl- glutathione.	17
C. Solution Preparation	18
D. Preparation of Hemolysed Erythrocytes.	23
E. Nuclear Magnetic Resonance Measurements.	24
1. General.	24
2. Measurement of Spin-Lattice Relaxation Times.	28
3. Measurement of 1H -NMR Spectra of Red Blood Cells.	35
F. Calibration Curve for Quantitative ^{113}Cd NMR	41
G. Non-Linear Least Squares Calculations.	47

CHAPTER	PAGE
III. ¹ H NMR STUDIES OF MIXED LIGAND COMPLEXES OF	
CADMIUM.	49
A. Introduction	49
B. Determination of Ligand Acid Dissociation	
Constants.	53
C. Determination of Formation Constants of	
Cd(NTA)L Mixed Complexes	57
1. Formation of the Only Mixed Ligand	
Complex.	58
2. Case of the Formation of CdL and Cd(NTA)L.	61
D. Results.	68
1. Formation Constant of Cd(NTA) ⁻	68
2. Mixed Ligand System Cd(NTA)-Glycine and	
Cd(NTA)-Glutamic Acid.	74
3. The Mixed Ligand System Cd(NTA) ⁻ -	
Penicillamine.	80
4. The Mixed Ligand System Cd(NTA)-	
N-acetylpenicillamine.	88
5. Mixed Ligand System (Cd(NTA) -	
Glutathione.	93
6. The Mixed Ligand System Cd(NTA) ⁻ -	
S-Methylglutathione.	114
7. Mixed Ligand Complexes of Cd(NTA) ⁻ and	
other Thiols	116
E. Discussion	122

CHAPTER	PAGE
IV. CHARACTERIZATION OF CADMIUM-GLUTATHIONE COMPLEXES BY ^{113}Cd NMR	128
A. Introduction	128
B. Results and Discussion	130
1. ^1H -NMR Studies	130
2. ^{13}C -NMR Studies	143
3. ^{113}Cd NMR Studies	158
a. Qualitative Studies	158
b. Quantitative Studies	164
i. pH Dependence of the Concentration of Cd^{2+} Species	165
ii. Dependence of the Concentration of Cd^{2+} Species on the Concentration of GSH at pH 9.5	169
iii. Effect of Dilution on the Distribution of Species	171
iv. Stoichiometry of Complexes	175
v. Comparative Study with PSH, N-PSH and Cysteine	182
C. Conclusion	189
V. DETERMINATION OF ^{113}Cd CHEMICAL SHIFTS OF Ca^{2+} COMPLEXED BY CARBOXYLATE LIGANDS	194
A. Introduction	194
B. Method	195

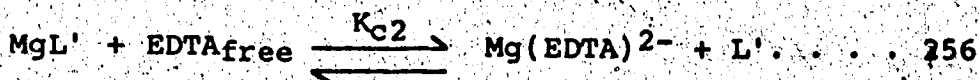
CHAPTER	PAGE
C. Results	199
1. Carboxylic Acid Complexes.	199
2. Acetylglycine Complexes.	209
3. Glycylglycine Complexes.	211
4. Histidine and N-acetylhistidine.	214
D. Discussion	227
VI. QUANTITATIVE STUDY OF CADMIUM COMPLEXATION IN HEMOLYSED RED BLOOD CELLS	230
A. Introduction	230
B. Method	232
C. Determination of Total Magnesium in Hemolysed Red Blood Cells (HRBC)	239
D. Calibration Curve for $Mg(EDTA)^{2-}$ in HRBC	244
E. Determination of the Equilibrium Constant K_{Cl} in HRBC.	246
F. Comparative Study of the Reaction of $Cd(EDTA)^{2-}$ with Selected Ligands in D_2O	257
1. Reaction of $Cd(EDTA)^{2-}$ with Glutathione.	262
2. Reaction of $Cd(EDTA)^{2-}$ with N-acetyl- penicillamine (N-PSH).	273
3. Reaction of $Cd(EDTA)^{2-}$ with Cysteine	278
4. Reaction of $Cd(EDTA)^{2-}$ with S-methyl- glutathione.	286
G. Discussion and Conclusions	286

CHAPTER	PAGE
REFERENCES	296
APPENDIX 1. Microprogram of Pulse Sequence Used to Obtain Totally Decoupled ^{13}C -NMR Spectra.	305
APPENDIX 2. Microprogram of the Pulse Sequence Used to Measure ^1H -NMR Spectra in H_2O	306

LIST OF TABLES

TABLE	PAGE
1. Chemical shifts and T_1 's of selected cadmium compounds.	43
2. The effect of gadolinium on the spin-lattice relaxation times of ^{113}Cd in CdCl_2 solutions . . .	45
3. Acidity constants of the sulfhydryl and amino groups in glutathione.	97
4. Summary of ^1H NMR studies of mixed ligand systems.	123
5. ^{113}Cd NMR spectral features during a pH titration of a 1 to 2 mixture of Cd^{2+} and GSH. . .	161
6. Species distribution versus pH of cadmium complexes of glutathione by ^{113}Cd NMR.	167
7. Molar ratio study at pH 9.5 of the reaction of Cd^{2+} and GSH by ^{113}Cd NMR	170
8. Species distribution of Cd-GSH at 273°K and 298°K by ^{113}Cd NMR	172
9. Dilution experiment at pH 9.5 for a 1:2 mixture of Cd^{2+} and GSH by ^{113}Cd NMR	174
10. Determination of the composition of complexes formed by Cd^{2+} and GSH from ^{113}Cd NMR and ^{13}C NMR intensity measurements (results deduced from spectra in Figure 63)	177

11.	^{113}Cd chemical shifts and measured % cadmium from mixtures containing Cd^{2+} and thiols in the ratio 1 to 5. pH = 9.5.	184
12.	^{113}Cd NMR study of Cd^{2+} -GSH system by Birgersson et al. [86] at 68°C	189
13.	^{113}Cd NMR chemical shifts of complexes of cadmium with selected carboxylic acids	206
14.	pK_a 's, Formation constants, ^1H and ^{113}Cd chemical shifts of histidine and N-acetylhystidine species.	222
15.	Determination of magnesium in hemolysed red blood cells of one donor during 40 days.	243
16.	Results of the titration of HRBC with $\text{Cd}(\text{EDTA})^{2-}$	251
17.	Results of the titration of (HRBC + Mg^{2+}) with $\text{Cd}(\text{EDTA})^{2-}$	252
18.	Results of the titration of HRBC with $\text{Cd}(\text{EDTA})^{2-}$	253
19.	Results of the titration of (HRBC + Mg^{2+}) with $\text{Cd}(\text{EDTA})^{2-}$	254
20.	Determination of the equilibrium constant for the reaction:	



21.	Equilibrium constants for the reaction $\text{Cd}(\text{EDTA})^{2-} + \text{Ca}^{2+} + \text{GSH}$	272
22.	Equilibrium constants for the reaction $\text{Cd}(\text{EDTA})^{2-} + \text{Ca}^{2+} + \text{NAC-PSH}$	281
23.	Equilibrium constants of the reaction $\text{Cd}(\text{EDTA})^{2-} + \text{Ca}^{2+} + \text{cysteine at pH} = 6.5$	285
24.	Equilibrium constants for the reaction $\text{Cd}(\text{EDTA})^{2-} + \text{Ca}^{2+} + \text{CH}_3\text{SG}$	289

LIST OF FIGURES

FIGURE	PAGE
1. Structure of Cd(NTA) ⁻ complex.	14
2. Single pulse experiment.	25
3. Power gated proton decoupling experiment	26
4. (A) Pulse sequence inversion recovery experiment, (B) behavior of the magnetization:	30
5. Recovery curves for nuclei having T ₁ values of 0.33, 0.7, 1.1 and 1.5 sec following application of the 180° pulse in the inversion recovery pulse sequence	31
6. Spectra obtained at different τ ₁ delay times of an inversion recovery experiment	33
7. Determination of the 90° pulse width Sample: CdBr ₂ (1.0 M)	34
8. Single pulse and spin-echo spectra of red blood cells.	36
9. Pulse sequence and behavior of the magnetization during a spin-echo experiment.	38
10. Intensity of resonances having T ₂ values of 0.1, 0.5, 1, 2 and 5 sec in the spin-echo spectra measured as a function of τ ₂	40
11. Calibration curve for Cd ²⁺ species	46

12. Names and structures of secondary ligands used in the study of $\text{Cd}(\text{NTA})\text{L}$ mixed ligand complexes. 49
13. Spectra of (A) $\text{Cd}(\text{NTA})^-$ and (B) of a mixture of $\text{Cd}(\text{NTA})^-$ (0.02M) and PSH (0.035M) showing displacement of NTA at pH 5.5. 64
14. 1) Chemical shift titration of NTA for pK_a determination. 2) Chemical shift titration of an equimolar mixture of Cd^{2+} and NTA 69
15. Spectra of titration of an equimolar mixture of Cd^{2+} and NTA. Total concentrations of Cd^{2+} and NTA = 0.02M 71
16. Spectra of equimolar solutions of $\text{Cd}(\text{NTA})^-$ and glycine at (A) pH 5 and (B) pH 9 75
17. The pH dependence of the chemical shift of (A) H_α during titration of glycine and the calculated curve from pK_{a2} determination, (B) H_α during titration of an equimolar solution of $\text{Cd}(\text{NTA})^-$ and glycine and the calculated curve from $\log K_f$ determination, (C) methylene protons on bound NTA during titration of an equimolar solution $\text{Cd}(\text{NTA})^-$ and glycine 77
18. Portions of spectra of equimolar solutions of $\text{Cd}(\text{NTA})^-$ and glutamic acid at (A) pH 4.5 and (B) pH 9.5 79

19. (A) The pH dependence of the chemical shift of glutamic acid H_{α} during titration of glutamic acid and the calculated curve from the pK_{a3} determination. (B) H_{α} during titration of an equimolar solution of $Cd(NTA)^-$ and glutamic acid and the calculated curve from $\log K_f$ determination. (C) Methylene protons in bound NTA during titration of an equimolar solution of $Cd(NTA)^-$ and glutamic acid. 81
20. Spectra of mixtures of $Cd(NTA)^-$ and PSH at pH 5. Initial concentrations $[Cd(NTA)^-] = 0.02M$ and $[PSH] =$ (A) $0.0M$, (B) $0.015M$ and (C) $0.07M$ 82
21. The pH dependence of the chemical shift of (A) H_{α} during titration of PSH and (B) H_{α} during titration of an equimolar mixture of $Cd(NTA)^-$ and PSH, (C) Methylene protons in bound NTA during a titration of an equimolar mixture of $Cd(NTA)^-$ and PSH and (D) methylene protons in NTA during a titration of an equimolar solution of Cd^{2+} and NTA. 84

22. Chemical shift of methylene protons in bound NTA as a function of PSH concentration and the calculated curve from K_{fc} and K_{eqc} determination 87
23. Spectra of the equimolar mixture of $Cd(NTA)^-$ and N-acetylpenicillamine at (A) pH 4.01, (B) 6.51 and (C) 8.01 89
24. The pH dependence of the chemical shift of (A) H_{α} during titration of the N-PSH, (B) H_{α} during titration of an equimolar mixture of $Cd(NTA)^-$ and N-PSH, (C) methylene protons in bound NTA during titration of an equimolar mixture of $Cd(NTA)^-$ and N-PSH and (D) methylene protons in NTA during titration of an equimolar mixture of Cd^{2+} and NTA. 90
25. Representative 1H NMR spectra of the pH titration of glutathione 94
26. Species of glutathione predominant in the pH region 4 to 12 95
27. The pH dependence of the chemical shift of g_5 proton (A) during titration of glutathione and (B) during titration of an equimolar mixture of glutathione and $Cd(NTA)$ 98

28. The pH dependence of the chemical shift of g2 protons (A) during the titration of glutathione and (B) during titration of an equimolar mixture of glutathione and $\text{Cd}(\text{NTA})^-$ 99
29. The pH dependence of the chemical shift of g7 proton (A) during titration of glutathione and (B) during titration of an equimolar mixture of glutathione and $\text{Cd}(\text{NTA})^-$ 101
30. Representative spectra of the titration of an equimolar solution of glutathione and $\text{Cd}(\text{NTA})^-$.
[$\text{Cd}(\text{NTA})^-$] = [GSH] = 0.02M 102
31. The pH dependence of the chemical shift of methylene protons in bound NTA during titration of an equimolar mixture of $\text{Cd}(\text{NTA})^-$ and glutathione. 103
32. Spectra obtained for solutions containing a fixed concentration of $\text{Cd}(\text{NTA})^-$ (~0.02M) and variable concentrations of GSH (0 - ~0.052M) at pH 6. 107
33. Dependence of the chemical shift of methylene protons in bound NTA on the concentration of GSH added to a solution of $\text{Cd}(\text{NTA})^-$ ~0.02M 109

34. The pH dependence of the chemical shifts of (A) cysteinyl C_{α} and (B) glutamyl C_{β} during titration of glutathione and (C) cysteinyl C_{α} and (D) glutamyl C_{α} during titration of an equimolar mixture of glutathione and $Cd(NTA)^{-}$ 111
35. The pH dependence of the chemical shift of (A) cysteinyl C_{β} and (B) glutamyl C_{β} during titration of glutathione; (C) cysteinyl C_{β} and (D) glutamyl C_{β} during titration of an equimolar mixture of glutathione and $Cd(NTA)^{-}$ 113
36. The pH dependence of the chemical shift of (A) g7 proton during titration of S-methylglutathione, (B) g7 proton and (C) methylene protons in bound NTA during titration of an equimolar mixture of S-methylglutathione and $Cd(NTA)^{-}$ 115
37. The pH dependence of the chemical shift of (A) H_{α} proton during titration of cysteine, (B) H_{α} and (C) methylene protons in bound NTA during titration of an equimolar mixture of cysteine and $Cd(NTA)^{-}$ 118
38. Spectra obtained when variable concentrations of cysteine ($0 + 1.4 \cdot 10^{-2}M$) are added to a solution

of Cd(NTA)⁻. Initial concentration of Cd(NTA)⁻ solution = 0.01M 119

39. Dependence of the chemical shift of methylene protons in bound NTA on the volume of 0.1M solution of cysteine added to a solution of Cd(NTA)⁻ (0.01M) at pH 7.5. 120

40. Spectrum of an equimolar mixture of Cd(NTA)⁻ and N-acetylcysteine (0.02M) at pH 7.276 121

41. ¹H NMR spectra of 1:2 mixtures of Cd²⁺ and glutathione at pH (A) 6.00, (B) 7.01, (C) 8.01, (D) 8.50, (E) 9.50, (F) 10.50, (G) 10.91, and (H) 12.05. 131

42. pH Dependence of the chemical shift of cysteinyl g5 protons (A) during titration of GSH (0.02M) and (B) during titrations of a 1:2 mixture of Cd²⁺ (0.1M) and GSH (0.2M) 134

43. pH Dependence of the chemical shift of g2 protons (A) during titration of GSH (0.02M) and (B) during titrations of a 1:2 mixture of Cd²⁺ (0.1M) and GSH 135

44. pH Dependence of the chemical shift of g3 protons (A) during titration of GSH (0.02M) and (B) during titrations of a 1:2 mixture of Cd²⁺ and GSH (0.2M) 136
45. pH Dependence of the chemical shift of glutamyl g4 protons (A) during titration of GSH (0.02M) and (B) during titrations of a 1:2 mixture of Cd²⁺ (0.1M) and GSH (0.2M) 137
46. pH Dependence of the chemical shift of glutamyl g7 protons (A) during titration of GSH (0.02M) and (B) during titrations of a 1:2 mixture of Cd²⁺ (0.1M) and GSH (0.2M) 138
47. pH Dependence of the chemical shift of glycy l g1 protons (A) during titration of GSH (0.02M) and (B) during titrations of a 1:2 mixture of Cd²⁺ (0.1M) and GSH (0.2M) 139
48. ¹H NMR spectra of glutathione solutions containing Cd²⁺ (0.01 M) at pH 9.5 and glutathione concentrations between ~0.02M to ~0.18M. 141
49. Dependence of chemical shift of g5, g1, g7, g2, g3, and g4 on the ratio [Cd]_t/[GSH] at pH 9.5. . . 142
50. ¹³C NMR spectra of glutathione at pH (A) 2.84, (B) 5.56, (C) 7.52, (D) 9.50 and (E) 11.52 144

51. ^{13}C NMR spectra of glutathione (0.2M) solutions containing Cd^{2+} (0.1M) at pH (A) 2.02, (B) 5.55, (C) 6.82, (D) 7.99, (E) 9.49, (F) 10.81, (G) 11.41 and (H) 12.00. 145

52. Expansion of the carbonyl region of spectrum of (A) glutathione and (B) a 1 to 2 mixture of Cd^{2+} and glutathione. pH = 9.5. 148

53. Expansion of the methylene region of the spectrum of (A) glutathione and (B) a 1 to 2 mixture of Cd^{2+} and glutathione. pH = 9.5. 149

54. Effects of Cd^{2+} complexation on the chemical shifts of cysteinyl C_β and glutamyl C_β resonances: pH dependence of the chemical shifts of (A) cys- C_β and (B) glu- C_β during titration of GSH and (C) cys- C_β and (D) glu- C_β during titration of a 1:2 mixture of Cd^{2+} and GSH. $[\text{Cd}]_t = 0.1\text{M}$ 150

55. Effects of Cd^{2+} complexation on the chemical shifts of cysteinyl C_β and glutamyl C_β resonances: pH dependence of the chemical shifts of (A) cys- C_α and (B) glu- C_α during titration of GSH and (C) cys- C_α and (D) glu- C_α during titration of a 1:2 mixture of Cd^{2+} and GSH: $[\text{Cd}]_t = 0.1\text{M}$ 152

56. ^{13}C NMR spectrum of GSH with (A) 0, (B) 0.02M and (C) 0.1M Cd^{2+} at pH = 6. 153
57. Chemical shifts of (A) cysteinyl C_β and (B) glutamyl C_β as a function of $[\text{Cd}]_t/[\text{GSH}]_t$ ratio at pH 6. $[\text{GSH}]_t = 0.2\text{M}$; $[\text{Cd}]_t = 0 + 0.14\text{M}$ 155
58. Chemical shifts of (A) cysteinyl C_α and (B) glutamyl C_β as a function of $[\text{Cd}]_t/[\text{GSH}]_t$ at pH 6. $[\text{GSH}]_t = 0.2\text{M}$, $[\text{Cd}]_t = 0 + 0.14\text{M}$ 156
59. Chemical shifts of (A) cysteinyl C_β and (B) glutamyl C_β as a function of $[\text{Cd}]_t/[\text{GSH}]_t$ concentration at pH 9.5. $[\text{GSH}]_t = 0.2\text{M}$, $[\text{Cd}]_t = 0 + 0.1\text{M}$ 157
60. ^{113}Cd NMR spectra of a 1 to 2 solution of Cd^{2+} and GSH at pH (A) 12.8, (B) 12.38, (C) 11.98, (D) 11.50, (E) 10.56, (F) 10.01, (G) 9.52, (H) 9.00. $[\text{Cd}^{2+}] = 0.25\text{M}$, $[\text{GSH}] = 0.5\text{M}$ 159
61. ^{113}Cd NMR spectrum of a 1 to 2 mixture of Cd^{2+} and GSH at pH = 9.5. $[\text{Cd}^{2+}] = 0.1\text{M}$; $[\text{GSH}] = 0.2\text{M}$ 166
62. ^{113}Cd NMR spectra of 1 to 2 mixture of Cd^{2+} (0.1M) and GSH (0.2M) at pH = 9.5 from $0^\circ\text{C} + 77^\circ\text{C}$ 173

63. (A) ^{113}Cd NMR and (B) ^{13}C NMR spectra of a 1:2 mixture of Cd^{2+} and GSH at pH 9.5. 176
64. ^{113}Cd NMR spectrum of a 1 to 1 mixture of Cd^{2+} and GSH at pH 10.5 180
65. The pH dependence of the ^{113}Cd chemical shift for (A) a $\text{Cd}(\text{NO}_3)_2$ solution and for (B) 1:1, (C) 1:2 and (D) 1:4 mixtures of Cd^{2+} and acetic acid 200
66. Names and structures of carboxylic acids used to determine ^{113}Cd chemical shifts of cadmium carboxylate complexes. 201
67. The pH dependence of the ^{113}Cd chemical shift for (A) 1:1, (B) 1:2 and (C) 1:4 mixtures of Cd^{2+} and chloroacetic acid 203
68. The pH dependence of the ^{113}Cd chemical shift for (A) 1:1, (B) 1:2 and (C) 1:4 mixtures of Cd^{2+} and formic acid. 204
69. The pH dependence of the ^{113}Cd chemical shift for (A) 1:1, (B) 1:2 and (C) 1:4 mixtures of Cd^{2+} and pivalic acid. 205
70. The pH dependence of the ^{113}Cd chemical shift for (A) 1:1 and (B) 1:2 mixtures of Cd^{2+} and acetylglycine. 210

71. The pH dependence of the ^{113}Cd chemical shift for (A) 1:1, (B) 1:2 and (C) 1:4 mixtures of Cd^{2+} and glycylglycine 213
72. Experimental and calculated curves of ^{113}Cd chemical shift versus pH for the determination of the ^{113}Cd chemical shift of the carboxylate complex of Cd-glycylglycine. 215
73. Experimental and calculated curves of ^{113}Cd chemical shift versus pH for the determination of the ^{113}Cd chemical shift of the amino complex of Cd-glycylglycine. 216
74. The pH dependence of the chemical shift of (A) H_2 and (B) H_4 protons during titration of histidine and (C) H_2 and (D) H_4 during titration of a 1:1 mixture of Cd^{2+} and histidine 218
75. The pH dependence of the chemical shift of H_4 proton (A) during titration of N-acetylhistidine and (B) during titration of a 1:1 mixture of Cd^{2+} and N-acetylhistidine 219
76. Experimental data and calculated curve of the chemical shift of H_β protons versus pH for the determination of (A) histidine's pK_a 's and (B) the formation constant of Cd-histidine complex . . 220

77. Experimental data and calculated curves of the chemical shift of H_4 proton versus pH for the determination of (A) N-acetylhistidine pK_a 's and (B) the formation constant of Cd-N-acetylhistidine complex. 221
78. Experimental data and calculated curve of ^{113}Cd chemical shifts versus pH for the determination of the ^{113}Cd chemical shift of Cd-N-acetylhistidine complex. 224
79. The pH dependence of the ^{113}Cd chemical shift for (A) 1:1, (B) 1:2 and (C) 1:4 mixtures of Cd^{2+} and N-acetylhistidine 225
80. The pH dependence of the ^{113}Cd chemical shift for (A) 1:2 and (B) 1:4 mixtures of Cd^{2+} and histidine. 226
81. Portion of a 360 MHz spin echo ^1H NMR spectrum of hemolysed erythrocytes ($\tau_2 = 0.06$ sec). 233
82. ^1H NMR spin echo spectrum of HRBC to which $\text{Cd}(\text{EDTA})^{2-}$ is added. $[\text{Cd}(\text{EDTA})^{2-}]_{\text{added}} = 2.621 \times 10^{-3}\text{M}$; $[\text{Mg}^{2+}]_{\text{total}} = 4.609 \times 10^{-3}\text{M}$ 234
83. ^1H NMR spectrum of an equimolar mixture of Cd^{2+} , Mg^{2+} and EDTA. 236

84. ^1H NMR spectrum of an equimolar mixture of Mg^{2+} and EDTA. 238
85. Titration of HRBC with EDTA: ^1H NMR spin echo spectra of HRBC obtained after addition of (A) 0 μl , (B) 15 μl , (C) 25 μl and (D) 35 μl of a 0.04M EDTA solution to 0.5 ml of HRBC. 240
86. Determination of Mg_{free} in HRBC: $I_{\text{EDTA}}/I_{\text{ref}}$ versus volume of EDTA added. Concentration of EDTA solution is 0.04M 241
87. Representative spectra used for the calibration of $\text{Mg}(\text{EDTA})^{2-}$ in HRBC. $[\text{Mg}]_{\text{t}} =$ (A) $4.65 \times 10^{-3}\text{M}$, (B) $6.09 \times 10^{-3}\text{M}$ and (C) $6.78 \times 10^{-3}\text{M}$ 245
88. Calibration curve for $\text{Mg}(\text{EDTA})^{2-}$ in HRBC 247
89. Spectra of the titration of HRBC with $\text{Cd}(\text{EDTA})^{2-}$. $[\text{Mg}]_{\text{tot}} = 4.6 \times 10^{-3}\text{M}$; $[\text{Cd}(\text{EDTA})]_{\text{added}} =$ (A) 0, (B) $1.778 \times 10^{-3}\text{M}$, and (C) $2.621 \times 10^{-3}\text{M}$ 249
90. ^1H NMR spectra of equimolar solutions of Cd^{2+} , Ca^{2+} and EDTA at pH (A) 7.02 and (B) 9.10. 260
91. ^1H NMR spectra of $\text{Ca}(\text{EDTA})^{2-}$ (equimolar solution of Ca^{2+} and EDTA at pH 6.9). 261
92. pH Dependence of the chemical shift of g_5 , g_1 , g_7 , g_2 , g_3 , g_4 during titration of GSH (darkened

circles) and during titration of a 1:2 mixture of Ca^{2+} and GSH (open circles) 263

93. Effect of the addition of GSH on the ^1H NMR spectrum of an equimolar solution (0.005M) of $\text{Cd}(\text{EDTA})^{2-}$ and Ca^{2+} at pH 6 (Spectrum A).
 (A) $[\text{GSH}] = 0 \text{ M}$, (B) $[\text{GSH}] = 1.84 \times 10^{-2} \text{ M}$,
 (C) $[\text{GSH}] = 3.77 \times 10^{-2} \text{ M}$, (D) $[\text{GSH}] = 5.68 \times 10^{-2} \text{ M}$ 264

94. Determination of $\text{Cd}(\text{EDTA})^{2-}$ from intensity measurements on g_4 resonance of GSH and resonance of ethylenic protons of $\text{Cd}(\text{EDTA})^{2-}$ 266

95. $\delta \text{ Cd}(\text{EDTA})$ versus pH during titration of a 1:1:1:10 mixture of Cd^{2+} , Ca^{2+} , EDTA and GSH 269

96. pH dependence of the ^{13}C chemical shifts of (A) cysteinyl C_β and (B) glutamyl C_β during titration of GSH and (C) cysteinyl C_β and (D) glutamyl C_β during titration of a 10:1:1 mixture of GSH, $\text{Cd}(\text{EDTA})^{2-}$ and Ca^{2+} 270

97. pH dependence of the chemical shift of H_α protons (A) during titration of N-PSH (0.02M) and (B) during titration of an equimolar solution of N-PSH and Ca^{2+} (0.02M). 274

98. ^1H NMR spectrum of a 1 to 1 to 10 mixture of $\text{Cd}(\text{EDTA})^{2-}$, Ca^{2+} and N-PSH at pH 6. $[\text{Cd}]_t = 0.005\text{M}$ 275
99. Portions of ^1H NMR spectra of Figure 98 mixture at pH (A) 5.4, (B) 5.9, (C) 7.1, and (D) 8.2 . . . 276
100. % $\text{Cd}(\text{EDTA})^{2-}$ vs. pH during titration of a 1:1:10 mixture of $\text{Cd}(\text{EDTA})^{2-}$, Ca^{2+} and N-PSH . . . 279
101. pH dependence of the chemical shift of H_α during titration of (A) cysteine (0.02M) and (B) an equimolar solution of Ca^{2+} and cysteine (0.02M). 280
102. Effect of addition of cysteine on the ^1H NMR spectrum of an equimolar mixture of $\text{Cd}(\text{EDTA})^{2-}$ and Ca^{2+} at pH 6.5. $[\text{Cd}(\text{EDTA})^{2-}] = [\text{Ca}^{2+}] = 0.005\text{M}$, $[\text{Cysteine}] =$ (A) 0, (B) $5.97 \cdot 10^{-3}\text{M}$, (C) $1.19 \cdot 10^{-2}\text{M}$ and (D) $1.59 \cdot 10^{-2}\text{M}$ 283
103. % $\text{Cd}(\text{EDTA})^{2-}$ versus concentration of cysteine at pH 6.5. 284
104. ^1H NMR spectra of 1:1:2 mixture of $\text{Cd}(\text{EDTA})^{2-}$, Ca^{2+} and CH_3SG at (A) 4.04, (B) 6.48, (C) 8.43, (D) 9.82 and (E) 12.00. $[\text{Cd}]_t = 0.01\text{M}$ 287
105. % $\text{Cd}(\text{EDTA})^{2-}$ versus pH during titration of a 1:1:2 mixture of $\text{Cd}(\text{EDTA})^{2-}$, Ca^{2+} and CH_3SG 288

CHAPTER I

INTRODUCTION

A. Toxicity of Cadmium

The toxic effects of cadmium in the form of Cd^{2+} are well established and documented [1]. It has been found to induce various pathological conditions, some of which may be fatal, such as the 'Itai-Itai' disease in northwestern Japan [1]. Other conditions include cardiovascular diseases [2,3], hypertension [4], and cancer [5].

It is known, however, that most of the Cd^{2+} in biological systems is not in the form of free Cd^{2+} ion; rather, it is complexed by the abundance of biological ligands therein [6-10]. For example, in animals, Cd^{2+} accumulates mainly in the liver and kidney where it is largely bound to thionein, a sulfur rich protein [11-13]. As a consequence, there has been considerable interest in the coordination chemistry of Cd^{2+} with biological ligands.

This thesis is concerned with 1H , ^{13}C and ^{113}Cd nuclear magnetic resonance studies of model systems for the complexation of Cd^{2+} in biological systems. In this chapter, the general coordination chemistry of Cd^{2+} is discussed, then the coordination chemistry of Cd^{2+} with biological ligands is reviewed, and finally the problems

addressed in this thesis are described.

B. The Coordination Chemistry of Cadmium

Divalent cadmium, (Cd^{2+}) is the most commonly encountered oxidation state of cadmium. It is a mildly soft acceptor with properties between those of the fairly hard Zn^{2+} and the very soft Hg^{2+} . With its $4d^{10}$ electronic configuration, Cd^{2+} adopts tetrahedral and especially octahedral coordination arrangements. 'Softer' ligands (e.g., S donors) prefer four coordination, while 'harder' ones (e.g., O and N donors) favor six coordination. Nonetheless, many exceptions to this generalization are known and departure from geometric regularity is quite frequent due to Jahn-Teller effects. As well, cases of higher and lower coordination numbers are well documented. Coordination numbers of seven and eight are found particularly with 'hard' chelating ligands such as nitrate and acetate [14-17]. Five coordinate compounds based on approximate trigonal bipyramidal or square pyramidal arrangements also occur for Cd^{2+} complexes in the solid state [15]. Lower coordination numbers of two and three are found in species with polarizable ligands of low effective electronegativity such as $(\text{CH}_3)_2\text{Cd}$, $\text{Cd}[\text{Mn}(\text{CO})_5]_2^-$ and CdI_3^- .

In solution, it is generally assumed that free Cd^{2+} is an octahedral $\text{Cd}(\text{solvent})_6^{2+}$ species unless the counter ions

show a strong tendency to ligate. Perchlorate, nitrate and sulfate have the least inner sphere involvement with Cd^{2+} [18,20].

C. Coordination Chemistry of Cd^{2+} with Biological Ligands

As suggested earlier, the complexation of Cd^{2+} by biological ligands plays a significant role in the toxicology of cadmium. The understanding of the interaction of Cd^{2+} in complex biological systems has been largely helped by the study of model systems in aqueous solutions. For example amino acids, peptides and related molecules are used to mimic the interactions of Cd^{2+} with proteins [21-23]. Simple amino acids coordinate through the amino and carboxylate groups, while N-protected amino acids coordinate solely through the carboxylate group [22]. In peptides, potential coordination sites are: the amino groups of the N-terminal amino acid residue, the carboxylate group of the C-terminal amino acid residue and the oxygen and nitrogen atoms of the peptide bonds. Depending on the residues, peptides can also coordinate to Cd^{2+} , through other nitrogen atoms (e.g., ring nitrogen in histidyl residues) and sulfur atoms (e.g., in cysteinyl residues).

Potentiometric titrations and polarographic studies have been extensively used to ascertain the nature of the complexes formed with amino acids and peptides and to deter-

mine their formation constants [21,22]. Nuclear magnetic resonance (NMR) spectrometry has also been used to study the complexation of Cd^{2+} by biological ligands providing detailed information at the molecular level about coordination at specific potential binding sites [21,23,24]. Also the change in NMR parameters, e.g., the change in chemical shifts upon complexation, can be used to determine formation constants [23,25]. In this respect NMR is a powerful tool for both the qualitative and quantitative characterization of the binding of metal ions by biological molecules.

Other ligands of interest include thiol containing molecules because of the strong affinity of Cd^{2+} for sulfur. A case that has attracted much interest is the formation of cadmium metallothionein in liver and kidney, which is considered to be a natural detoxification mechanism [26-28]. Thioneins are a class of cysteine-rich proteins found in a variety of species including mammals, birds, fish, etc. For example, 20 of the 61 amino acid residues of the thionein found in mammals are cysteine residues. Heavy metals such as mercury, zinc and cadmium have been found to bind to thionein through the cysteinyl side chains, wherefore the name metallothionein. It is the high metal content of these metallothioneins (usually 7 metals/mole) which led to the proposal that thionein may function as a detoxifying agent. Complexes of Cd^{2+} with thiols have relatively large formation constants. For example the 1 to 1 complex of Cd^{2+}

and penicillamine has a formation constant of $10^{11.4}$ [29]. Thiols also tend to form polynuclear species with Cd^{2+} in solution as well as in the solid state [30-32]. For example, both penicillamine and cysteine form polynuclear complexes with Cd^{2+} in aqueous solutions [30-32].

The interactions of Cd^{2+} in some real biological systems have been studied. Of interest to this thesis is the study conducted on the complexation of Cd^{2+} in human red blood cells [33]. The identity of the components of the erythrocytes which bind Cd^{2+} was established from changes in high resolution spin-echo $^1\text{H-NMR}$ spectra of intact erythrocytes. It was found that intracellular cadmium binds to the tripeptide glutathione (GSH) and to hemoglobin (Hb). Though the exact nature of complexes formed was not established in this study, it was suggested that besides complexes of the nature $\text{Cd}(\text{GSH})$ and $\text{Cd}(\text{Hb})$, ternary complexes involving Cd^{2+} and both GSH and Hb might exist. The latter conclusion was drawn from differences in the changes observed for resonances from GSH in red blood cells and in aqueous solutions upon the addition of Cd^{2+} . From the same study, it was found that the binding of Cd^{2+} by GSH in erythrocytes is reversible. When a red blood cell lysate containing CdCl_2 was titrated with EDTA, the $^1\text{H-NMR}$ spectra of the lysate indicated complete release of GSH.

The most common treatment for cadmium poisoning is to increase the rate of elimination of cadmium from the body.

and dithiols. The relative effectiveness of various thiol-containing chelating agents for removing Cd^{2+} from its complexes in erythrocytes was determined from their effect on the GSH resonances of Cd^{2+} -containing red cell lysates. The following order of effectiveness was observed: mercaptosuccinic acid > N-acetylpenicillamine > penicillamine > mercaptoacetic acid > cysteine > 2,3-dimercaptopropane-sulfonic acid > dithioerythritol > 2,3-dimercaptosuccinic acid.

Since blood plasma contains small molecules and proteins which potentially can bind Cd^{2+} , the uptake of Cd^{2+} by erythrocytes in suspension in isotonic solution was compared with uptake by erythrocytes in whole blood. This was done by measuring time courses for the uptake of Cd^{2+} by erythrocytes in the two media, using as an indicator of the uptake the intensity of the resonance for the cysteinyl protons of GSH. The time courses for the uptake of Cd^{2+} by erythrocytes in the two media were found to be similar. In both cases, the intensity of the glutathione resonance reached a minimum after approximately 30 minutes, indicating little if any interaction of Cd^{2+} with plasma components.

The complexation of Cd^{2+} by biological macromolecules (e.g., metalloproteins) has been studied by ^{113}Cd -NMR. Naturally occurring cadmium contains two isotopes of spin $1/2$. The natural abundance of ^{111}Cd is 12.75% and that of ^{113}Cd is 12.26%. The ^{113}Cd isotope is the one most commonly observed by cadmium NMR. The ^{113}Cd -isotope has a sensitivity of 1.34×10^{-3} with respect to ^1H at isotopic natural abundance and constant field, which makes it approximately eight times as sensitive as the ^{13}C nucleus.

^{113}Cd chemical shifts cover some 900 ppm, consistent with large paramagnetic contributions to the shielding constant [43]. Though a strict relationship between chemical shifts and the nature of the Cd^{2+} complex has not been determined, it is well established that the number and nature of donor groups plus the geometry of the complex are major factors determining the chemical shift. For example, oxygen donors cause an upfield shift whereas nitrogen and sulfur donors produce a downfield shift, with sulfur causing the largest shift [20]. Also, cadmium in a tetrahedral coordination geometry appears to be deshielded relative to that in octahedral coordination by approximately 50-100 ppm [34]. A similar degree of deshielding of ^{113}Cd is known to exist between octahedral and heptacoordinated oxygen ligands [35]. Outer-sphere effects have been reported as

thiolate ligands brings about a shift of the order of 15 to 20 ppm per alkyl substitution [36]. From a compilation of ^{113}Cd chemical shifts for Cd^{2+} -substituted metalloproteins, Armitage and Boulanger [37] summarized the effect of the donor groups as follows: resonances from cadmium bound exclusively to oxygen ligands are invariably found in the region of 0 to -125 ppm, those bound to a combination of oxygen and nitrogen ligands appear between 0 and 300 ppm, whereas resonances from cadmium bound to two or more thiolate sulfur ligands are found in the most downfield region, between 450-750 ppm. These chemical shifts are reported relative to 0.1 M $\text{Cd}(\text{ClO}_4)_2$ solution to which 0.0 ppm is generally assigned.

One of the most significant applications of ^{113}Cd -NMR has been its use as a surrogate probe for zinc and calcium in biological systems. For example, zinc(II) is substituted by cadmium(II) in its metallothioneins, and the environment of the Cd^{2+} is probed by ^{113}Cd -NMR. The ^{113}Cd NMR signal of metalloproteins was first observed by Armitage, Coleman and coworkers [38], followed by Sudmeier [39], Drakenberg and coworkers [40] and Myers [41]. Significant progress has been made in the elucidation of the structure and the nature of the binding of Cd^{2+} metallothioneins. Human liver metallothionein, for example, exhibits ^{113}Cd resonances in the region between 600 and 680 ppm, which have been attri-

sulfur [28].

The calcium-binding muscle protein, troponin C, was investigated by Ellis and coworkers [43]. Individual resonances were observed and assigned for all four calcium binding sites in Cd^{2+} -substituted protein. These signals appeared in the region between -100 and -120 ppm, 2 for structural sites and 2 for regulatory sites.

Given that the ^{113}Cd -NMR chemical shift has the potential to provide detailed information about the chemical environment and structure of Cd^{2+} complexes, there has been an increasing need for benchmark chemical shifts of model Cd^{2+} compounds. ^{113}Cd -NMR parameters from these model complexes can provide data relevant to the interpretation of the ^{113}Cd -NMR parameters of more complex biological systems. For this reason, model compounds of Cd^{2+} have been investigated by ^{113}Cd -NMR both in the solid state and aqueous solutions. Bulman et al. have reported ^{113}Cd chemical shifts and ^{113}Cd - ^{113}Cd coupling constants for cadmium complexes of the bis(ethyl cysteinate) amide of EDTA [44] which are close to those observed for metallothionein in aqueous solution. Similar couplings were measured in ^{113}Cd -NMR spectra of polycadmium thiolate/chalcogenide aggregates of known crystal structure by Dance and Saunders [45]. Small dynamically stable Cd^{2+} complexes were recently investigated by Keller et al. [46]. The ^{113}Cd -NMR parameters from these

model complexes proved to be useful for the interpretation of those from Zn^{2+} and Ca^{2+} substituted proteins. Honkonen and Ellis measured ^{113}Cd -NMR parameters for single crystals of cadmium salts of selected carboxylic acids and cadmium diammonium disulfate hexahydrate as a basis for understanding the characteristic shielding of the resonances corresponding to Cd-substituted parvalbumin [40], troponin C [48], calmodulin [49], insulin [50] and concanavalin A [51].

In aqueous solution as well as in biological systems, chemical exchange can hamper the direct use of the ^{113}Cd -NMR chemical shifts to determine the chemical environment of species. The worst case is the total loss of the NMR signal due to excessive exchange broadening. A direct consequence of the high sensitivity of ^{113}Cd NMR to small changes in the chemical environment of cadmium is large differences in resonance frequencies of closely related species. Exchange of Cd^{2+} among these species can cause the NMR signal to disappear from the spectrum due to intermediate exchange rates. Exchange may also affect parameters, not directly observed such as the nuclear Overhauser enhancement and the spin lattice relaxation times [52]. Consequently, interpretation of NMR parameters can be totally inaccurate if the effect of chemical exchange is not considered. This apparent liability can, however, be turned into an asset not available with the most commonly used NMR

nuclei and ^{113}Cd . Thus, a detailed study by ^{113}Cd -NMR of the "well known" $\text{Cd}(\text{EDTA})$ complex [52] proved useful for accommodating conflicting reports on the solution structure of Cd-EDTA [53]. Investigation of the pH dependence of the ^{113}Cd chemical shift and spin-lattice relaxation time and of ^{113}Cd - $\{^1\text{H}\}$ nuclear Overhauser effects at three magnetic field strengths, provided new evidence for a pH dependence of the solution structure of the Cd-EDTA complex. This study, by Jensen and coworkers is an elegant demonstration of the detailed information attainable with ^{113}Cd -NMR and emphasizes the crucial need for a careful interpretation of relaxation parameters in order to draw accurate conclusions.

To circumvent the problem of the lost signal by exchange, Ackerman and Ackerman used supercooled emulsions to impose the NMR slow exchange regime upon labile $\text{Cd}(\text{II})$ glycine complexes [54]. However, the assignment of the resonances was not unambiguous, as remarked by the authors, who observed a signal at a chemical shift which they had attributed to a $\text{Cd}(\text{II})$ glycine complex from supercooled solutions containing varying amounts of $\text{Cd}(\text{II})$ and NO_3^- in the absence of glycine. It was suggested that this signal might have been derived from the aquated or ion-pair forms of $\text{Cd}(\text{II})$. The general applicability of this technique using supercooled solutions is, therefore, questionable.

A somewhat more favorable situation is that of suf-

ficiently rapid exchange to produce a single ^{113}Cd resonance for all species in a given system. The observed chemical shift is then a weighted average of the chemical shifts of the various species. Individual chemical shifts can be deduced with knowledge of the formation constants of the species, assuming exact reaction models were used for the determination of the formation constants [19,55]. This method relies upon the accuracy of formation constants determined previously by other techniques.

E. This Thesis

As discussed earlier, Cd^{2+} can have coordination numbers up to 6 or larger. Many biological ligands have fewer dentates and thus the Cd^{2+} in complexes of such ligands is coordinatively unsaturated, with solvent molecules occupying the other coordination sites. The solvent molecules in these sites can be replaced by other ligands, forming mixed complexes of the type MLL' where M stands for metal and L and L' stand for the two different ligands. As discussed earlier (33), mixed Cd^{2+} complexes have been suggested to occur in red blood cells on the basis of $^1\text{H-NMR}$ measurements. In Chapter III, results obtained from a study of model systems for the formation of Cd^{2+} mixed complexes are reported. The objective of this study was to characterize the tendency of various biological ligands to react with a

Cd-ligand complex to form mixed ligand complexes. The system studied consists of a primary ligand, nitrilotriacetic acid (NTA), which forms a stable 1 to 1 complex with Cd^{2+} above pH 4 in solutions containing equimolar amounts of Cd^{2+} and NTA. The proposed structure of this complex is shown in Figure 1. The tetradentate NTA (one nitrogen and three oxygen donor groups) blocks four of the six coordination sites on Cd^{2+} , leaving two vacant sites in a cis configuration [56]. The secondary ligands used in this work were the amino acids glycine (gly), glutamic acid (glu), penicillamine (PSH), N-acetylpenicillamine (N-PSH), cysteine (cys), N-acetylcysteine (N-cys), mercaptosuccinic acid (MSA), the peptide glutathione (GSH) and its derivative S-methylglutathione (CH_3SG).

As mentioned earlier, ^1H -NMR evidence has been presented for the complexation of Cd^{2+} by glutathione in intact erythrocytes. Given the ubiquity of GSH in biological systems and thus the probable importance of the binding of Cd^{2+} by GSH in the toxicology of Cd^{2+} , the binding of Cd^{2+} by GSH has been studied in detail by ^1H , ^{13}C and ^{113}Cd NMR. Results are presented in Chapter IV. Results of studies conducted in order to establish ^{113}Cd -NMR chemical shifts for Cd^{2+} in certain model complexed forms are presented in Chapter V.

In Chapter VI are presented the results of a study in which the binding of Cd^{2+} in hemolyzed red blood cells is

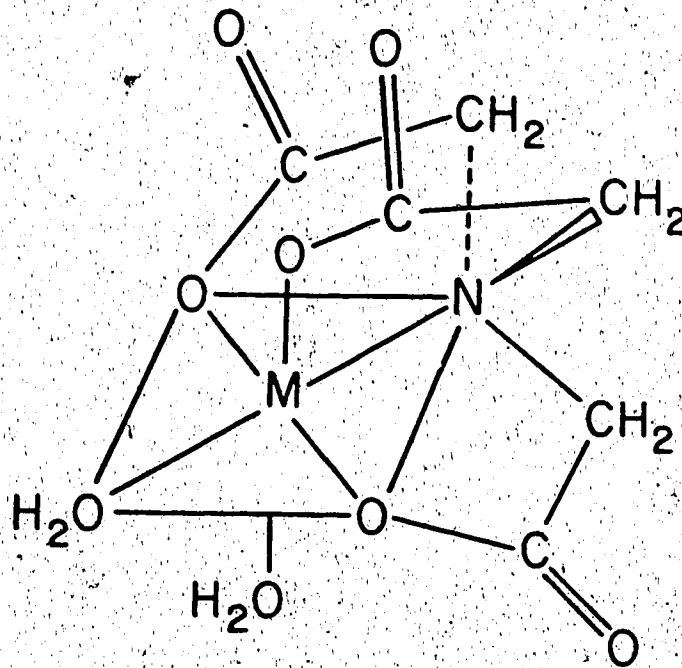


Figure 1. Structure of Cd(NTA)⁻ complex.

quantitatively characterized. Equilibrium constants are estimated by using a reaction in which EDTA competes with ligands in the red blood cells for Cd^{2+} . Equilibrium constants for the reaction were calculated from the intensity of resonances in spin echo ^1H NMR spectra. This approach was also used to determine equilibrium constants for several model systems for comparison.

CHAPTER II

EXPERIMENTAL

A. Chemicals

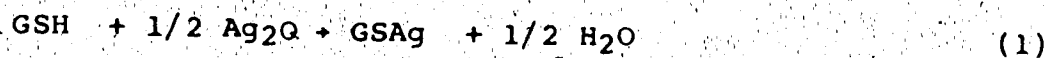
Cadmium nitrate, $\text{Cd}(\text{NO}_3)_2 \cdot 4\text{H}_2\text{O}$, calcium nitrate, $\text{Ca}(\text{NO}_3)_2$, sodium hydroxide (carbonate free), t-butyl alcohol (TBA), potassium diphthalate, potassium dihydrogen phosphate, disodium hydrogen phosphate, zinc metal, silver oxide (Ag_2O) and methyl iodide (CH_3I) were obtained from J.T. Baker Chemical Company. Cadmium bromide and cadmium perchlorate were obtained from Alfa Products, sodium nitrate and magnesium chloride from Mallinckrodt Chemical Co., 1,4-dioxane and glycine from BDH and D_2O from Stohler Isotope Chemicals. Sodium deuterioxide (NaOD), deuterated nitric acid (DNO_3), glutathione, penicillamine, N-acetylpenicillamine, cysteine, N-acetylcysteine, mercaptosuccinic acid and N-acetylhistidine were from Sigma Chemical Company. The disodium salt of nitrilotriacetic acid, cadmium chloride, cadmium iodide and gadolinium nitrate were from Aldrich Chemical Company and glutamic acid, ethylenediaminetetraacetic acid, sodium acetate, chloroacetic acid, sodium formate and histidine were from Fisher Scientific Company. All were used as obtained without further purification.

Doubly distilled and deionized (DDD) water was used in

the preparation of solutions. S-methylglutathione (CH₃SG) was prepared as detailed in the next section.

B. Synthesis and Analysis of S-Methylglutathione

S-methylglutathione was prepared according to the method described by Martin and Edsall [57]. The following reactions were used:



where GSH represents glutathione. 15 mmole of GSH (4.6095 g) were dissolved in about 20 ml of deionized water and deoxygenated by bubbling N₂ through it. 7.5 mmole of Ag₂O (1.7380 g) were added to the solution in the dark and the solution was stirred for one hour. The black silver oxide precipitate was replaced by a white precipitate of GSAg. 17 mmole of CH₃I (2.412 g or 1.05 ml) were added to this precipitate and the mixture was stirred for 42 hours. The yellow precipitate of AgI was removed from the solution by filtration. The S-methylglutathione was then precipitated from the filtrate by the addition of acetone. The yield was 78% before purification. The white powder of CH₃SG was recrystallized by dissolving in a minimum amount of H₂O and then adding acetone. The powder was dried under vacuum overnight.

A microanalysis of the product thus obtained yielded the following results: C, 41.2%; H, 5.99%; N, 13.07%; S, 9.86%. The theoretical percentages are respectively 41.1, 5.96, 13.07 and 9.79.

C. Solution Preparation

Solvents were 0.4 M NaNO₃ in D₂O for most ¹H-NMR measurements and 0.3 M NaNO₃ in 5% D₂O/95% H₂O for ¹³C and ¹¹³Cd NMR measurements. The chemical shift reference substances, tert-butyl alcohol (TBA) (0.04% v/v) and 1,4-dioxane (0.15% v/v) were added to the solvents.

Solutions were prepared in a thermostated cell at 25°C in 25 or 50 ml of the appropriate solvent. Argon was bubbled through solutions containing thiols in order to prevent their oxidation by air. Titrant solutions used for pH adjustments (NaOD, DNO₃, NaOH, HNO₃) generally were about 2 M and were delivered with a Mettler/DV11 autoburet through a Pederson 5 μl micropipet.

Samples to be used for NMR measurements were withdrawn from the cell with 1 ml polyethylene syringes. For ¹H-NMR measurements, ~0.5 ml of sample were transferred to a 5 mm diameter NMR tube while for ¹³C and ¹¹³Cd-NMR, ~2 ml of sample were transferred to a 10 mm-diameter NMR tube.

For the study of the mixed ligand complexes, Cd(NTA)L, two kinds of experiments were performed. In the first

category, mixtures containing equimolar amounts of Cd^{2+} , NTA and ligand were titrated with NaOD and DNO_3 to make samples at different pH values. The concentration of each species was kept generally at $\sim 0.02\text{M}$ except in the case of N-acetylpenicillamine, where it was kept at 0.01M due to its lower solubility. The sodium salt of NTA and the cadmium nitrate were dissolved separately in the solvent before mixing. This approach prevented precipitation of $\text{Cd}(\text{OH})_2$ which results from local saturation. The ligand was then added as a solid. Alternatively, a stock solution of $\text{Cd}(\text{NTA})^-$ was prepared in the solvent. To 25 or 50 ml of this solution, the ligand was added. For the second category of experiments, the pH and the concentrations of Cd^{2+} and NTA were kept constant while the ligand concentration was varied. For these experiments, a sample (25 ml) of the stock solution of $\text{Cd}(\text{NTA})^-$ was brought to the desired pH. Increments of the ligands were added to this solution as a solid or as a concentrated stock solution.

For the determination of pK_a values from chemical shift measurements, solutions of a ligand alone at different pH values had to be prepared. NMR tubes as many as selected pH values of measurements were used. Samples (0.5 ml) were withdrawn from the solution of the ligand as its pH was adjusted. This was a faster way of acquiring data when there was no need to know the exact concentration as in the case of pK_a determination. The chemical shift depends

the pH.

When formation and/or equilibrium constants were deduced from NMR measurements, it was necessary to know exact concentrations of metal and ligand, and a different sample preparation was used. A single NMR tube was used, and the sample was returned to the titration vessel after each NMR measurement. After the pH and/or concentration were adjusted, the tube was rinsed at least twice with the experimental solution and a new sample withdrawn. A dilution factor could be calculated and the change in concentrations monitored easily this way. This procedure was also used when preparing samples for quantitative ^{113}Cd NMR where concentrations of species were deduced from the NMR experiments.

For other ^{113}Cd and ^{13}C NMR measurements, a two tube procedure was employed. The use of two tubes was realized as follows: at the beginning of the experiment sample 1 and sample 2 were prepared and transferred to tubes 1 and 2. When NMR measurements on sample 1 were completed, it was returned to the titration vessel for the preparation of sample 3. While the NMR measurements were being made on sample 2, the pH of the solution in the titration vessel was adjusted and sample 3 was then withdrawn from the vessel and transferred to tube 1. When the measurements on sample 2 were

... of the longer accumulation times required for ^{13}C and ^{113}Cd NMR measurements, this procedure proved to be more efficient than the use of one NMR tube.

For the measurement of ^{113}Cd chemical shifts of Cd^{2+} -carboxylate complexes, titrations were performed on mixtures of 1 to 1, 1 to 2 and 1 to 4 Cd^{2+} to ligand. Solutions of cadmium nitrate were prepared so as to keep the sum of the concentrations of ligand and NaNO_3 constant at 0.4 M.

Therefore, stock solutions of 0.1 M $\text{Cd}(\text{NO}_3)_2$ in 0.3 M, 0.2 M and 0.0 M NaNO_3 in 5% $\text{D}_2\text{O}/95\% \text{H}_2\text{O}$ were prepared for the 1 to 1, 1 to 2 and 1 to 4 mixtures, respectively. 25 ml were used for each titration and the ligand was added in the solid form to give the appropriate concentrations of 0.1 M, 0.2 M and 0.4 M. The pH was adjusted with 2.0 M NaOH or HNO_3 solutions. One NMR tube was used according to the procedure already described. The stock solutions of $\text{Cd}(\text{NO}_3)_2$ were made from a more concentrated solution of $\text{Cd}(\text{NO}_3)_2$ which had been standardized by EDTA titration. The EDTA was first standardized with Zn^{2+} solution prepared from Zn metal and concentrated HCl [58], then the $\text{Cd}(\text{NO}_3)_2$ solution was titrated with the standardized EDTA solution in the presence of xylenol orange [58].

All solutions used for the experiments on the red blood cells were prepared in D_2O and their pH adjusted to 7.4. For the determination of magnesium in the red blood cells, a

solution prepared from MgCl_2 had a concentration of $\sim 0.05 \text{ M}$. The solution of the complex $\text{Cd}(\text{EDTA})^{2-}$ was prepared by dissolving $\text{Cd}(\text{NO}_3)_2$ and the disodium salt of EDTA in equimolar quantities to make 0.025 M . When the pH is adjusted to 7.4, the complex is readily formed in solution.

Calibrations of the pH meter were done with buffers $\text{pH} = 4.008$ and $\text{pH} = 6.865$ freshly prepared in double distilled and deionized water. The $\text{pH} 4.008$ buffer was a 0.05 M solution of potassium biphthalate [59]. The $\text{pH} 6.865$ buffer was a solution of 0.025 M potassium dihydrogen phosphate and 0.025 M disodium hydrogen phosphate [59]. The phthalate as well as the phosphate salts were ground to a powder and dried at 120°C for 2 hours before use.

Measurements of pH were made with an Orion model 701A or a Fisher Accumet pH meter equipped with a standard glass electrode and a double junction saturated calomel reference electrode. The outer junction of the reference electrode contained a solution of ionic strength close to that of the solution under investigation. A microcombination electrode was used for a few pH measurements.

Throughout this thesis, pH refers to the meter reading not corrected for the deuterium isotope effect.

The erythrocytes were obtained from venous blood which was collected in vacutainers (Becton, Dickinson and Co.) containing heparin. The whole blood was poured into a large beaker (250 ml) and oxygenated. It was then transferred into polyethylene tubes and centrifuged for 5 to 7 minutes. The plasma and buffy coat were removed. The cells were washed two or three times by suspension in an equal volume of a D₂O solution of isotonic saline (0.9% NaCl) followed by centrifugation to separate the cells from the wash solution. The D₂O replaces most of the intracellular H₂O. After washing, the cells were oxygenated again and then were lysed by taking them through three freeze-thaw cycles in dry ice. NMR measurements were made on 0.5 ml of lysed cells. The lysed cells were transferred into the NMR tube with an Eppendorf pipette. The NMR tube was centrifuged to bring the sample down the tube. The solutions of EDTA, MgCl₂ or Cd(EDTA)²⁻ were added to the lysed cells in the NMR tube with 10 µl microsyringes. The tube was shaken and centrifuged to achieve complete mixing and to bring the sample to the bottom of the NMR tube.

1. General

All NMR measurements were performed on a Bruker WM-360 spectrometer operating in the pulse Fourier Transform mode. ^{13}C and ^{113}Cd NMR spectra were measured at spectrometer frequencies of 90.5 and 79.8 MHz, respectively.

Most experiments were performed at an ambient probe temperature of -25°C . When additional temperature control was needed, cool air was blown into the probe and the temperature regulated by the heater and thermocouple contained in the probe. Air was cooled by passing it through a metal coil immersed in dry ice which was contained in a dewar. It was necessary to cool the sample to maintain a temperature of 25°C when measuring ^{13}C spectra due to the sample heating which results from broadband proton decoupling.

Most ^1H and ^{113}Cd NMR spectra were measured by the single pulse experiment (Figure 2). Proton decoupled ^{13}C -NMR spectra were obtained by using power gated proton decoupling (Figure 3). In this experiment, the broadband ^1H decoupling is switched between high and low power during and prior to the acquisition of the free induction decay (FID) by using the microprogram listed in Appendix 1. In so doing, heating of the sample is kept at a minimum without sacrificing too much the Nuclear Overhauser Enhancement (NOE) advantage. Prior to acquisition of the FID, a low power

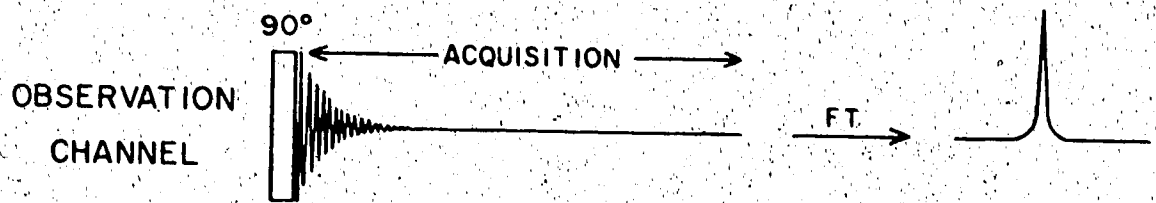


Figure 2. Single pulse experiment.

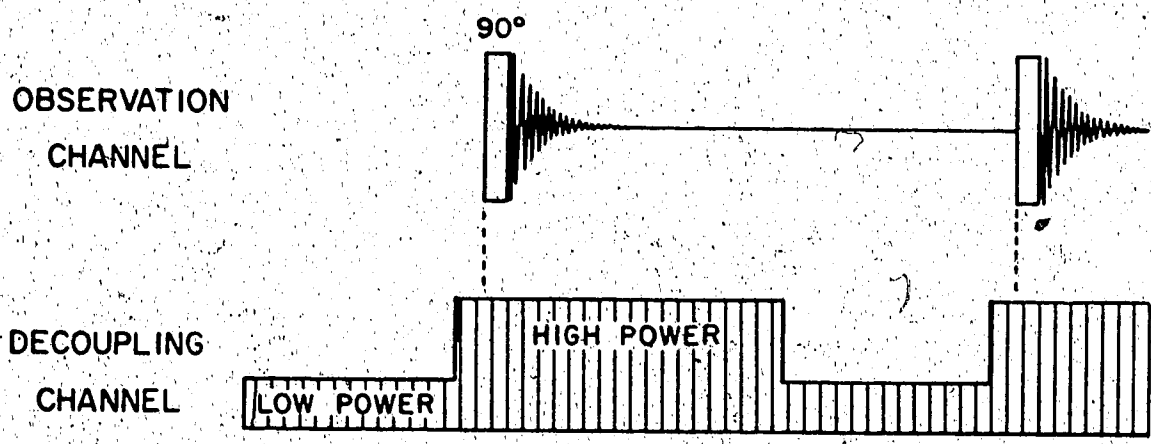


Figure 3. Power gated proton decoupling experiment.

(0.4 watt), broad band decoupling is applied during 1 second to build the NOE with minimum heating. Approximately .01 sec prior to acquisition, the high power (2 watts) decoupling is turned on to assure total decoupling during acquisition. Overheating of the sample causes a drift in the lock signal, and consequently broadening of the resonance signal.

In the measurement of ^1H NMR spectra of aqueous solutions, the large water signal was suppressed by applying through the decoupling channel a strong selective radio frequency pulse at the water resonance frequency for about 2 sec prior to the application of the nonselective observation pulse. The purpose of the decoupler pulse is to saturate the H_2O resonance so that there is only a small net magnetization due to H_2O along the direction of the applied field (z') when the observation pulse is applied and thus only a small contribution from the H_2O magnetization to the free induction decay. The time between the saturation and the observation pulses must be kept short to prevent return of the magnetization from H_2O along the z' axis by spin-lattice relaxation. The microprogram used is given in Appendix 2.

^1H -NMR chemical shifts were measured relative to the methyl resonance of *t*-butanol, which was added as an internal reference, but are reported relative to the methyl resonance of sodium 2,2-dimethyl-2-silapentane-5-sulfonate (DSS). The chemical shift of the *t*-butanol methyl resonance is 1.2365 ppm relative to the DSS resonance. ^{13}C -NMR chemical

shifts were measured relative to the ^{13}C resonance for 1,4-dioxane but are reported relative to tetramethylsilane (TMS). The chemical shift of the dioxane resonance is 67.4 ppm relative to TMS. ^{113}Cd -NMR chemical shifts were measured and are reported relative to the ^{113}Cd resonance for a 0.1M solution of $\text{Cd}(\text{ClO}_4)_2$ set at 0.0 ppm. Initially a ^{113}Cd NMR spectrum of a concentrated solution of $\text{Cd}(\text{NO}_3)_2$ (4.5 M) was recorded. The resonance in the spectrum was spotted and assigned its known chemical shift relative to 0.1 M $\text{Cd}(\text{ClO}_4)_2$, -49.4 ppm [18]. This produced a spectral reference (SR) value which was subsequently typed in to calibrate all other spectra.

2) Measurement of Spin-Lattice Relaxation Times

For quantitative NMR measurements, it is necessary to know the spin-lattice relaxation times (T_1) of the resonance from which quantitative information is obtained to ensure that a sufficiently long repetition time, i.e., the total time between successive pulses, is used. The repetition time must be long enough to allow all nuclei to relax back to equilibrium, i.e. to relax so that the magnetization along the z' axis has returned to its equilibrium value, before the next pulse is applied. If the magnetization of some resonances is only partially recovered, these resonances will be partially saturated and concentrations determined from integral measurements will be in error. To

obtain accurate quantitative information, the repetition time must be at least 5 times the longest T_1 of resonances of interest; at $5 T_1$, magnetization along the z axis will be 99.3% of its equilibrium value with a 90° pulse angle.

The inversion-recovery pulse sequence ($180^\circ - \tau - 90^\circ$ - acquisition-RD), where RD is a relaxation delay time, was used to determine spin lattice relaxation times.

This pulse sequence and the behavior of the magnetization during the pulse sequence are depicted in Figure 4. The 180° pulse inverts the magnetization. During the following relaxation period of length τ , the magnetization is relaxed back towards its equilibrium value. The recovery of the magnetization by spin lattice relaxation is described by equation 3, where M_τ

$$M_\tau = M_0(1 - e^{-\tau/T_1}) \quad (3)$$

is the value of the magnetization at time τ and M_0 is the value of the magnetization at equilibrium. The latter value will be reached faster or slower depending on the spin-lattice relaxation time. The dependence of the recovery curves on T_1 is depicted in Figure 5, showing fast recovery with short T_1 and long recovery period with long T_1 's. After the relaxation period, the 90° sampling pulse is applied to determine the magnitude of the magnetization at time τ . Since the signal strength is directly proportional to the magnitude of the magnetization in the x'y' plane,

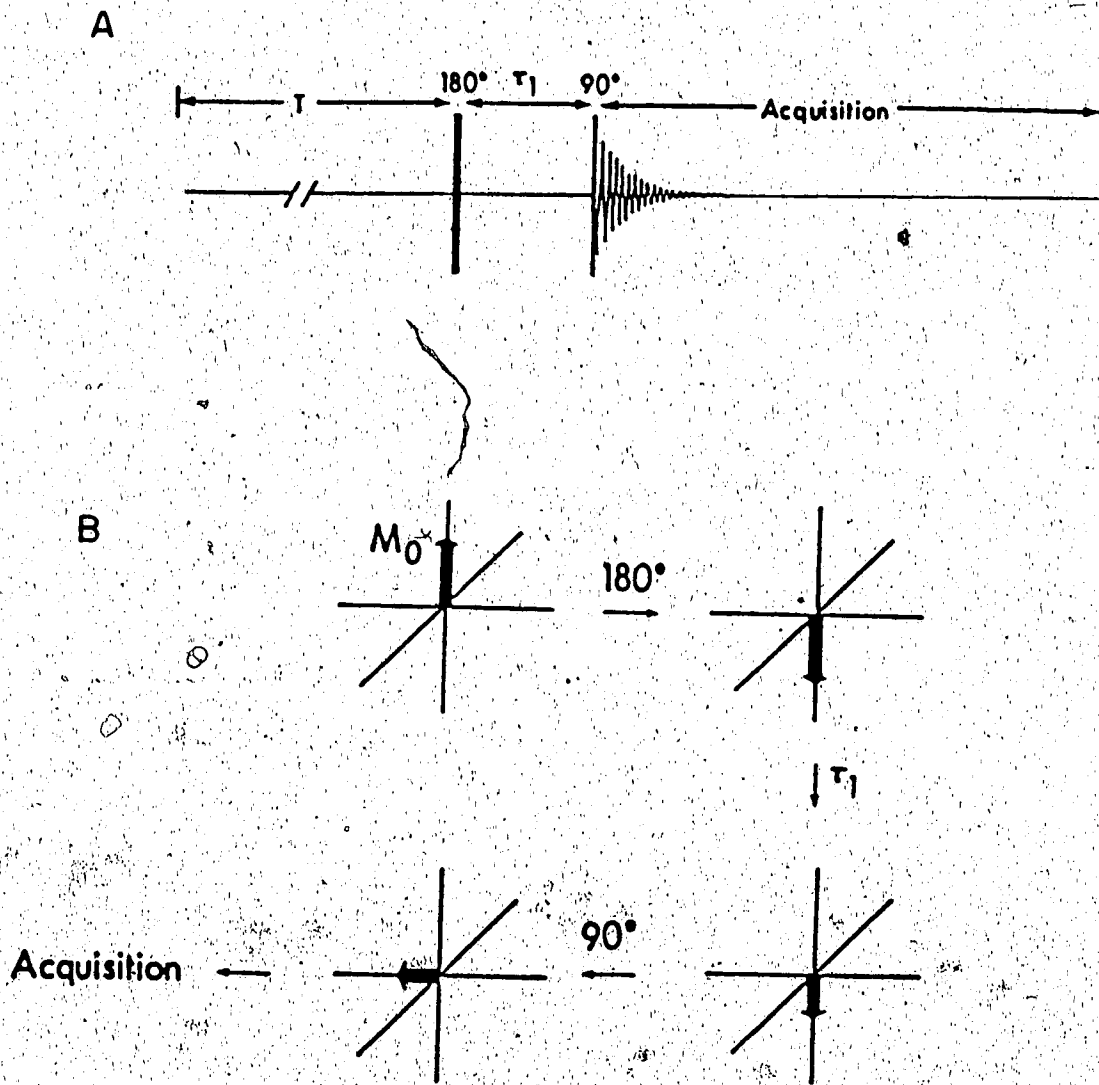


Figure 4. (A) Pulse sequence inversion recovery experiment, (B) behavior of the magnetization.

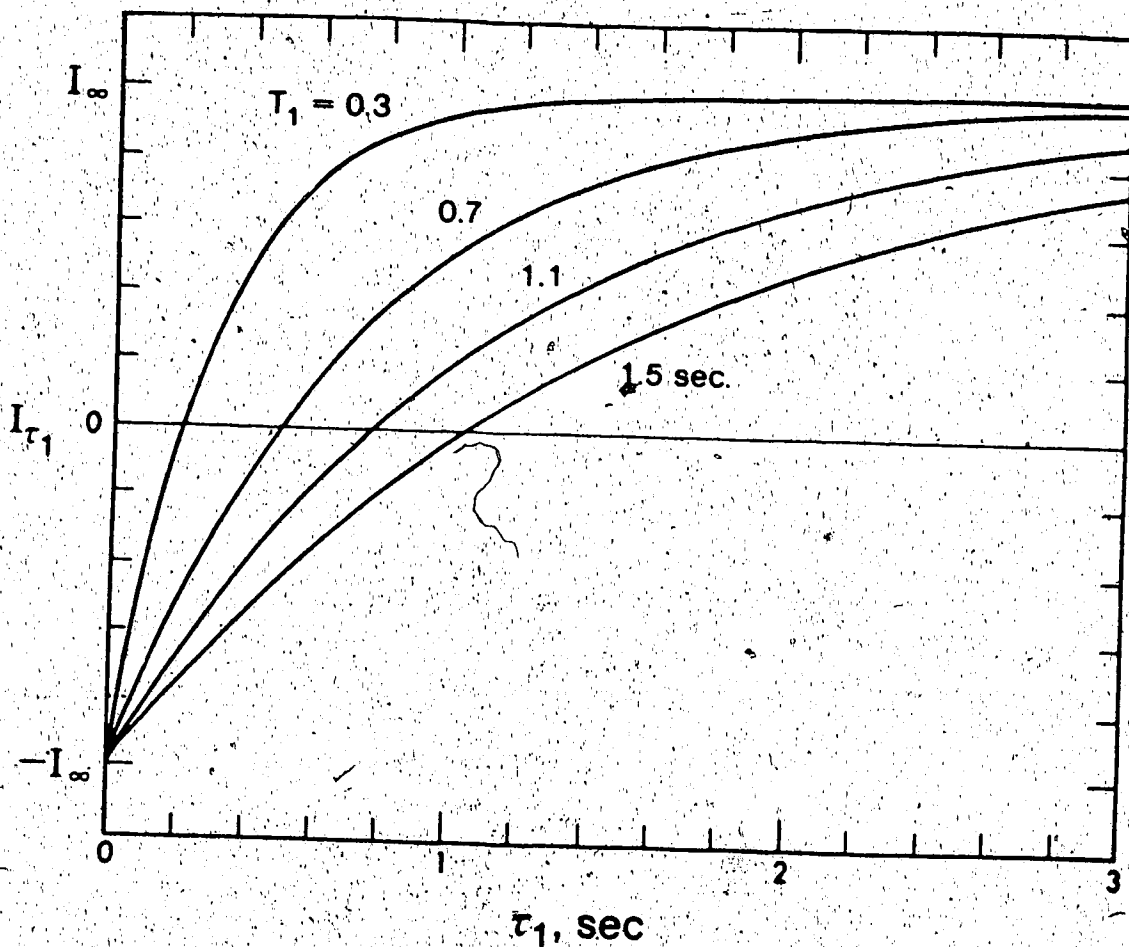


Figure 5. Recovery curves for nuclei having T_1 values of 0.3, 0.7, 1.1 and 1.5 sec following application of the 180° pulse in the inversion recovery pulse sequence. [Reproduced with permission from D.L. Rabenstein, *J. Biochem. Biophys. Methods*, 9, 277 (1984)].

$$I_{\tau} = I_0(1 - 2e^{-\tau/T_1}) \quad (4)$$

where I_{τ} is the intensity of the signal after a time τ and I_0 is the intensity of the signal at $\tau \geq 5T_1$. If τ is long enough, the magnetization will return completely to its equilibrium value M_0 and the intensity is equal to the equilibrium intensity. A series of spectra recorded at different τ values in the measurement of a spin-lattice relaxation time are shown in Figure 6. Spin-lattice relaxation times were obtained by fitting the intensity versus τ data to equation 4 with the nonlinear least squares computer program KINET; this program and its use are described in Section G of this chapter. When only an approximate value for T_1 was required, it was obtained from the τ at the point where the intensity of the signal is at a null. At this point, τ is related to T_1 by:

$$\tau = 0.69 T_1 \quad (5)$$

To measure T_1 values by the inversion recovery pulse sequence, it is necessary that the pulse lengths for 90° and 180° flip angles be known. These pulse lengths were determined by measuring spectra as a function of the length of the pulse. A typical series of spectra obtained during the determination of the pulse lengths at 79.8 MHz for ^{113}Cd -NMR are shown in Figure 7. The sample was a 1 M solution of CdBr_2 . The signal intensity goes through a maximum at >20

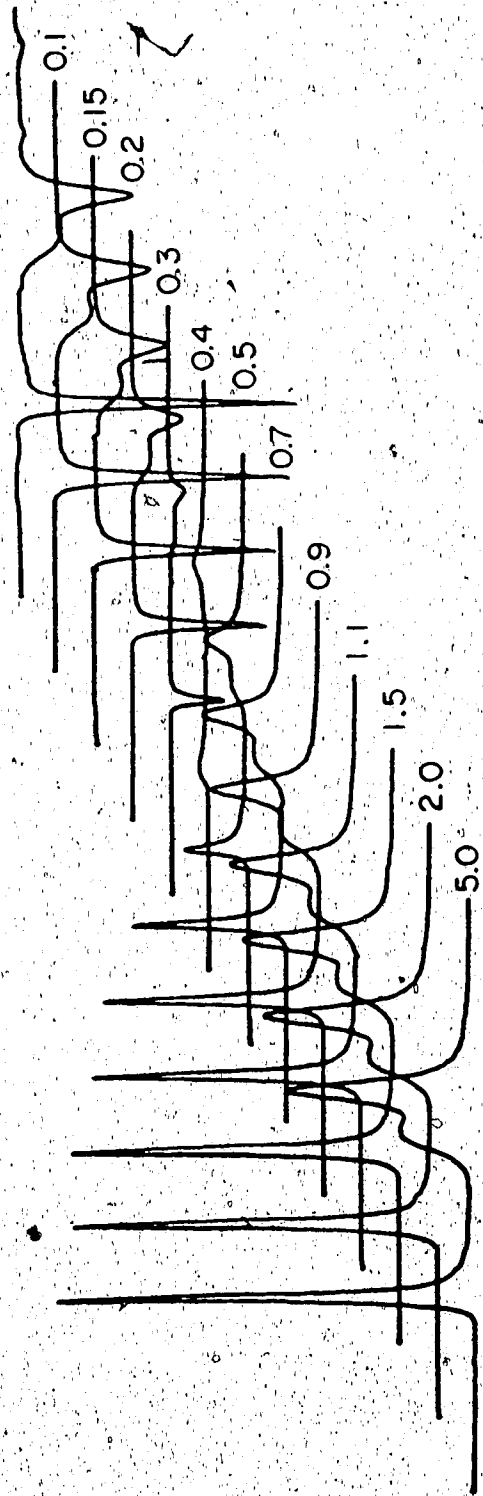


Figure 6. Spectra obtained at different t_1 delay times of an inversion recovery experiment.

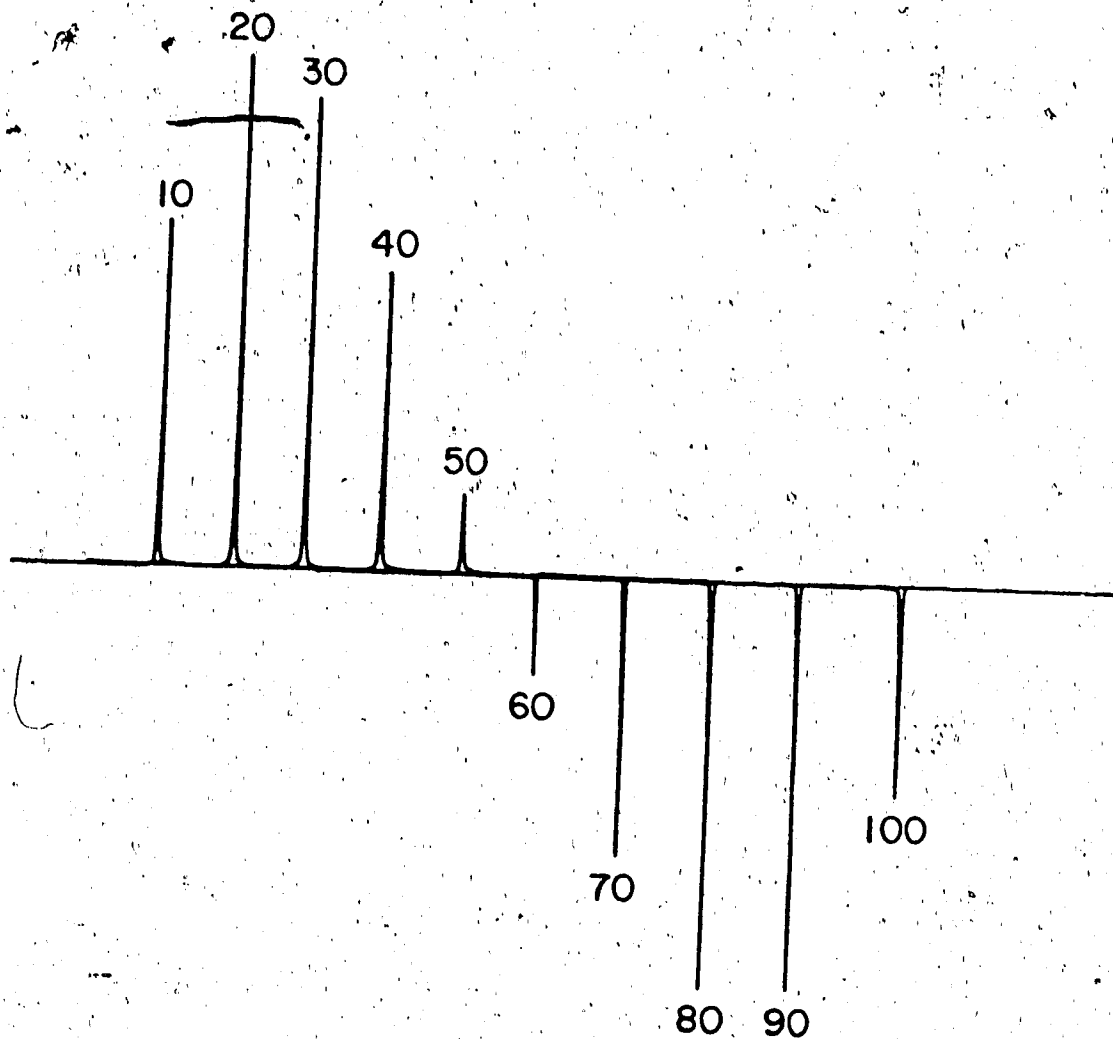


Figure 7. Determination of the 90° pulse width.
Sample: CdBr₂ (1.0 M).

μs , which correspond to a 90° pulse, and a null at $\sim 50 \mu\text{s}$, which corresponds to a 180° pulse. The procedure used involved making measurements at fairly widely spaced pulse lengths, e.g. $10 \mu\text{sec}$, to locate approximately the 180° pulse. The spectra were measured using more closely spaced pulse lengths to locate more precisely the length for a 180° pulse. The length for a 90° pulse was then taken as one half the value for a 180° pulse. Whenever concentrations of species in solution were to be determined from resonance intensities, T_1 values were first measured for the resonances of interest, and then appropriate repetition times were used.

3. Measurement of ^1H -NMR Spectra of Red Blood Cells

^1H -NMR measurements on red blood cells were performed using the spin-echo pulse sequence (90° - τ_2 - 180° - τ_2 -acquisition). From the ^1H -NMR point of view, the erythrocyte is a complicated sample; it is made up of a very large number of compounds, most of which contain hydrogen, and signals are obtained simultaneously for all of these compounds. There is some spreading of resonances due to chemical shift dispersion, however the ^1H chemical shift range is small and thus there is extensive overlap. The result is a spectrum which consists of a broad, rather featureless envelope of resonances (Figure 8A). The majority of the resonance intensity in Figure 8A is from the

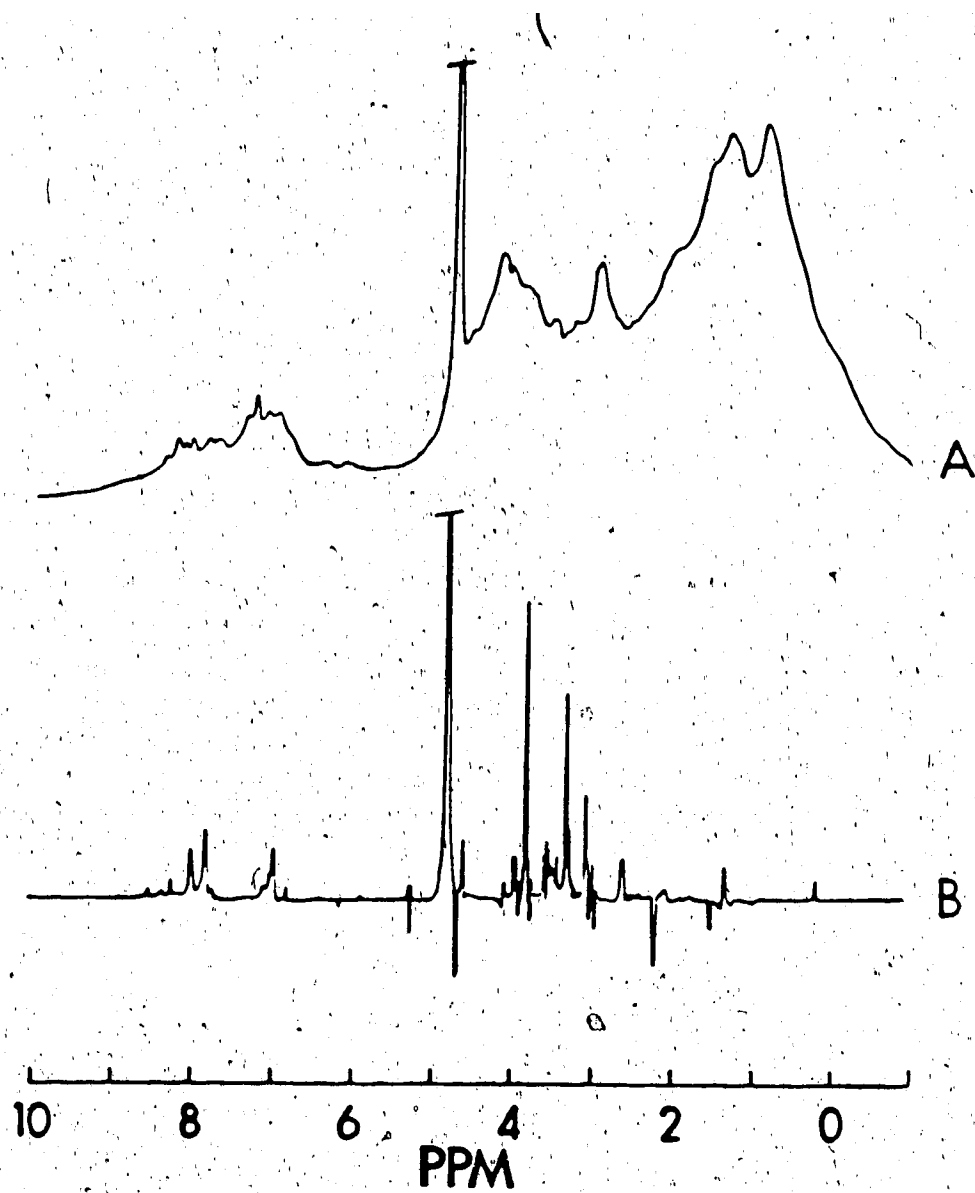


Figure 8. Single pulse and spin-echo spectra of red blood cells. [Reproduced with permission from D.L. Rabenstein, *J. Biochem. Biophys. Methods*, **9**, 277 (1984)].

^1H nuclei of hemoglobin. Hemoglobin is present at the 5 mM level in erythrocytes and, with a molecular weight of 68000, the concentration of hemoglobin ^1H nuclei is much larger than that of the smaller molecules in the erythrocytes. To observe resonances from the small molecules, those from hemoglobin must be suppressed or eliminated. Two methods have been used to accomplish this: one is based on the transfer of saturation throughout the hemoglobin proton spin system by cross relaxation [61], while the other takes advantage of differences in the spin-spin relaxation times of protons in large and small molecules [62,65]. The spin-echo Fourier transform NMR method belongs to the latter category. With this method the entire hemoglobin envelope can be partially or completely eliminated [62,64,65].

The spin-echo pulse sequence consists of a 90° pulse, a delay period of length τ_2 , a 180° pulse, a second delay of length τ_2 , at the end of which a free induction decay is collected (Figure 9A). The behavior of the nuclear magnetization during this pulse sequence is depicted in Figure 9B. Starting with the equilibrium net magnetization M_0 , the 90° pulse rotates M_0 through 90° around the x' axis and generates a component of magnetization in the $x'y'$ plane ($M_{x'y'}$). During the first delay period of length τ_2 , $M_{x'y'}$ decays due to spin-spin relaxation and magnetic field inhomogeneity. The 180° pulse rotates $M_{x'y'}$ through 180° around the x' axis, and then during the following delay the magne-

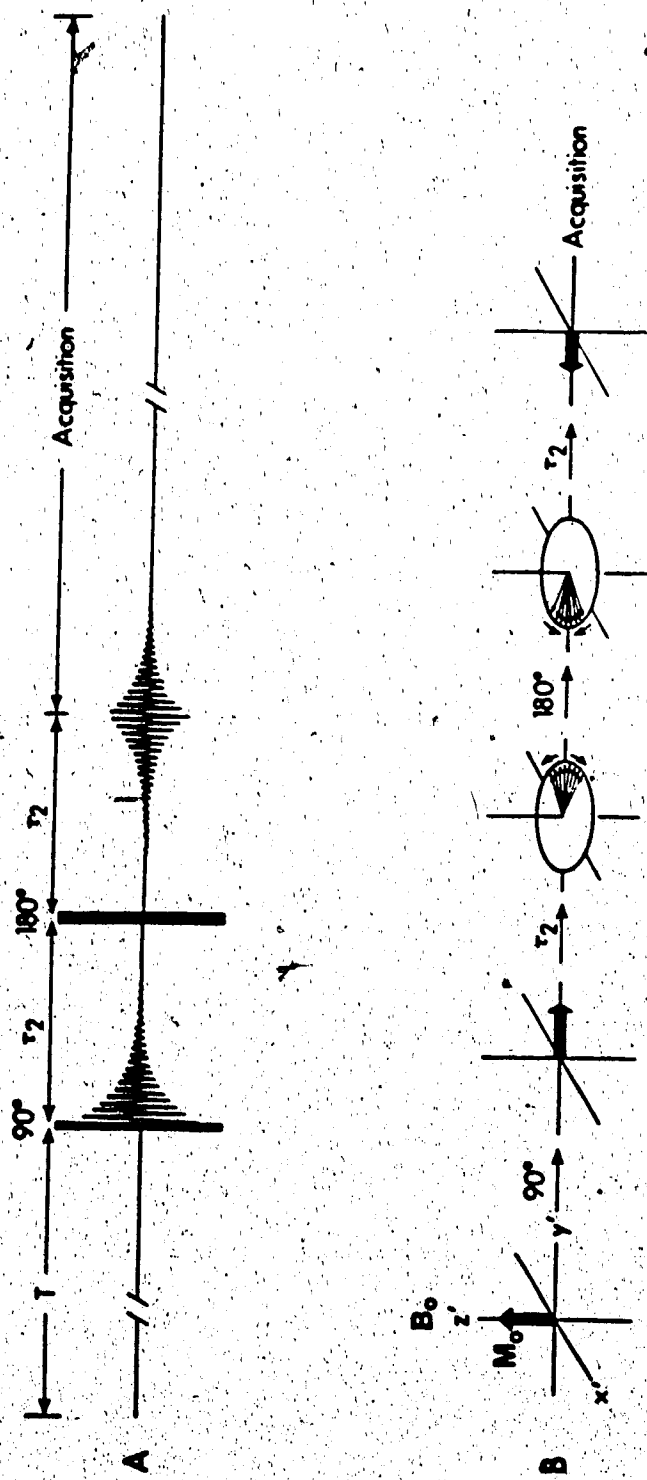


Figure 9. Pulse sequence and behavior of the magnetization during a spin-echo experiment.

tization which has spread out due to the magnetic field inhomogeneity is refocussed. The result is that $M_x'y'$ reforms (an echo) during the second delay, reaching a maximum at time $2\tau_2$ after the 90° pulse. The intensity of the echo at time $2\tau_2$ is given by the equation

$$I_{2\tau_2} = I_0(\exp((-2\tau_2/T_2) - (2D\gamma^2G^2\tau_2^3/3)))f(J) \quad (6)$$

where γ is the magnetogyric ratio, D the diffusion coefficient, G the magnetic field gradient across the sample and T_2 the spin-spin relaxation time. $f(J)$ accounts for modulations of resonances in homonuclear spin coupled multiplets. The second term in the exponent accounts for incomplete refocussing due to diffusion of molecules during the two delay periods to regions where the magnetic field is different. If diffusion is negligible, this term can be ignored and the intensity of the echo depends on T_2 and $2\tau_2$ as shown in Figure 10. It is obvious from this diagram that resonances from protons having short T_2 values (e.g., resonances from hemoglobin protons) can be selectively eliminated by making τ_2 long enough. Figure 8B shows a spectrum of packed erythrocytes measured by the spin-echo Fourier transform method using a τ_2 of 60 msec. With this delay time, the hemoglobin resonances are completely eliminated from the 0-6 ppm region; the spectrum consists of a number of sharp resonances from small molecules in the erythrocyte. The spectrum is also characterized by positive, negative

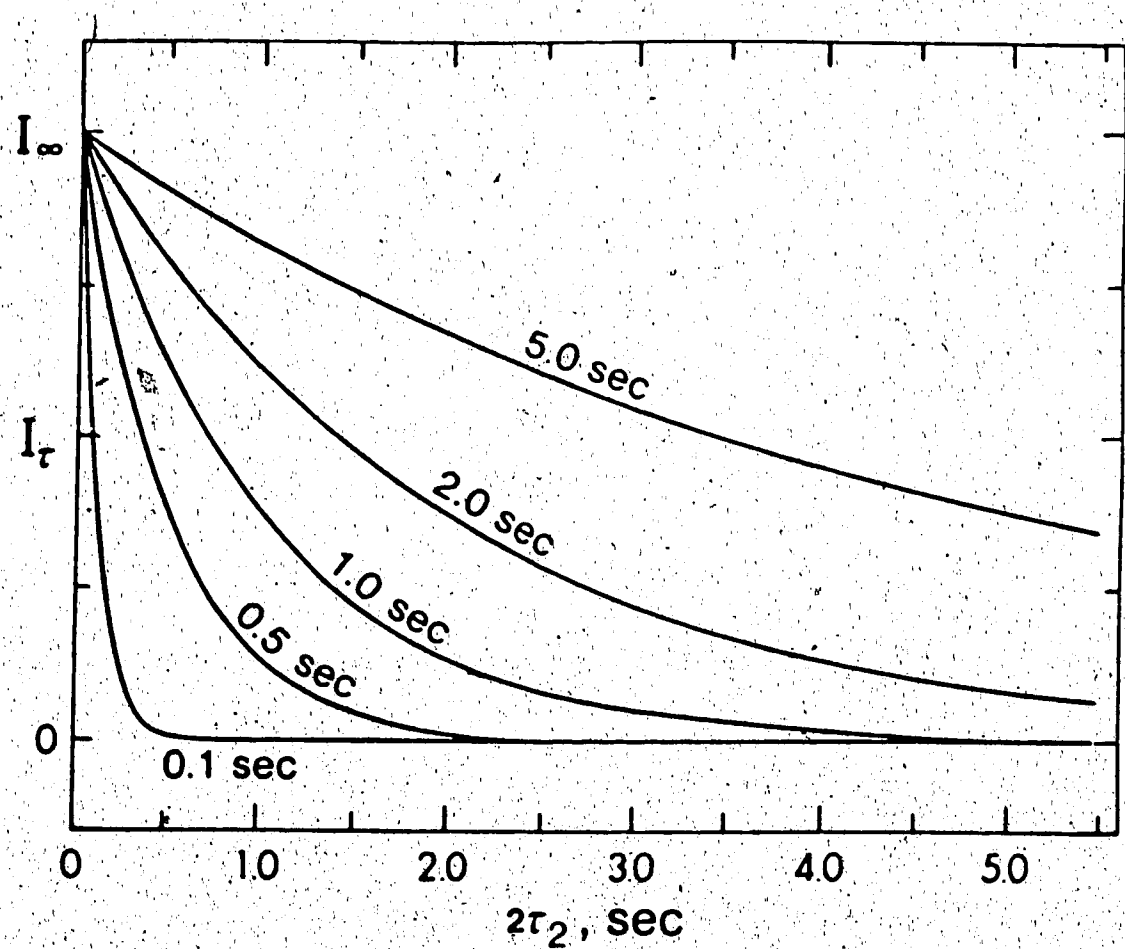


Figure 10. Intensity of resonances having T_2 values of 0.1, 0.5, 1, 2 and 5 sec in the spin-echo spectra measured as a function of τ_2 . [Reproduced with permission from D.L. Rabenstein, *J. Biochem. Biophys. Methods*, 9, 277 (1984)].

and out-of-phase resonances for the components of multiplet patterns due to homonuclear spin-spin coupling [65,66]. The phase modulation is caused by the 180° pulse in the spin echo pulse sequence; the 180° pulse changes the spin states of the nuclei which cause the multiplet structure, and thus the individual components of a multiplet pattern precess at different frequencies during the two delay periods.

F. Calibration Curve for Quantitative ^{113}Cd NMR

To completely characterize the Cd^{2+} -GSH system by ^{113}Cd NMR, a question to be addressed was that of exchange and its consequences already mentioned in the introductory chapter. When resonance(s) were observed in the ^{113}Cd NMR spectrum, it was necessary to know if all the cadmium in solution was represented by the observed signal(s) in order to assess the extent to which exchange had affected the spectrum. To determine the relative concentrations of species under two or more resonances, the previous question must first be answered as well.

A common procedure used in NMR spectroscopy to determine an unknown concentration of a given compound is to add a compound of known concentration and compare the intensities of the resonances due to the two compounds. The two resonances must be well resolved and the reference compound should not interfere in ways which would affect the inten-

sity of the compound of interest (e.g., through a reaction). The latter condition can not be met for the present study. If a cadmium compound is added to a solution of cadmium complex(es) of glutathione for example, it will interfere and disturb the equilibria already established. This problem was solved by placing the reference compound in a concentric capillary separate from the solution of interest.

Because the volumes of the reference and sample solutions were different, it was necessary to use a calibration curve to determine unknown concentrations. The calibration curve was prepared by measuring the ratio of the intensities of the resonances from the reference and standard solutions.

To select the standard and reference compounds, the estimates of T_1 values and the chemical shifts of a number of cadmium compounds were measured; the results are given in Table 1. $\text{Cd}(\text{NO}_3)_2$ at a concentration of $\sim 1.5 \text{ M}$ was selected as the reference compound because its resonance is well separated from those of the other compounds. CdCl_2 was chosen as the standard compound because it had the shortest T_1 of 3.6 sec. Even with the latter T_1 , a repetition time of at least 18 seconds was required. To reduce this time, a relaxation agent was employed. The nitrate salt of gadolinium was added to solutions of CdCl_2 having concentrations within the range to be used in establishing the calibration curve, and the T_1 of the resonance due to CdCl_2 determined

Table 1. Chemical shifts and T_1 's of selected cadmium compounds.

Compounds	Chemical shift (ppm)	T_1 (seconds)
1 $\text{Cd}(\text{NO}_3)_2$ (1.5 M)	-30.6	>13
2 CdCl_2 (0.18 M)	62.8	>3.6
3 CdCl_2 (0.10 M)	54.2	
4 CdCl_2 (0.04 M)	42.1	
5 CdBr_2 (1.00 M)	107.7	>12.0
6 CdI_2 (1.00 M)	62.8	>14.5

90° pulse width = 23 μs

using the inversion recovery experiment. Values obtained are listed in Table 2. A concentration of 0.05 M Gd^{3+} proved sufficient; the T_1 for a 0.2 M $CdCl_2$ solution was reduced from ~6 seconds to 0.25 sec from 0.001 M to 0.05 M of Gd^{3+} . The longest T_1 measured in the presence of 0.05 M Gd^{3+} was 0.33 sec from a 0.05 M $CdCl_2$ solution, for which a repetition time of 1.65 sec would be sufficient. However, a repetition time of 2.39 sec was used to meet the T_1 requirement for the longest T_1 (0.44 sec) measured for the resonances due to cadmium-glutathione complexes.

Solutions containing varying concentrations of $CdCl_2$ (0.06 to 0.16 M) and 0.05 M Gd^{3+} were used for the preparation of the calibration curve. Two milliliters of $CdCl_2$ solution were transferred to 10 mm NMR tubes. A melting point capillary (10 cm length, 2 mm external diameter) containing 1.5 M $Cd(NO_3)_2$ was positioned in the 10 mm NMR tube with two teflon spacers. The spacers were cut from a teflon sheet of about 2 mm thickness. A length of thin teflon tubing was fitted over the upper end of the capillary to remove the capillary from the tube. The same capillary was used for all experiments. The intensities of the integrals of the two signals were measured and their ratio (I_S/I_R) plotted against the concentration of $CdCl_2$ (Figure 11). To obtain unknown concentrations from this calibration curve, the capillary containing the reference was to be placed in the sample under investigation and the

Table 2. The effect of gadolinium on the spin-lattice relaxation times of ^{113}Cd in CdCl_2 solutions.

$[\text{CdCl}_2]$ (M)	$[\text{Gd}(\text{NO}_3)_3]$ (M)	T_1 (seconds)
0.20	0.001	~6
0.20	0.010	~1
0.20	0.05	.25 sec
0.10	0.05	.28 sec
0.05	0.05	.33 sec

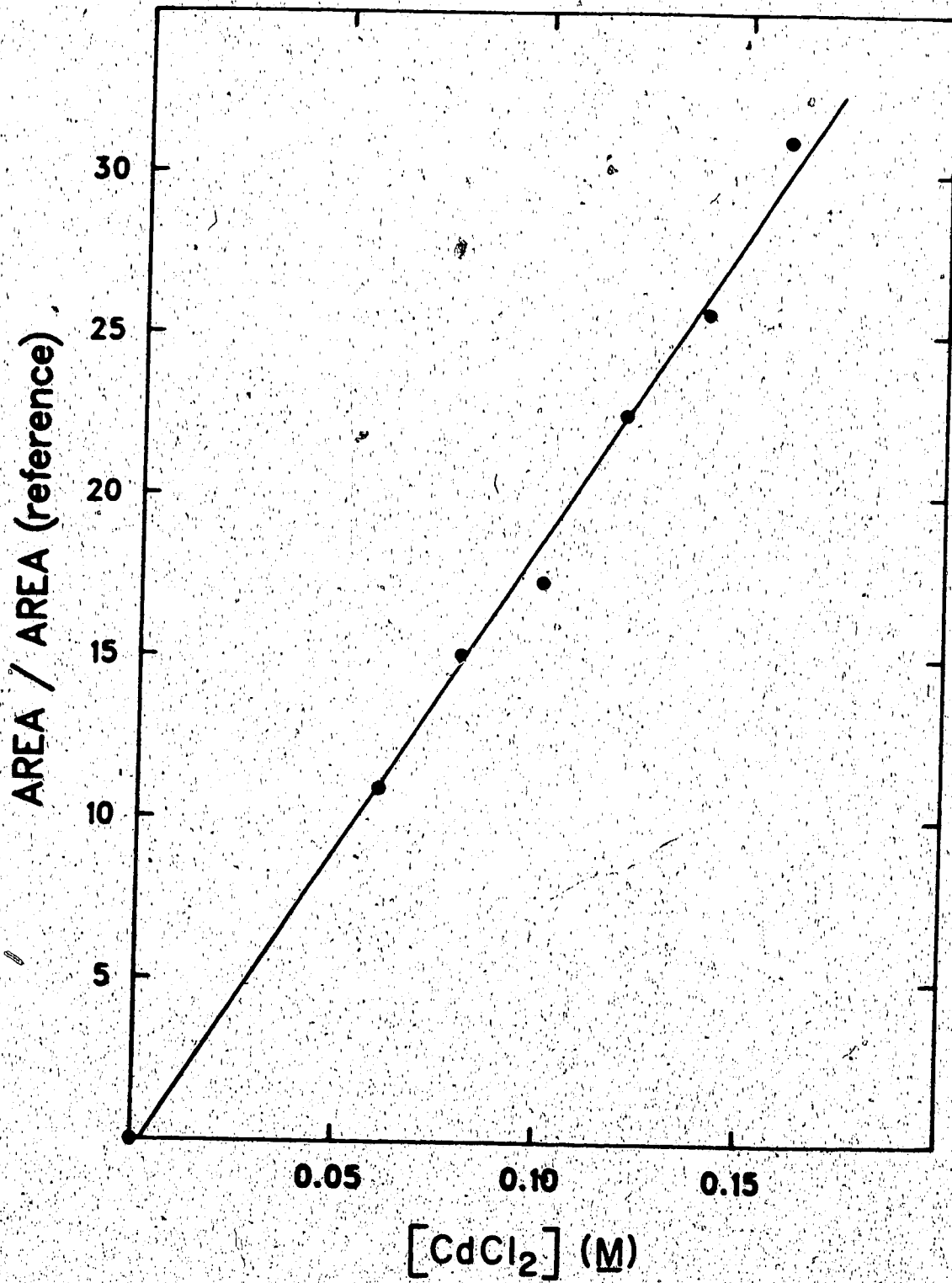


Figure 11. Calibration curve for Cd²⁺ species.

ratio I_u/I_r where I_u is the intensity of a signal of unknown concentration was measured. With this ratio, the concentration was read from the calibration curve.

G. Non-Linear Least Squares Calculations

The non-linear least squares program, Kinet, has been used to obtain parameters from experimental data in this thesis. Kinet is a general purpose curve-fitting program developed by Dye and Nicely [67]. Kinet fits data by varying estimates of unknown parameters, so as to minimize the sums of the squares of deviations of experimental values from calculated values. A subroutine (EQN in the program) must be provided, which defines the known experimental variables, constants and unknowns. The equations in the subroutine are derived from an equilibrium model if one is solving for formation, dissociation or equilibrium constants. Data files were created using a program called PIDEK, which puts data in a format suitable for Kinet. Data files included the experimental variables, e.g., chemical shift, pH, concentration, known constants and estimates of the unknown parameters. Results from Kinet are reported with a linear estimate of the standard deviation which indicates the quality of the fit. A multicorrelation factor, which is a measure of how strongly the parameters are "coupled", is listed as part of the output when more than one unknown is evaluated.

¹H NMR STUDIES OF MIXED LIGAND COMPLEXES OF CADMIUM

A. Introduction

As discussed in Chapter I, cadmium can form complexes having coordination numbers of four, six or even larger. If cadmium combines with a ligand having fewer donor groups, the remaining coordination sites on cadmium can be occupied by solvent molecules or by other ligands to form mixed ligand complexes. Biological molecules which might complex cadmium and thus be of importance in cadmium toxicology, generally either do not have a sufficient number of donor groups to saturate the coordination sites of cadmium, or the donor groups can not simultaneously coordinate to cadmium. For example, it was discussed in Chapter I that ¹H NMR measurements suggested that a ternary complex of cadmium with glutathione (GSH) and hemoglobin is one of the species formed when cadmium is present in human erythrocytes.

Although GSH is potentially a hexadentate ligand with its two carboxylate groups, an amino group, a sulfhydryl group and two peptide groups (Figure 12), the arrangement of the donor groups is such that they can not all simultaneously coordinate to a metal ion.

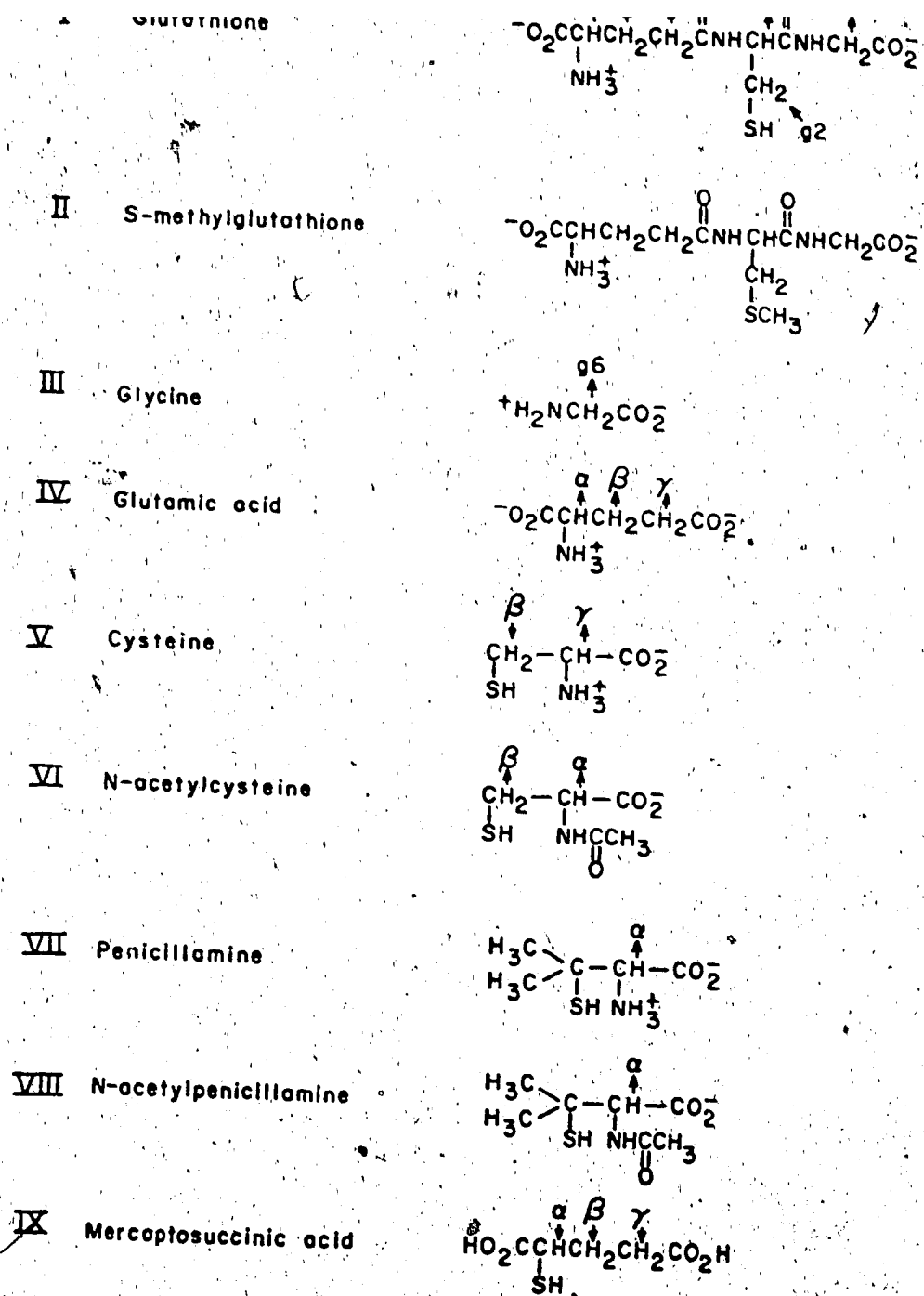
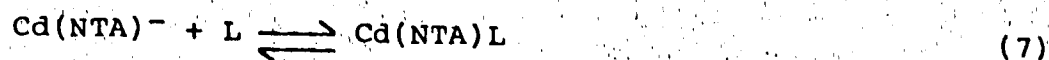


Figure 12. Names and structures of secondary ligands used in the study of Cd(NTA)L mixed ligand complexes.

of mixed ligand complexes involving Cd^{2+} are presented. The model system investigated involves Cd^{2+} complexed by nitrilotriacetic acid (NTA) as the primary ligand and GSH as well as a series of ligands which contain carboxylate, amino and thiol donor groups as secondary ligand (L). The objective is to characterize the formation of mixed ligand complexes involving Cd^{2+} and GSH. NTA was chosen as the primary ligand because it forms a stable 1 to 1 complex with Cd^{2+} in aqueous solutions which contain equimolar amounts of Cd^{2+} and NTA above pH 4. The $\text{Cd}(\text{NTA})^-$ complex has been the subject of several investigations, including the measurement of its formation constant. The following values have been reported for the logarithm of the formation constant ($\log K_f$): 9.8 [73], 9.2 [74] and 9.4 [75]. In the structure generally accepted for $\text{Cd}(\text{NTA})^-$, the tetradentate ligand occupies four of the six coordination sites in a cis configuration as shown in Figure 1. The remaining two positions may be occupied by a secondary ligand with the formation of mixed complexes $\text{Cd}(\text{NTA})\text{L}$.

The use of NTA as the primary ligand simplifies to a great extent the chemistry to be studied. Because of its large formation constant, essentially all the Cd^{2+} in a solution containing equimolar concentrations of Cd^{2+} and NTA will be present as $\text{Cd}(\text{NTA})^-$, which reduces the complexation equilibrium involved in the formation of the mixed $\text{Cd}(\text{NTA})\text{L}$



$$K_f = \frac{[\text{Cd(NTA)L}]}{[\text{Cd(NTA)}^-][\text{L}]} \quad (8)$$

where L represents the ligand with its donor groups deprotonated.

In the results described in this chapter, $^1\text{H-NMR}$ has been used to monitor both NTA and the secondary ligand for a range of solution conditions. From these data, formation constants, as defined by equation 8, have been determined for several Cd(NTA)L complexes. The secondary ligands which were studied in this research, and their structures, are given in Figure 12, with assignments of their protons for future use in the text. These ligands were chosen as models for the various potential coordination groups of glutathione. For example, glycine (gly), glutamic acid (glu) and cysteine (cys) were chosen because they are the constituent amino acids of GSH. Furthermore, glycine serves as a model for the free amino and α -carboxylate groups of the γ -glutamyl residue of GSH. The interaction with these two donor groups was further studied using the S-methylated derivative of GSH. Penicillamine (PSH), N-acetylpenicillamine (N-PSH), mercaptosuccinic acid (MSA) and N-acetylcysteine (N-Cys) were studied to characterize the interaction of

latter ligands are also of interest because they were shown, in studies on Cd^{2+} in red blood cells, to be effective at displacing Cd^{2+} from its complex with GSH and hemoglobin [33].

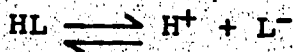
A detailed analysis of the ^1H -NMR measurements is given for a wide range of pH and secondary ligand concentration. Formation and equilibrium constants are determined from chemical shift and intensity measurements. In some systems, for example those involving thiol ligands, not only do mixed complexes form but in addition, the thiol ligand can displace NTA as a result of the large formation constants of the $\text{Cd}(\text{thiol})$ complexes. The displacement of NTA is accompanied by the formation of complexes of the type CdL_n . The formation constants for the latter complexes were also determined from ^1H -NMR data. Evidence for the displacement of NTA from the $\text{Cd}(\text{NTA})^-$ complex could be obtained directly through the appearance in the ^1H -NMR spectrum of a separate resonance for free NTA and the disappearance of the doublet which is due to coupling of the NTA protons of $\text{Cd}(\text{NTA})^-$ to the 25% of the cadmium which is ^{111}Cd and ^{113}Cd .

In order to calculate the formation constants of the various complexes, the acid dissociation constants of the ligands, under the conditions used in this study, were required. They were determined for all ligands from ^1H -NMR chemical shift measurements. Also, the formation constant

... complex was redetermined under the same conditions; this constant was needed to evaluate the formation constants in those systems where the secondary ligand displaced NTA with the formation of CdL_n type complexes.

B. Determination of Ligand Acid Dissociation Constants

The acid dissociation constants of the ligands are required in the evaluation of the formation constants of their complexes. They were obtained from 1H -NMR chemical shift data which were measured as a function of pH for each of the ligands. For all the ligands studied, exchange of ligand between protonated and deprotonated forms is sufficiently fast on the NMR time scale that only exchange-averaged resonances are observed for the ligand protons. In those pH regions where an acidic group is being titrated and thus both protonated and deprotonated forms are present, the observed chemical shift for a particular ligand proton is the sum of the chemical shifts of the protonated and deprotonated species weighted according to their fractional concentrations. For resonances which are affected by ionization of a single acidic group, as represented by equations 9 and 10, the chemical shift δ_{obs} is given by equation 11 where



(9)

[HL]

(10)

$$\delta_{\text{obs}} = \delta_{\text{HL}} P_{\text{HL}} + \delta_{\text{L}^-} P_{\text{L}^-} \quad (11)$$

δ_{HL} and δ_{L^-} are the chemical shifts of the protonated (HL) and deprotonated (L^-) forms, and P_{HL} and P_{L^-} are the fractional concentrations of HL and L^- . P_{HL} and P_{L^-} depend on the pH of the solution and the pK_a of the group being ionized as expressed in equations 12 and 13.

$$P_{\text{HL}} = \frac{[\text{HL}]}{[\text{HL}] + [\text{L}^-]} = \frac{[\text{H}^+]}{K_a + [\text{H}^+]} \quad (12)$$

$$P_{\text{L}^-} = \frac{[\text{L}^-]}{[\text{HL}] + [\text{L}^-]} = \frac{K_a}{K_a + [\text{H}^+]} \quad (13)$$

Knowing that the sum of P_{HL} and P_{L^-} is unity and replacing P_{HL} with $(1 - P_{\text{L}^-})$ and P_{L^-} with $(1 - P_{\text{HL}})$ in equation 11, the following two expressions can be derived:

$$P_{\text{HL}} = \frac{\delta_{\text{obs}} - \delta_{\text{L}^-}}{\delta_{\text{HL}} - \delta_{\text{L}^-}} \quad (14)$$

$$P_{\text{L}^-} = \frac{\delta_{\text{obs}} - \delta_{\text{HL}}}{\delta_{\text{L}^-} - \delta_{\text{HL}}} \quad (15)$$

These equations show that the fractions may be obtained from the observed chemical shift. If δ_{HL} and δ_{L^-} could be obtained from the chemical shift versus pH data, P_{L^-} and P_{HL} were calculated directly from δ_{obs} . With these values, K_a was calculated using the relation:

$$K_a = \frac{[H^+][L^-]}{[HL]} = \frac{[H^+]}{P_{HL}} \quad (16)$$

If δ_{HL} and δ_{L^-} could not be obtained directly from the data, for example, due to overlap of the resonance for HL or L with another resonance, they were determined simultaneously with K_a by fitting the chemical shift versus pH data with KINET. The model to which the chemical shift data were fit for a monoprotic acid or for a resonance whose chemical shift is affected by ionization of a single acidic group is described by equation 17, which is obtained by substitution of equations 12 and 13 into equation 11.

$$\delta_{obs} = \frac{\delta_{HL} [H^+] + \delta_{L^-} K_a}{K_a + [H^+]} \quad (17)$$

The acid-base equilibria for a diprotic acid, H_2L , are described by equations 18-21



$$K_{a1} = \frac{[HL^-][H^+]}{[H_2L]} \quad (19)$$



$$K_{a2} = \frac{[L^{2-}][H^+]}{[HL^-]} \quad (21)$$

When the ionization of the two acidic groups affects the chemical shift of the resonance being monitored, the observed chemical shift will be the sum of the chemical shifts of the three species H_2L , HL^- and L^{2-} , weighted according to their fractional concentrations.

$$\delta_{obs} = \delta_{H_2L} P_{H_2L} + \delta_{HL^-} P_{HL^-} + \delta_{L^{2-}} P_{L^{2-}} \quad (22)$$

where P_{H_2L} , P_{HL^-} and $P_{L^{2-}}$ as defined by equations 23-25.

$$P_{H_2L} = \frac{[H_2L]}{[H_2L] + [HL^-] + [L^{2-}]}$$

$$= \frac{[H^+]^2}{[H^+]^2 + K_{a1}[H^+] + K_{a1}K_{a2}} \quad (23)$$

$$P_{HL^-} = \frac{[HL^-]}{[H_2L] + [HL^-] + [L^{2-}]}$$

$$= \frac{K_{a1}[H^+]}{[H^+]^2 + K_{a1}[H^+] + K_{a1}K_{a2}} \quad (24)$$

$$P_{L^{2-}} = \frac{[L^{2-}]}{[H_2L] + [HL^-] + [L^{2-}]}$$

$$= \frac{K_{a1}K_{a2}}{[H^+]^2 + K_{a1}[H^+] + K_{a1}K_{a2}} \quad (25)$$

Following the steps described in the derivation of equation 17, equation 22 is transformed to equation 26.

$$\delta_{\text{obs}} = \frac{\delta_{\text{H}_2\text{L}}[\text{H}^+]^2 + \delta_{\text{HL}^-}[\text{H}^+]K_{\text{a}1} + \delta_{\text{L}^{2-}}K_{\text{a}1}K_{\text{a}2}}{[\text{H}^+]^2 + [\text{H}^+]K_{\text{a}1} + K_{\text{a}1}K_{\text{a}2}} \quad (26)$$

This equation expresses the observed chemical shift for the resonance of a diprotic acid in terms of the acid dissociation constants of the two groups and the pH. $K_{\text{a}1}$ and $K_{\text{a}2}$ were obtained by fitting chemical shift versus pH data to this equation with the program KINET. Chemical shifts $\delta_{\text{H}_2\text{L}}$, δ_{HL^-} and $\delta_{\text{L}^{2-}}$ were also treated as unknowns. This was more critical for δ_{HL^-} because it could not be obtained directly from titration curves due to superimposition of ionizations. The treatment for a triprotic acid is similar.

C. Determination of Formation Constants of Cd(NTA)_nL
Mixed Complexes

Depending on the stability of the CdL complex, addition of L to a solution containing Cd(NTA)⁻ can result in formation of Cd(NTA)L only or in displacement of NTA with formation of CdL_n type complexes as well as the mixed complex. The methods used to evaluate the formation constants of the mixed complexes from NMR data were different in the two cases.

1. Formation of Only the Mixed Ligand Complex

The ligand L reacts with $\text{Cd}(\text{NTA})^-$ to form $\text{Cd}(\text{NTA})\text{L}$ as described by equations 27 and 28,



$$K_f = \frac{[\text{Cd}(\text{NTA})\text{L}]}{[\text{Cd}(\text{NTA})^-][\text{L}]} \quad (28)$$

It was found that the chemical shifts of resonances from L change more upon formation of $\text{Cd}(\text{NTA})\text{L}$ from $\text{Cd}(\text{NTA})^-$ and L than does the resonance from NTA. Thus, changes in the chemical shifts of resonances from L were used for the evaluation of formation constants of the $\text{Cd}(\text{NTA})\text{L}$ complexes. The exchange of L between the free form and $\text{Cd}(\text{NTA})\text{L}$ is fast on the NMR time scale and thus only a single exchange-averaged resonance was observed. The chemical shift of the exchange-averaged resonance is given by equation 29, where f stands

$$\delta_{\text{obs}} = P_f \delta_f + P_c \delta_c \quad (29)$$

for free ligand (protonated and deprotonated) and c for the complex ligand ($\text{Cd}(\text{NTA})\text{L}$). The fractional concentrations P_f and P_c can be expressed in terms of the acidity constants, the formation constant and the pH. By substituting these expressions for the fractional concentration into equation 29, a model equation is obtained to which the chemical shift data can be fitted to evaluate the formation constant. To

illustrate the procedure, the derivation of the model equation for the case where the ligand is a monoprotic acid will be described in detail. For such a system, the observed chemical shift is given by

$$\delta_{\text{obs}} = \delta_{\text{HL}} P_{\text{HL}} + \delta_{\text{L}} P_{\text{L}} + \delta_{\text{C}} P_{\text{C}} \quad (30)$$

The total concentration of the secondary ligand and of cadmium are given by

$$L_t = [\text{HL}] + [\text{L}] + [\text{Cd}(\text{NTA})\text{L}] \quad (31)$$

$$\text{Cd}_t = [\text{Cd}(\text{NTA})] + [\text{Cd}(\text{NTA})\text{L}] \quad (32)$$

The terms $[\text{HL}]$ and $[\text{Cd}(\text{NTA})\text{L}]$ can be substituted by

$$[\text{HL}] = \frac{[\text{H}^+][\text{L}]}{K_a} \quad (33)$$

and

$$[\text{Cd}(\text{NTA})\text{L}] = K_f [\text{Cd}(\text{NTA})][\text{L}] \quad (34)$$

Rearrangement of equation 32 to express $[\text{Cd}(\text{NTA})]$ in terms of Cd_t , $[\text{L}]$ and K_f yields:

$$[\text{Cd}(\text{NTA})] = \frac{\text{Cd}_t}{1 + K_f[\text{L}]} \quad (35)$$

Substitution of equations 33, 34 and 35 into equation 31 leads to

$$([H^+]K_f + K_aK_f) [L]^2 +$$

$$([H^+] + K_a + Cd_tK_fK_a + L_tK_aK_f) [L] - L_tK_a = 0 \quad (36)$$

This quadratic equation in terms of [L] was solved by a subroutine (DTRMI, from the scientific subroutines library of the University of Alberta) incorporated in the KINET program. This subroutine uses the estimates of K_f and the known parameters (H^+ , K_a , Cd_t , L_t) to calculate [L]. With this estimate of [L], the three fractions needed to calculate a value for δ_{obs} with equation 30 and the concentration of the species are deduced as follows:

$$P_L = \frac{[L]}{L_t} \quad (37)$$

$$P_{HL} = \frac{[HL]}{L_t} = \frac{[H^+][L]}{K_a L_t} \quad (38)$$

$$[HL] = P_{HL} \times L_t$$

$$P_C = \frac{[Cd(NTA)L]}{L_t} = \frac{L_t - [HL] - [L]}{L_t} \quad (39)$$

$$[Cd(NTA)L] = P_C \times L_t$$

The procedure for obtaining K_f from the experimental chemical shift data with KINET involves first giving the program estimated values for K_f and δ_c . With these estimates, the program then calculates for each data point P_L , P_{HL} and P_C according to equations 37-39, and finally these values are used to calculate δ_{obs} . It then uses these values for [L] to calculate the chemical shift substituting equations 37 to

39 in equation 30. K_a , δ_L and δ_{HL} obtained as detailed in the previous section are provided as known parameters. Residuals for each point, given by equation 40 where

$$\text{Residual} = \delta_{\text{calc}} - \delta_{\text{obs}} \quad (40)$$

δ_{calc} is the calculated chemical shift, are calculated. KINET will continue to vary the estimates of K_f and δ_c so as to minimize the sum of the squares of the residuals. Until the sum of the squares of the residuals is minimized, the previously described procedure is repeated to calculate $[L]$ and δ_{calc} .

2. Case of the Formation of CdL and Cd(NTA)L

For each of the thiol-containing ligands investigated, at least two reactions occurred which could be detected by changes of the NTA resonances. They were the formation of Cd(NTA)L, as described by equation 27, and the displacement of NTA by the secondary ligand as described by equations 41 and 42.



$$K_{\text{eq}} = \frac{[\text{CdL}][\text{NTA}^{3-}]}{[\text{Cd(NTA)}^-][L]} \quad (42)$$

The formation constant of the species CdL, K_{CdL} , as defined in equations 43 and 44, can be obtained from K_{eq} if

the formation constant of $\text{Cd}(\text{NTA})^-$ is known, by combining equations 42 and 45 to yield 46.



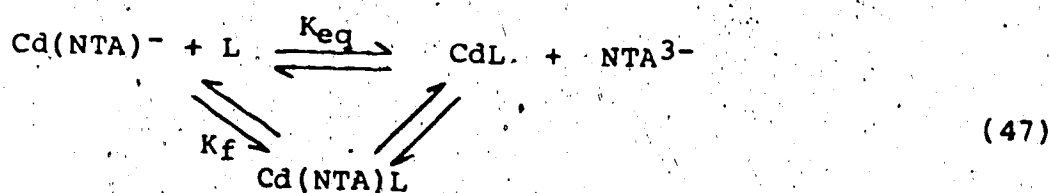
$$K_{\text{CdL}} = \frac{[\text{CdL}]}{[\text{Cd}^{2+}][\text{L}]} \quad (44)$$

$$K_{\text{Cd}(\text{NTA})^-} = \frac{[\text{Cd}(\text{NTA})^-]}{[\text{Cd}^{2+}][\text{NTA}^{3-}]} \quad (45)$$

$$K_{\text{CdL}} = K_{\text{eq}} \times K_{\text{Cd}(\text{NTA})^-} \quad (46)$$

The remaining portion of this section describes the general procedure used to deduce K_f and K_{CdL} from NMR measurements.

The NMR data used in this case were obtained at a constant pH and varying the concentration of the secondary ligand or by varying the pH and keeping the concentrations constant. The following scheme describes the equilibria of the system:



K_f and K_{eq} were determined from chemical shift data, and then the formation constant of the complex CdL was calculated from K_{eq} and the formation constant of $\text{Cd}(\text{NTA})^-$. The procedure used involved determining the relative concentrations of the various species from intensities and from the chemical shifts of resonances of free (NTA_f) and bound

NTA (NTA_b). Shown in Figure 13 is a spectrum which illustrates the changes which occur when both $\text{Cd}(\text{NTA})\text{L}$ and CdL are formed. $\text{Cd}(\text{NTA})^-$ exhibits the spectrum A, with only one resonance flanked by two satellites due to coupling of ^1H with ^{113}Cd and ^{111}Cd . Spectrum B was obtained from a mixture of $\text{Cd}(\text{NTA})^-$ and PSH. The two resonances around 1.2 ppm are due to the protons of the two methyl groups of PSH, the singlet at 3.679 ppm is due to H_α proton of PSH, the singlet at 3.80 ppm is due to free NTA and the resonance at 3.25 ppm is due to $\text{Cd}(\text{NTA})^-$ species (i.e., $\text{Cd}(\text{NTA})^-$ and $\text{Cd}(\text{NTA})\text{L}$). Exchange between the species $\text{Cd}(\text{NTA})^-$ and $\text{Cd}(\text{NTA})\text{L}$ is fast and thus an exchange averaged resonance is observed. Formation of $\text{Cd}(\text{NTA})\text{L}$ causes a shift of the $\text{Cd}(\text{NTA})^-$ resonances whereas formation of CdL results in displacement of NTA as evidenced by the appearance of the resonance due to free NTA. Relative concentrations of free and bound NTA were obtained from relative areas under the signals from free and bound NTA respectively, as described below.

$$A_t = A_f + A_b \quad (48)$$

$$P_f = \frac{A_f}{A_t} \quad (49)$$

$$[\text{NTA}]_f = P_f \times [\text{NTA}]_t \quad (50)$$

$$P_b = \frac{A_b}{A_t} \quad (51)$$



Figure 13. Spectra of (A) $\text{Cd}(\text{NTA})^-$ and (B) of a mixture of $\text{Cd}(\text{NTA})^-$ (0.02M) and PSH (0.035M) showing displacement of NTA at pH 5.5.

$$[\text{NTA}]_b = P_b \times [\text{NTA}]_t \quad (52)$$

A_t , A_f and A_b stand for total area, area under the free and area under the bound NTA resonances respectively, and P_f and P_b stand for fraction of free and bound NTA respectively, the bound NTA being the sum of $\text{Cd}(\text{NTA})^-$ and $\text{Cd}(\text{NTA})_L$.

To obtain the relative concentration of $\text{Cd}(\text{NTA})^-$ and $\text{Cd}(\text{NTA})_L$ from $[\text{NTA}]_b$, the observed exchange averaged chemical shift of bound NTA was employed. The latter chemical shift is given by:

$$\delta_{\text{obs}} = \delta_{\text{Cd}(\text{NTA})^-} P_{\text{Cd}(\text{NTA})^-} + \delta_{\text{Cd}(\text{NTA})_L} P_{\text{Cd}(\text{NTA})_L} \quad (53)$$

From the sum of the fractional concentrations

$$P_{\text{Cd}(\text{NTA})^-} + P_{\text{Cd}(\text{NTA})_L} = 1 \quad (54)$$

$P_{\text{Cd}(\text{NTA})^-}$ and $P_{\text{Cd}(\text{NTA})_L}$ are replaced alternatively in equation 53 by $1 - P_{\text{Cd}(\text{NTA})_L}$ and $1 - P_{\text{Cd}(\text{NTA})^-}$ respectively. After rearrangement, the fractional concentrations are given by equations 55 and 57 from which the concentration of species are calculated as in equations 56 and 58

$$P_{\text{Cd}(\text{NTA})^-} = \frac{\delta_{\text{obs}} - \delta_{\text{Cd}(\text{NTA})_L}}{\delta_{\text{Cd}(\text{NTA})^-} - \delta_{\text{Cd}(\text{NTA})_L}} \quad (55)$$

$$[\text{Cd}(\text{NTA})^-] = P_{\text{Cd}(\text{NTA})^-} \times [\text{NTA}]_b \quad (56)$$

$$P_{\text{Cd}(\text{NTA})_L} = \frac{\delta_{\text{obs}} - \delta_{\text{Cd}(\text{NTA})^-}}{\delta_{\text{Cd}(\text{NTA})_L} - \delta_{\text{Cd}(\text{NTA})^-}} \quad (57)$$

$$[\text{Cd}(\text{NTA})\text{L}] = P_{\text{Cd}(\text{NTA})\text{L}} \times [\text{NTA}]_D \quad (58)$$

The chemical shift of $\text{Cd}(\text{NTA})^-$ is obtained directly from a spectrum of $\text{Cd}(\text{NTA})^-$ formed in an equimolar mixture of Cd^{2+} and NTA at $\text{pH} > 4$, and is 3.162 ppm. The chemical shift of $\text{Cd}(\text{NTA})\text{L}$ is the limiting chemical shift on the curve of δ_{obs} versus total concentration of the secondary ligand L_t . The other quantity needed to calculate the formation and equilibrium constants is the concentration of the free secondary ligand, as given by:

$$L_f = L_t - [\text{CdL}] - [\text{Cd}(\text{NTA})\text{L}] \quad (59)$$

Under the conditions used in this work, ($\text{Cd}_t/\text{NTA}_t = 1$), the concentration of CdL is equal to the concentration of the free NTA according to equation 41. The concentration of free NTA can be deduced from the intensity of the resonance for free NTA. With all these concentrations, the conditional formation and equilibrium constants defined by equation 60 and 62 may be calculated. K_{eq} and K_f can then be calculated from the conditional constants using fractional concentration of reactive species (α) which are obtained from the acidity constants of NTA and the secondary ligand and the pH.

$$K_{\text{fc}} = \frac{[\text{Cd}(\text{NTA})\text{L}]}{[\text{Cd}(\text{NTA})^-][\text{L}]_f} \quad (60)$$

$$K_f = K_{\text{fc}}/\alpha_L \quad (61)$$

$$K_{eqc} = \frac{[CdL][NTA]_f}{[Cd(NTA)^-][L]_f} \quad (62)$$

$$K_{eq} = K_{eqc} \frac{\alpha_{NTA}^{3-}}{\alpha_L} \quad (63)$$

In the case of a monoprotic acid α is given by:

$$\alpha_L = \frac{K_a}{[H^+] + K_a} \quad (64)$$

A model equation was also derived to obtain K_{fc} and K_{eqc} simultaneously from the chemical shift data using Kinet. Replacing $P_{Cd(NTA)^-}$ and $P_{Cd(NTA)L}$ by equations 65 and 66, equation 53 is transformed to equation 67.

$$P_{Cd(NTA)^-} = \frac{Cd(NTA)^-}{Cd(NTA)^- + Cd(NTA)L} = \frac{1}{1 + K_{fc}[L]_f} \quad (65)$$

$$P_{Cd(NTA)L} = \frac{Cd(NTA)L}{Cd(NTA)^- + Cd(NTA)L} = \frac{K_{fc}[L]_f}{1 + K_{fc}[L]_f} \quad (66)$$

$$\delta_{obs} = \frac{\delta_{Cd(NTA)^-} + \delta_{Cd(NTA)L} K_{fc}[L]_f}{1 + K_{fc}[L]_f} \quad (67)$$

Substitution of $[L]_f$ in equation 67 by equation 68 gives the model equation used by Kinet to fit the data.

$$[L]_f = \frac{L_t}{1 + K_{eqc} \frac{[Cd(NTA)^-]}{[NTA]_f} + K_{fc}[Cd(NTA)^-]} \quad (68)$$

This expression of $[L]_f$ is obtained by replacing $[CdL]$ and $[Cd(NTA)L]$ by equations 69 and 70 in equation 59. Equations 69 and 70 are derived from equations 62 and 60 respectively.

$$[\text{CdL}] = \frac{K_{\text{egc}}[\text{Cd}(\text{NTA})^-][\text{L}]_f}{[\text{NTA}]_f} \quad (69)$$

$$[\text{Cd}(\text{NTA})\text{L}] = K_{\text{fc}}[\text{Cd}(\text{NTA})^-][\text{L}]_f \quad (70)$$

D. Results

1. Formation Constant of Cd(NTA)⁻

The formation constant of Cd(NTA)⁻ has been determined by Rabenstein and Kula using proton NMR measurements, and by others using potentiometric titrations [21,22]. Because this constant will be needed for further calculations, it was redetermined under the conditions used for this study in order to maintain self consistency in all the values to be reported and because it is needed for the determination of the formation constants of complexes.

The acid dissociation constant of the monoprotonated form of NTA, HNTA²⁻, was first determined using chemical shift measurements and the method of calculation described in Section III-B for a monoprotic acid. The ¹H-NMR spectrum of NTA is a single resonance due to the six equivalent methylene protons. The change in the chemical shift of these protons as a function of pH is shown in Figure 14. A pK_a of 9.36 was obtained from these data, along with values of 3.798 and 3.126 ppm for the chemical shifts of the monoprotonated and totally deprotonated NTA, respectively. This pK_a value agrees well with literature values of 9.32

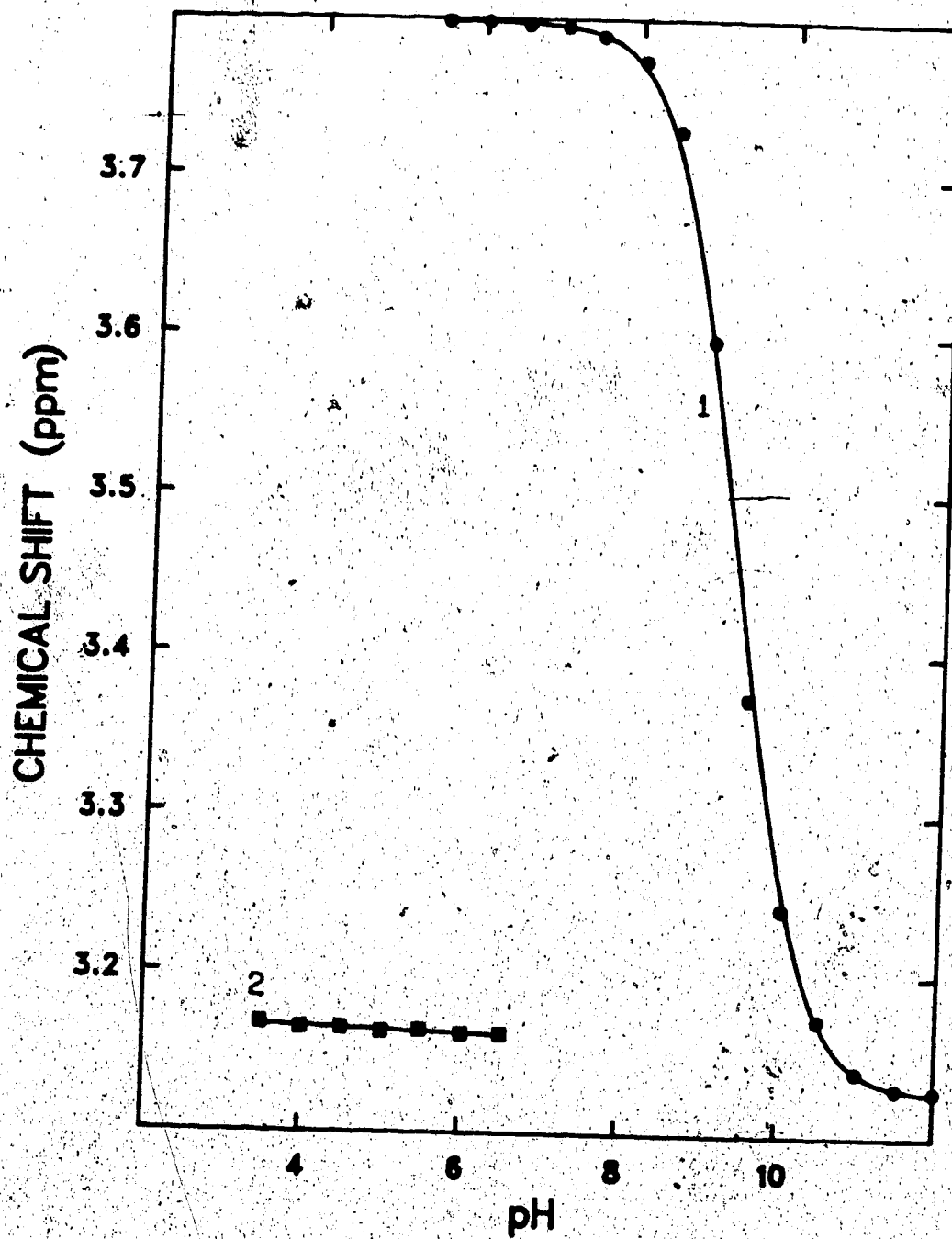


Figure 14. 1) Chemical shift titration of NTA for pK_a determination.
2) Chemical shift titration of an equimolar mixture of Cd^{2+} and NTA.

[76] and 9.4 [75]. Given the pK_a values 1.8 and 2.5 [76] for the tri- and diprotonated NTA respectively, the NHTA^{2-} and NTA^{3-} species are the most predominant forms in which NTA is present in the pH region of interest in this study. Hence, above pH 4 the three carboxylic acid groups are totally dissociated and in HNTA^{2-} the proton is on the amino group.

^1H -NMR spectra for NTA in solutions containing 0.02M Cd^{2+} and 0.02M NTA are shown as a function of pH in Figure 15. Above pH 4, a singlet resonance flanked symmetrically by two weaker satellite resonances is observed; the chemical shift of the central resonance is 3.162 ppm and remains constant above pH 4 as shown in Figure 14. This resonance is due to NTA in the $\text{Cd}(\text{NTA})^-$ complex; the satellite resonances result from spin-spin coupling of the NTA protons to the 12.7% ^{111}Cd and 12.3% ^{113}Cd . The separation of the satellite resonances in hertz is the spin-spin coupling constant (14.7 Hz). Below pH 4, NTA is not completely bound by Cd^{2+} and two resonances are observed, one around 3.16 ppm and the other at a chemical shift which is dependent on pH. The former is due to the $\text{Cd}(\text{NTA})^-$ complex while the latter resonance is due to NTA free in solution. At much lower pH, for example, pH 2.1, a broad signal is observed. In this region, the NTA is exchanging between its free and bound forms at an intermediate rate on the NMR time scale, thus causing a broad signal. The chemical shift of this signal depends on the relative amounts of free and

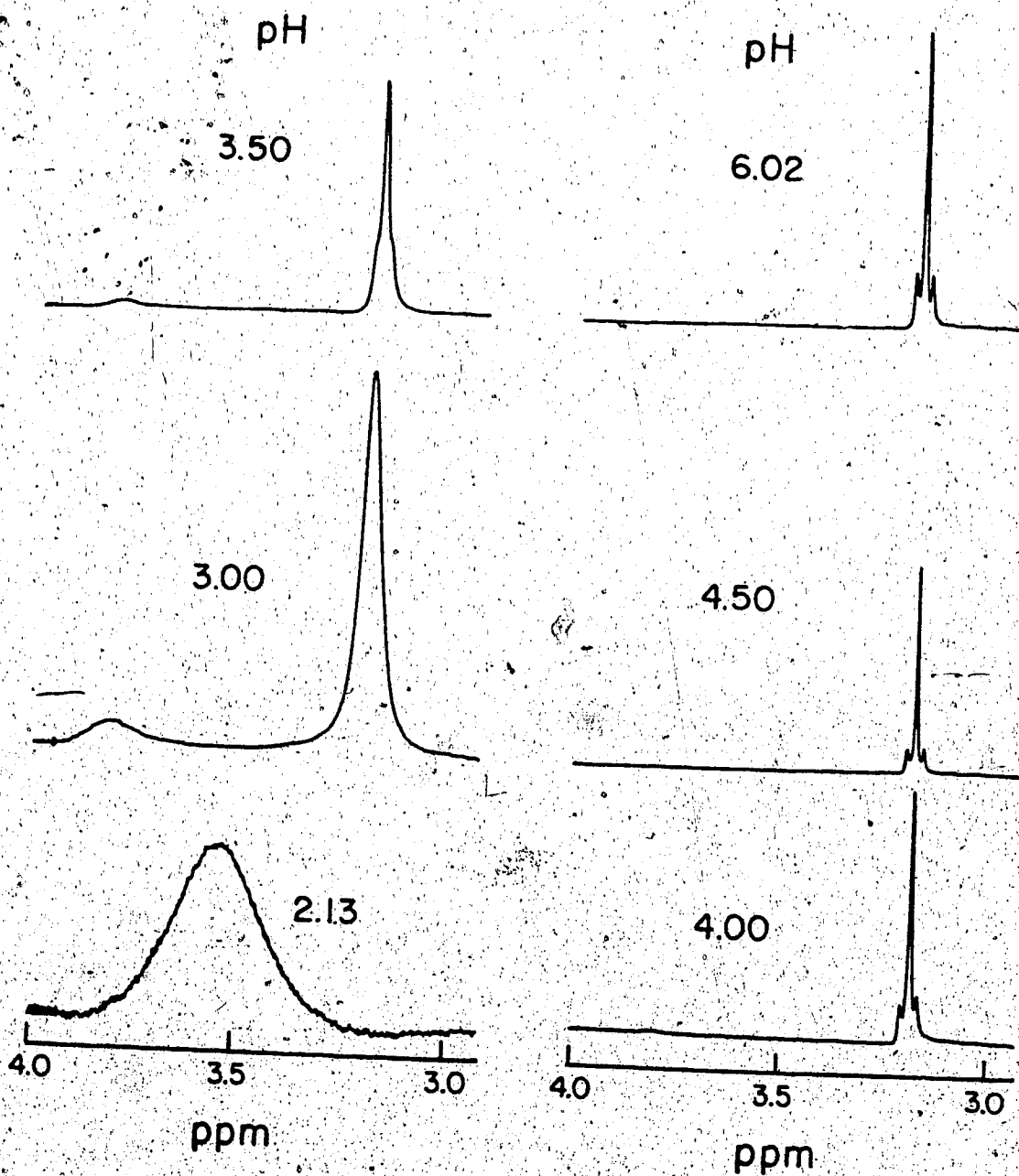
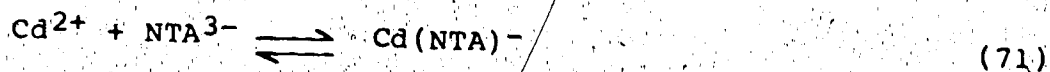


Figure 15. Spectra of titration of an equimolar mixture of Cd^{2+} and NTA. Total concentrations of Cd^{2+} and NTA = $\sim 0.02\text{M}$.

bound NTA and is located between 3.162 ppm, the chemical shift of the bound NTA, and 3.8 ppm, the chemical shift of monoprotonated free NTA, the predominant free NTA species in this pH region. To calculate the formation constant of $\text{Cd}(\text{NTA})^-$, as expressed by equations 71 and 72, NMR data were obtained in the pH region (2.5-4) where resonances are observed for both free and bound NTA.



$$K_f = \frac{[\text{Cd}(\text{NTA})^-]}{[\text{Cd}^{2+}][\text{NTA}^{3-}]} \quad (72)$$

The concentrations of free and bound NTA were obtained from resonance intensities by the following procedure. The total area under the resonance for free and bound NTA is given by equation 73.

$$A_t = A_f + A_b \quad (73)$$

where A_f and A_b are the area under the resonances due to free and bound NTA respectively. The fractions of the total NTA in the bound and free forms, P_b and P_f , were calculated from the resonance intensity using equation 74 and 75. Knowing the total concentration of NTA ($[\text{NTA}]_t$),

$$P_f = \frac{A_f}{A_t} \quad (74)$$

$$P_b = \frac{A_b}{A_t} \quad (75)$$

the concentrations of free ($[NTA]_f$) and bound ($[NTA]_b$) NTA were obtained from equation 76 and 77.

$$[NTA]_f = P_f [NTA]_t \quad (76)$$

$$[NTA]_b = P_b [NTA]_t \quad (77)$$

The concentration of free cadmium is the difference between the total concentration of cadmium, $[Cd]_t$, and the concentration of bound $[NTA]_b$, which is equal to the concentration of $Cd(NTA)^-$.

$$[Cd]_f = [Cd]_t - [Cd(NTA)^-] \quad (78)$$

A conditional formation constant, as defined by equation 79 was calculated from these concentrations.

$$K_{fc} = \frac{[Cd(NTA)^-]}{[Cd]_f [NTA]_f} \quad (79)$$

A value for the formation constant, as defined by equation 72 was then calculated from each value of K_{fc} using equation 80

$$K_f = \frac{K_{fc}}{\alpha_{NTA3-}} \quad (80)$$

where α_{NTA3-} is the fraction of free NTA in the fully deprotonated form.

$$\alpha_{\text{NTA}^{1-}} = \frac{K_a}{K_a + [\text{H}^+]} \quad (81)$$

The free cadmium is all in the form of Cd²⁺, because cadmium does not form complexes with NTA other than the Cd(NTA)⁻ complex, under the conditions used in this study; i.e., equimolar concentrations of cadmium and NTA and low pH. An average value of 2.69 ± 0.10 x 10⁹ was obtained for K_f (log K_f = 9.43). For comparison, values reported previously are 9.23 [74], 9.4 [75] and 9.8 [73].

2. Mixed Ligand Complexes of Cd(NTA)-Glycine and Cd(NTA)-Glutamic Acid

Among the mixed ligand complexes investigated, those formed with glycine and glutamic acid had the simplest behavior. For both systems only the mixed complex Cd(NTA)L is formed.

Solutions containing equimolar amounts of Cd(NTA)⁻ and secondary ligand were titrated and spectra obtained for different pH values. Two spectra obtained from the titration of the mixture of Cd(NTA)⁻ and glycine are shown in Figure 16, one at a low pH of 4 and another at a high pH of 9. In both spectra two resonances are observed which are pH dependent. The chemical shift of the resonance at low fields is due to glycine H_α protons and is affected by ionization of glycine's amino group and the binding of glycine to Cd(NTA)⁻. The resonance around 3.16 ppm is due to bound NTA and is

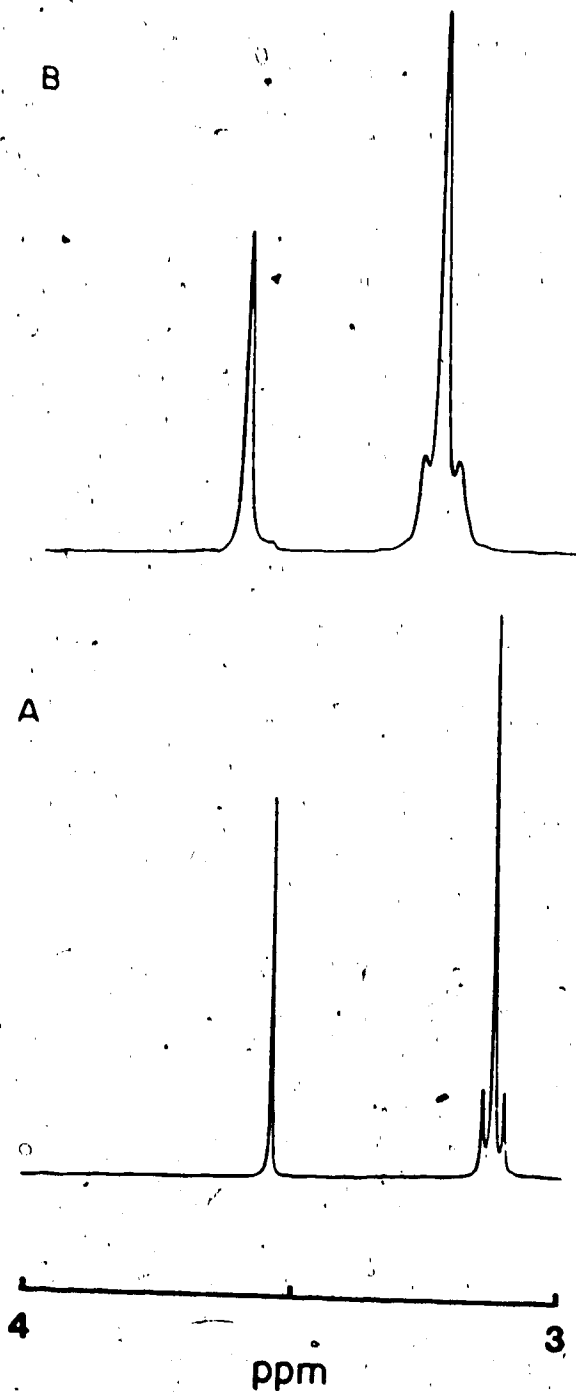


Figure 16. Spectra of equimolar solutions of Cd(NTA)⁻ and glycine at (A) pH 5 and (B) pH 9.

shifted to lower field as compared to that of $\text{Cd}(\text{NTA})^-$ (3.162 ppm). The change in the NTA chemical shift as the pH increases is a result of glycine binding to $\text{Cd}(\text{NTA})^-$. The pH dependence of the chemical shift of glycine H_α resonance and bound NTA resonance are depicted in Figure 17. In Figure 17 points on curve A represent chemical shifts of the glycine H_α resonance in a solution of glycine alone, these data were used to determine the $\text{pK}_{\text{a}2}$ of glycine. The carboxylic acid group of glycine is essentially completely deprotonated at $\text{pH} > 4$ [71]. The solid line through these data points was calculated by KINET with a $\text{pK}_{\text{a}2}$ of 9.85 ± 0.01 and chemical shifts of (3.5550 ± 0.0005) ppm and (3.1599 ± 0.0006) ppm for the protonated and deprotonated forms of glycine. Experimental data on curve B are chemical shifts of the glycine H_α resonance for an equimolar solution of $\text{Cd}(\text{NTA})^-$ and glycine. The curve defining these points is shifted from that of the titration of glycine alone from $\text{pH} \sim 6$ due to complexation of glycine by $\text{Cd}(\text{NTA})^-$. Curve C is defined by experimental chemical shifts of methylene protons in $\text{Cd}(\text{NTA})^-$. Only a small shift is experienced by this resonance upon complexation (~ 0.012 ppm) as was stated earlier. Hence, the pH dependence of the chemical shift of H_α protons of glycine, which experiences a more important shift upon complexation, was used to determine the formation constant of the mixed complex $\text{Cd}(\text{NTA})(\text{gly})$. Using the procedure described in Section B, the solid line

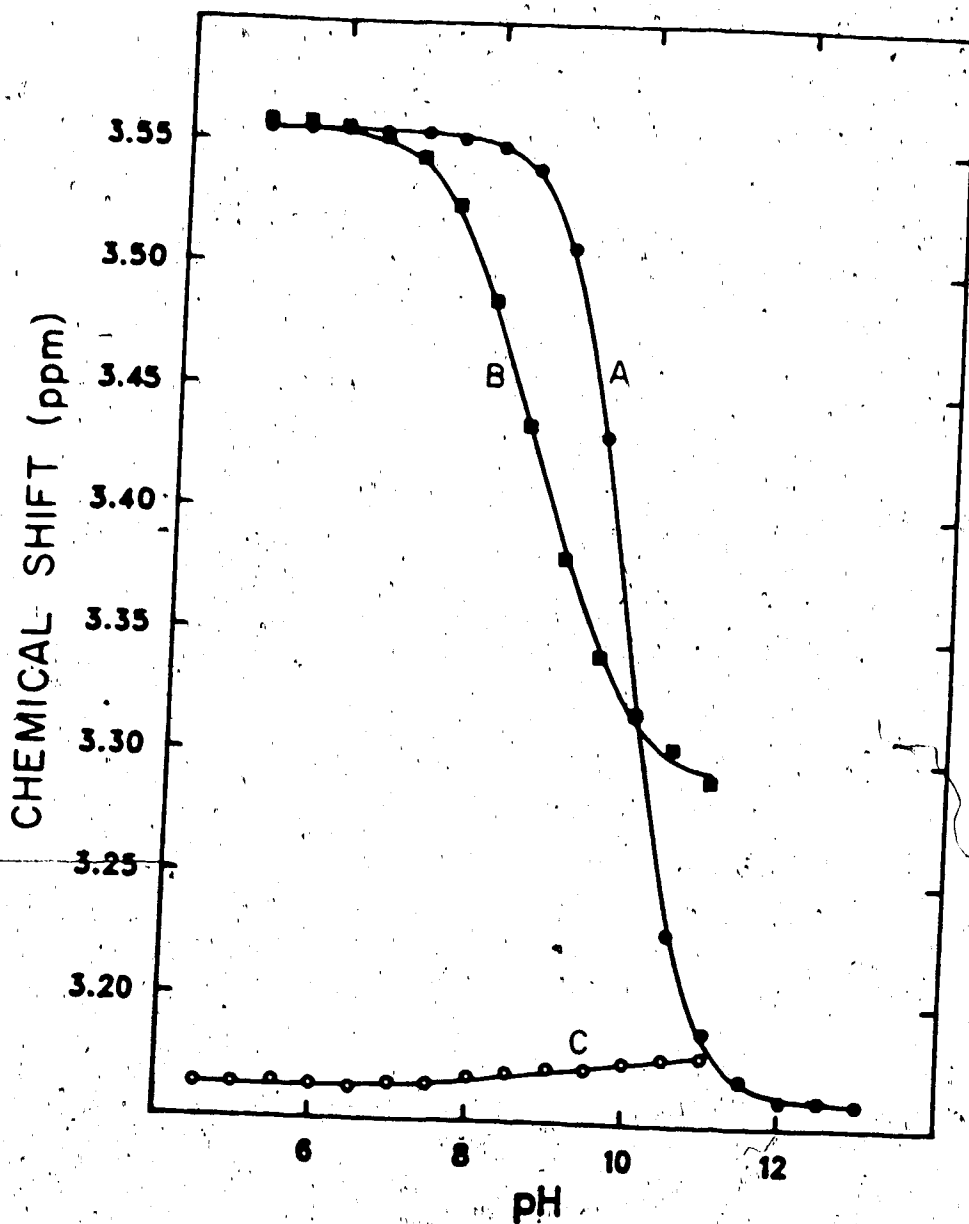


Figure 17. The pH dependence of the chemical shift of (A) H_α during titration of glycine and the calculated curve from pK_{a2} determination, (B) H_α during titration of an equimolar solution of Cd(NTA)⁻ and glycine and the calculated curve from log K_f determination, (C) methylene protons on bound-NTA during titration of an equimolar solution Cd(NTA)⁻ and glycine.

through the data points was calculated by Kinet with a log K_f of 3.26 ± 0.02 and a δ_C of (3.314 ± 0.0002) ppm. For comparison some literature values previously reported for log K_f are 3.62 [71], 3.25 [78] and 3.05 [79].

The complexation of glutamic acid by $\text{Cd}(\text{NTA})^-$ is reflected in spectral features and chemical shift behavior similar to that of glycine. Complexation was investigated in equimolar mixtures of $\text{Cd}(\text{NTA})^-$ and glutamic acid. Changes in the glutamic acid H_α resonance and bound NTA resonance are depicted in Figure 18. As was the case with glycine, all NTA remains bound to Cd^{2+} and a single resonance is observed for NTA protons. However as the pH increases, this resonance is shifted slightly downfield as compared to $\text{Cd}(\text{NTA})^-$ (3.162 ppm to 3.176 ppm) as a result of the binding of glutamic acid to $\text{Cd}(\text{NTA})^-$. The chemical shift of the resonance due to glutamyl H_α is also pH dependent. It is affected by the acid-base chemistry of glutamic acid as well as the complexation of glutamic acid by $\text{Cd}(\text{NTA})^-$. pK_{a3} of glutamic acid was determined from chemical shift data for the H_α resonance of solutions of glutamic acid alone. The experimental data and the curve calculated by KINET are given in Figure 19 (curve A). A pK_{a3} of 9.72 ± 0.03 and chemical shifts of (3.754 ± 0.001) ppm and (3.218 ± 0.002) ppm for the protonated and deprotonated species were obtained. The formation constant of the mixed complex $\text{Cd}(\text{NTA})(\text{glu})$ was determined from the pH dependence

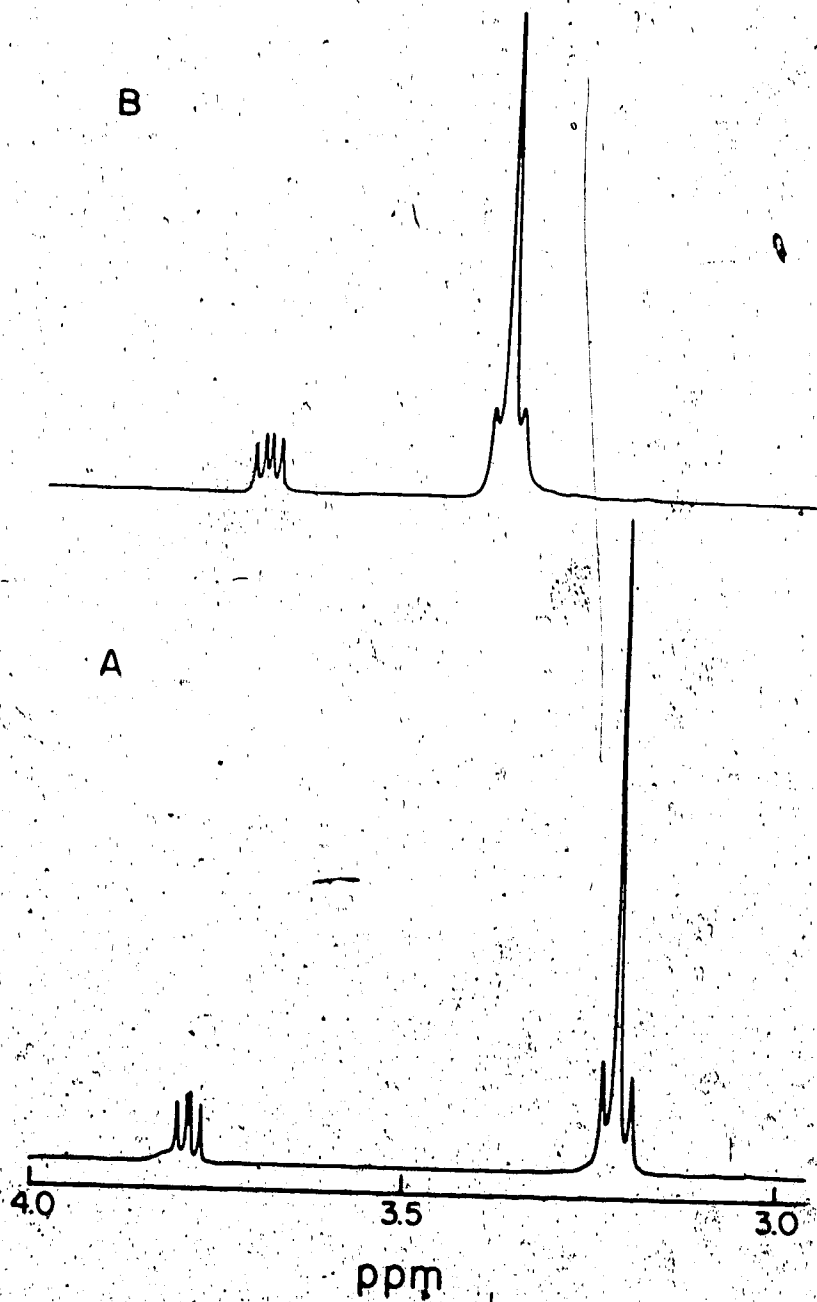


Figure 18. Portions of spectra of equimolar solutions of $\text{Cd}(\text{NTA})^-$ and glutamic acid at (A) pH 4.5 and (B) pH 9.5.

of the chemical shift of H_{α} in the equimolar mixture of $Cd(NTA)^{-}$ and glutamic acid also shown in Figure 19. Points on curve B are experimental results and the solid curve through them was calculated by Kinet with a $\log K_f$ of 2.79 ± 0.04 and a chemical shift of H_{α} in the complex (δ_c) of (3.439 ± 0.004) ppm.

3. The Mixed Ligand System $Cd(NTA)^{-}$ -Penicillamine

The equilibria established in the mixed ligand system $Cd(NTA)^{-}$ -PSH were investigated by 1H -NMR chemical shift and resonance intensity measurements. When PSH is reacted with $Cd(NTA)^{-}$ in a 1 to 1 ratio, there is some displacement of NTA by PSH. This is indicated by the presence of a resonance around 3.8 ppm for free NTA. Figure 20 shows the changes in the spectrum for a pH 5.5 solution of $Cd(NTA)^{-}$ as PSH is added. A pH of 5.5 was used to avoid overlap of resonances for NTA and PSH. The concentration of $Cd(NTA)^{-}$ was kept at 0.02M. Addition of PSH causes the displacement of NTA from its $Cd(NTA)^{-}$ complexes, as indicated by the appearance of a resonance at 3.8 ppm (Figure 20, spectrum B). As more PSH is added the intensity of the resonance at 3.8 ppm is increased as illustrated by spectrum C in Figure 20. The displacement of NTA by PSH signifies the formation of $Cd(PSH)$ complexes. As the intensity of the resonance due to free NTA increases, that of the resonance due to bound NTA decreases. The latter resonance is also shifted downfield due to the formation of the mixed complex $Cd(NTA)(PSH)$. The

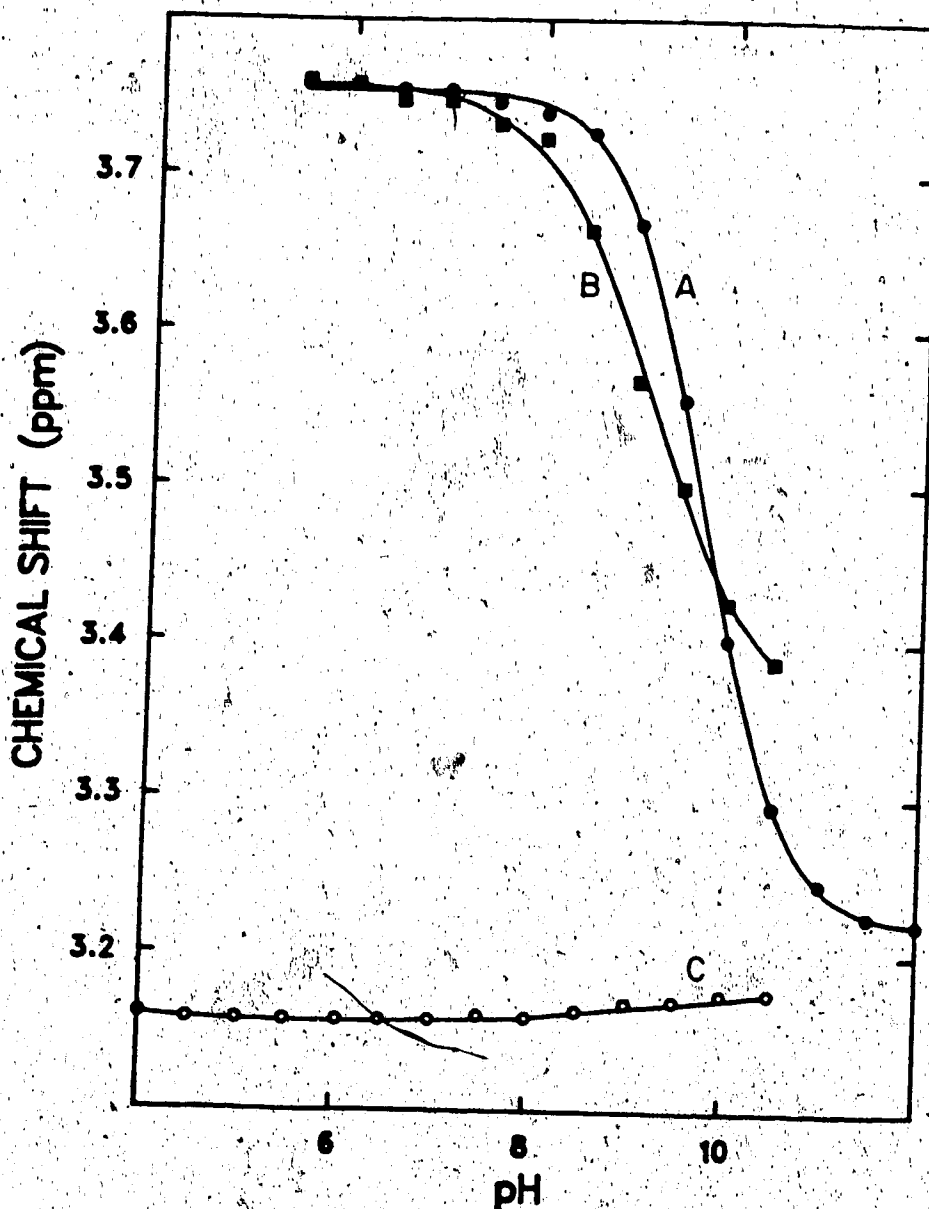


Figure 19. (A) The pH dependence of the chemical shift of glutamic acid H_{α} during titration of glutamic acid and the calculated curve from the pK_{a3} determination. (B) H_{α} during titration of an equimolar solution of $Cd(NTA)^-$ and glutamic acid and the calculated curve from $\log K_f$ determination. (C) Methylene protons in bound NTA during titration of an equimolar solution of $Cd(NTA)^-$ and glutamic acid.

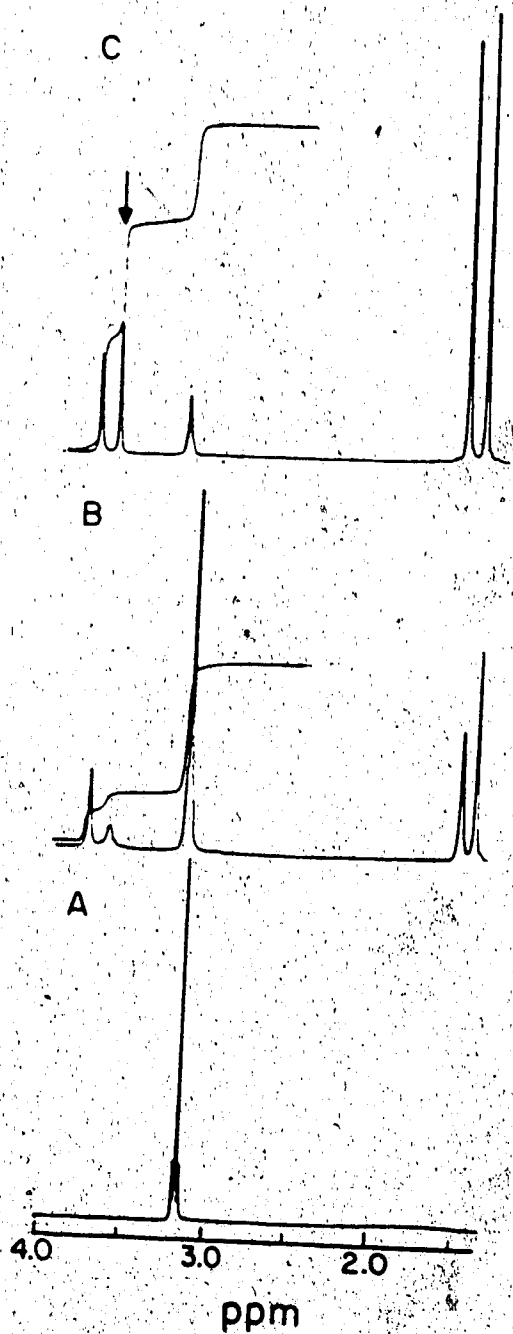


Figure 20. Spectra of mixtures of Cd(NTA)^- and PSH at pH 5. Initial concentrations $[\text{Cd(NTA)}^-] = 0.02\text{M}$ and $[\text{PSH}] =$ (A) 0.0M , (B) 0.015M and (C) 0.07M .

satellites due to ^1H - ^{111}Cd and ^1H - ^{113}Cd coupling are broadened which suggests weaker bonding.

Changes in the chemical shifts of the resonances due to the H_α proton of PSH (curve B), and the protons of bound NTA (curve C) are shown in Figure 21. The chemical shift titration for PSH alone (curve A) and $\text{Cd}(\text{NTA})^-$ alone (curve D) are also shown in the figure for comparison. The chemical shift for the protons of bound NTA increases above pH 4.5, and reaches a plateau of ~ 3.31 ppm above pH 9. The chemical shift of the resonance for the H_α proton of PSH is shifted from that of its resonance in a solution of the ligand alone in the pH region where the sulfhydryl group is being titrated. It also reaches a plateau of about 3.2 ppm above pH 10.

Data for the chemical shift titration of PSH between pH 6 and 11 (curve A on Figure 21) were used to determine the acidity constants. In this pH region the H_α resonance monitors the ionization of the sulfhydryl and amino groups. The carboxylic acid group is much more acidic and is dissociated at lower pH [29]. Hence, the acidity constants pK_{a2} and pK_{a3} as defined by equations 82 and 83 were determined from H_α chemical shift titration data of PSH.



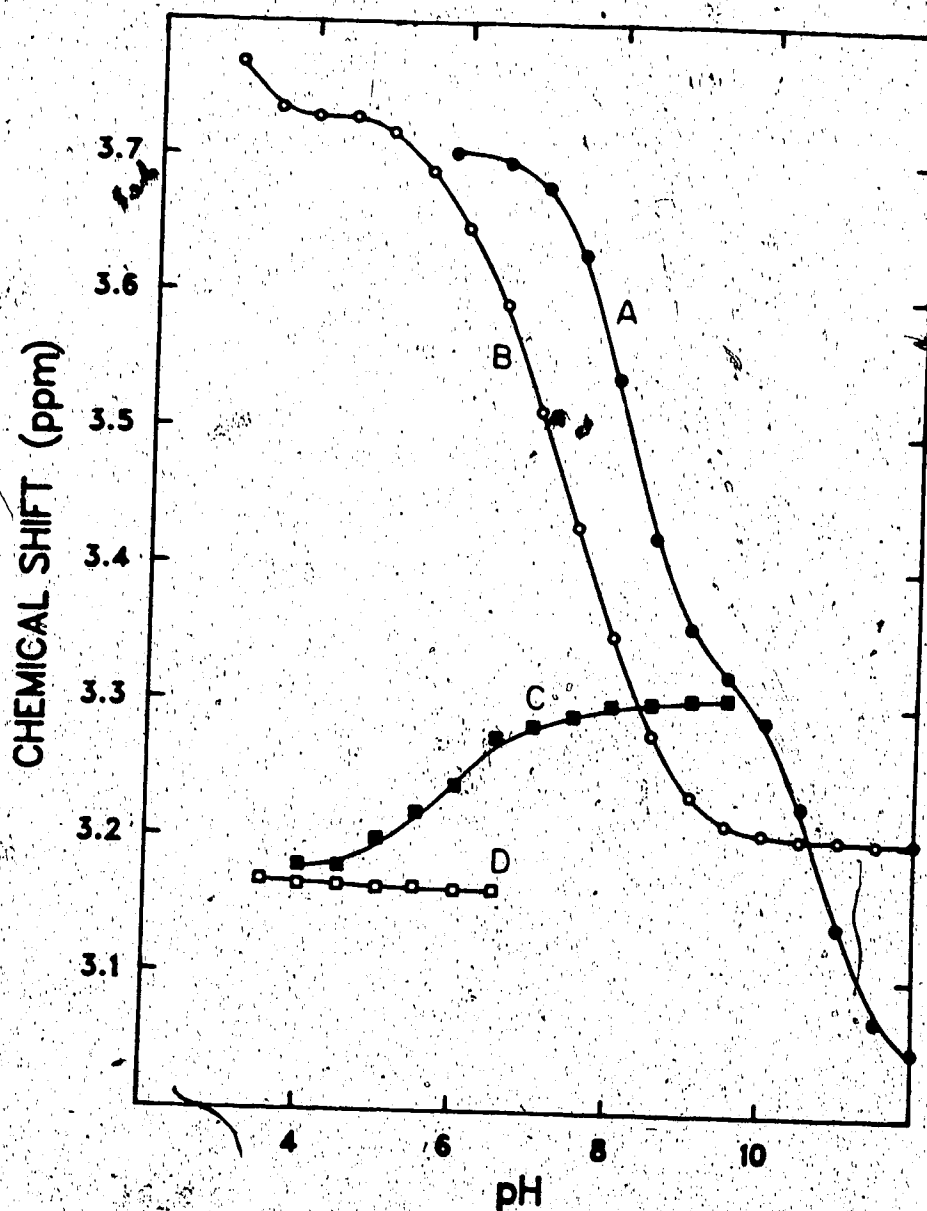
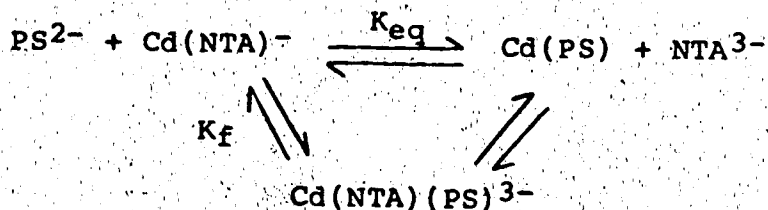


Figure 21. The pH dependence of the chemical shift of (A) H_{α} during titration of PSH and (B) H_{α} during titration of an equimolar mixture of $Cd(NTA)^-$ and PSH, (C) Methylene protons in bound NTA during a titration of an equimolar mixture of $Cd(NTA)^-$ and PSH and (D) methylene protons in NTA during a titration of an equimolar solution of Cd^{2+} and NTA.



A $\text{p}K_{a2}$ of 8.09 ± 0.02 and a $\text{p}K_{a3}$ of 10.79 ± 0.03 were obtained. The chemical shifts obtained for H_α in PSH, PS^- and PS^{2-} were (3.706 ± 0.002) ppm, (3.322 ± 0.003) ppm and (3.029 ± 0.003) ppm respectively.

The equilibria established in solutions containing $\text{Cd}(\text{NTA})^-$ and PSH are described by the scheme:



It involves the formation of the mixed complex $\text{Cd}(\text{NTA})(\text{PS})^{3-}$ as well as displacement of NTA with formation of $\text{Cd}(\text{PS})$.

Data obtained at a constant pH of 5.5 were used to evaluate the K_f and K_{eq} . First, the conditional formation constant for $\text{Cd}(\text{NTA})(\text{PS})^{3-}$, K_{fc} , and for the displacement of NTA by PSH, K_{eqc} , as defined by equations 84 and 85 were obtained by

$$K_{fc} = \frac{[\text{Cd}(\text{NTA})(\text{PS})^{3-}]}{[\text{Cd}(\text{NTA})^-][\text{PSH}]_f} \quad (84)$$

$$K_{eqc} = \frac{[\text{Cd}(\text{PS})][\text{NTA}]_f}{[\text{Cd}(\text{NTA})^-][\text{PSH}]_f} \quad (85)$$

fitting the chemical shift of the resonance for bound NTA versus the concentration of PSH using the procedure

described in section C.2 of this chapter. The values obtained were $K_{fc} = 52.1 \pm 0.5$ and $K_{eqc} = (1.14 \pm 0.49) \times 10^{-2}$. The experimental data and the chemical shift versus [PSH] curve predicted with these constants are shown in Figure 22. Then K_f and K_{eq} were calculated using equations 86 and 87

$$K_f = K_{fc} / \alpha_{PS^{2-}} \quad (86)$$

$$K_{eq} = K_{eqc} \times \frac{\alpha_{NTA^{3-}}}{\alpha_{PS^{2-}}} \quad (87)$$

where $\alpha_{PS^{2-}}$ and $\alpha_{NTA^{3-}}$ are the fractions of PS^{2-} and NTA^{3-} in the solution at pH 5.5. The values obtained were $K_f = 4.22 \times 10^9$ and $K_{eq} = 1.26 \times 10^2$. The formation constant of $Cd(PS)$ was calculated from K_f and K_{eq} using equation 88 and 89. The value obtained is 3.41×10^{11} ($\log K_{f,Cd(PS)} = 11.53$)

$$K_{f,Cd(PS)} = \frac{[Cd(PS)]}{[Cd^{2+}][PS^{2-}]} \quad (88)$$

$$K_{f,Cd(PS)} = K_{f,Cd(NTA)} \times K_{eq} \quad (89)$$

in good agreement with reported literature values of 10.92 by Sugiura and Yokoyama [80], 11.4 by Kuchinkas and Rosen [29], 12.68 by Corrie, Walker and Williams [81] and 11.51 by Strand, Lund and Aaseth [82].

In the solutions used to determine the above formation constants, there is free NTA and free PSH. Since the complexes $Cd(NTA)_2$ and $Cd(PSH)_2$ are known to form [56, 29], calculations were done to determine if any $Cd(PS)_2$ or

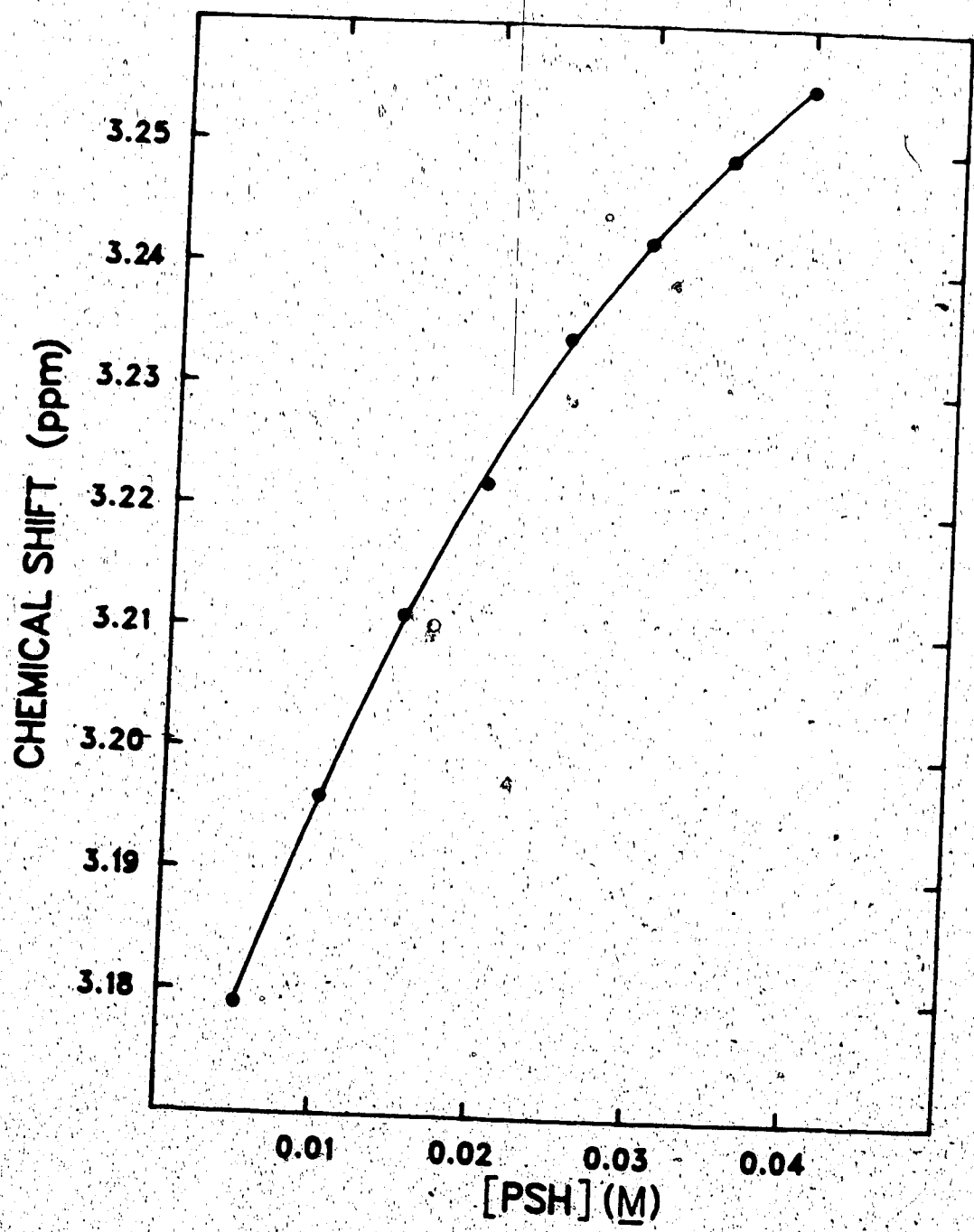


Figure 22. Chemical shift of methylene protons in bound NTA as a function of PSH concentration and the calculated curve from K_{fc} and K_{eqc} determination.

$\text{Cd}(\text{NTA})_2$ formed under these conditions. Literature values for the formation constants for the $\text{Cd}(\text{PS})_2$ and $\text{Cd}(\text{NTA})_2$ complexes were used [8,30] together with reaction conditions used in this study. At the highest PSH concentration, where the highest concentration of $\text{Cd}(\text{PS})_2$ and $\text{Cd}(\text{NTA})_2$ would form, less than 2.5% of the cadmium was predicted to be present in either of these forms, indicating that neglect of the 2:1 complexes was justified.

4: The Mixed Ligand System $\text{Cd}(\text{NTA})$ -N-acetylpenicillamine

A mixture of 1 to 1 $\text{Cd}(\text{NTA})^-$ and N-PSH was titrated and ^1H -NMR spectra recorded between pH 2 and 12. Representative spectra are shown in Figure 23. Only the portion of spectrum containing the H_α resonance of N-PSH and the NTA resonances is shown. These spectra indicate displacement of NTA as was the case with PSH. The resonance due to bound NTA is shifted to lower fields with increasing pH values. Broadening and loss of the coupling between ^{111}Cd and ^{113}Cd and the ^1H resonance of the bound NTA is also observed. All these changes point to the formation of both the mixed complex $\text{Cd}(\text{NTA})(\text{N-PSH})$ and the complex $\text{Cd}(\text{N-PSH})$.

The effects of the binding on the chemical shifts of the resonances of H_α proton of N-PSH (curve B) and of the methylene protons of bound NTA (curve C) are summarized in Figure 24. The chemical shift titration data for the N-PSH

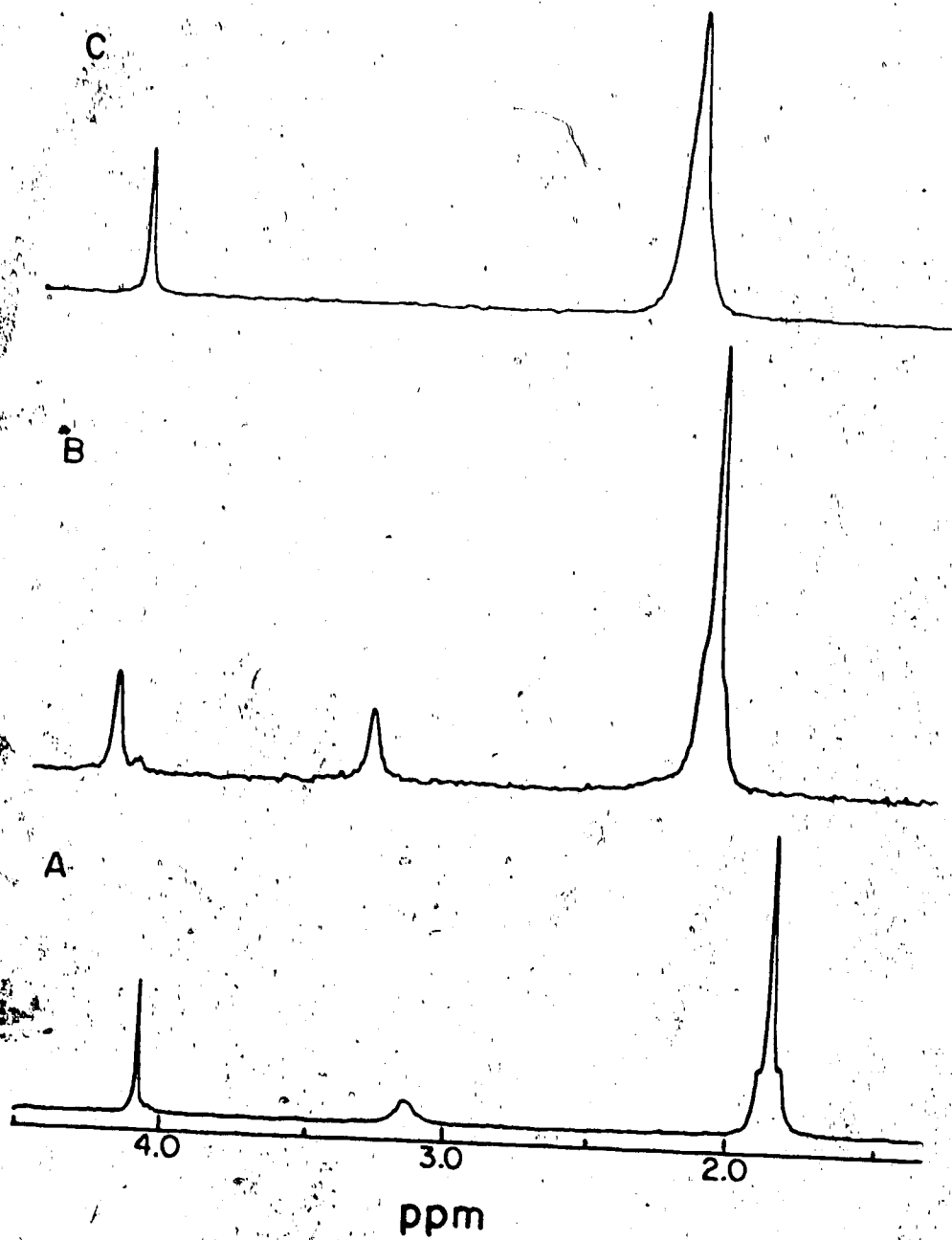


Figure 23. Spectra of the equimolar mixture of $\text{Cd}(\text{NTA})^-$ and N-acetylpenicillamine at (A) pH 4.01, (B) 6.51 and (C) 8.01.

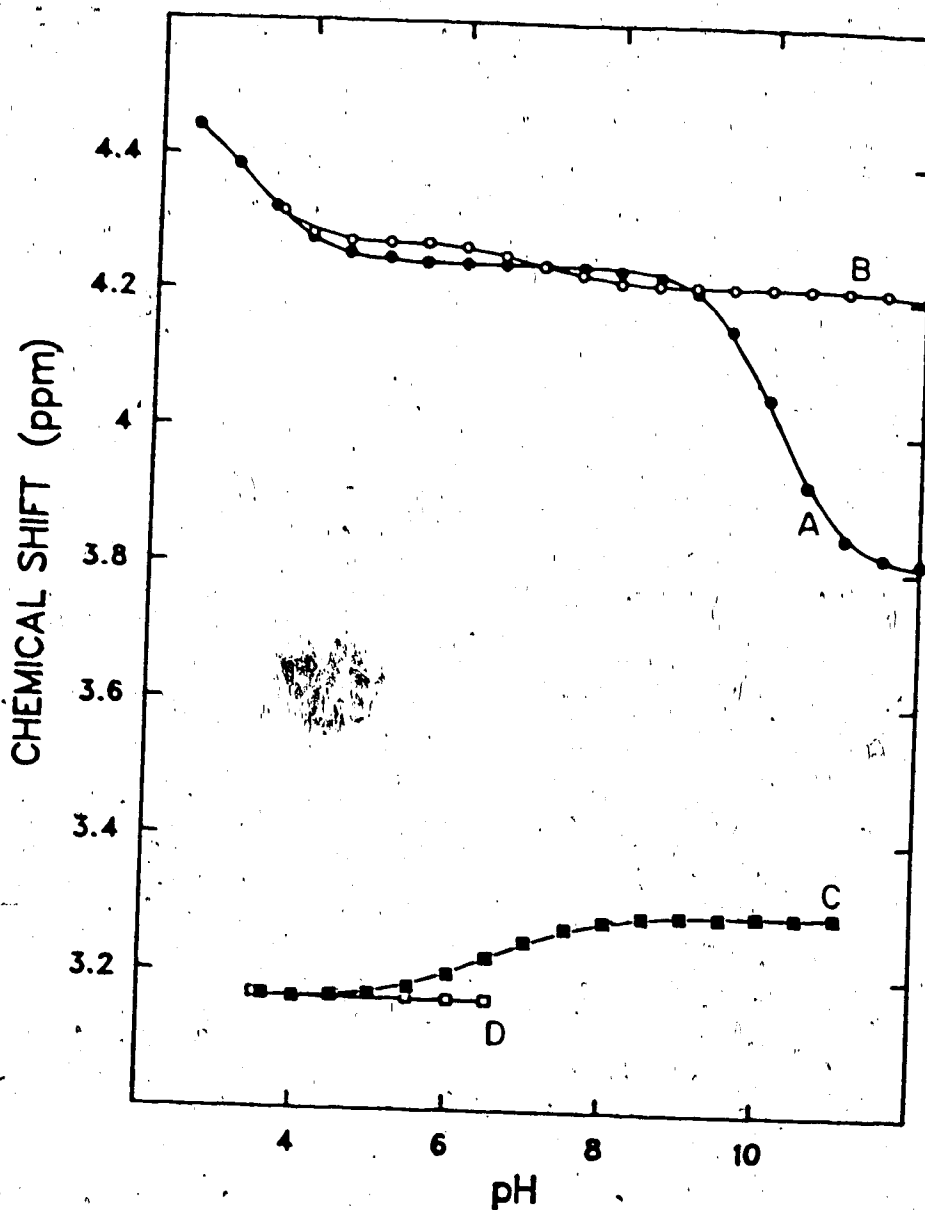
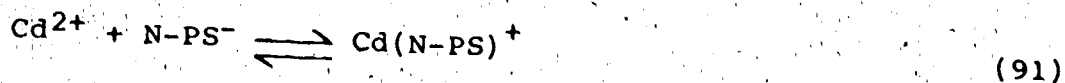
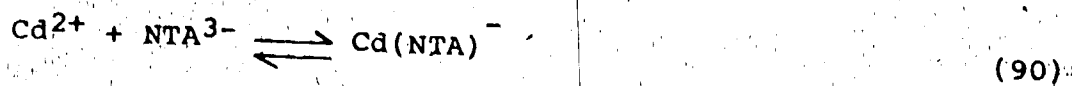


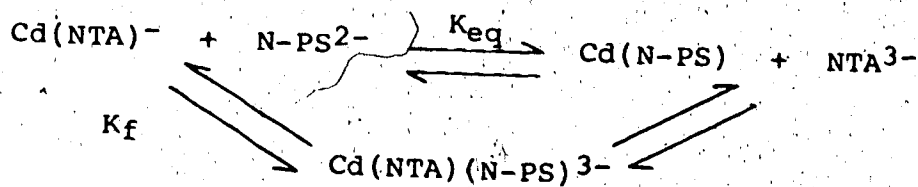
Figure 24. The pH dependence of the chemical shift of (A) H_a during titration of the N-PSH, (B) H_a during titration of an equimolar mixture of $Cd(NTA)^-$ and N-PSH, (C) methylene protons in bound NTA during titration of an equimolar mixture of $Cd(NTA)^-$ and N-PSH and (D) methylene protons in NTA during titration of an equimolar mixture of Cd^{2+} and NTA.

alone (curve A) and $\text{Cd}(\text{NTA})^-$ alone (curve D) are plotted on the same figure for comparison. Data for the titration of the ligand were used to determine the acidity constants pK_{a1} and pK_{a2} of N-PSH. The solid curves through the experimental data were calculated by KINET with a pK_{a1} of 3.21 ± 0.02 , pK_{a2} of 10.09 ± 0.01 and H_a chemical shifts of (4.477 ± 0.004) ppm, (4.243 ± 0.001) ppm and (3.806 ± 0.002) ppm in N-PSH, N-PS^- and N-PS^{2-} .

The chemical shift of H_a in the mixture of $\text{Cd}(\text{NTA})^-$ and N-PSH is shifted from that in N-PSH alone from pH 3.8 upwards, indicating complexation of N-PSH. The chemical shift of methylene protons in the bound NTA is constant (3.162 ppm) up to pH ~ 5.5 indicating that the reaction occurring below this pH does not involve the formation of the mixed complex $\text{Cd}(\text{NTA})(\text{N-PSH})$. Experimental measurements on an equimolar mixture of Cd^{2+} and NTA have indicated the presence of NTA free below pH 4.5, meaning that some free Cd^{2+} exists in solution below this pH. It is therefore the species Cd^{2+} which is complexing N-PSH in the region of pH (3.8-5.5) where no change is observed on the chemical shift of methylene protons of bound NTA. The donor group in this pH region is most likely the carboxylate group of N-PSH which is titrated between pH ~ 2 and ~ 5 . The complexation equilibria effective in the pH region ~ 3.8 to 5.5 are therefore:



Above pH 5.5, the chemical shift of the methylene protons in bound NTA is shifted to higher frequencies and reaches a plateau of ~3.30 ppm above pH 8.5. This shift results from the formation of the mixed complex, $\text{Cd}(\text{NTA})(\text{N-PSH})$. Displacement of NTA by N-PSH is also effective as evidenced by the spectra shown in Figure 23. Therefore, the scheme below describes the equilibria of the system above pH 5:



The formation constant K_f of the mixed ligand complex $\text{Cd}(\text{NTA})(\text{N-PS}^{3-})$:

$$K_f = \frac{[\text{Cd}(\text{NTA})(\text{N-PS})^{3-}]}{[\text{Cd}(\text{NTA})^{-}][\text{N-PS}^{2-}]} \quad (92)$$

was calculated using data above pH 5. The intensities of resonances for bound and free NTA were used to determine the concentrations of the species in solution, as described in Section C-2 of this chapter. The equilibrium constant K_{eq} for the displacement of NTA, with binding of Cd^{2+} to the sulfhydryl group of N-PSH:

$$K_{eq} = \frac{[Cd(N-PS)][NTA^{3-}]}{[Cd(NTA)^-][N-PS^{2-}]} \quad (93)$$

was calculated using data between pH 6 and 7. The values obtained are $K_f = (8.39 \pm 0.24) \times 10^4$ and $K_{eq} = (5.0 \pm 0.5) \times 10^{-1}$. The formation constant of $Cd(N-PS)^+$, where Cd^{2+} is binding to the sulfhydryl group of N-acetylpenicillamine, was calculated from the formation constant of $Cd(NTA)^-$ and K_{eq} :

$$K_{f,Cd(N-PS)} = K_{f,Cd(NTA)^-} \times K_{eq} \quad (94)$$

The value obtained was 1.44×10^9 .

5. Mixed Ligand System Cd(NTA) - Glutathione

In this study, the chemical shifts of the g2 and g5 protons of the cysteinyl residue and the g3, g4 and g7 protons of the glutamyl residue were used to determine the fractional titration of the sulfhydryl and amino groups. Representative spectra of the titration of GSH are shown in Figure 25 with the assignment of the resonances. Only data recorded between pH 4 and 12 were treated. In this pH region both carboxylic acid groups of GSH are deprotonated given the $pK_{a1} = 2.12$ and $pK_{a2} = 3.53$ for GSH [84]. Therefore in the pH range 4-12 only the sulfhydryl and amino groups are being titrated. Species present in this pH range are given in Figure 26.

The resonances due to cysteinyl protons are affected

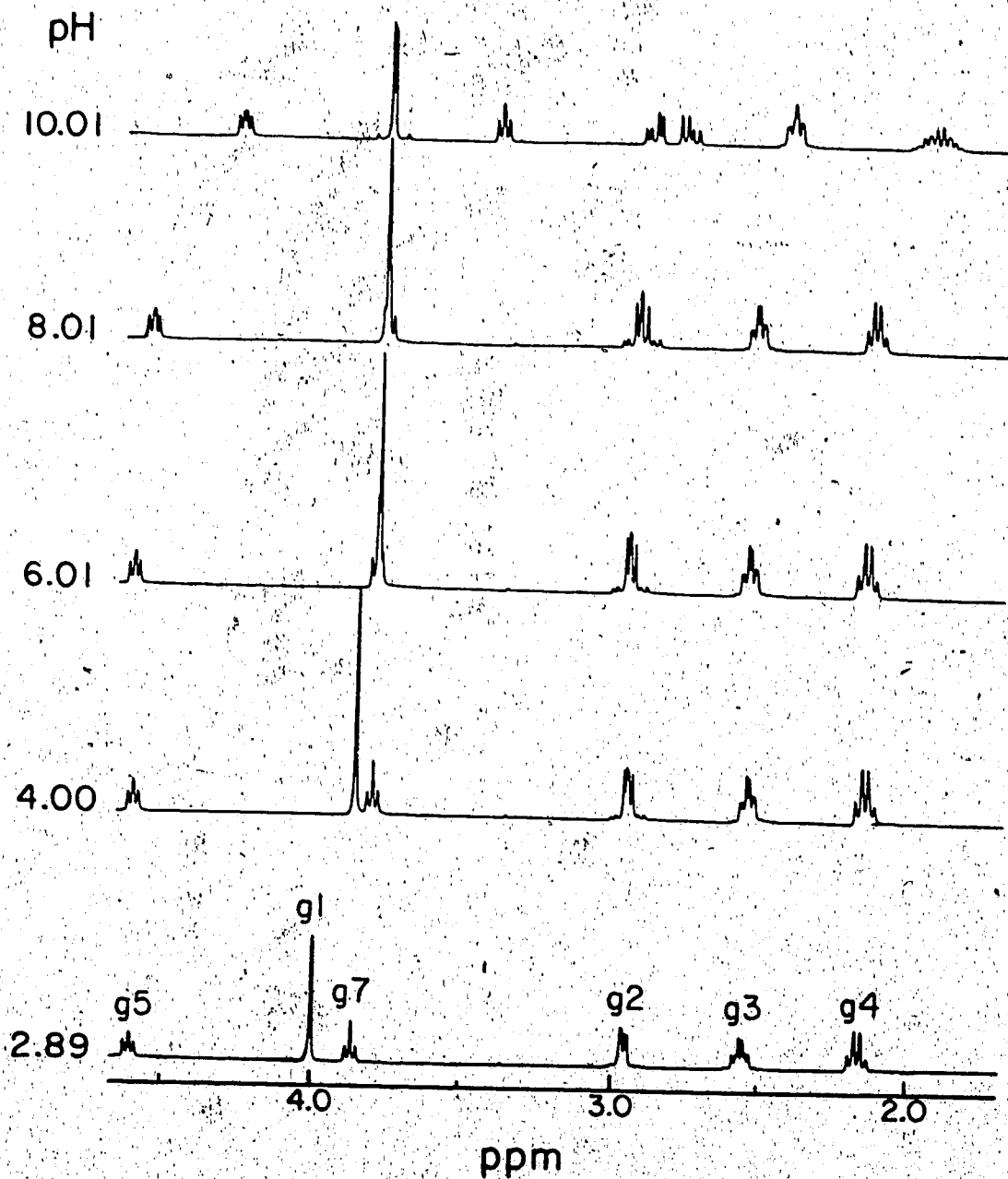


Figure 25. Representative ¹H NMR spectra of the pH titration of glutathione.

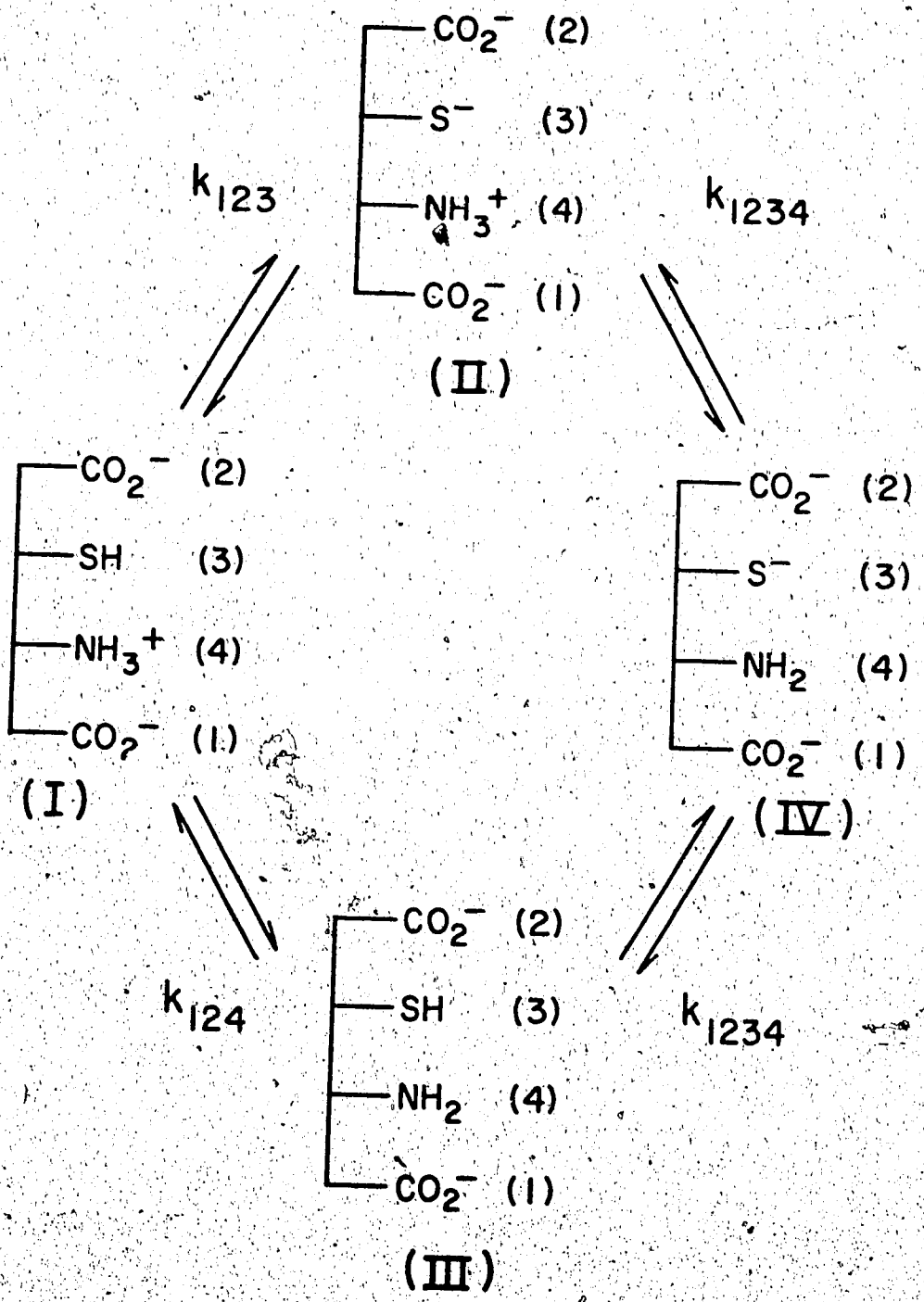


Figure 26. Species of glutathione predominant in the pH region 4 to 12.

solely by ionization of the sulfhydryl group. The pH dependences of their chemical shifts are depicted in Figure 27 for g5 (curve A) and in Figure 28 for g2 (curve A). The equilibrium monitored by the resonances for these protons is:



$$K_{\text{SH}} = \frac{[\text{GS}^-][\text{H}^+]}{[\text{GSH}]} \quad (96)$$

where GSH represents all the species of glutathione with the sulfhydryl group protonated (i.e., I, III in Figure 26) and GS^- species with the sulfhydryl group deprotonated (i.e., II and IV in Figure 26). The acidity constant K_{SH} was determined using the monoprotic acid model with Kinet. An average value of 8.87 ± 0.01 was obtained for $\text{p}K_{\text{SH}}$ which yielded the fit shown in Figure 27 for g5 proton and Figure 28 for g2 protons. The individual $\text{p}K_{\text{SH}}$ and chemical shifts of protonated and deprotonated species are listed in Table 3.

Similarly to the resonances for the cysteinyl protons, resonances g3, g4 and g7 of the glutamyl residue monitor the ionization of the amino group as described by equations 97 and 98 where

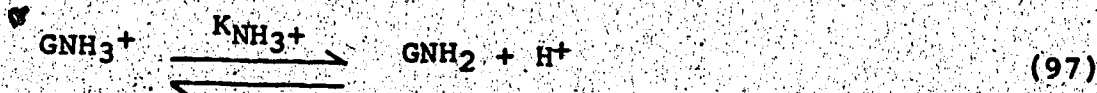


Table 3. Acidity constants of the sulfhydryl and amino groups in glutathione.

Resonance	pK	δ	δ_{HL}	δ_L
1 g5	8.87 ^a ±0.01		4.569±0.002	4.224±0.001
2 g2	8.87 ^a ±0.01		2.942±0.002	2.837±0.001
3 g7	9.48 ^b ±0.01		3.779±0.001	3.264±0.001
4 g4	9.47 ^b ±0.01		2.549±0.001	2.396±0.001
5 g3	9.49 ^b ±0.01		2.159±0.001	1.881±0.001

^apK_{SH}

^bpK_{NH₃⁺}

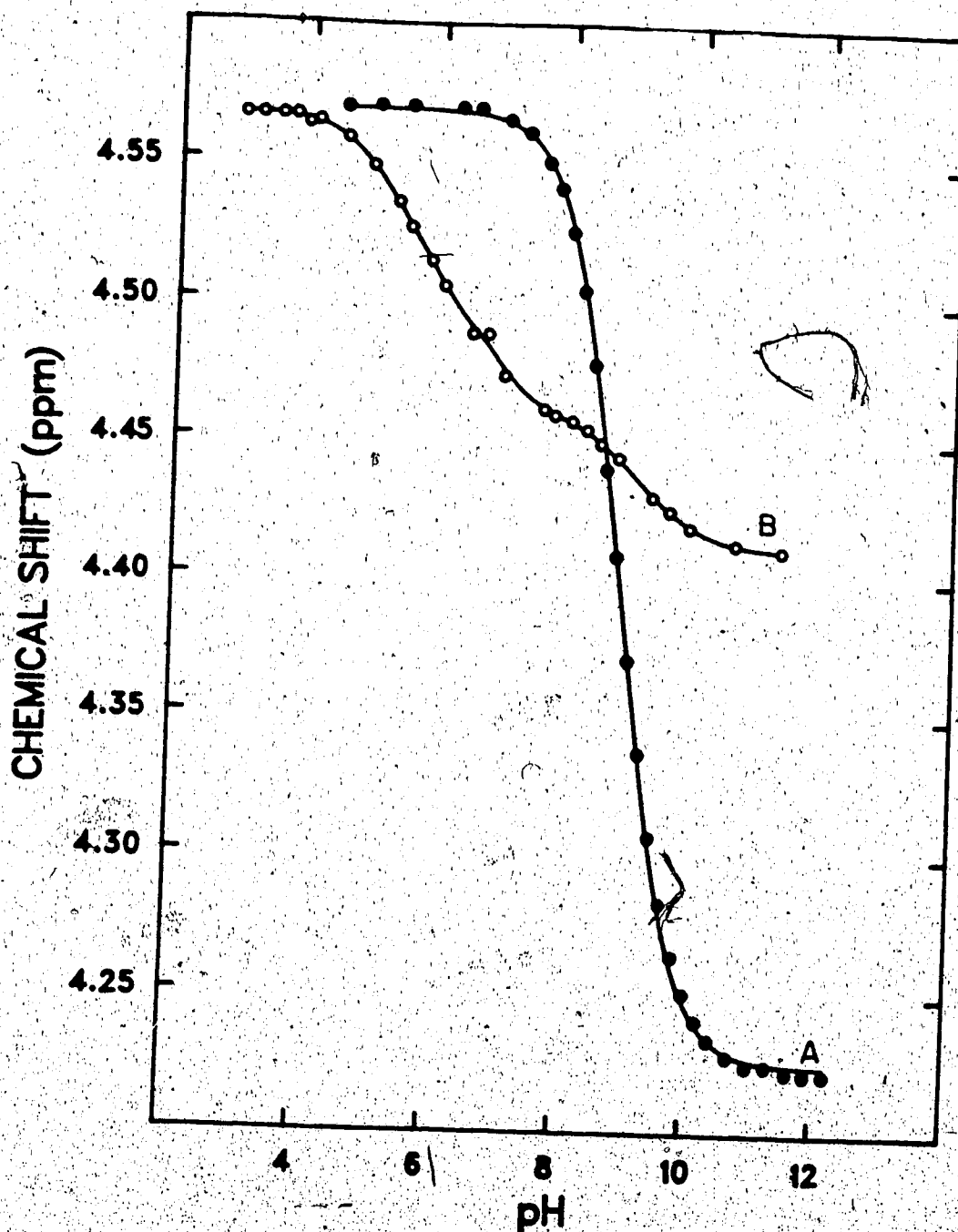


Figure 27. The pH dependence of the chemical shift of g5 proton (A) during titration of glutathione and (B) during titration of an equimolar mixture of glutathione and Cd(NTA).

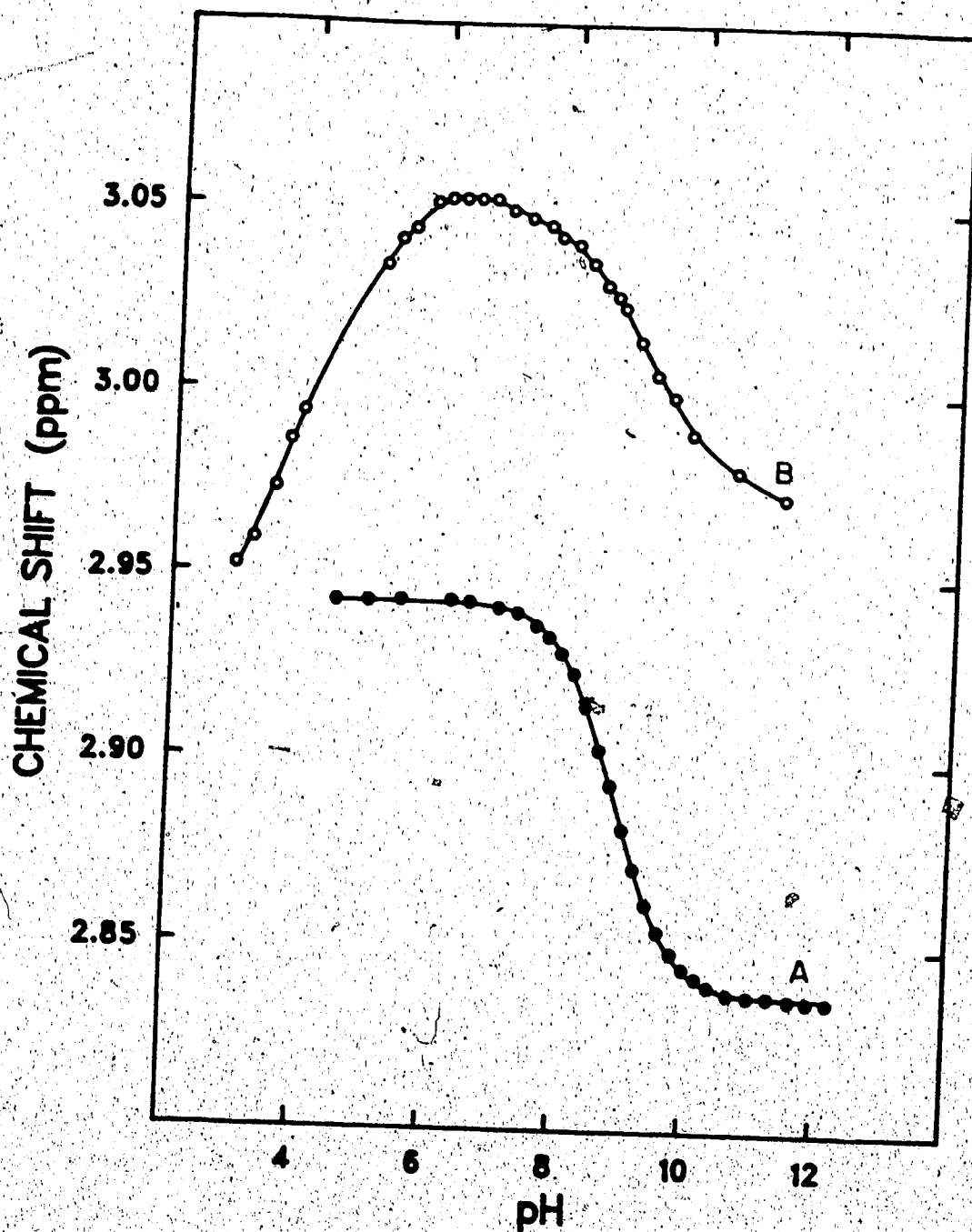


Figure 28. The pH dependence of the chemical shift of g_2 protons (A) during the titration of glutathione and (B) during titration of an equimolar mixture of glutathione and $Cd(NTA)^-$.

$$K_{\text{NH}_3^+} = \frac{[\text{GNH}_2][\text{H}^+]}{[\text{GNH}_3^+]} \quad (98)$$

GNH_3^+ and GNH_2 represent all species of glutathione with the amino group protonated (i.e., I and II in Figure 26) and deprotonated (i.e., III and IV in Figure 26) respectively. The pH dependence of the chemical shift of resonance g7 is depicted in Figure 29 (curve A). The solid line drawn through the experimental data is the curve calculated using the monoprotic acid model with KINET. Similar data treatment were done with g3 and g4 resonances. Results obtained for $\text{p}K_{\text{NH}_3^+}$ and the chemical shifts of protonated and deprotonated species are given in Table 3. An average value of $\text{p}K_{\text{NH}_3^+} = 9.48 \pm 0.01$ was calculated from the three data sets.

Having thus characterized the acid-base chemistry, glutathione was titrated in the presence of $\text{Cd}(\text{NTA})^-$. Figure 30 shows representative spectra for samples taken during the titration of a 1 to 1 mixture of $\text{Cd}(\text{NTA})^-$ and GSH. Clearly evident in the spectra is the downfield shift of the resonance due to methylene protons in bound NTA as the pH is increased, which indicates formation of the mixed complex $\text{Cd}(\text{NTA})(\text{GSH})$. The pH dependence of the chemical shift of the bound NTA resonance in the mixture is shown in Figure 31. The satellites due to coupling to ^{111}Cd and ^{113}Cd are broadened and lost suggesting weak bonding between Cd^{2+} and NTA and displacement of NTA. The resonance for

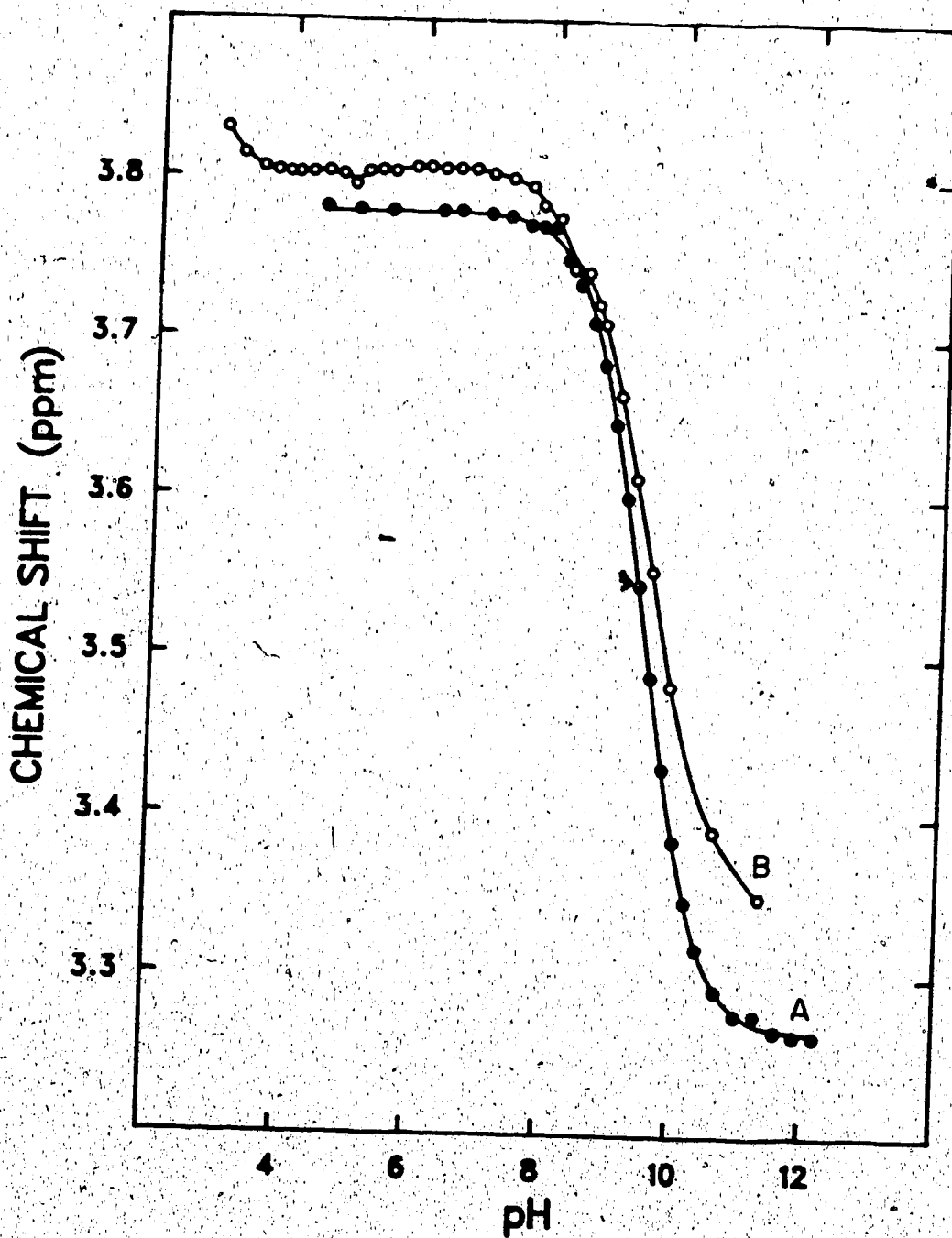


Figure 29. The pH dependence of the chemical shift of g7 proton (A) during titration of glutathione and (B) during titration of an equimolar mixture of glutathione and Cd(NTA)⁻.

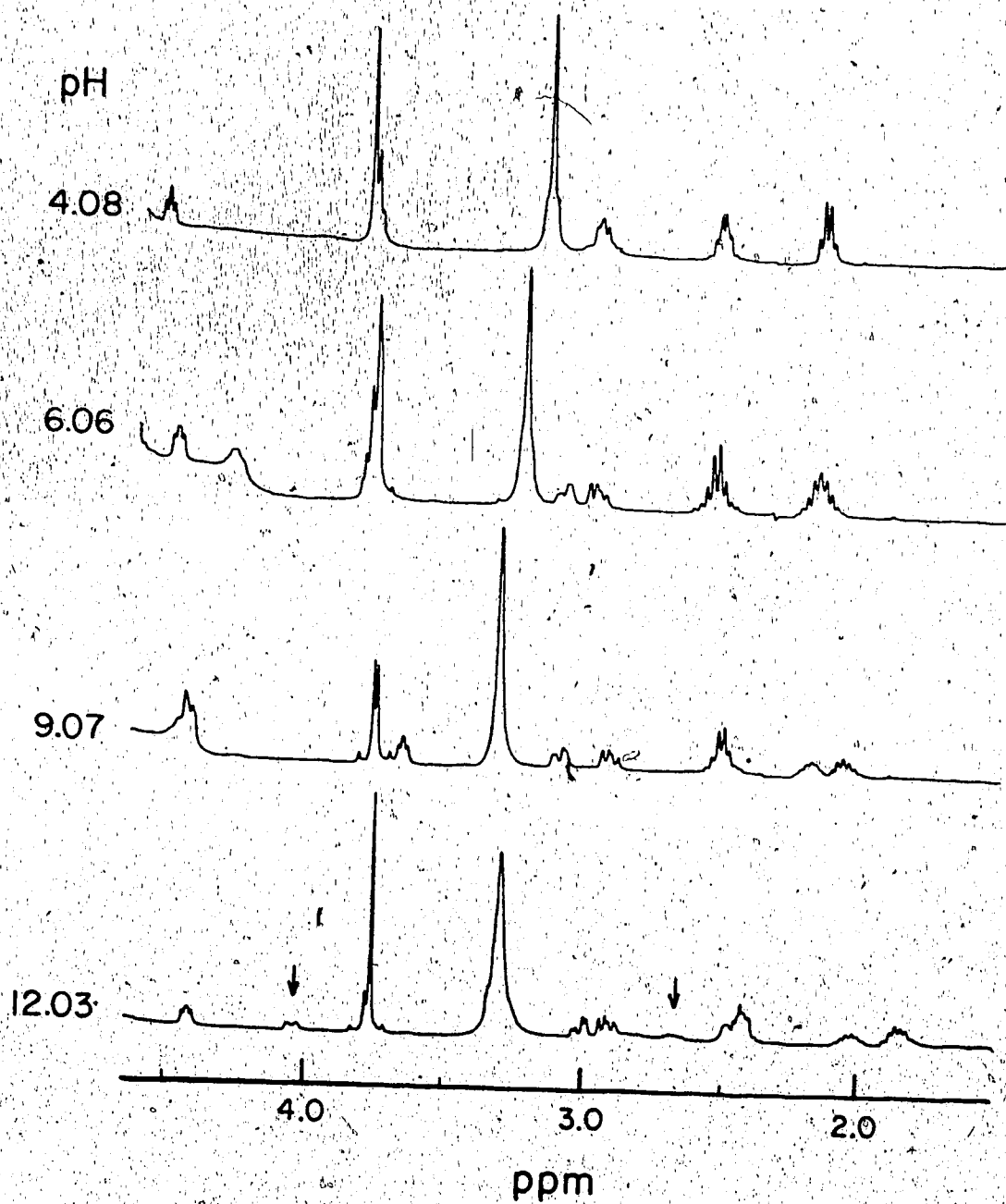


Figure 30. Representative spectra of the titration of an equimolar solution of glutathione and Cd(NTA)^- . $[\text{Cd(NTA)}^-] = [\text{GSH}] = 0.02\text{M}$.

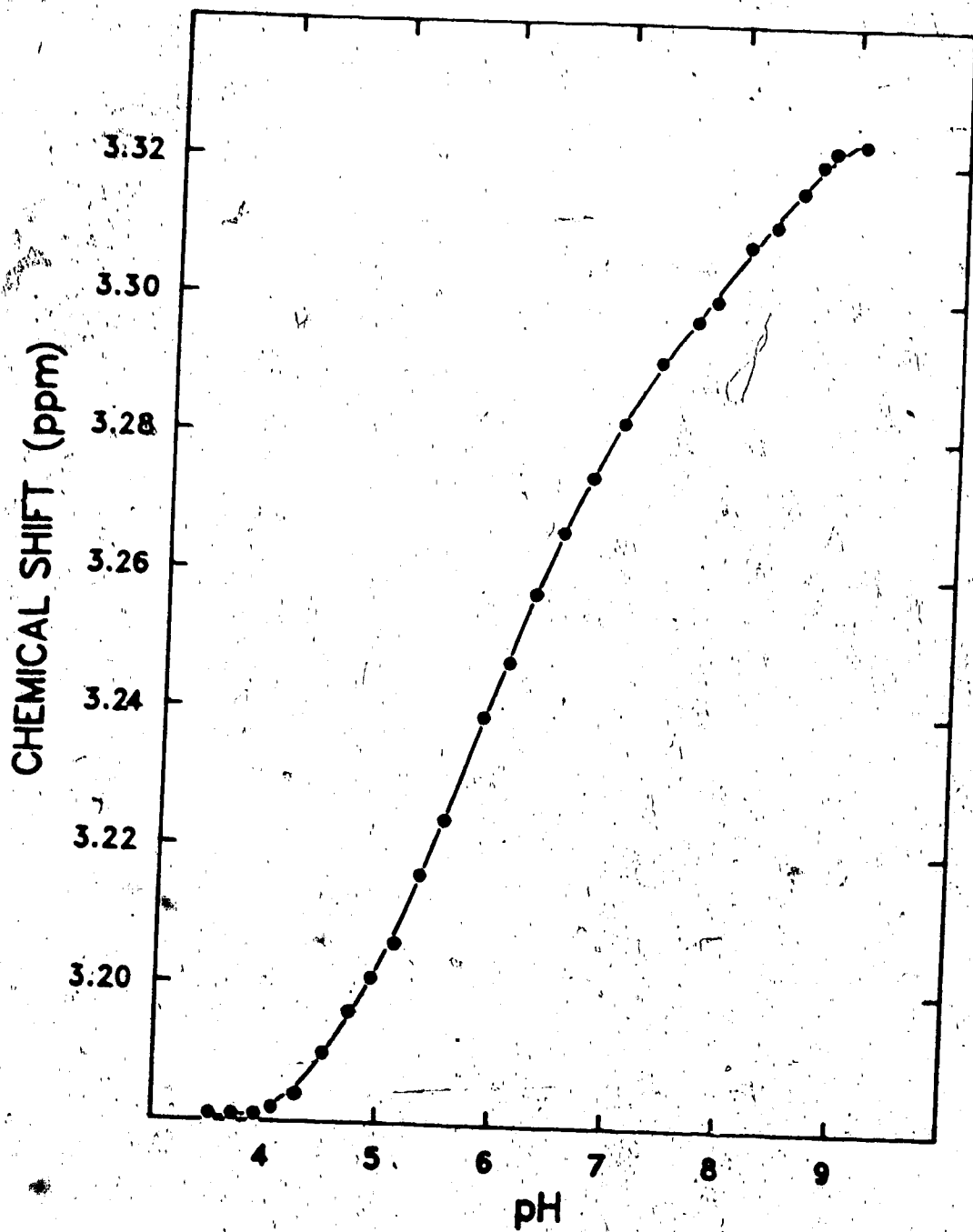


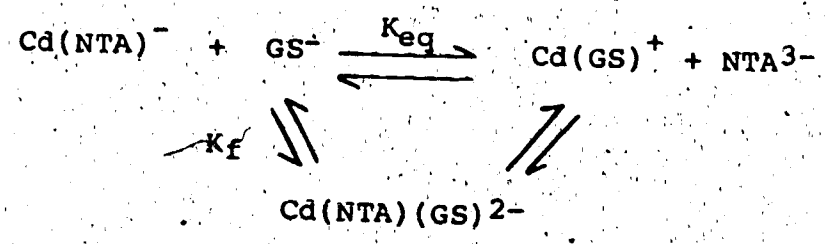
Figure 31. The pH dependence of the chemical shift of methylene protons in bound NTA during titration of an equimolar mixture of $\text{Cd}(\text{NTA})^-$ and glutathione.

free NTA falls under the resonances due to glutamyl g7 and glycyI g1 protons, and thus it is not possible to detect the displacement of NTA from $\text{Cd}(\text{NTA})^-$ by the appearance of a resonance for free NTA. Changes in the ratio A_b/A_{ref} where A_b and A_{ref} are integrated intensities of the resonance for bound NTA ($\text{Cd}(\text{NTA})^- + \text{Cd}(\text{NTA})(\text{GSH})$) and the resonance due to the chemical shift reference (t-butanol) respectively, were measured to detect the displacement of NTA and to determine its concentration. Additional resonances are observed for GSH at high pH. They are indicated by arrows in Figure 30 on the spectrum of a pH 12 sample. These resonances are due presumably to the complex $\text{Cd}(\text{GSH})$ which forms upon displacement of NTA from $\text{Cd}(\text{NTA})^-$ by GSH. To support this assumption, similar resonances are observed in mixtures of Cd^{2+} and only GSH at high pH values.

Changes in the chemical shifts of cysteinyl resonances g5 (curve B in Figure 27) and g2 (curve B in Figure 28) indicate that two main reactions are occurring in the pH range studied. Both resonances suggest one event between pH ~ 4 and ~ 7 affecting mostly the sulfhydryl group when compared to the changes of the glutamyl resonance (Figure 29). The sulfhydryl group must be binding in this region to cadmium possibly with participation of the amino group suggested by the smaller shift in the glutamyl resonances, or two kinds of mixed complexes are formed; one, predominant with binding to the sulfhydryl group and the other with

binding to the amino and carboxylate groups of the glutamyl residue. Above pH ~ 6 a different reaction starts to occur, best demonstrated by the chemical shift behavior of the cysteinyl g2 resonance (Figure 28). A reverse in the direction in which the resonance is shifting is noted. This could signify the decomposition of the earlier formed complex or simply a lesser contribution of the sulfhydryl group to the binding taking place in this region. The downfield shift was caused by binding to Cd(NTA)⁻, therefore the reversal may result from release of GSH or binding to a different species, in this case Cd²⁺. Supporting the binding to Cd²⁺ instead of Cd(NTA)⁻ is broadening of the NTA resonance and the loss of the satellites due to 1H-111Cd, 113Cd coupling (Figure 30).

From the previous discussion, changes observed on the resonances of NTA and GSH protons suggest the following reactions:



To determine K_f and K_{eq}, the above equilibria were studied at a constant pH of 6. Increasing amounts of GSH were added to a solution of Cd(NTA)⁻ and the change in the chemical shift and intensity of the resonance due to bound

NTA was used to determine the concentrations of species in solution. Spectra obtained for a $\sim 0.02M$ solution of $Cd(NTA)^-$ with 0 to $\sim 0.052M$ of GSH are shown in Figure 32. Addition of glutathione caused downfield shifts of the resonance of bound NTA due to the formation of the mixed complex $Cd(NTA)(GSH)$. The dependence of the chemical shift on the concentration of GSH is depicted in Figure 33. From these chemical shifts, the relative amounts of $Cd(NTA)^-$ and $Cd(NTA)(GSH)$ were determined following a procedure similar to that described in section C.2 of this chapter. The concentration of total bound NTA ($Cd(NTA)^- + Cd(NTA)(GSH)$) was obtained from the intensity of the bound NTA resonance. The intensity of this resonance is seen to decrease in Figure 32 as GSH is added due to displacement of free NTA whose resonance overlaps with glutathione's g7 and g1 resonances.

First, the ratio $(A_b/A_{ref})_{Cd(NTA)^-}$ was obtained from the spectrum of the solution of $Cd(NTA)^-$ of known concentration (Cd_t) to which GSH was subsequently added. The ratio A_b/A_{ref} was obtained from the subsequent spectra and the concentration of bound NTA was calculated as follows:

$$[NTA]_b = \frac{Cd_t \times (A_b/A_{ref})}{(A_b/A_{ref})_{Cd(NTA)^-}} \quad (99)$$

The concentration of free NTA was then obtained by difference

$$[NTA]_f = Cd_t - [NTA]_b \quad (100)$$

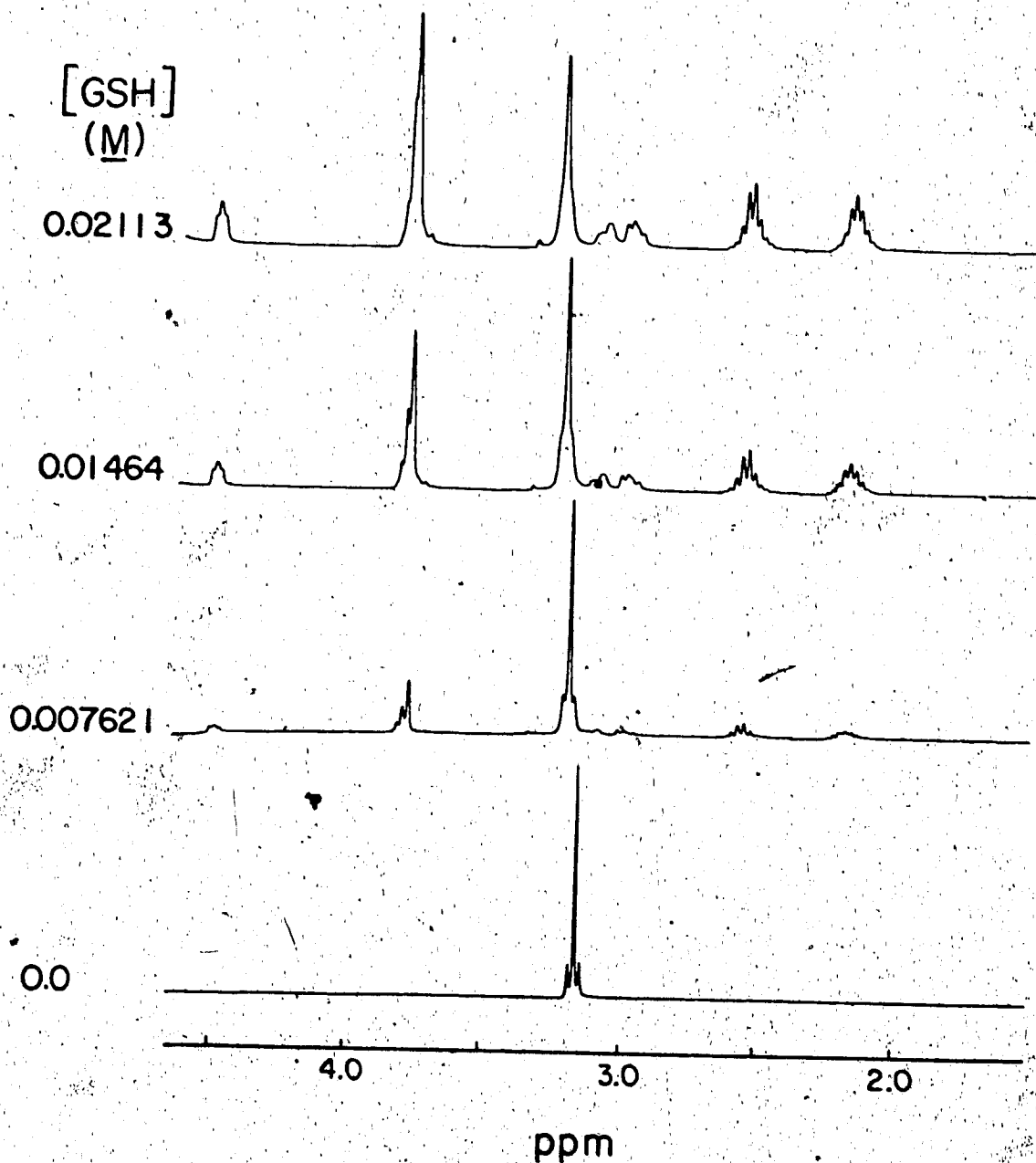


Figure 32. Spectra obtained for solutions containing a fixed concentration of $\text{Cd}(\text{NTA})^-$ ($\sim 0.02\text{M}$) and variable concentrations of GSH ($0 - \sim 0.052\text{M}$) at pH 6.

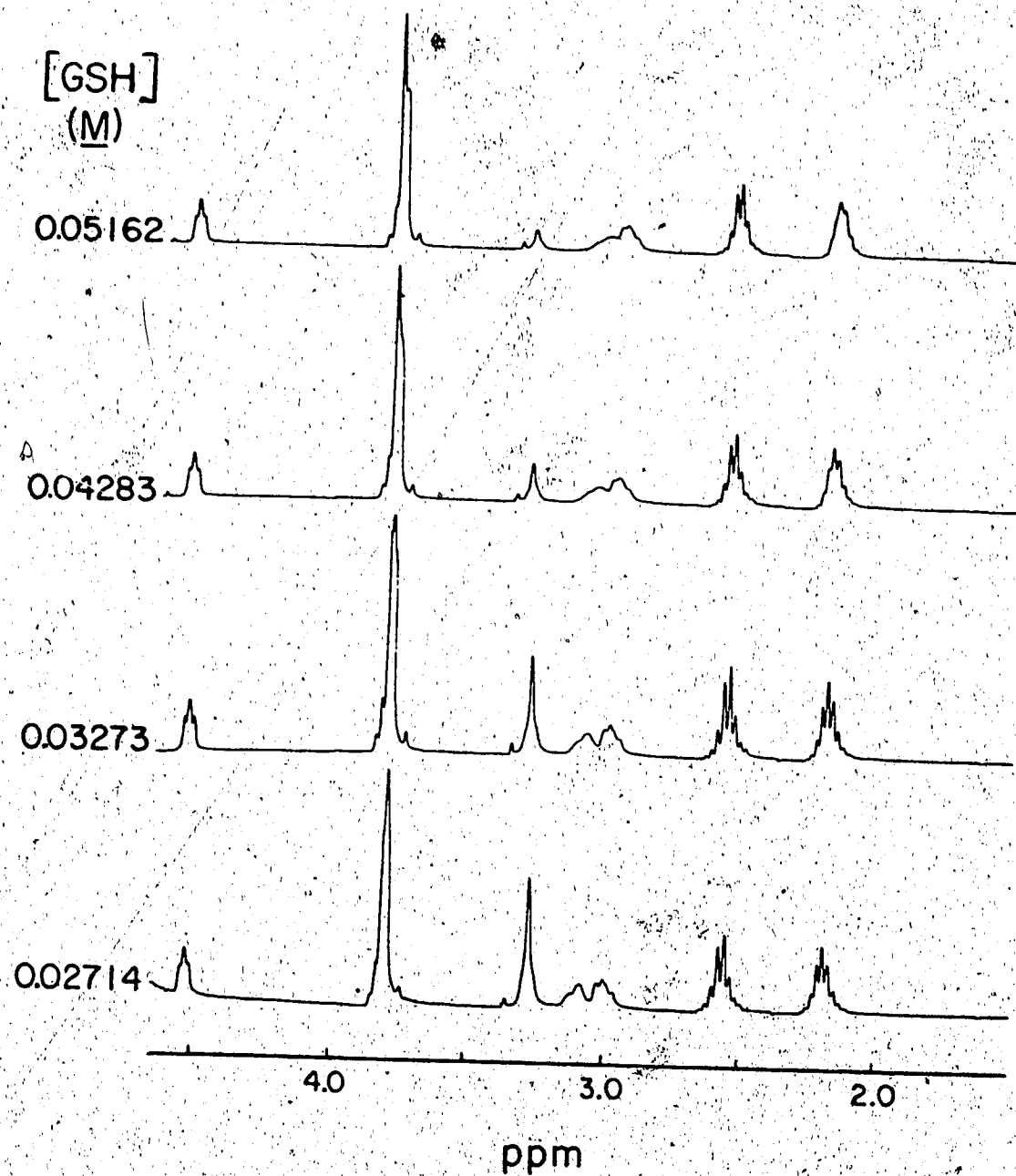


Figure 32. (cont.)

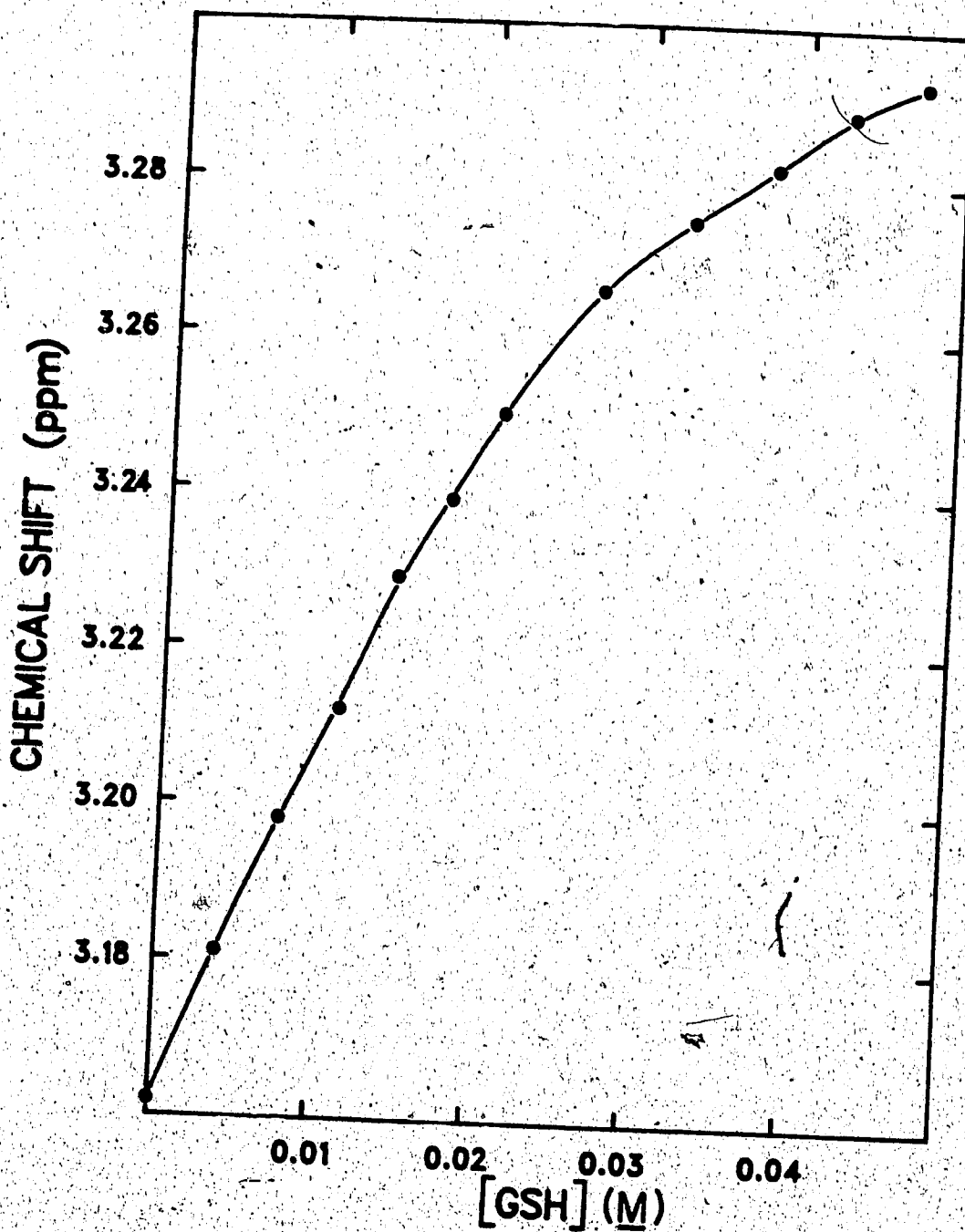


Figure 33. Dependence of the chemical shift of methylene protons in bound NTA on the concentration of GSH added to a solution of Cd(NTA) - 0.02M.

Having determined the concentration of all the species, estimates of K_f and K_{eq} were first obtained for each data point in Figure 33 using expressions given in Section C.2. The values obtained were then refined using KINET to fit the change of the chemical shift of bound NTA versus the total concentration of glutathione. The values obtained are $K_f = (1.02 \pm 0.02) \times 10^5$ and $K_{eq} = (1.64 \pm 0.58) \times 10^{-3}$.

The formation constant of $Cd(SG)$ was deduced from K_{eq} and the formation constant of $Cd(NTA)^-$:

$$K_{f,Cd(SG)} = K_{f,Cd(NTA)^-} \times K_{eq} \quad (101)$$

The value deduced $\log K_{f,Cd(SG)} = 6.64$ is comparable to $\log K_{f,Cd(SG)} = 6.16$ obtained by Rabenstein et al. from potentiometric measurements on solutions containing only Cd^{2+} and GSH [83].

^{13}C NMR measurements made on mixtures containing equimolar amounts of $Cd(NTA)^-$ and GSH also revealed a strong effect on the resonance due to cysteinyl carbons upon complexation. The chemical shifts of cysteinyl C_α , the carbon to which γ_5 proton is attached and glutamyl C_α , the carbon to which γ_7 proton is attached are plotted as a function of pH for solutions of glutathione alone and for mixtures of GSH and $Cd(NTA)^-$ in Figure 34. No data points from mixtures below pH ≈ 6 are plotted because precipitation occurred due to the higher concentrations which had to be used for the ^{13}C NMR measurements. There is a large change in the

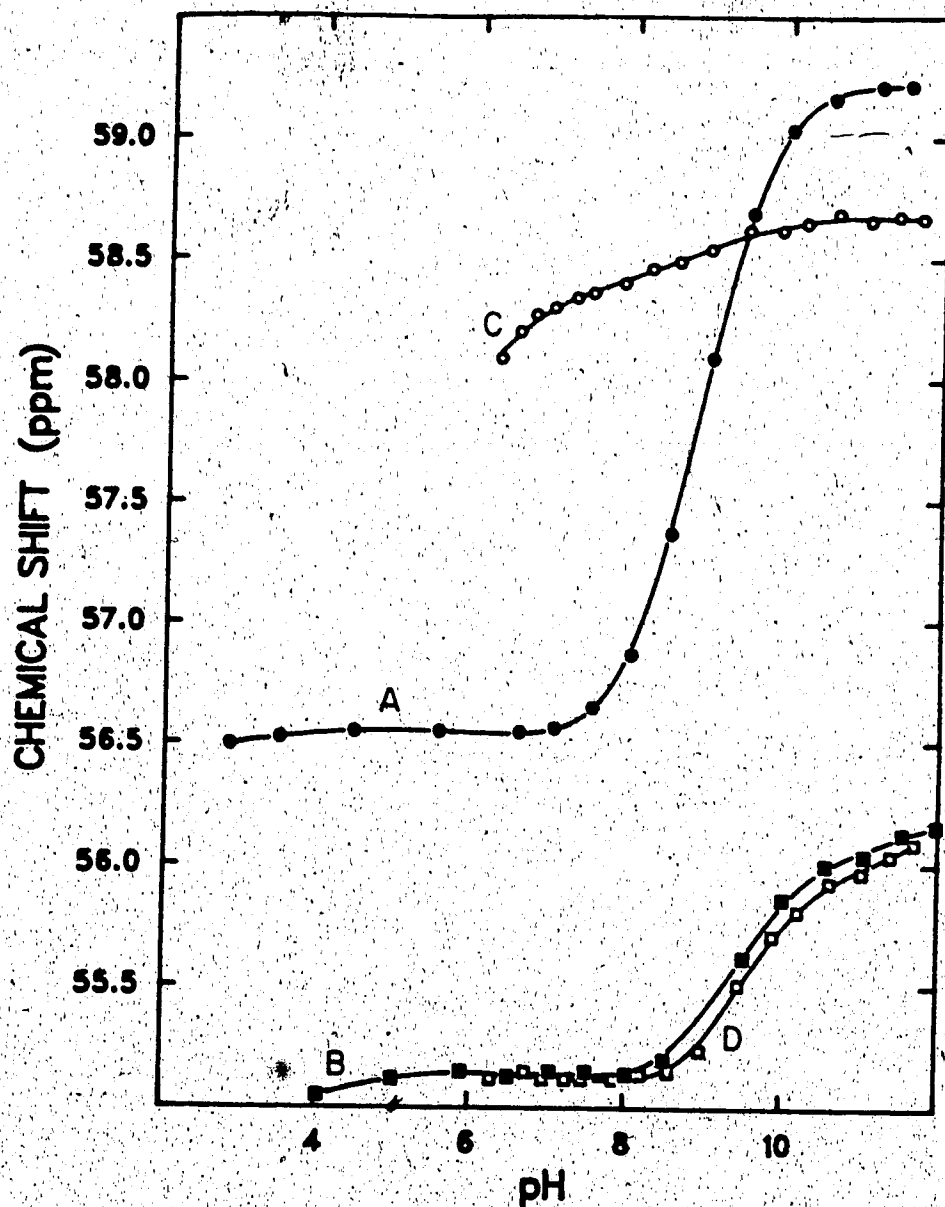


Figure 34. The pH dependence of the chemical shifts of (A) cysteinyl C_{α} and (B) glutamyl C_{α} during titration of glutathione and (C) cysteinyl C_{α} and (D) glutamyl C_{α} during titration of an equimolar mixture of glutathione and $Cd(NTA)^{-}$.

chemical shift of cysteinyl C_α in the mixture (curve B) as compared to GSH solution (curve A) indicating binding to the sulfhydryl group. Between pH 6 and 8, the chemical shifts of glutamyl C_α in the mixture (curve D) are superimposed on those from GSH solutions (curve C). Above pH 8, the latter C_α resonance experiences a shift, however it is much smaller than that of the cysteinyl C_α . This shift occurs in the region where the amino group is being titrated, which suggests some binding to the amino group of the glutamyl residue.

Figure 35 depicts the pH dependence of the chemical shifts of cysteinyl C_β , the carbon to which g2 protons are attached and glutamyl C_β , the carbon to which g4 protons are attached. The titration of GSH alone is represented by curve A for cysteinyl C_β resonance and curve C for glutamyl C_β resonance, while the titration of the 1 to 1 mixture of GSH and $Cd(NTA)^-$ is represented by curve B for cysteinyl C_β resonance and by curve D for glutamyl C_β resonance. The behavior of these resonances reproduces more or less that of cysteinyl and glutamyl C_α resonances. The chemical shift of the resonance due to cysteinyl C_β in the mixture experiences the reversal of direction of change observed with the analogous curve for the g2 protons in Figure 28. The chemical shift of the glutamyl C_β resonance in the mixture experiences a slightly larger shift than that of glutamyl C_α resonance. Thus shifts are observed from

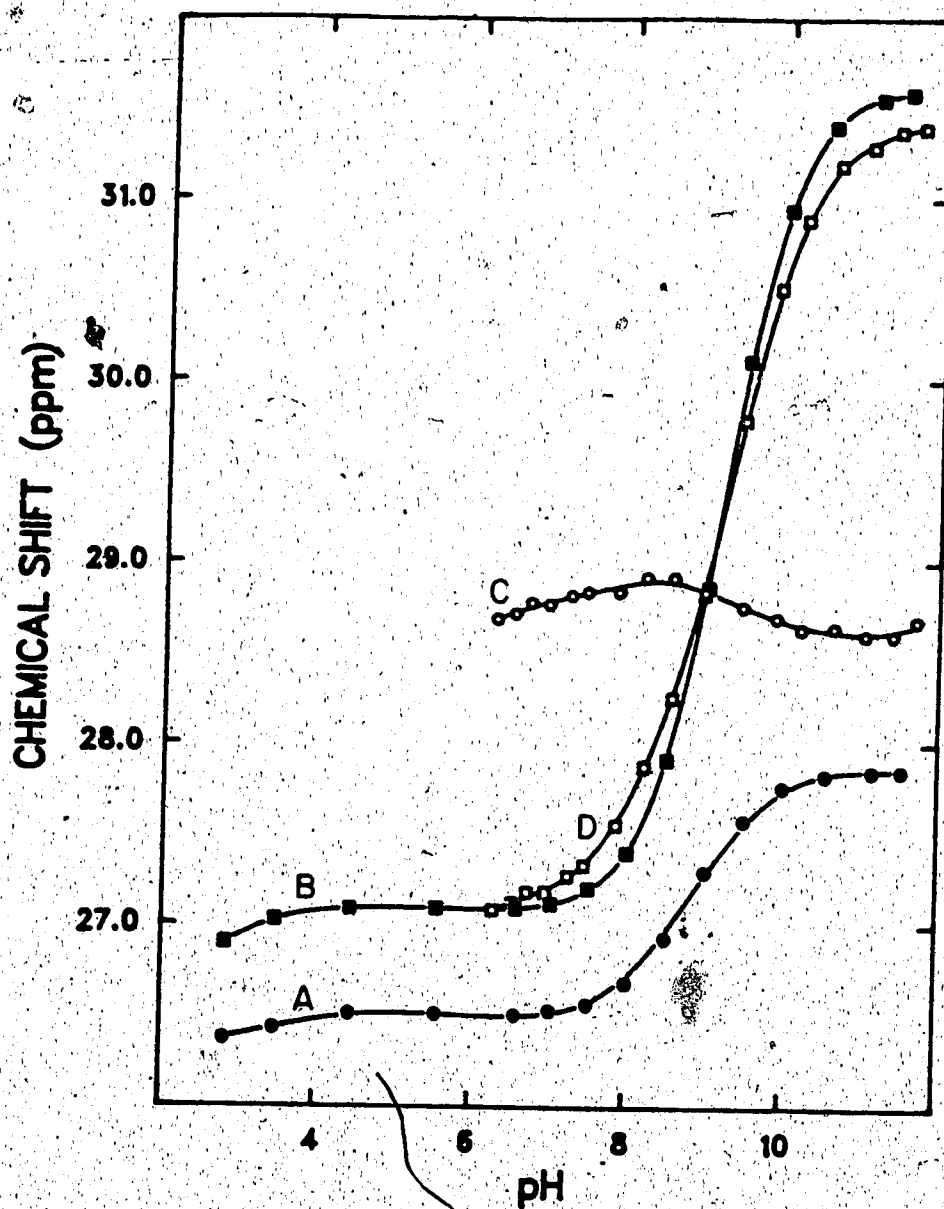


Figure 35. The pH dependence of the chemical shift of (A) cysteinyl C_{β} and (B) glutamyl C_{β} during titration of glutathione; (C) Cysteinyl C_{β} and (D) glutamyl C_{β} during titration of an equimolar mixture of glutathione and $Cd(NTA)^{-}$.

approximately pH 7, which is still higher than the pH's where shifts occur in the resonance due to g7 proton (Figure 29).

6. The Mixed Ligand System Cd(NTA)⁻-S-Methylglutathione

The S-methylated derivative of glutathione was selected to characterize further the contribution of binding to the amino group in the Cd(NTA)⁻-GSH system.

¹H NMR titration of an equimolar mixture of Cd(NTA)⁻ and CH₃SG reveals a behavior very similar to that of the Cd(NTA)⁻-glycine and glutamic acid systems. No free NTA is detected and the resonance for the complexed NTA undergoes a small change in chemical shift as shown by curve C in Figure 36, indicating the formation of the mixed complex Cd(NTA)(CH₃SG). Changes of the chemical shifts of the resonance due to glutamyl g7 protons depicted in Figure 36 indicate that up to pH ~ 6.4 no complexation has taken place. Curve A is defined by experimental data for the titration of the ligand and curve B by experimental data for the titration of the equimolar solution of Cd(NTA)⁻ and CH₃SG. The two curves diverge only above pH 7 indicating that complexation starts to occur at this point. The pH dependence of the chemical shift of g7 during titration of the ligand alone was used to determine the acid dissociation constant (pK_{a3}) using the monoprotic acid model with Kinet. A value of 9.38±0.02 was obtained for pK_{a3} with the fit shown in Figure 36.

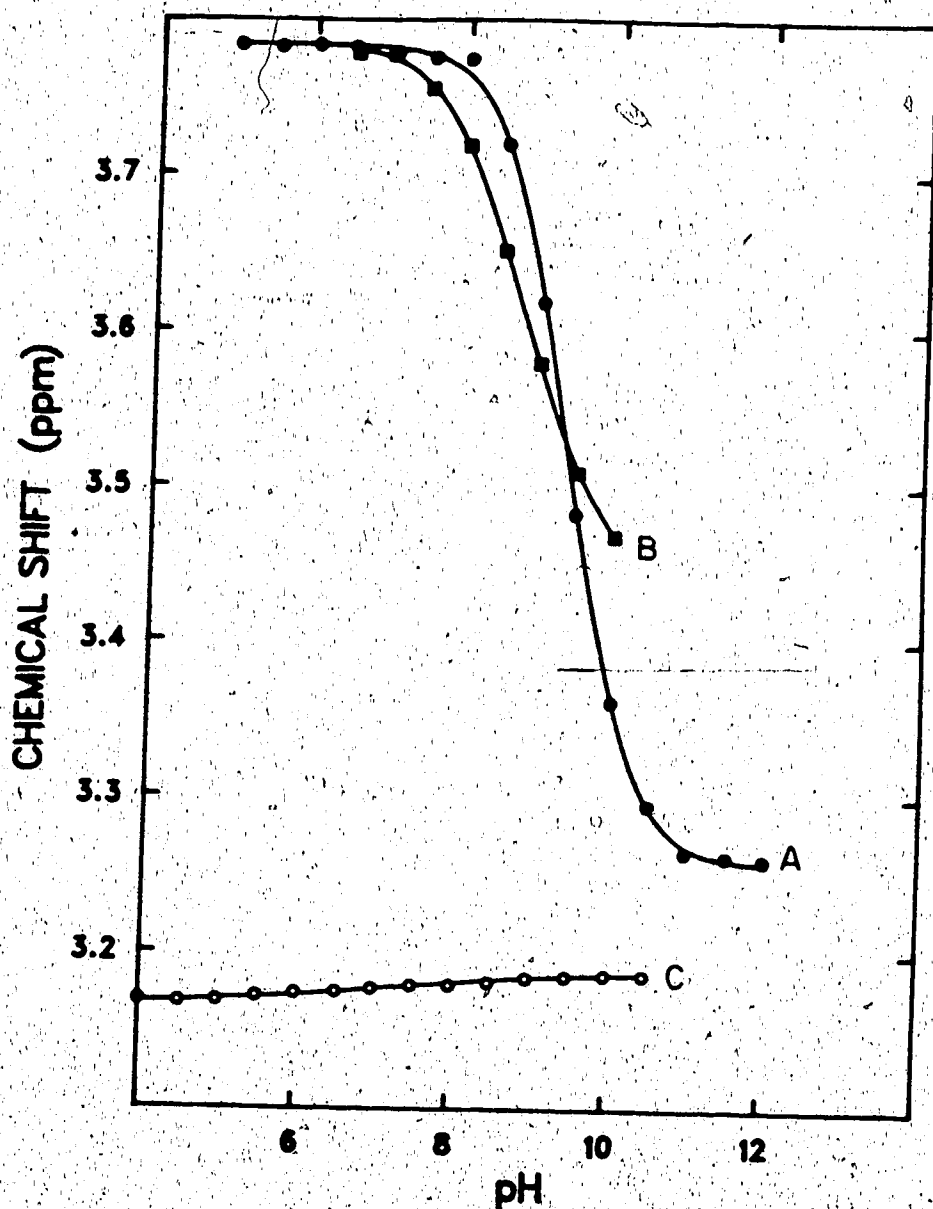


Figure 36. The pH dependence of the chemical shift of (A) g7 proton during titration of S-methylglutathione, (B) g7 proton and (C) methylene protons in bound NTA during titration of an equimolar mixture of S-methylglutathione and Cd(NTA)⁻.

Then the formation constant of the mixed complex was obtained by fitting the chemical shift versus pH data of the titration of the mixture as described in section C.1. The solid line through the experimental data is the calculated curve yielded by KINET with $\log K_f = 2.55 \pm 0.02$. This value is the smallest K_f for all of the mixed ligand complexes which were characterized.

7. Mixed Ligand Complexes of $\text{Cd}(\text{NTA})^-$ and other Thiols

The reactions of $\text{Cd}(\text{NTA})^-$ with cysteine, N-acetylcysteine and mercaptosuccinic acid were also investigated. Cysteine and mercaptosuccinic acid cause extensive displacement of NTA from its $\text{Cd}(\text{NTA})^-$ complex. This displacement is accompanied by a decrease in the intensity of the resonance due to methylene protons in $\text{Cd}(\text{NTA})^-$. In the presence of cysteine and MSA this signal is strongly reduced and broadened, thus precluding accurate measurements of its intensity or chemical shifts. When N-acetylcysteine was allowed to react with $\text{Cd}(\text{NTA})^-$ a number of resonances appeared in the spectra overlapping with the resonances due to N-acetylcysteine's protons and the resonance of bound NTA (Figure 40), hence, the equilibria established in this system could not be quantified. With MSA the resonances were too broadened upon complexation and no quantitative data were obtained. Only a semiquantitative study was accomplished with cysteine.

The chemical shift behavior for the cysteinyl H_α and bound NTA resonances is depicted in Figure 37 as a function of pH for an equimolar solution of cysteine and $Cd(NTA)^-$. Curve A is for the titration of cysteine alone. This data was used to determine the pK_{a2} and pK_{a3} of cysteine. Results obtained were $pK_{a2} = 8.21 \pm 0.01$ and $pK_{a3} = 10.43 \pm 0.01$. Curve B shows the effect of complexation on the chemical shift of the cysteinyl H_α resonance. Curve C shows the shift of the resonance of bound NTA indicating the formation of the mixed complex $Cd(NTA)(Cys)$. The chemical shifts of the resonance of free NTA, not plotted, vary between ~ 3.80 and ~ 3.28 ppm. Consequently the resonance of free NTA overlaps with the cysteinyl H_α resonance. The chemical shift of the resonance due to bound NTA varies between ~ 3.18 ppm and ~ 3.28 ppm, thus some overlap occurs with the resonance due to cysteinyl H_β whose chemical shifts vary between ~ 3.08 ppm and ~ 2.89 ppm.

To quantitate the equilibria, the reaction of $Cd(NTA)^-$ and cysteine was studied at a constant pH of 7.5 where the resonance due to bound NTA is free of interferences. The spectra obtained when increasing amounts of cysteine are added to a solution of $Cd(NTA)^-$ are shown in Figure 38. As was stated before, the resonance for bound NTA is shifted due to formation of the mixed complex (Figure 39) and its intensity decreases indicating the displacement of NTA. The satellites due to the coupling $1H-111Cd$, $113Cd$ are totally

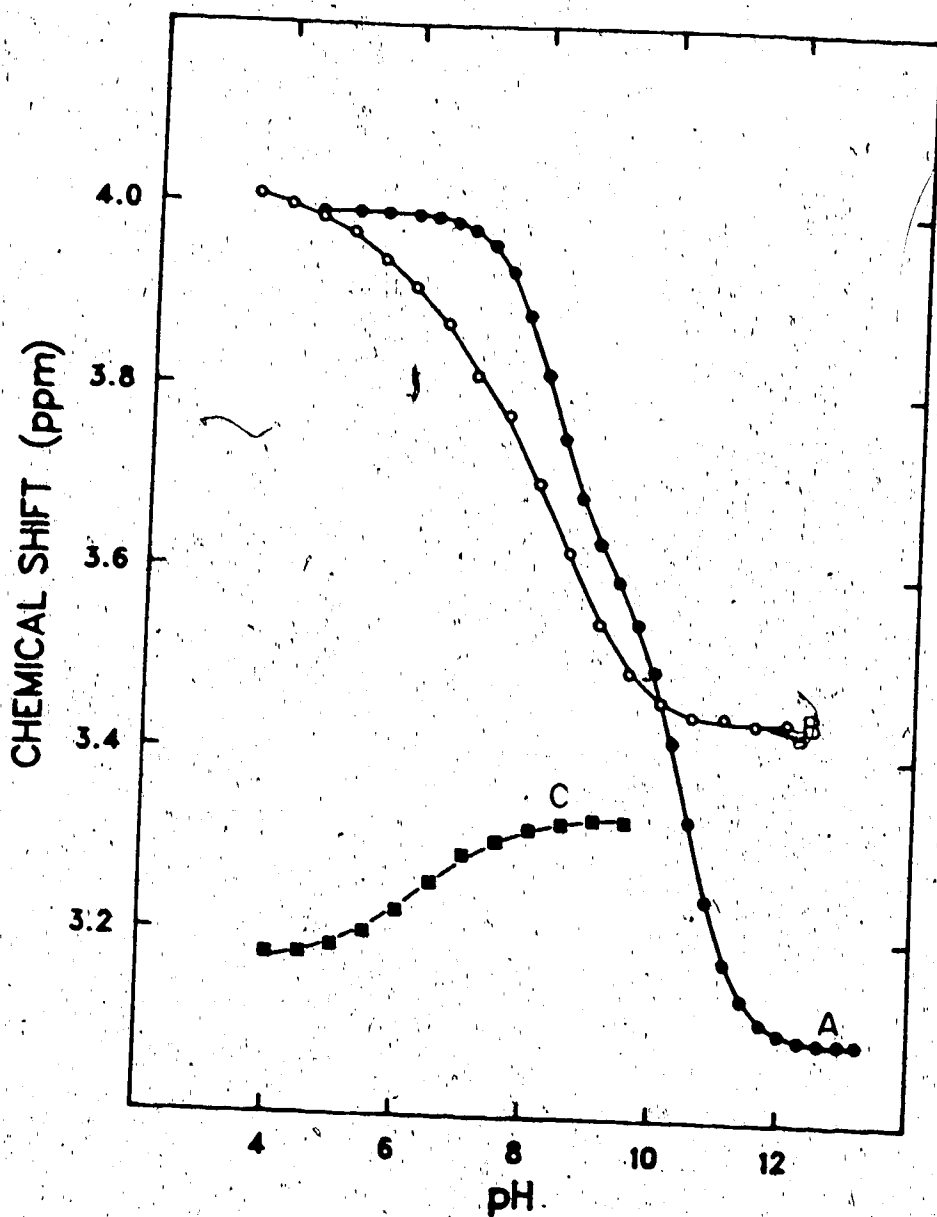


Figure 37. The pH dependence of the chemical shift of (A) H_{α} proton during titration of cysteine, (B) H_{α} and (C) methylene protons in bound NTA during titration of an equimolar mixture of cysteine and $Cd(NTA)^{-}$.

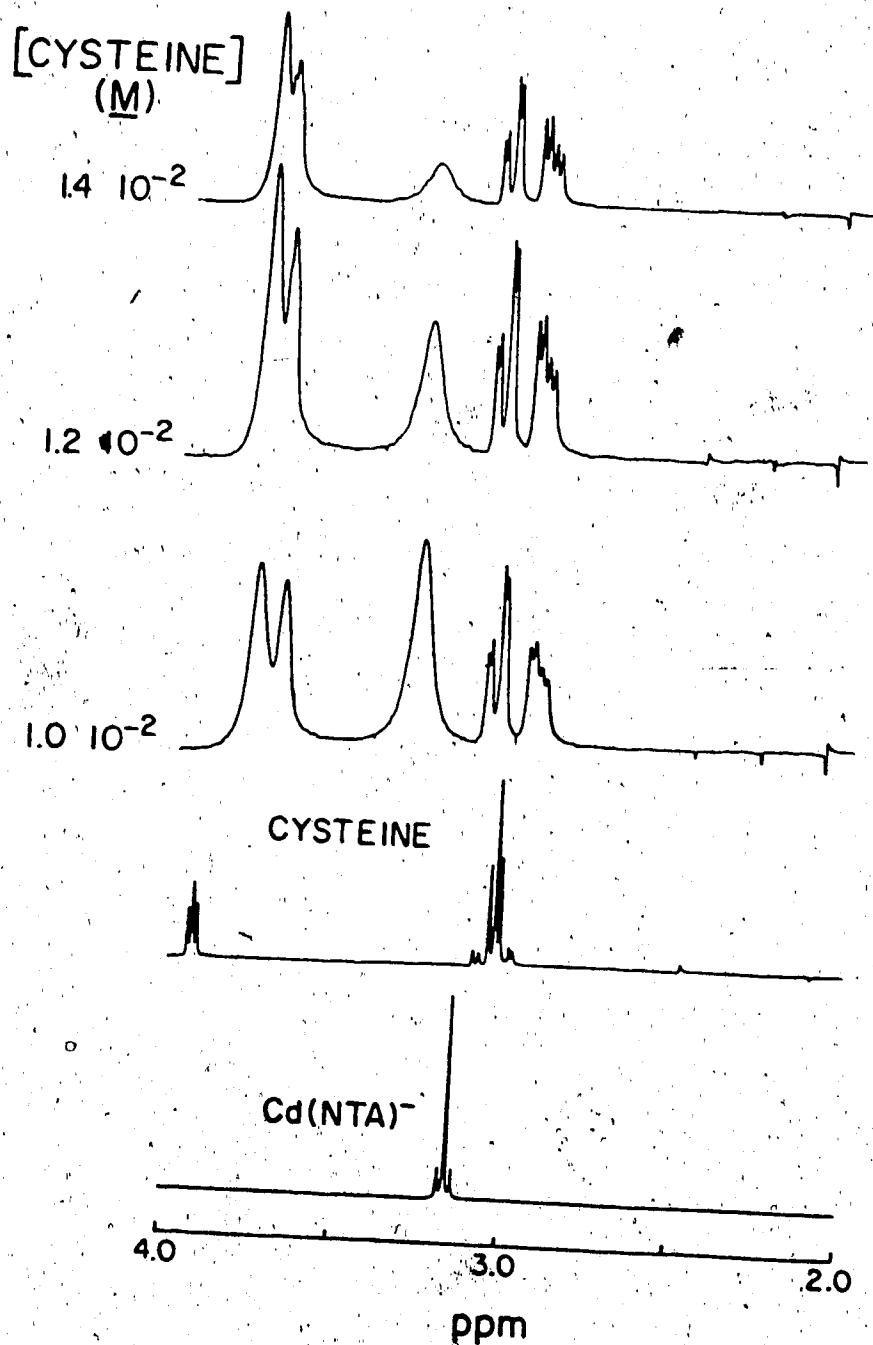


Figure 38. Spectra obtained when variable concentrations of cysteine ($0 \rightarrow 1.4 \times 10^{-2}M$) are added to a solution of Cd(NTA)⁻. Initial concentration of Cd(NTA)⁻ solution = 0.01M.

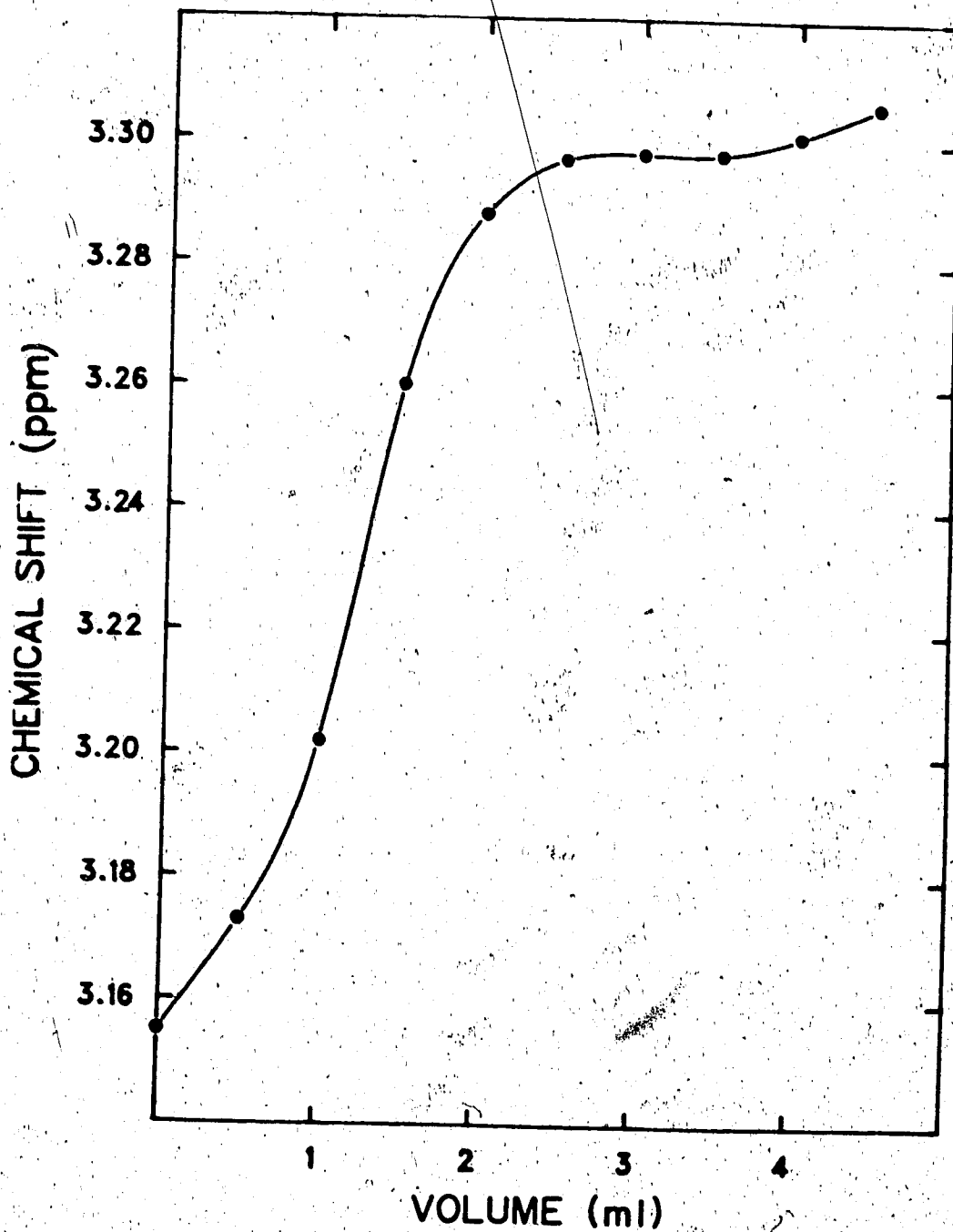


Figure 39. Dependence of the chemical shift of methylene protons in bound NTA on the volume of 0.1M solution of cysteine added to a solution of Cd(NTA)- (0.01M) at pH 7.5.

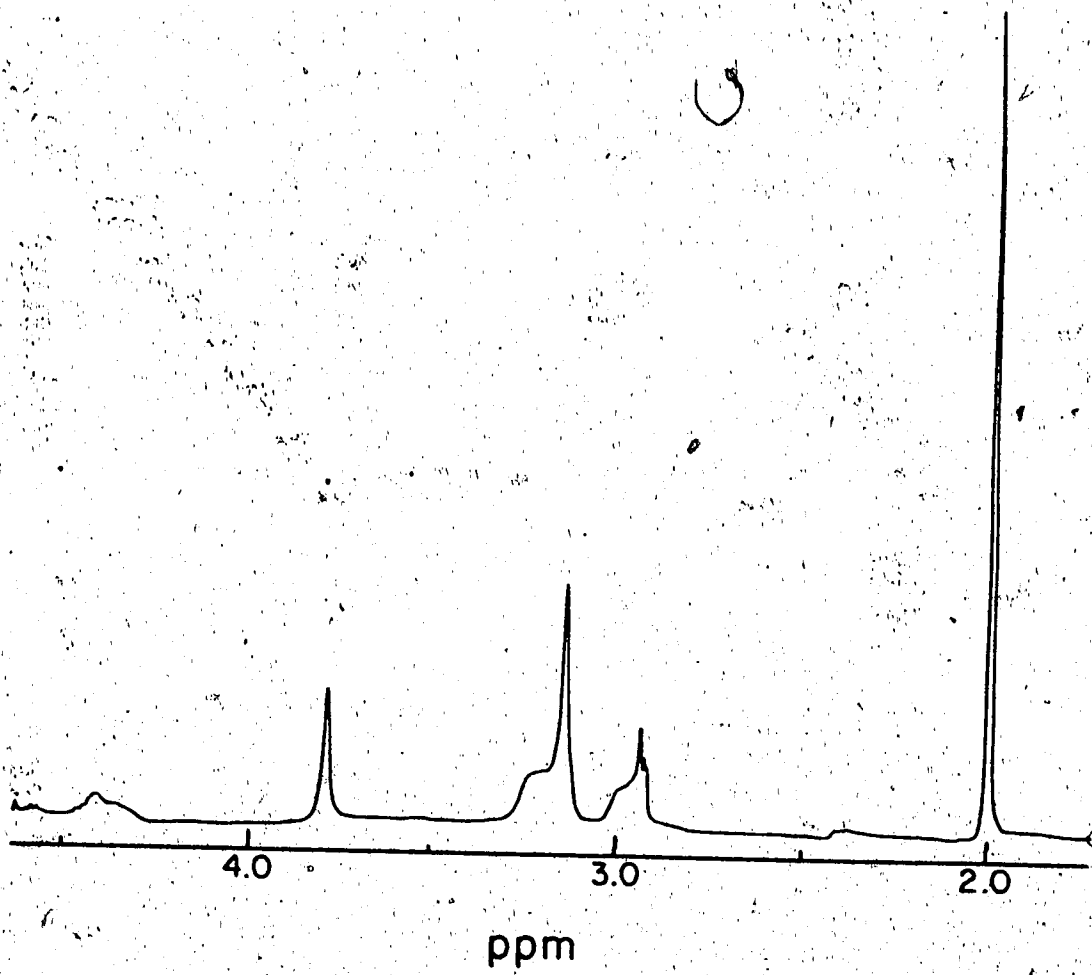


Figure 40. Spectrum of an equimolar mixture of Cd(NTA)- and N-acetylcysteine (0.02M) at pH 7.276.

lost even at low concentrations of cysteine and the resonance is very broad. Due to uncertainty in the measured limiting chemical shift and the intensity of the bound resonance, the determination of K_f and K_{eq} was done for a single experimental data set ($[Cysteine]_t = 5.63 \cdot 10^{-3} M$). The formation constant of the complex $Cd(Cys)$ formed upon displacement of NTA was calculated using K_{eq} and the formation constant of $Cd(NTA)^-$ similarly to the previous thiol systems studied. Results obtained $\log K_f = 9.3$ and $\log K_{f,Cd(Cys)} = 13$ are considered semi-quantitative for the reasons mentioned above.

E. Discussion

The values of the stability constants of the mixed ligand complexes formed by reaction of $Cd(NTA)^-$ with the ligands glycine, glutamic acid and CH_3SG (Table 4) increase with increasing basicity of the ligand, i.e., $CH_3SG < \text{glutamic acid} < \text{glycine}$. However, besides basicity a steric effect contributes to the stability of the mixed complexes. Though all the three ligands have the group $H_2N-CHX-CO_2^-$ which may chelate through the amino and carboxylate groups, the nature of the group X seems to be an important factor in the stability of the mixed complex. In glycine -X is -H, in glutamic acid -X is $-CH_2CH_2CO_2^-$ and in CH_3SG -X is $-CH_2CH_2CONHCH(CH_2SCH_3)CONHCH_2CO_2^-$, resulting in increased

Table 4. Summary of ^1H NMR studies of mixed ligand systems.

Ligand	pK_{a1}	pK_{a2}	pK_{a3}	$\log K_{fCd}(\text{NTA})\text{L}$	$\log K_{fCd}(\text{L})$
NTA			9.36 ± 0.02		9.43
CH_3SG			9.38 ± 0.02	2.55 ± 0.02	
glutamic acid		9.72 ± 0.03		2.79 ± 0.04	
glycine		9.85 ± 0.01		3.26 ± 0.02	
N-PSH	3.21 ± 0.02	10.09 ± 0.01		4.92	9.16
Glutathione		$8.87^a \pm 0.02$	$9.36^b \pm 0.01$	5.01	6.64
PSH		8.09 ± 0.02	10.79 ± 0.03	9.62	11.50
Cysteine		8.21 ± 0.01	10.43 ± 0.01	9.3c	13c
N-Cysteine		9.24 ± 0.01			
MSA		10.20 ± 0.01			

aPKSH

bPK NH_3^+

cSemiquantitative

steric crowding in the mixed complexes in the order given. For these ligands only mixed complexes are formed, and the formation of the mixed complex causes only a small change (~ 0.02 ppm) in the chemical shift of the resonance for bound NTA. The coupling between ^{113}Cd and ^{111}Cd and the NTA protons is retained even at high pH values, meaning that the binding of these ligands to $\text{Cd}(\text{NTA})$ does not significantly alter the strength of the binding between Cd^{2+} and NTA.

With the thiol-containing ligands, the situation is different. For example, the mixed complexes formed with N-PSH and GSH have comparable stability constants (4.92 and 5.02, respectively) even though the pK_a values for their sulfhydryl groups are quite different (pK_a of 10.09 and 8.87). This result supports binding only to the sulfhydryl group in the glutathione system at the pH where K_f was determined. Also, steric effects probably lower the stability of the mixed complex with glutathione. PSH forms a mixed complex with a higher formation constant ($\log K_f = 9.62$). Only the formation of a five member chelate ring in the case of PSH, with S^- and NH_2 acting as donor groups, would account for the large difference between the formation constants of $\text{Cd}(\text{NTA})(\text{GS})$ and $\text{Cd}(\text{NTA})(\text{PS})$. Molecular models were used to explore the possibility of chelate formation in the case of glutathione. Such a complex can be formed according to space filling molecular models. However, a

9-membered chelate ring would be formed, which presumably would be less stable than the 5-member chelate ring. The formation constant of the mixed complex $\text{Cd}(\text{NTA})(\text{GS})$ was determined at pH 6, where ^{13}C NMR data indicate absence of binding to the amino group.

The relative stability of the mixed complexes increases in the order $\text{CH}_3\text{SG} < \text{glutamic acid} < \text{glycine} < \text{N-acetylpenicillamine} = \text{glutathione} < \text{penicillamine} < \text{cysteine}$. As far as the thiols are concerned, this order is the same as that found for the relative effectiveness of the thiols for releasing GSH from its Cd^{2+} complexes in the erythrocytes [33]. GSH was displaced by thiols which have a higher formation constant for their mixed complex $\text{Cd}(\text{NTA})(\text{thiol})$ as compared to that of glutathione's.

Exchange of the ligand between free and $\text{Cd}(\text{NTA})$ -bound forms was rapid on the NMR time scale over the entire pH range studied for glycine, glutamic acid, CH_3SG , penicillamine, N-acetyl penicillamine, cysteine and mercaptosuccinic acid. Two exceptions were the N-acetylcysteine and glutathione at pH higher than 7. Additional resonances were observed at higher pH with glutathione, which were attributed to $\text{Cd}(\text{GSH})$ complex(es). ^{13}C NMR data indicated shifts in the resonances due to glutamyl C_α and C_β above pH 7 suggesting binding to the amino group. The chemical shifts of cysteinyl resonances indicate binding to the sulfhydryl group in this region as well. The smaller

lability of GSH in these complexes with binding to the sulfhydryl and the amino group suggests that glutathione forms with cadmium complexes of fairly rigid structure. Quantitative measurements were done under conditions of rapid exchange where single exchange averaged resonances having a chemical shift between those of free and bound ligand are observed. The use of the changes in the chemical shifts of the ligand resonances for characterizing the formation constants was more favorable than the use of the NTA resonance, in the cases involving the formation of the mixed complexes with glycine, glutamic acid and S-methylglutathione. The effect of this binding is much more pronounced on the ligand resonances than on the NTA resonance. The shift of the resonance due to the ligand could be as large as 0.15 ppm while that of the resonance due to NTA was never more than 0.02 ppm. Also, the ^1H - ^{111}Cd , ^1H - ^{113}Cd coupling in the resonance for bound NTA is always present in the ^1H -NMR spectra for these systems. The retention of this coupling and the small effect of the binding on the chemical shift of $\text{Cd}(\text{NTA})^-$ resonance means that the solution structure of $\text{Cd}(\text{NTA})^-$ complex (Figure 1) is probably retained in the presence of these ligands, which bind through their carboxylate and amino groups.

Thiols, however, cause a strong shift in the resonance of bound NTA as well as broadening of the satellites due to ^1H - ^{111}Cd , ^1H - ^{113}Cd coupling and even their disappearance.

This suggests that the binding of NTA to Cd^{2+} in the mixed complexes $\text{Cd}(\text{NTA})(\text{thiol})$ must be quite different from that in $\text{Cd}(\text{NTA})^-$ alone. Some bonds between NTA and Cd^{2+} must be weakened or broken to cause the loss of the coupling between its protons and the central cadmium ion. The fact that thiols cause NTA to be displaced from $\text{Cd}(\text{NTA})^-$ supports such an alteration in the bonds between Cd^{2+} and NTA.

The release of NTA by thiols is noted by the appearance of a resonance due to free NTA. The $1\text{H}-111\text{Cd}$, $1\text{H}-113\text{Cd}$ coupling is observed in spectra showing release of NTA. The exchange of NTA between its free and bound forms ($\text{Cd}(\text{NTA})^-$ $\text{Cd}(\text{NTA})\text{L}$) is therefore slow on the NMR time scale. Consequently, the change observed in the chemical shift of the resonance for bound NTA is solely caused by the formation of the mixed complex and was used to determine the relative concentrations of $\text{Cd}(\text{NTA})^-$ and $\text{Cd}(\text{NTA})\text{L}$ species. However, at higher pH (e.g., pH 8 for N-acetylpenicillamine), only one broad resonance is observed for the NTA protons, meaning that NTA is exchanging more rapidly between its free and bound forms at high pH values.

CHAPTER IV

CHARACTERIZATION OF CADMIUM-GLUTATHIONE COMPLEXES

BY ^{113}Cd NMR

A. Introduction

The nuclear magnetic resonance characteristics of cadmium were reviewed in the introductory chapter. Illustrations were also given of the utility of ^{113}Cd NMR in probing the solution structure, interactions and dynamics of a wide variety of cadmium compounds. The first reports of the observations of ^{113}Cd NMR signals, about a decade ago, indicated the potential of ^{113}Cd NMR in elucidating the nature of cadmium complexes [18,19]. It was evident from the studies conducted that the position of the resonance was extremely sensitive to the nature of the coordinating group; upfield shifts were produced by oxygen ligands, downfield by nitrogen and sulfur ligands.

Development of the pulse Fourier Transform (P/FT) technique made possible a faster acquisition of ^{113}Cd NMR spectra. As a result a larger number of ^{113}Cd NMR studies of Cd(II) systems appeared [20,85,86]. Subsequently, the use of ^{113}Cd NMR has expanded to the study of the binding of Cd^{2+} by more complicated biological macromolecules. The characteristic chemical shift of ^{113}Cd bonded to a certain

type of donor group, the extreme sensitivity of the chemical shift to subtle changes in the environment of the cadmium ion, and to ligand exchange dynamics, make ^{113}Cd NMR a powerful tool for the study of biological systems [37,43,87]. Observation of ^{113}Cd NMR signals from metal binding macromolecules were made by Armitage, Coleman et al. [38], Sudmeier [39], Ellis et al. [51], Drakenberg et al. [40] and Myers [41]. The solution structures of human [28], rabbit [88] and calf [89] liver Cd(II)-substituted metallothioneins were elucidated by Armitage et al. Several ^{113}Cd multiplet resonances were observed in the chemical shift range 600-670 ppm, consistent with tetrahedral binding of four sulfur atoms to the Cd(II). For comparison, the resonance for the tetrahedral Cd(II) in the CdS_4 site of the polynuclear $\text{Cd}_{10}(\text{SCH}_2\text{CH}_2\text{OH})_{16}^{4+}$ complex has a chemical shift of 652 ppm [90]. Selective homonuclear decoupling experiments led to the assignment of the resonances for the Cd(II)-substituted metallothioneins to four and three metal clusters which are bridged by sulfur.

The Cd(II)-substituted form of the calcium binding muscle protein, troponin C, was investigated by Ellis et al. [43]. They were able to resolve and assign four resonances between -103 ppm and -113 ppm to four different binding sites in the protein. The observed resonances are strongly shielded and result from ^{113}Cd which is complexed by oxygen donor groups.

Reported in this chapter is a detailed study of the Cd^{2+} -glutathione system by ^{113}Cd NMR. Interest in this study stems from the finding, reported in the introduction, that Cd^{2+} in human erythrocytes binds primarily to GSH and hemoglobin [33], and thus the importance of Cd-GSH complexes in the toxicology of cadmium. The dependence of the observed ^{113}Cd NMR resonances on the pH, the concentration and the temperature was investigated. ^{13}C NMR measurements were also made on the system, in an attempt to determine the stoichiometry of the complexes formed. ^{13}C and ^1H NMR measurements are also used to support the interpretation of the ^{113}Cd NMR results. ^{113}Cd NMR measurements were also made on solutions containing Cd^{2+} and cysteine, Cd^{2+} and penicillamine and Cd^{2+} and N-acetylpenicillamine for comparison.

B. Results and Discussion

1. ^1H -NMR Studies

The investigation of the complexation of glutathione by cadmium using ^{113}Cd NMR was preceded by preliminary measurements by ^1H and ^{13}C NMR. Solutions used in this study were prepared in H_2O which contained 5% D_2O for a spectrometer lock signal. ^1H NMR spectra recorded for solutions having a ratio of $\text{GSH}/\text{Cd}^{2+}$ of 2 are shown in Figure 41 as a function of pH. Starting at the low pH end, the spectra of mixtures

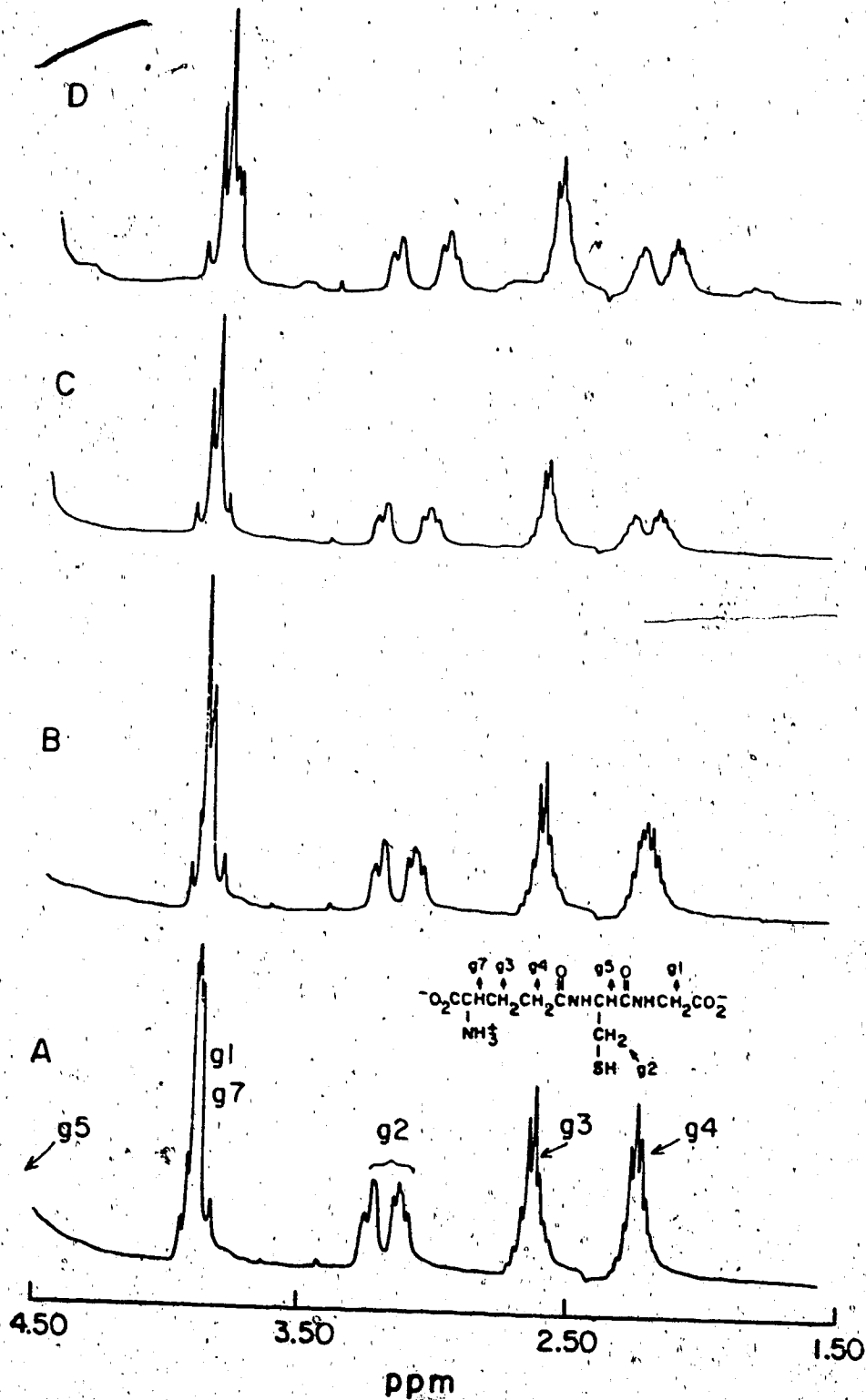


Figure 41. ^1H NMR spectra of 1:2 mixtures of Cd^{2+} and glutathione at pH (A) 6.00, (B) 7.01, (C) 8.01, (D) 8.50, (E) 9.50, (F) 10.50, (G) 10.91, and (H) 12.05. $[\text{Cd}^{2+}] = 0.1\text{M}$

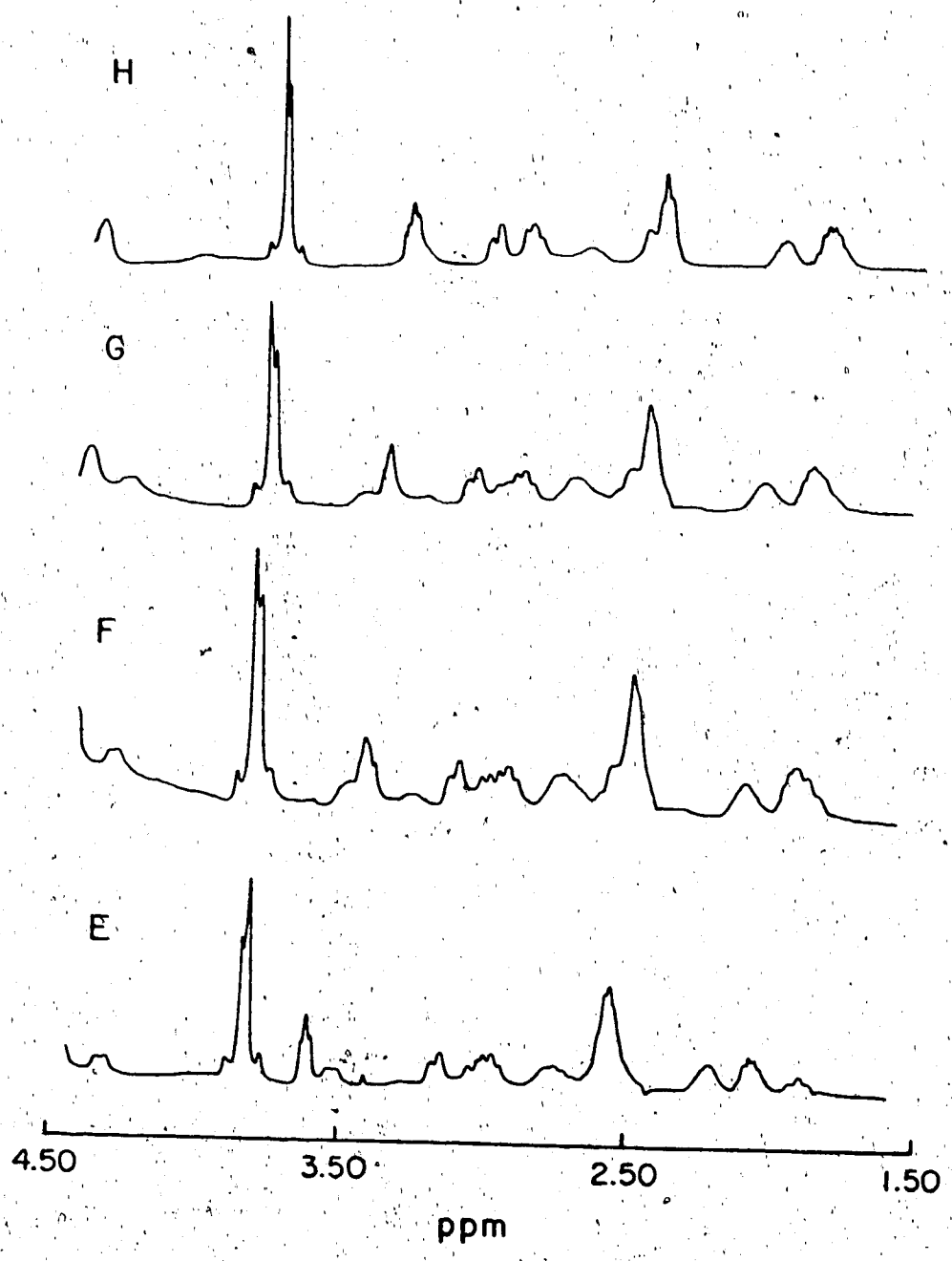


Figure 41. (continued)

of Cd^{2+} and glutathione resemble those of glutathione alone in that the number of resonances observed is the same in both cases. Resonances have undergone shifts, compared to their chemical shifts in GSH alone, due to complexation. This effect is illustrated in Figures 42 to 47. The methine protons (g5) and methylene protons (g2) of the cysteinyl residue experience the largest shifts (Figures 42 and 43) indicating the importance of the binding of Cd^{2+} to the sulfhydryl group. Resonances due to the glutamyl protons (Figures 44 to 46) are also shifted, although the shifts are somewhat smaller, suggesting that the amino and/or carboxylate groups of the glutamyl residue are also involved in the complexation. The resonance due to glycyl g1 protons (Figure 47) experiences a small shift as well. This shift results most probably from the close proximity of the glycyl protons g1 to the reacting site on the cysteinyl residue. New resonances appear in the spectra of mixtures starting at pH 8.5 (Figure 41). This indicates the formation of kinetically stable complexes meaning that exchange among them is slow on the NMR time scale. The new resonances are found beside the resonances due to cysteinyl protons g2 and g5 and glutamyl protons g3, g4 and g7. Because the 'new resonances' occur only at high pH where the amino group is being titrated, they were attributed to coordination of the amino group of the glutamyl residue. Given that new sets of resonances are also observed for the cysteinyl protons, the

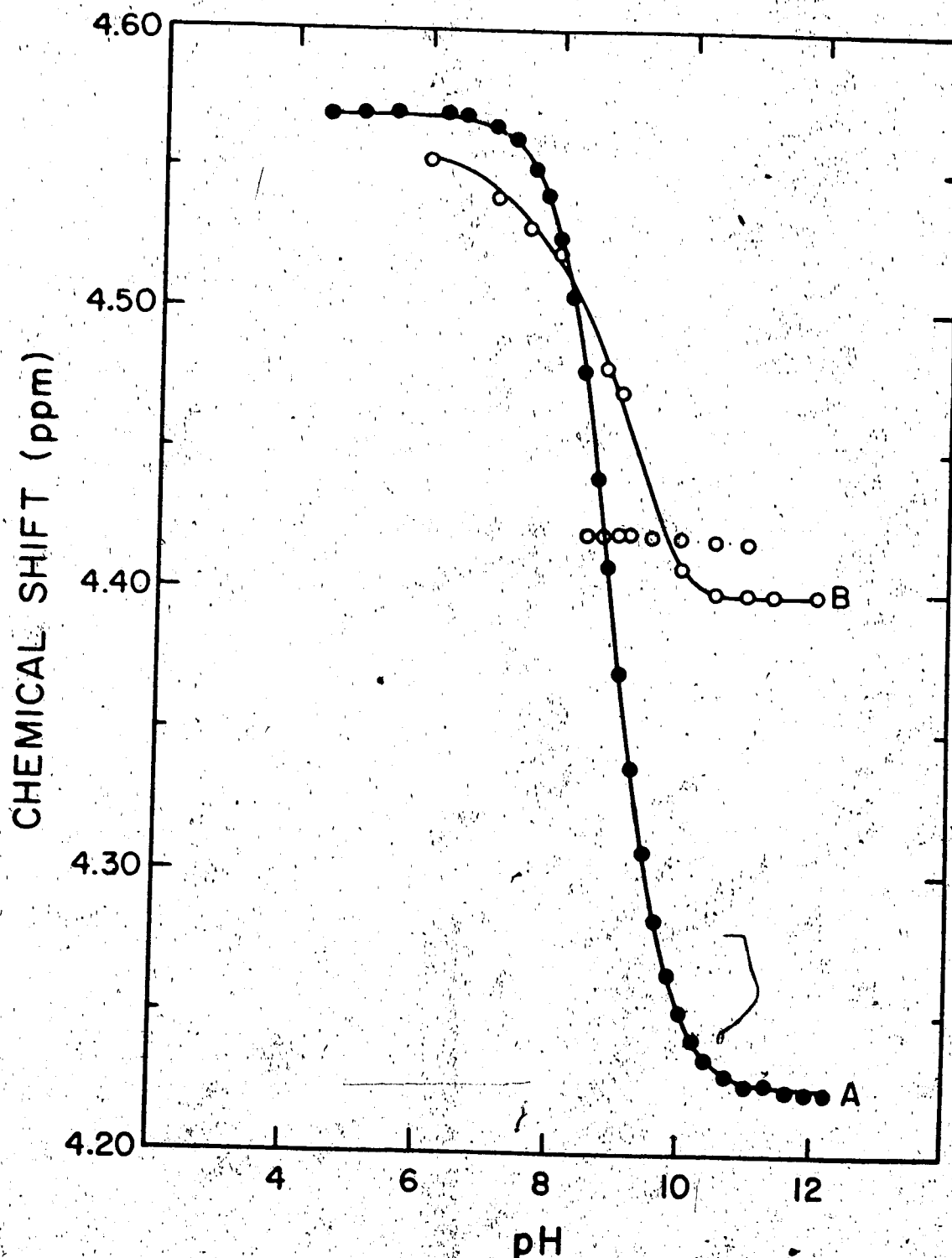


Figure 42. pH Dependence of the chemical shift of cysteinyl g5 protons (A) during titration of GSH (0.02M) and (B) during titrations of a 1:2 mixture of Cd^{2+} (0.1M) and GSH (0.2M). The points in (B) which are off the smooth curve are for the additional slow exchange resonances.

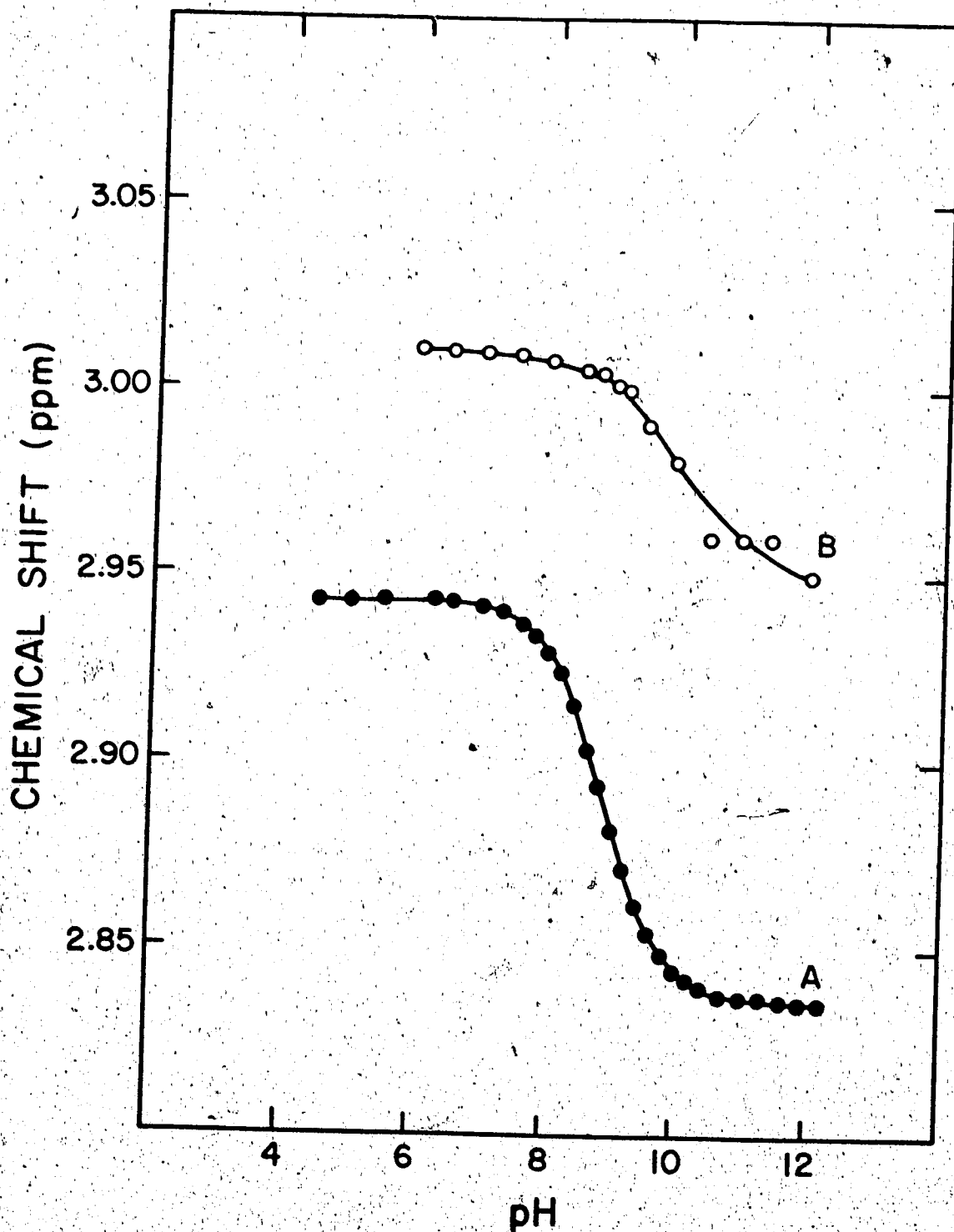


Figure 43. pH Dependence of the chemical shift of cysteinyl g2 protons (A) during titration of GSH (0.02M) and (B) during titrations of a 1:2 mixture of Cd^{2+} (0.1M) and GSH (0.2M). The points in (B) which are off the smooth curve are for the additional slow exchange resonances.

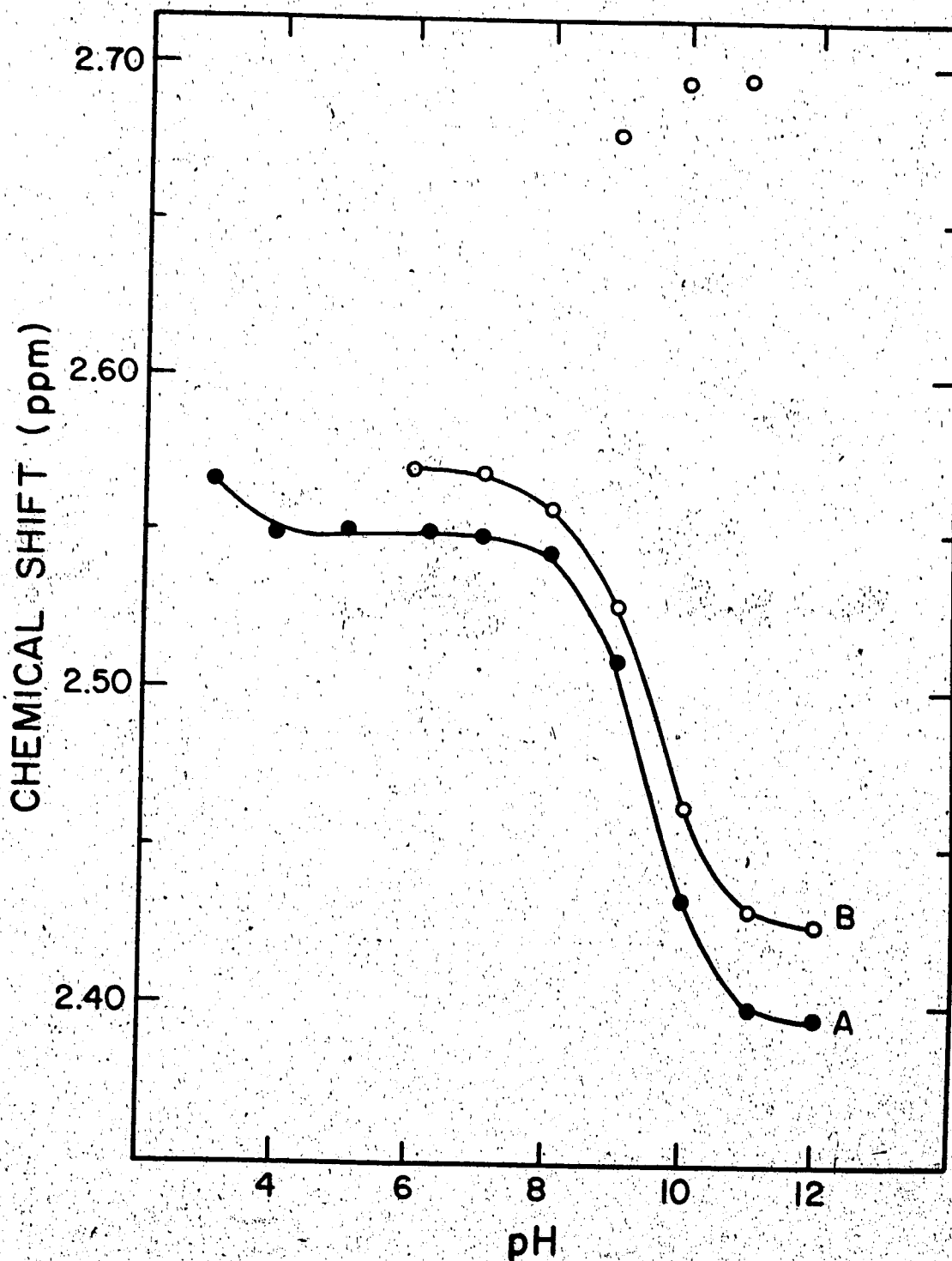


Figure 44. pH Dependence of the chemical shift of glutamyl g3 protons (A) during titration of GSH (0.02M) and (B) during titrations of a 1:2 mixture of Cd^{2+} (0.1M) and GSH (0.2M). The points in (B) which are off the smooth curve are for the additional slow exchange resonances.

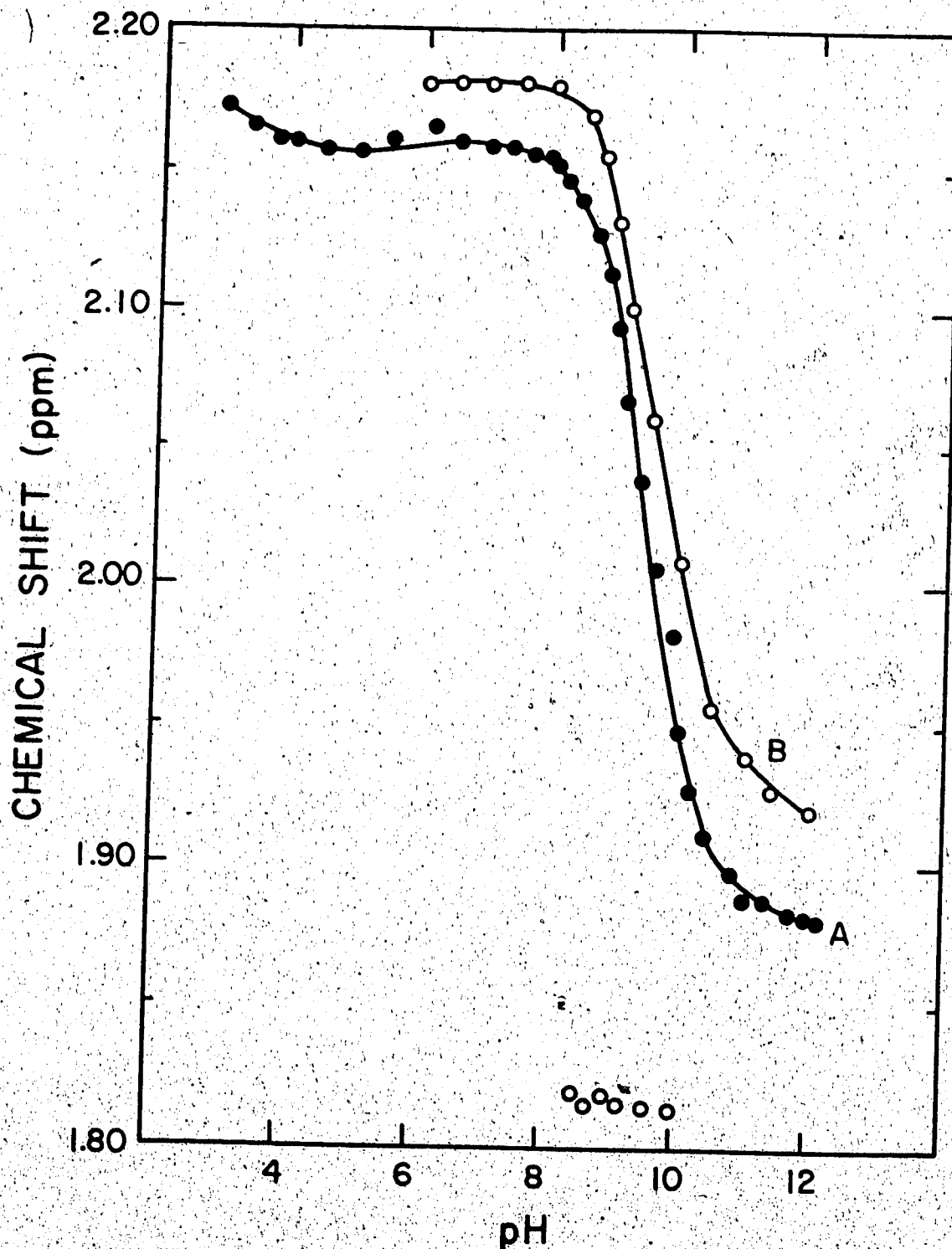


Figure 45. pH Dependence of the chemical shift of glutamyl 94 protons (A) during titration of GSH (0.02M) and (B) during titrations of a 1:2 mixture of Cd^{2+} (0.1M) and GSH (0.2M). The points in (B) which are off the smooth curve are for the additional slow exchange resonances.

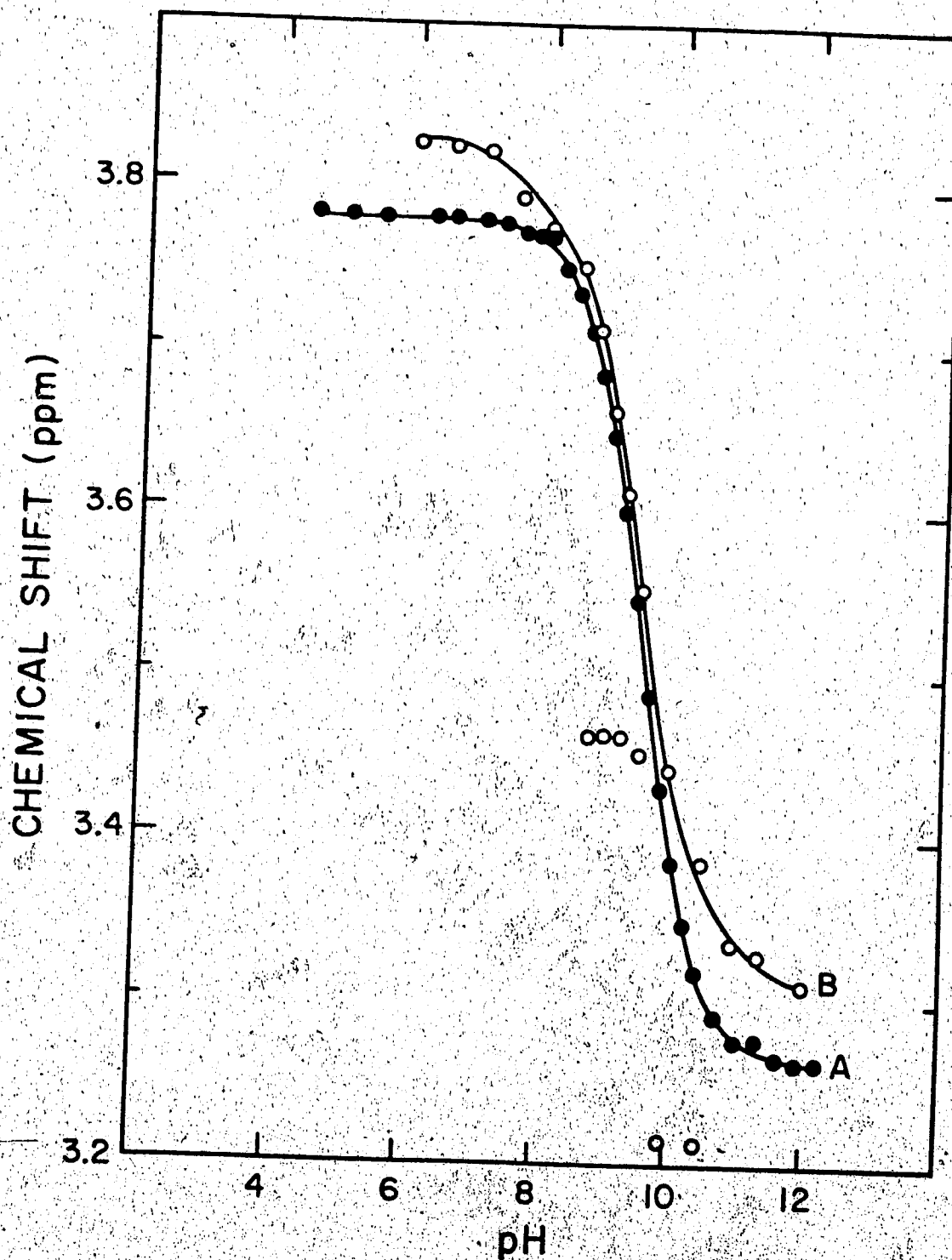


Figure 46. pH Dependence of the chemical shift of glutamyl g7 protons (A) during titration of GSH (0.02M) and (B) during titrations of a 1:2 mixture of Cd^{2+} (0.1M) and GSH (0.2M). The points in (B) which are off the smooth curve are for the additional slow exchange resonances.

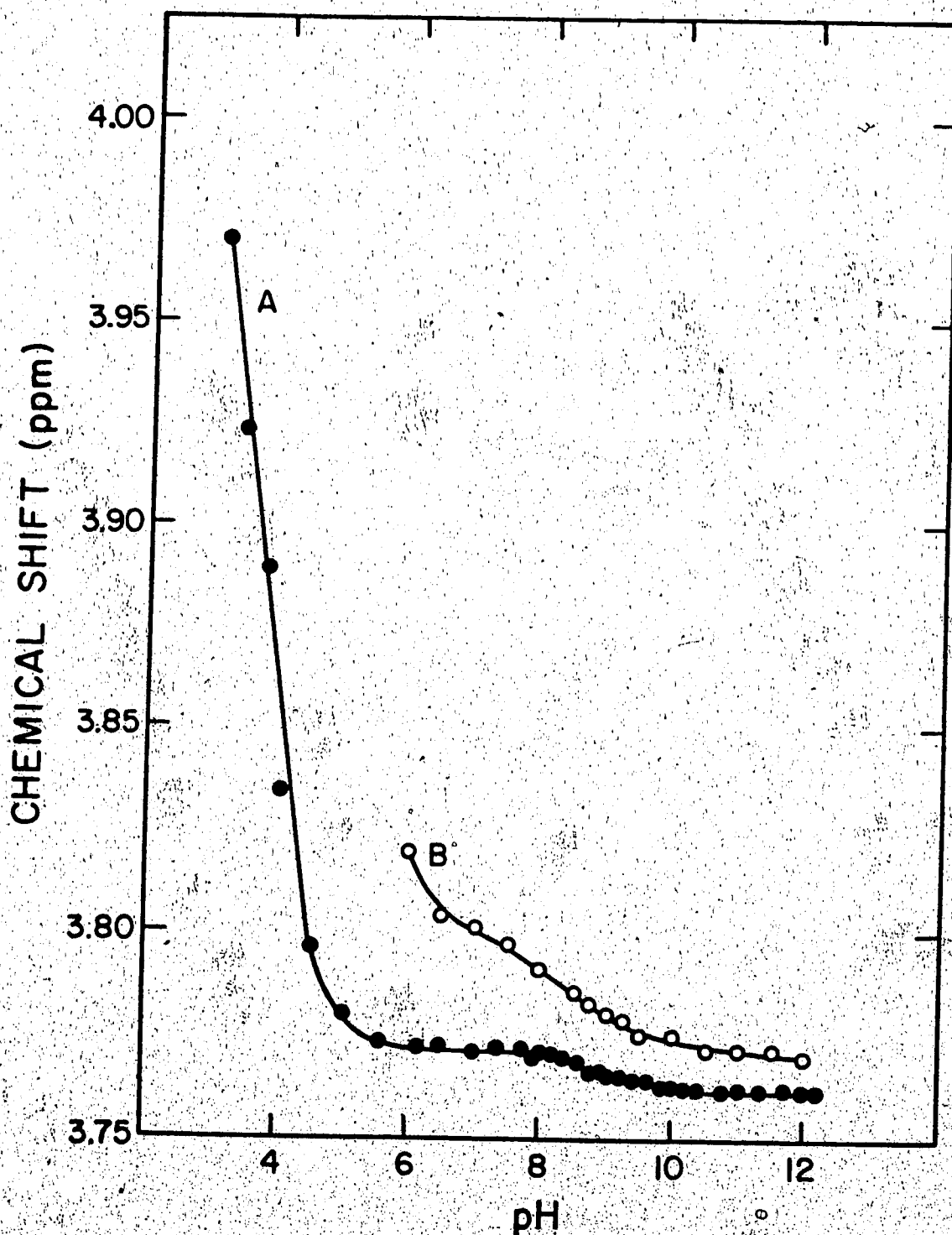


Figure 47. pH Dependence of the chemical shift of glyceryl glycolate protons (A) during titration of GSH (0.02M) and (B) during titrations of a 1:2 mixture of Cd^{2+} (0.1M) and GSH (0.2M).

complexes formed must involve binding to the sulfhydryl groups as well as to the amino group.

A mole ratio study was done at pH 9.5, where the new resonances are the most intense. The total concentration of cadmium was kept at $\sim 0.1M$ and that of glutathione was varied from $\sim 0.2M$ to $\sim 0.8M$. Such high concentrations were used to maintain similar experimental conditions for 1H , ^{13}C and ^{113}Cd NMR measurements. It was not possible to use a glutathione concentration less than $0.2M$ due to precipitation of $Cd(OH)_2$. Representative spectra are shown in Figure 48. From a ratio GSH/Cd^{2+} of 3 and above, the resonances for the kinetically stable complexes do not appear in the spectra and the multiplets of the remaining single sets of resonances become better resolved. Changes can be observed in the resonance due to glycy1 g1 protons. Its multiplet lines are sharper and better resolved. Its chemical shift however remains constant from a ratio Cd^{2+}/GSH of 0.1 to 0.5 (Figure 49), suggesting that the glycy1 residue is not directly involved in the complexation of Cd^{2+} as mentioned earlier. Contrary to glycy1 g1 protons, increase in the concentrations of GSH causes the resonances due to cysteinyl and glutamyl protons to shift (Figure 49). The largest changes in chemical shifts are undergone by both the cysteinyl g2 and g5 resonances, 0.086 and 0.097 ppm, respectively, as compared to 0.01 ppm for resonances due to protons g7 and g3 and 0.036 ppm for g4 protons. The previous

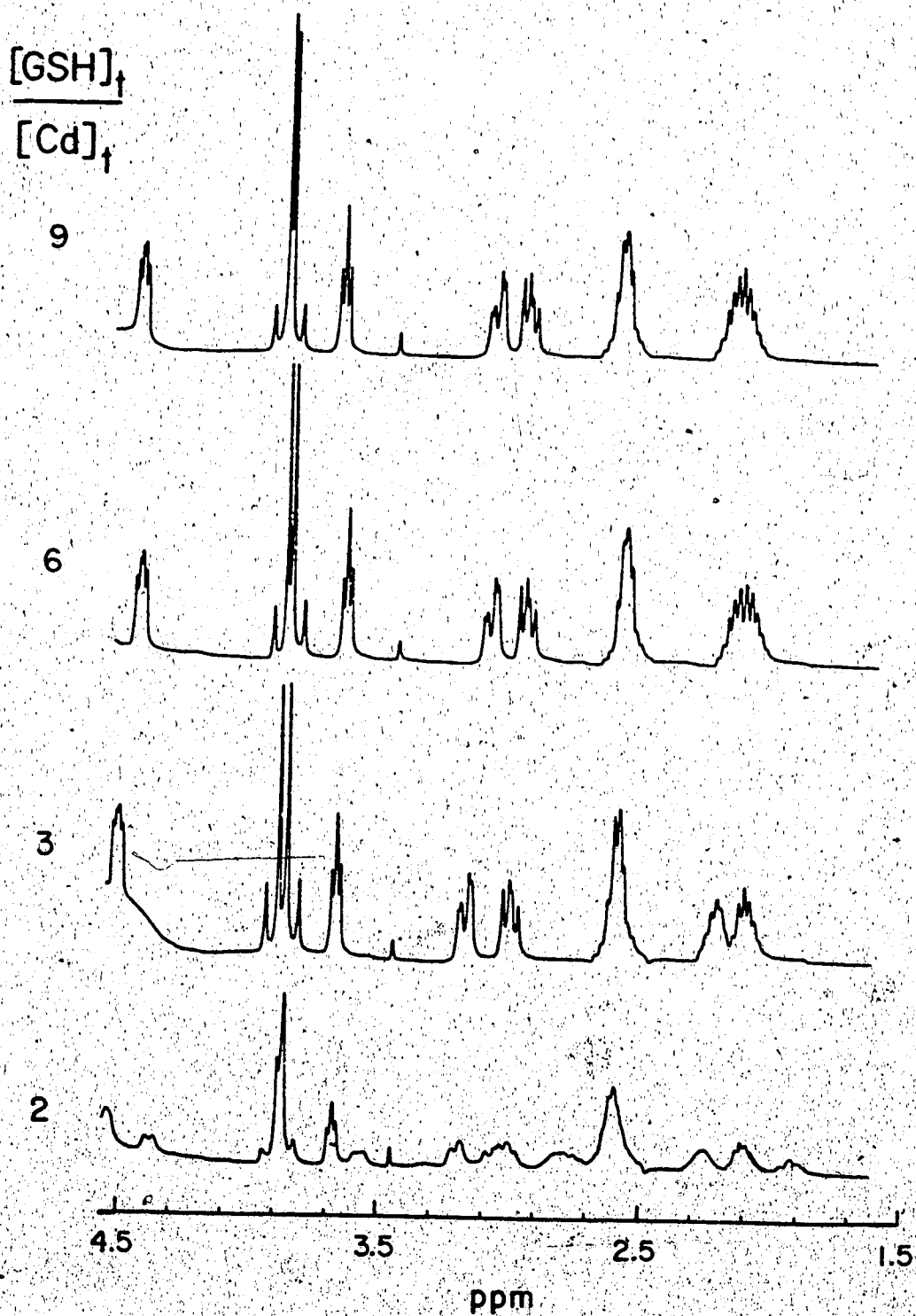


Figure 48. ^1H NMR spectra of glutathione solutions containing Cd^{2+} (0.1M) at pH 9.5 and glutathione concentrations between $\sim 0.2\text{M}$ to $\sim 0.8\text{M}$.

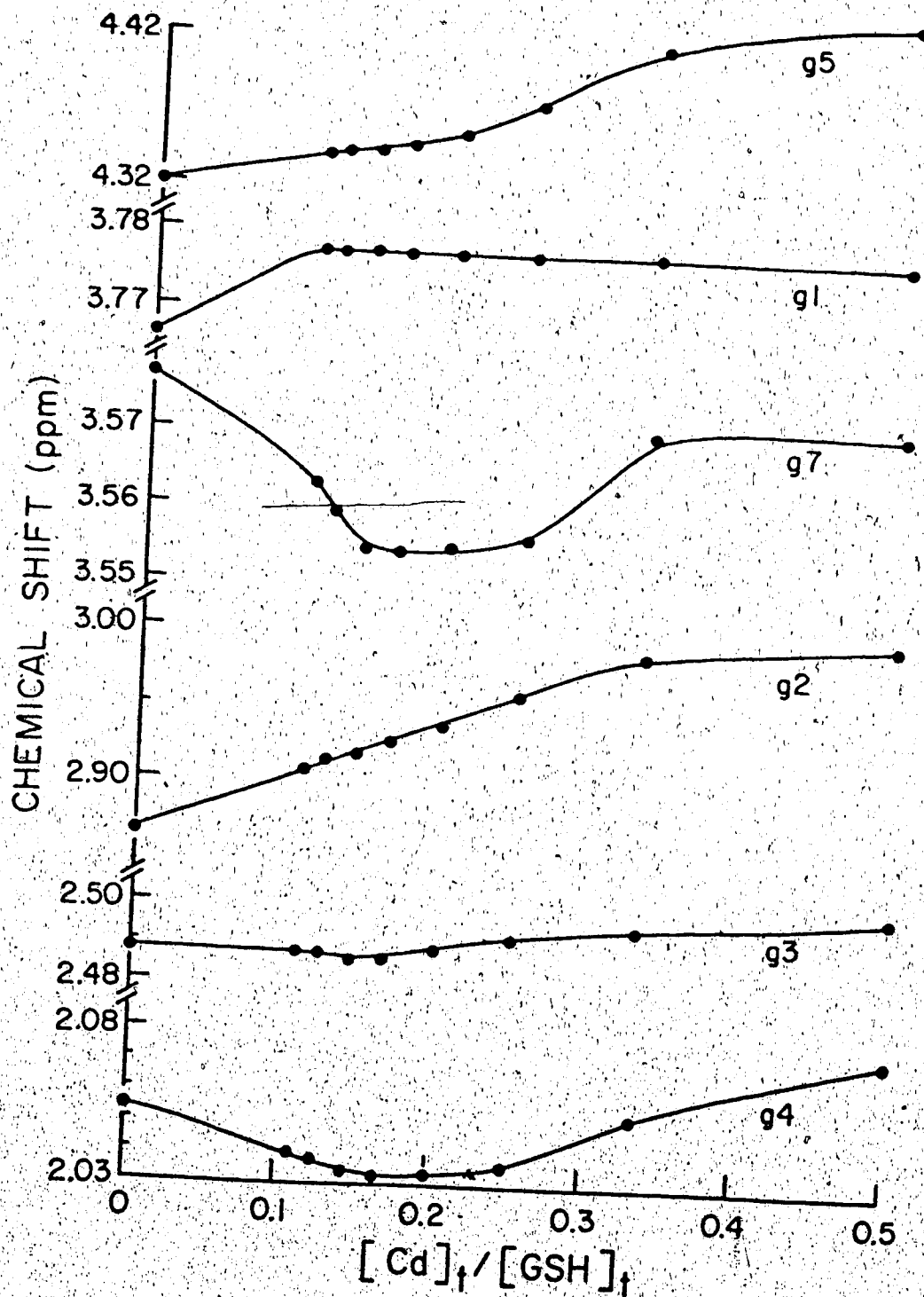


Figure 49. Dependence of chemical shift of g5, g1, g7, g2, g3, and g4 on the ratio $[Cd]_t/[GSH]_t$ at pH 9.5.

observations suggest that Cd^{2+} still binds predominantly to the sulfhydryl group at pH 9.5.

2. ^{13}C NMR Studies

Similarly to the ^1H NMR measurements, ^{13}C NMR spectra were recorded as a function of pH for mixtures containing Cd^{2+} and GSH in the ratio 1:2. Representative spectra are shown in Figure 51. For comparison, Figure 50 contains ^{13}C NMR spectra of glutathione alone at different pH values with assignment of resonances. For glutathione alone, ten resonances due to the four carbonyl groups (~ 175 ppm), two cysteinyl carbons (α , β), three glutamyl (α , β , γ) and one glycyl carbon are observed over the whole pH range. The shifts of the resonances as the pH is increased result from ionization of the acidic groups glycyl- CO_2H , glutamyl- CO_2H , cysteinyl-SH and glutamyl- NH_3^+ . In Figure 51, the resonance due to cysteinyl C_β is shown shifted and has lost intensity. The signal not observed is most probably lost through exchange of species at intermediate exchange rates. As the pH is increased, cysteinyl C_β resonance regains its intensity indicating faster exchange rates between the species formed. Up to pH 8, only ten resonances are present in the spectrum consistent with the ten carbons in glutathione. However, in the spectrum of the mixture at pH 9.5, the number of resonances has doubled at least, as was also observed in the ^1H NMR spectrum. This multiplication of

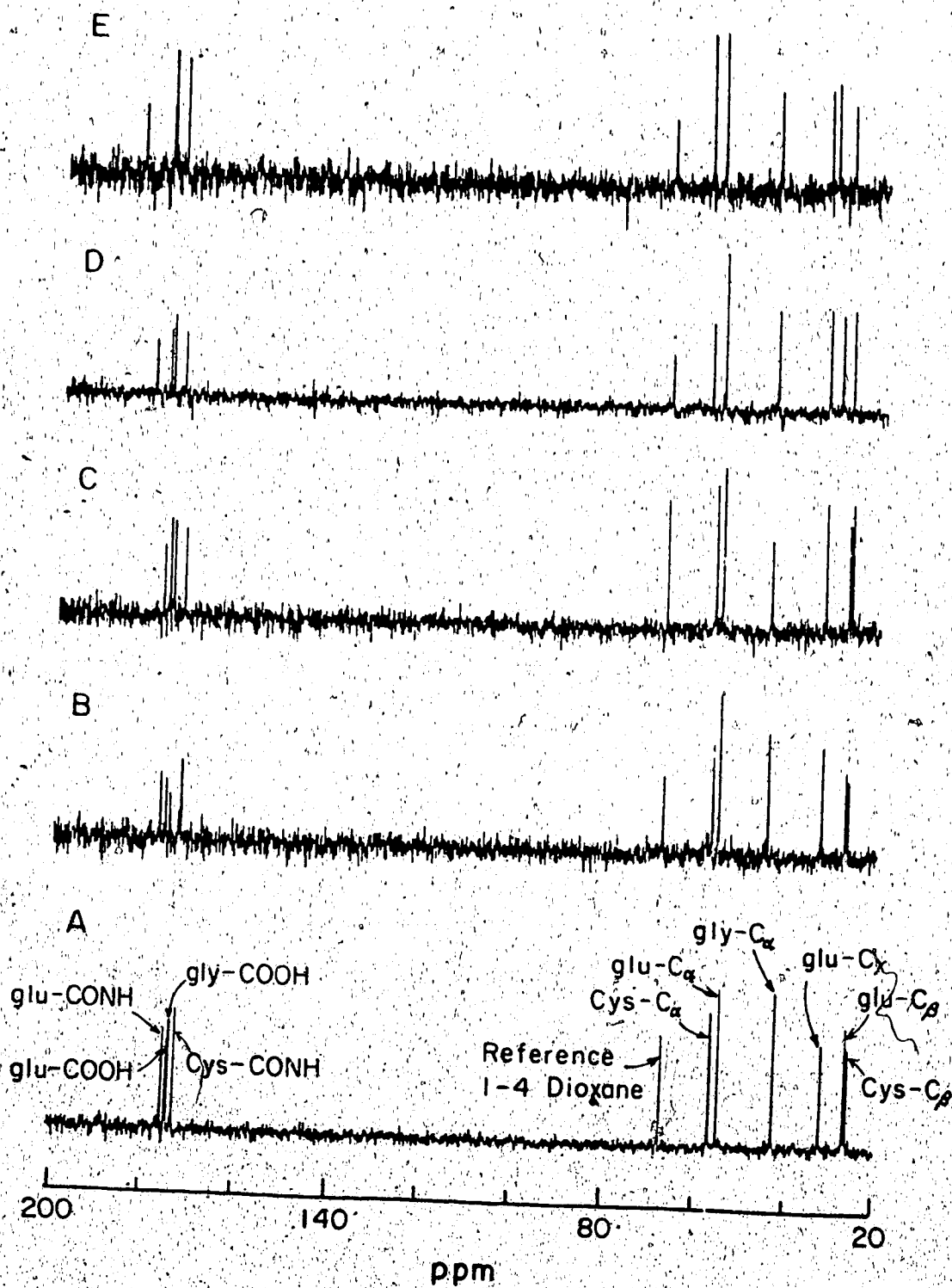


Figure 50. ^{13}C NMR spectra of glutathione at pH (A) 2.84, (B) 5.56, (C) 7.52, (D) 9.50 and (E) 11.52.

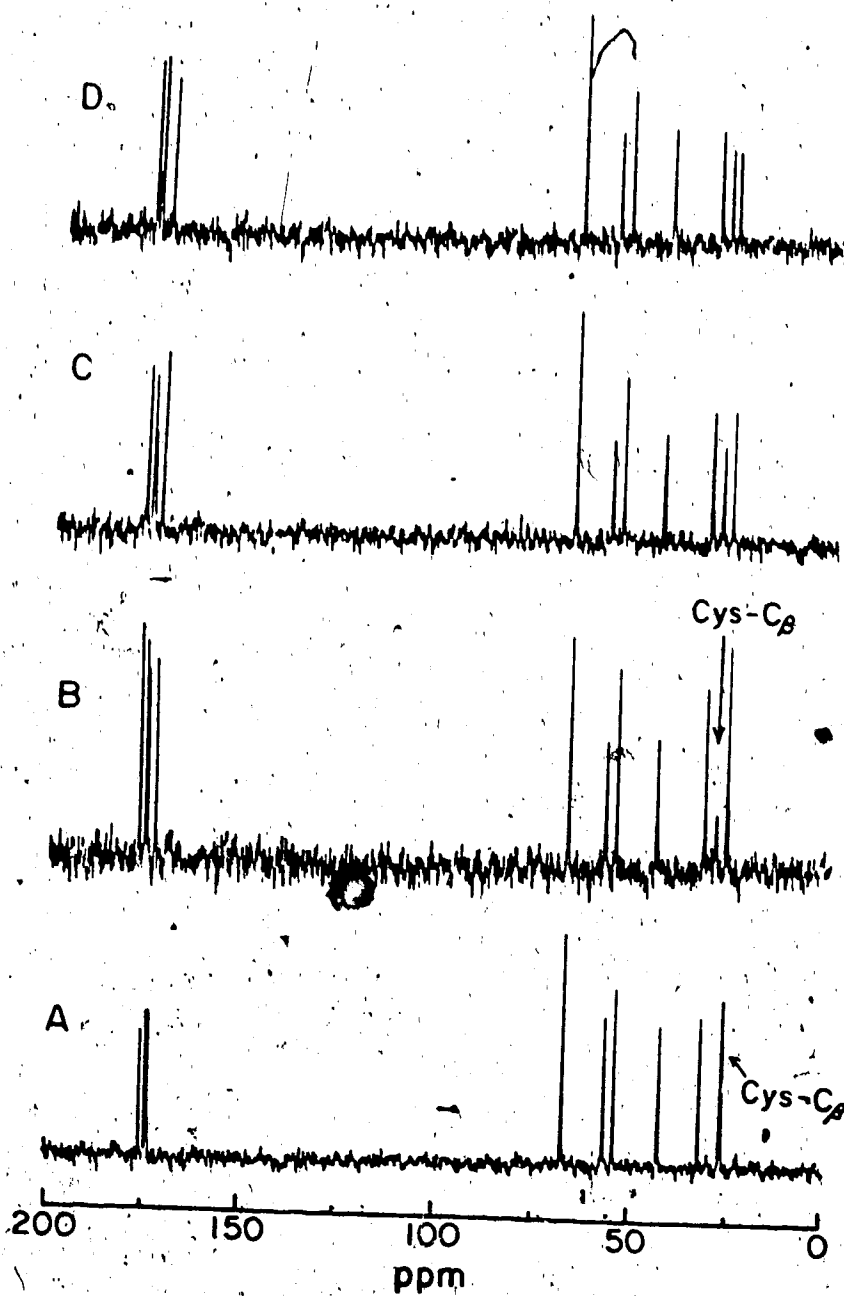


Figure 51. ^{13}C NMR spectra of glutathione (0.2M) solutions containing Cd^{2+} (0.1M) at pH (A) 2.02, (B) 5.55, (C) 6.82, (D) 7.99, (E) 9.49, (F) 10.81, (G) 11.41 and (H) 12.00.

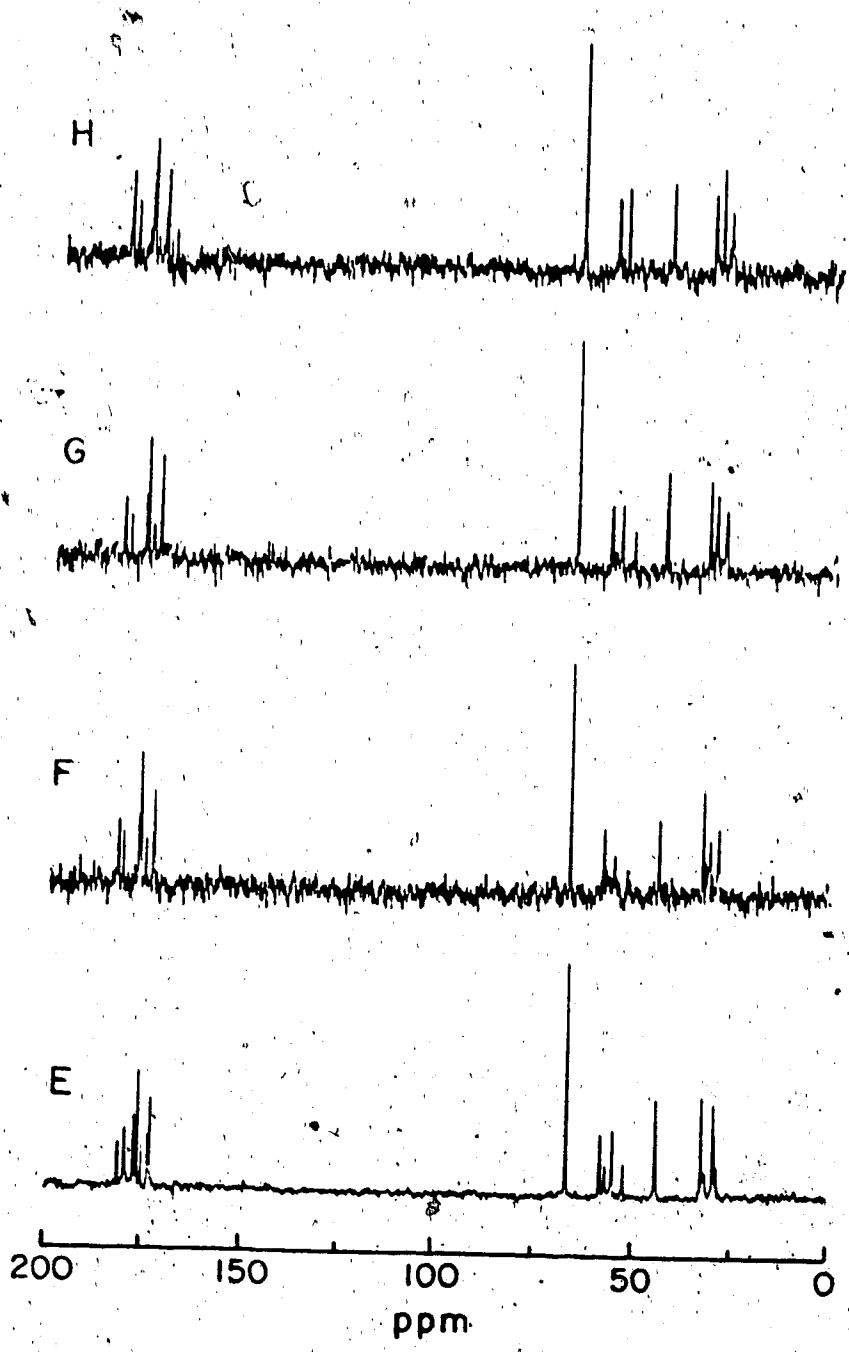


Figure 51. (continued)

resonances is observed in both the carbonyl region and the methylene region. Figures 52 and 53 show these two regions of the spectrum expanded for a sample at pH 9.5. This indicates that exchange between the complexes formed is also slow on the ^{13}C NMR time scale at pH 9.5 as was the case for ^1H NMR. Complexation is also indicated by the chemical shifts of the resonances in the mixtures of Cd^{2+} and glutathione compared to the chemical shifts of resonances in glutathione solutions. The effects of the complexation on the chemical shift of cysteinyl C_β and glutamyl C_β resonances are depicted in Figure 54. The chemical shifts of the two resonances are plotted versus the pH for solutions containing glutathione ((A) = cyst C_β , (B) = glu C_β) and glutathione and Cd^{2+} ((C) = cyst C_β ; (D) = glu C_β). Below pH 4, there are no data points for the Cd^{2+} -containing solution because of precipitation of Cd^{2+} -GSH complexes at lower pH. However, even at pH 4, the cysteinyl C_β resonance in the mixture is shifted to higher frequency. This shift increases as the pH is increased up to pH ~ 8. Between pH 6 and 8 the shift is very small compared to the one undergone between pH 4 and 6. Above pH 8, this resonance undergoes a smaller shift to lower frequency. The earlier shift to higher frequency is certainly due to binding at the sulfhydryl group. The reverse shift could be caused by a reversal of the earlier reaction, i.e., decomposition of the complex(es) formed at low pH, a change in the nature of the

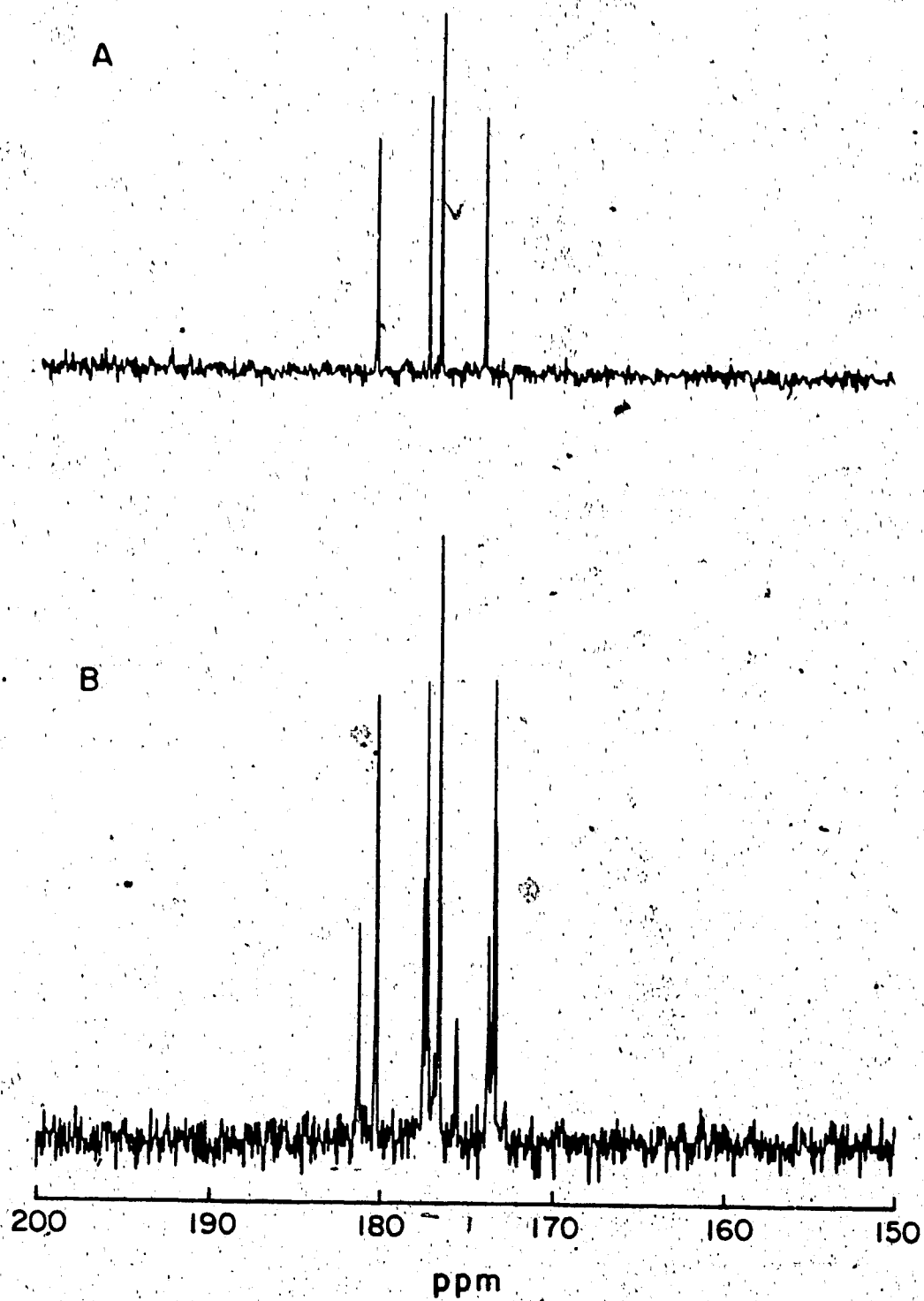


Figure 52. Expansion of the carbonyl region of the spectrum of (A) glutathione and (B) a 1 to 2 mixture of Cd²⁺ and glutathione. pH = 9.5.

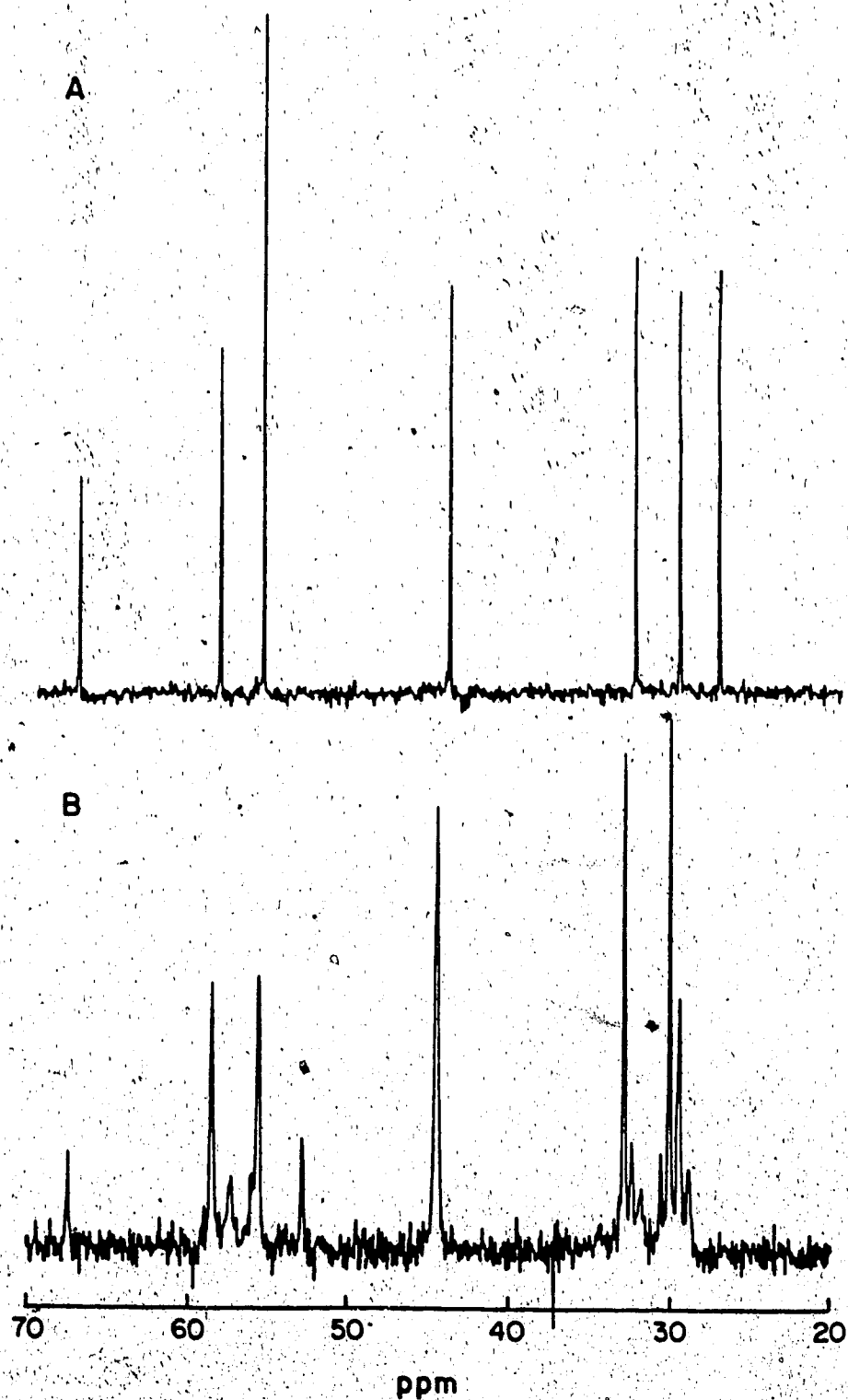


Figure 53. Expansion of the methylene region of the spectrum of (A) glutathione and (B) a 1 to 2 mixture of Cd²⁺ and glutathione. pH = 9.5.

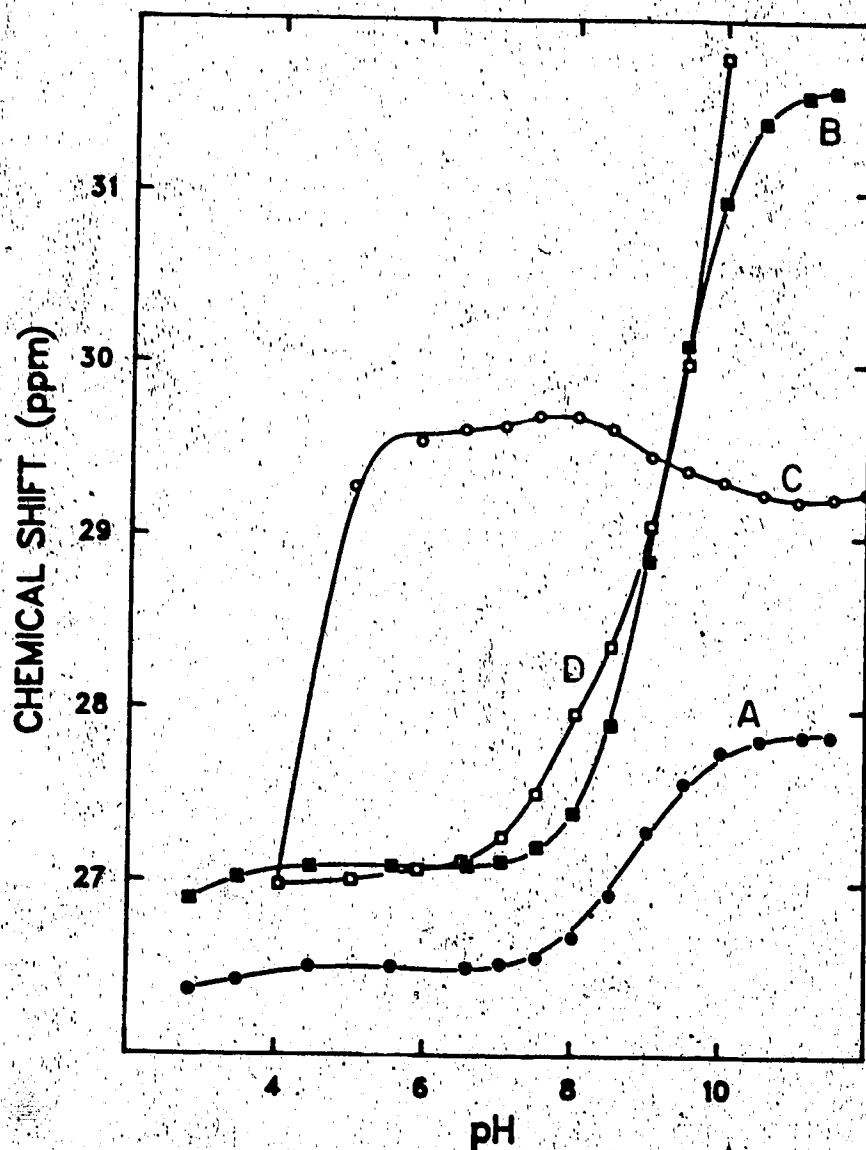


Figure 54. Effects of Cd^{2+} complexation on the chemical shifts of cysteinyl C_β and glutamyl C_β resonances: pH dependence of the chemical shifts of (A) cys- C_β and (B) glu- C_β during titration of GSH and (C) cys- C_β and (D) glu- C_β during titration of a 1:2 mixture of Cd^{2+} and GSH. $[\text{Cd}]_t = 0.1\text{M}$.

complex already formed, or formation of a new complex with binding to the sulfhydryl group and other coordinating sites (e.g., amino group).

The behavior of the glutamyl C_{β} resonance supports the involvement of the glutamyl donor group(s) in the complexation. Between pH 4 and ~7, the glutamyl C_{β} resonance in the mixture of Cd^{2+} and GSH experiences only a small shift as can be seen in Figure 54. However, above pH ~ 7 a larger shift is observed. Because the latter shift occurs in the region where the amino group is being titrated, it was attributed to the complexation of the amino group. The smaller shifts below pH 7 are possibly due to weak bonding to the carboxylate group of the glutamyl residue.

The resonances due to cysteinyl C_{α} and glutamyl C_{α} experience changes similar to those previously discussed for cysteinyl C_{β} and glutamyl C_{β} . Figure 55 depicts the dependence of their chemical shifts on the pH for GSH alone and for solutions containing Cd^{2+} and GSH. The resonance due to cysteinyl C_{α} does not, however, undergo a reverse shift above pH 8, instead the rate of increase in the chemical shift as the pH is increased above pH 8 is smaller than below pH 8. Cysteinyl C_{α} is further away from the reaction site than cysteinyl C_{β} ; changes in reactions occurring at the sulfhydryl group affect more the latter than the former.

^{13}C NMR mole ratio studies were conducted at pH 6, 9.5, 10 and 10.5. In Figure 56 the spectrum of glutathione at pH

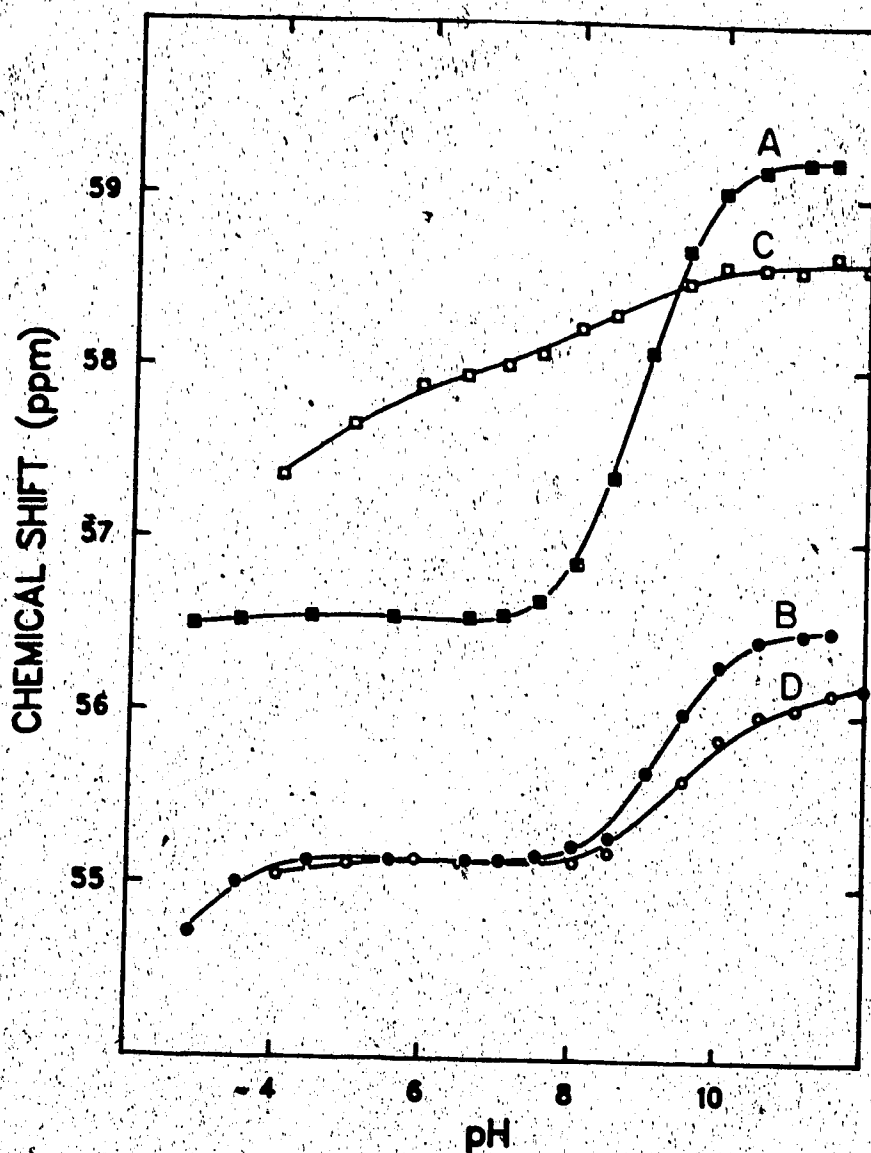


Figure 55. Effects of Cd^{2+} complexation on the chemical shifts of cysteinyl C_β and glutamyl C_β resonances: pH dependence of the chemical shifts of (A) cys- C_α and (B) gly- C_α during titration of GSH and (C) cys- C_α and (D) glu- C_α during titration of a 1:2 mixture of Cd^{2+} and GSH. $[\text{Cd}]_t = 0.1\text{M}$.

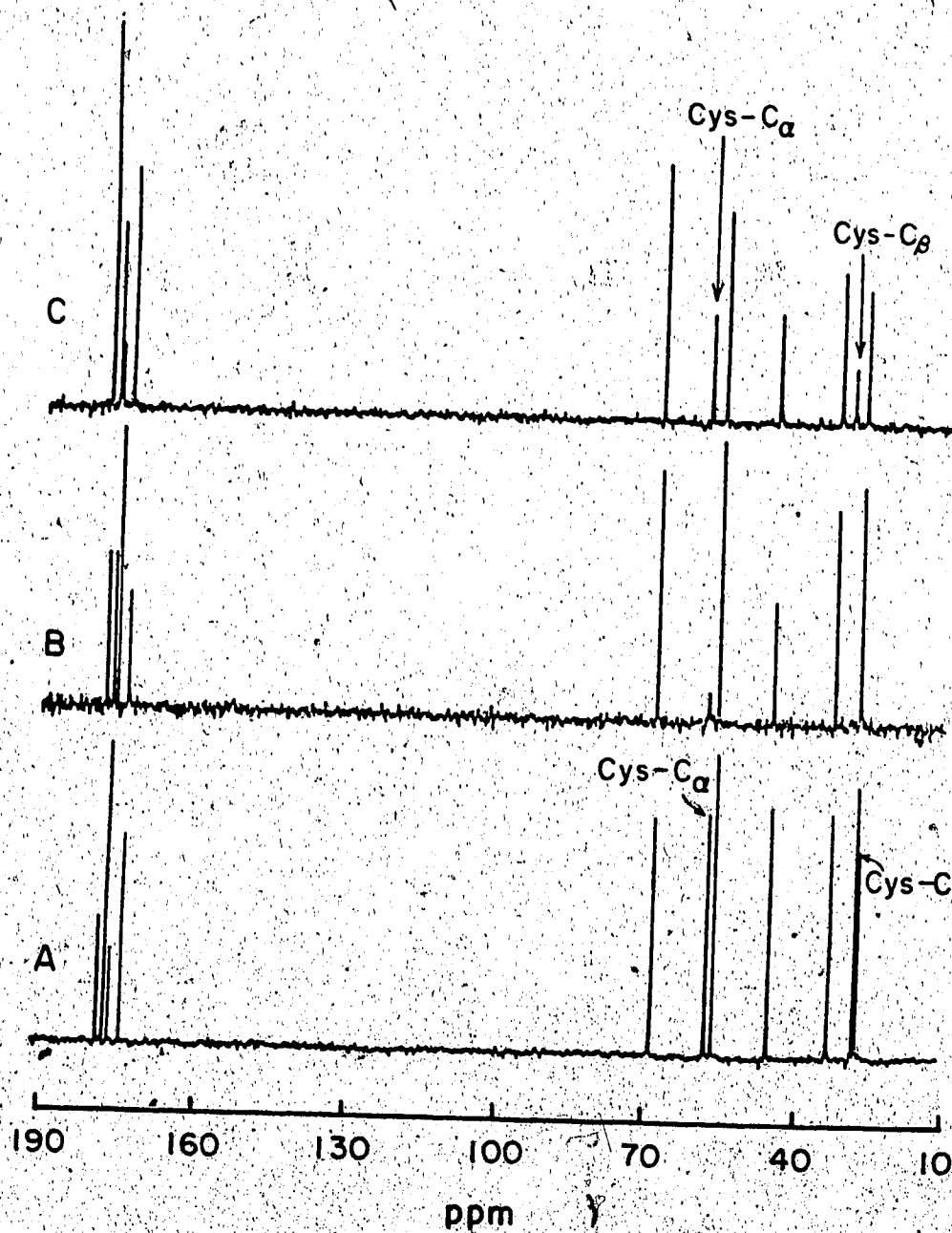


Figure 56. ^{13}C NMR spectrum of GSH (0.2M) with (A) 0, (B) 0.02M and (C) 0.1M Cd^{2+} at pH = 6.

6 is compared to those obtained when Cd^{2+} was added to glutathione at concentrations of 0.02M and 0.1M . The concentration of glutathione was kept at 0.2M . Addition of only 0.02M Cd^{2+} causes complete loss of the cysteinyl C_β resonance and an important decrease of the intensity of cysteinyl C_α resonance. At Cd^{2+} concentration of 0.1M both resonances have regained intensity indicating a faster exchange rate. Figure 57 depicts the dependence of the chemical shifts of cysteinyl C_β (A) and glutamyl C_β (B) resonances on the Cd^{2+} /glutathione ratio. The cysteinyl C_β resonance is shifted downfield with increasing concentrations of glutathione and reaches a plateau around a ratio of Cd^{2+} /GSH of approximately 0.5. The chemical shift of glutamyl C_β is practically invariant up to this point then is slightly shifted upfield. Similar behavior was observed for cysteinyl C_α (A) and glutamyl C_α (B) (Figure 58). These results indicate that at pH 6, the glutamyl residue is not complexed by cadmium up to ratio of GSH/cadmium of 2. They also point to the formation of a 1 to 2 Cd^{2+} to GSH complex.

However, at pH 9.5 changes in the chemical shifts of cysteinyl and glutamyl resonances indicate that both the cysteinyl and glutamyl residues are involved in the complexation. Dependence of the chemical shifts of the cysteinyl C_β (A) and glutamyl C_β (B) resonances on the concentration of glutathione at pH 9.5 is shown in Figure 59.

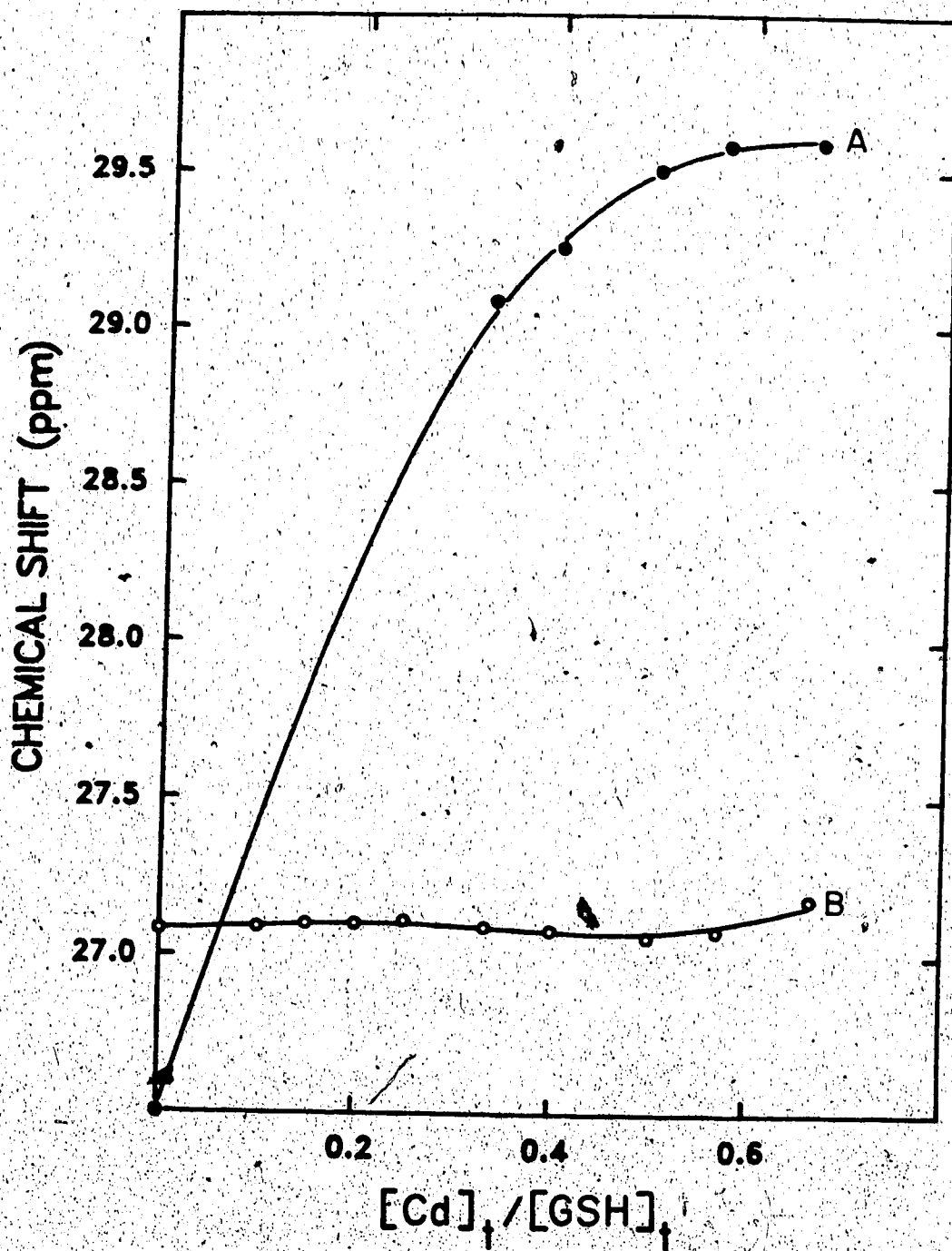


Figure 57. Chemical shifts of (A) cysteinyl C β and (B) glutamyl C β as a function of $[Cd]_t/[GSH]_t$ ratio at pH 6. $[GSH]_t = 0.2M$; $[Cd]_t = 0 \rightarrow 0.14M$.

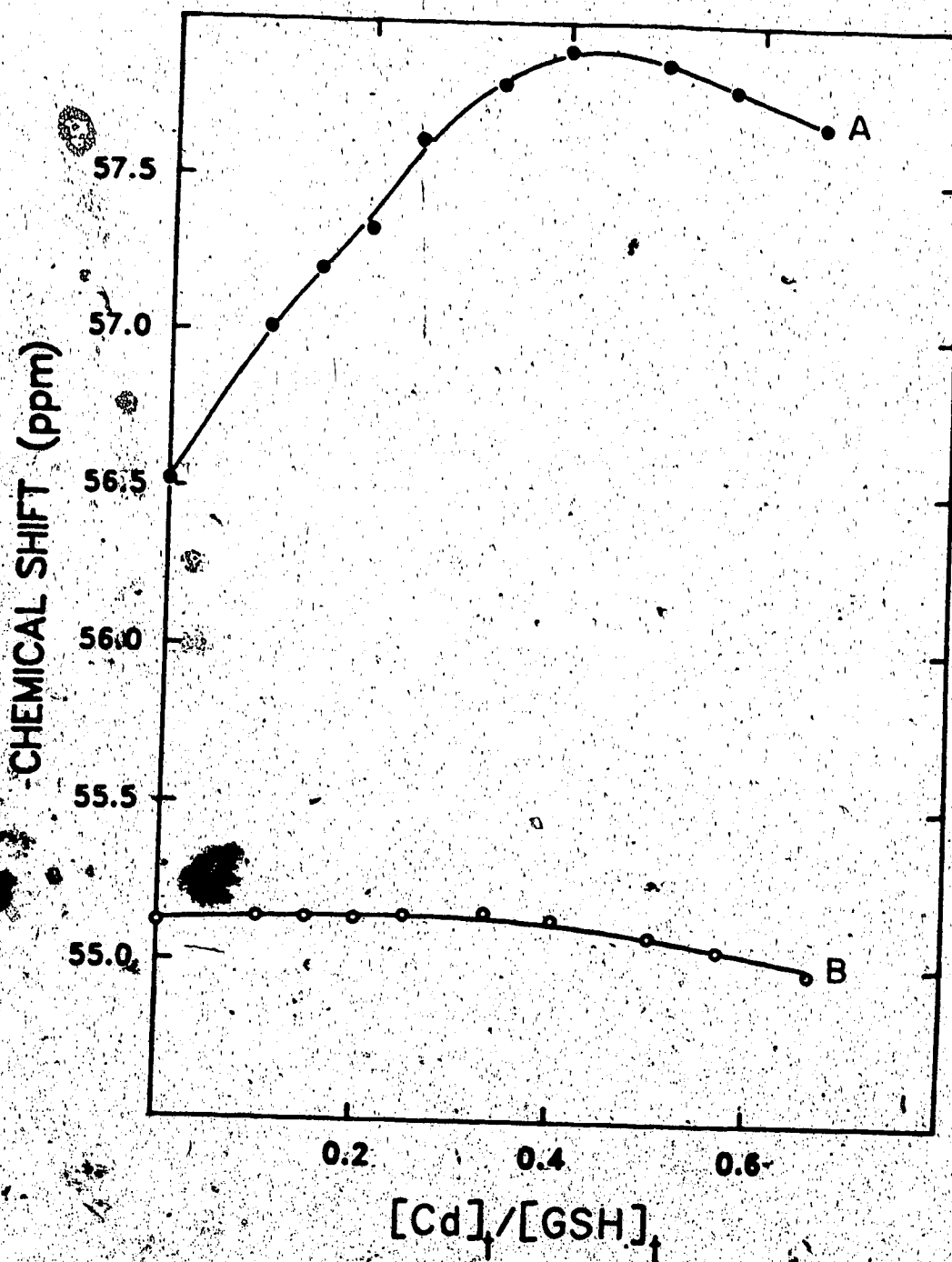


Figure 58. Chemical shifts of (A) cysteinyl C_α and (B) glutamyl C_β as a function of $[Cd]_t/[GSH]_t$ at pH 6. $[GSH]_t = 0.2M$, $[Cd]_t = 0 + \sim 0.14M$.

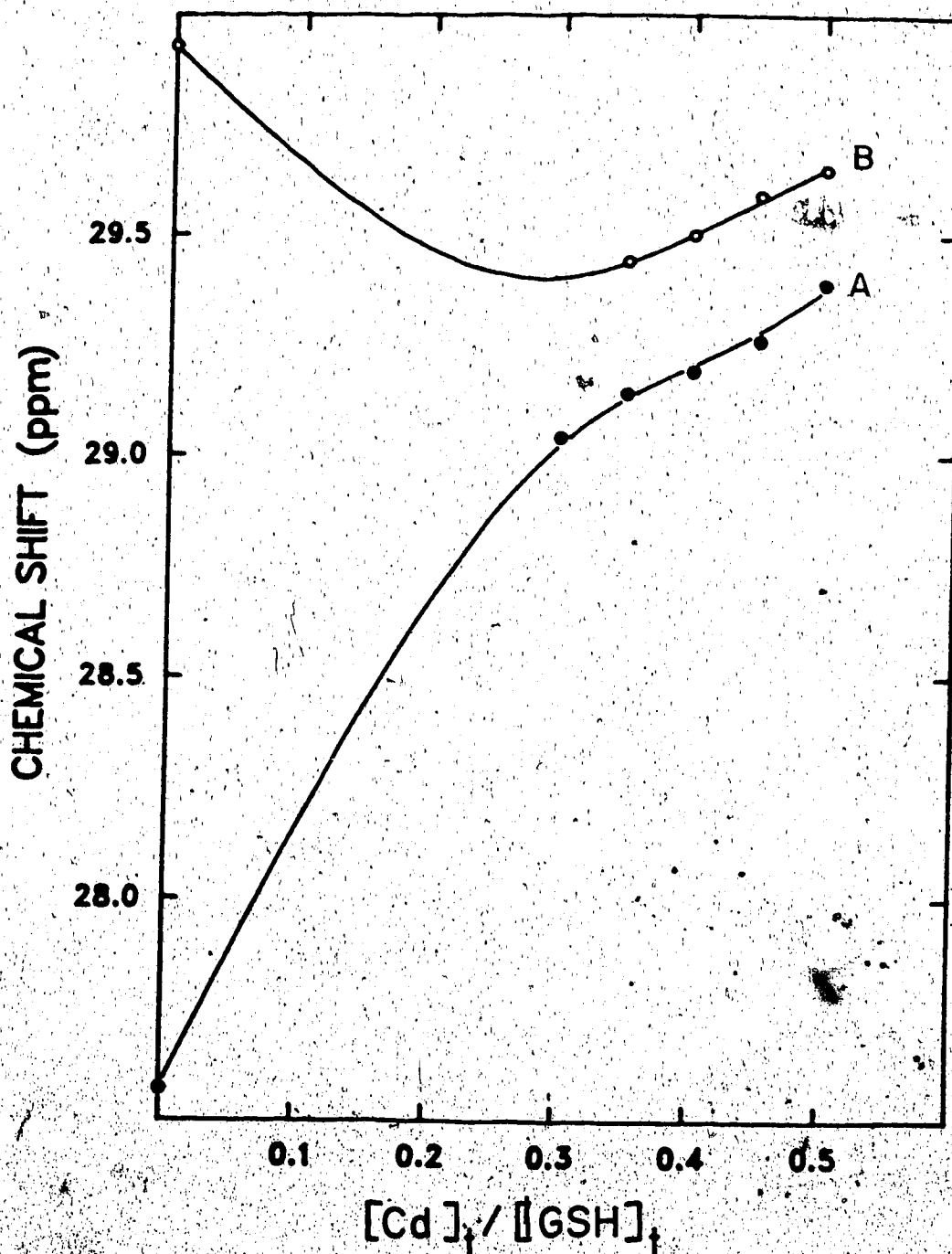


Figure 59. Chemical shifts of (A) cysteinyl C_β and (B) glutamyl C_β as a function of $[Cd]_t/[GSH]_t$ concentration at pH 9.5. $[GSH]_t = 0.2M$, $[Cd]_t = 0 + 0.1M$.

Between ratios of 0.1 and 0.3 the cysteinyl $C\beta$ resonance is not observed, therefore no data points exist in that range of ratio. The cysteinyl $C\beta$ resonance is shifted downfield with increasing concentration of cadmium, as was observed at pH 6 except that the shifts are smaller than those of pH 6. The glutamyl $C\beta$ resonance seems to have shifted to a minimum chemical shift and is then shifted to higher chemical shift values at higher ratios where data could be secured.

In summary from 1H and ^{13}C NMR studies two main reactions take place between Cd^{2+} and glutathione. A reaction involving predominantly the sulfhydryl group occurs at low pH (-2-7). The second reaction involves the sulfhydryl as well as the amino group and is detected at pH > 8 . Above pH 8 at least two kinds of complexes are formed in solution which are dynamically stable on the NMR time scale.

3. ^{113}Cd NMR Studies

a.. Qualitative Studies

The pH dependence of the ^{113}Cd NMR spectra of solutions in which the GSH/ Cd^{2+} ratio is kept at 2 is shown in Figure 60. Results are also summarized in Table 5. Starting at the high pH end, several resonances occur between 700 and 300 ppm. Groups of resonances are centered around 670 ppm, 565 ppm and 324 ppm. From pH ~ 10.5 the spectrum is reduced to only two resonances at 673.8 ppm and 320.4 ppm. These two resonances are observed down to pH 8.5 and their chemical

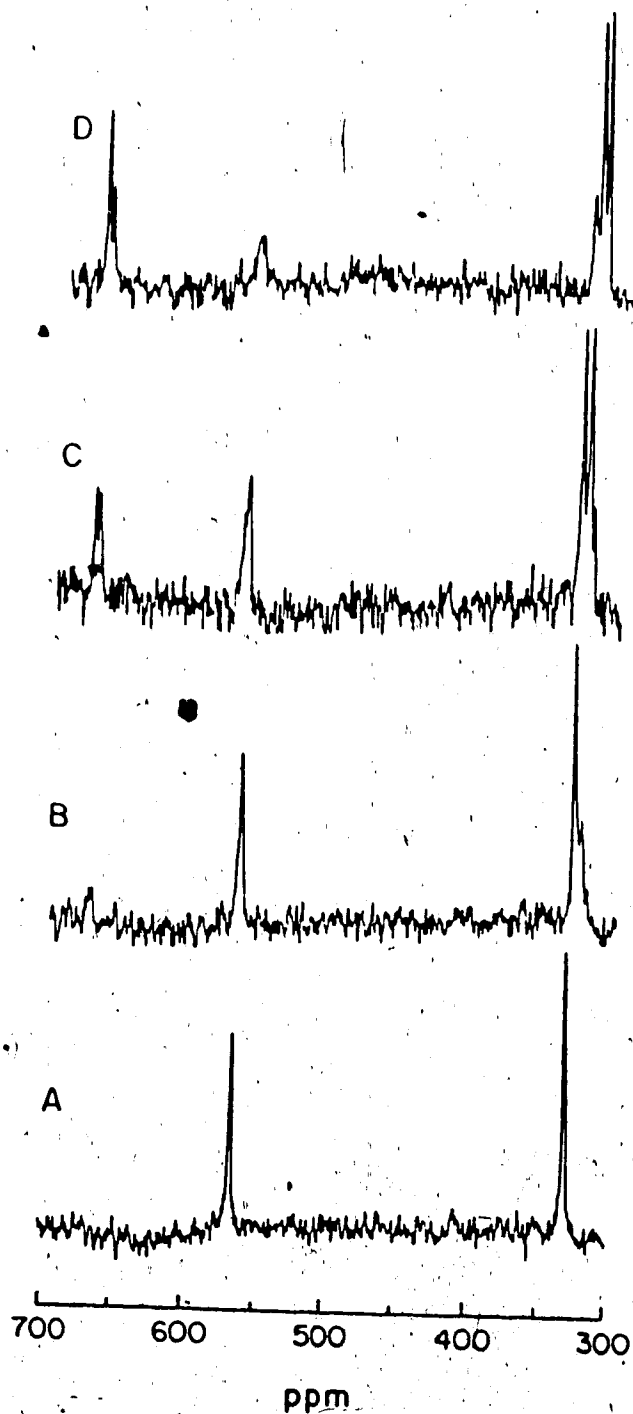


Figure 60. ^{113}Cd NMR spectra of a 1 to 2 solution of Cd^{2+} and GSH at pH (A) 12.8, (B) 12.38, (C) 11.98, (D) 11.50, (E) 10.56, (F) 10.01, (G) 9.52, (H) 9.00. $[\text{Cd}^{2+}] = 0.25\text{M}$, $[\text{GSH}] = 0.5\text{M}$.

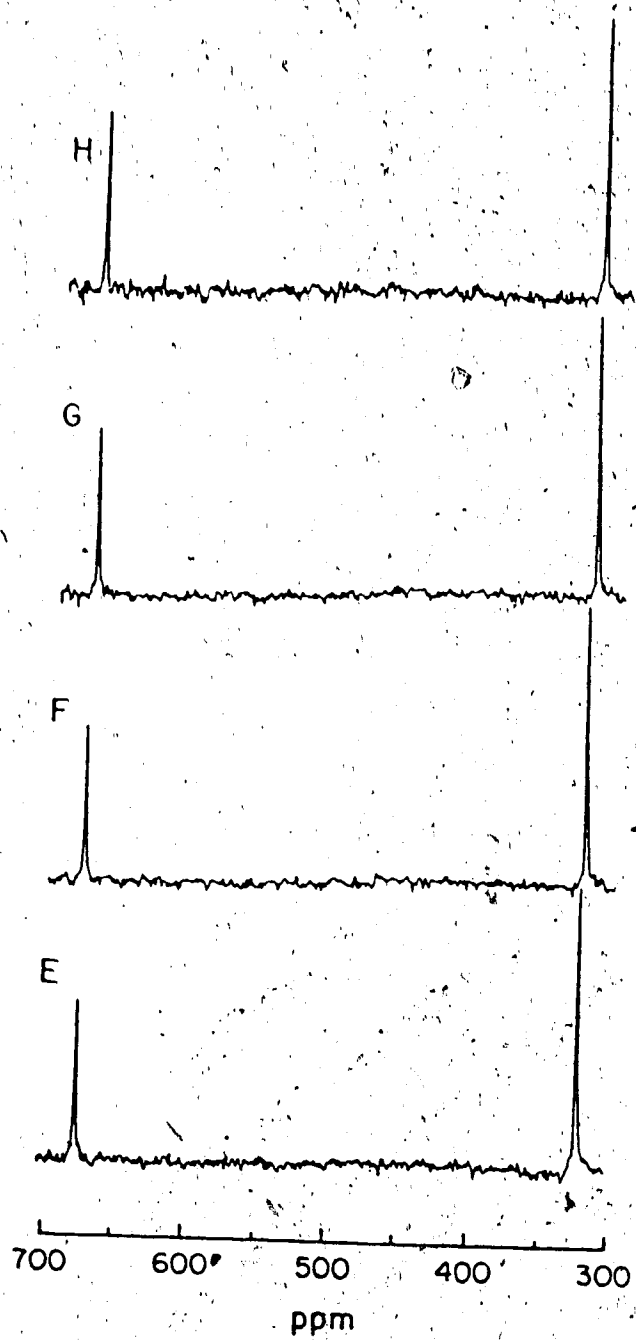


Figure 60. (continued)

Table 5. ^{113}Cd NMR spectral features during a pH titration of a 1 to 2 mixture of Cd^{2+} and GSH.

pH	Spectral events
12.38	Two groups of resonances centered around 566 ppm and 330 ppm.
11.98	Three groups of resonances centered around 670 ppm, 565 ppm and 324 ppm.
11.53	Three groups of resonances centered around 670 ppm, 565 ppm and 324 ppm.
	The intensity of the 565 ppm group of signals has decreased while that for the two other groups has increased.
11.05	One resonance is observed at 674 ppm and two at 325 and 320 ppm, the one at 325 ppm being the least intense.
10.56	Two resonances at 673.8 ppm and 320.4 ppm.
10.00	Two resonances at 673.8 ppm and 320.4 ppm with increase of intensity compared to previous pH.
9.50	Same as pH 10.
9.00	Decrease of the intensity of the two resonances.
8.50	The resonance signal at 673 ppm is decreasing faster in intensity than the one at 320 ppm.
8.00	Only the 320 ppm resonance still appears.
7.50	No detectable signal.
7-4	No detectable signal.

$$[\text{Cd}]_t = \sim 0.25\text{M}, [\text{GSH}]_t = 0.5\text{M}$$

shifts are unchanged.

The appearance of the ^{113}Cd NMR spectra parallels that of the ^{13}C and ^1H NMR spectra in that the two resonances are observed in the pH region where multiplication of resonances occurs in the ^1H and ^{13}C NMR spectra. Hence, the resonances in the ^1H and ^{13}C NMR spectra were due to GSH with cadmium complexed in different environments. The chemical shift of the cadmium resonance at high frequency falls in the region of chemical shifts generally attributed to Cd^{2+} bonded to multiple sulfur donors. The chemical shift of the resonance at low frequency does not coincide with the regions assigned to nitrogen binding, or a combination of nitrogen and oxygen or sulfur binding. From a compilation of the chemical shifts of resonances occurring in spectra of cadmium substituted metalloproteins [37], it was concluded that resonances from cadmium bound to sites consisting exclusively of oxygen ligands are found in the region 0 to -125 ppm, those from cadmium in sites containing a combination of oxygen and nitrogen ligands appear between 0-300 ppm, whereas those resonances from sites containing 2 or more thiolate sulfur ligands are found in the downfield region between 450 and 750 ppm. The resonance at 320 ppm falls in the non-assigned region between 300 and 450, however not far outside the region of chemical shifts of cadmium sites containing a combination of oxygen and nitrogen.

From pH 8 to 4, there are no detectable signals in the

^{113}Cd NMR spectrum. ^{13}C NMR data attest, however, that complexation to the sulfhydryl group occurs. The absence of ^{113}Cd resonances must be due to excessive broadening of the ^{113}Cd NMR resonance(s) resulting from chemical exchange.

An exchange averaged resonance is observed when the rate of exchange is much larger than the chemical shift difference and separate resonances are observed when the exchange rate is much smaller than the chemical shift difference. The broad signal of cysteinyl C_β at pH 5.5 (Figure 51) in the ^{13}C NMR spectrum indicates that the rate of exchange is intermediate on the ^{13}C NMR time scale. This resonance became sharper at higher pH, which means the exchange rate had increased. Relative to the ^{113}Cd NMR time scale the abovementioned intermediate and fast exchange are moved to fairly slow and intermediate rates due to the large chemical shift range of ^{113}Cd . Thus equivalent resonances to those in the ^{13}C NMR spectra are not observed in the ^{113}Cd NMR spectra due to the difference in time scales.

The single resonances observed in the ^{13}C NMR spectra at lower pH are, therefore, exchange averaged resonances due to a number of complexes formed with predominance of binding to the sulfhydryl group. Species of the type $\text{Cd}(\text{SG})$, $\text{Cd}(\text{SG})_2$ have been proposed to occur at $\text{pH} < 7$ [83]. The formation of a 1:2 complex between Cd^{2+} and glutathione is also supported by the curve of the dependence of the chemical shift of cysteinyl C_α and C_β resonances on the ratio

$\text{Cd}^{2+}/\text{GSH}$ (Figure 57 and 58); the two curves reach a plateau at a ratio of ~ 0.5 .

b. Quantitative Studies

Besides the qualitative information from the chemical shifts, the concentrations of species giving rise to resonances in the ^{113}Cd NMR spectra are determined from intensity measurements. These experiments were done to determine how much of the total cadmium in solution was represented by the observed resonances and eventually to determine the stoichiometry of the complexes by correlation with ^{13}C NMR data.

Details about the method used to generate the calibration curve were given in Chapter II. Briefly, a capillary containing the reference compound ($\text{Cd}(\text{NO}_3)_2$) with a fixed concentration was placed in NMR tubes containing solutions of known concentration of a standard compound (CdCl_2) and spectra were recorded for a range of CdCl_2 concentrations. The ratio of the intensities of the resonances due to CdCl_2 over that of the resonance due to the reference having a fixed concentration (I_S/I_R) were plotted against the concentration of CdCl_2 and yielded the straight line in Figure 11 of Chapter II.

For quantitative measurement the same capillary containing the reference was placed in the NMR tubes containing samples of interest. The integrated intensities of the resonances in the spectrum were measured and the ratio

$I_{\text{sample}}/I_{\text{R}}$ was calculated. This ratio was used with the calibration curve to deduce the concentration of the species giving the sample resonance(s). The procedure is illustrated in Figure 61, which shows the ^{113}Cd NMR spectrum of a 1 to 2 mixture of Cd^{2+} and GSH at pH 9.5.

i. pH Dependence of the Concentration of Cd^{2+} Species

A quantitative study was conducted in the pH region where two signals are observed in the ^{113}Cd NMR spectra (pH 9.5 to 8.5). The two resonances are well resolved ($\Delta\delta = 354$ ppm) and integration measurements can be performed on each separately without interferences.

Initially, the apparent T_1 values of the two resonances were determined in an inversion recovery experiment described in Chapter II, section 2. They were found to be 0.29 sec and 0.44 sec for the 320 ppm and 674 ppm resonances respectively. The repetition time (2.39 sec) used in the NMR experiments to establish the calibration curve was based on these T_1 values. The repetition time was set to be at least five times the longest T_1 , i.e., $5 \times 0.44 \text{ sec} = 2.2 \text{ sec}$, in order to avoid saturation of the signals. An example of the measurements done on the two signals was given previously in Figure 61 for a sample at pH 9.5. Table 6 lists the results obtained for the ratios of intensities of the two signals at pH 9.5, 9.0 and 8.5 and the concentration of cadmium under each resonance, as determined from the calibration curve. The concentrations were calculated using

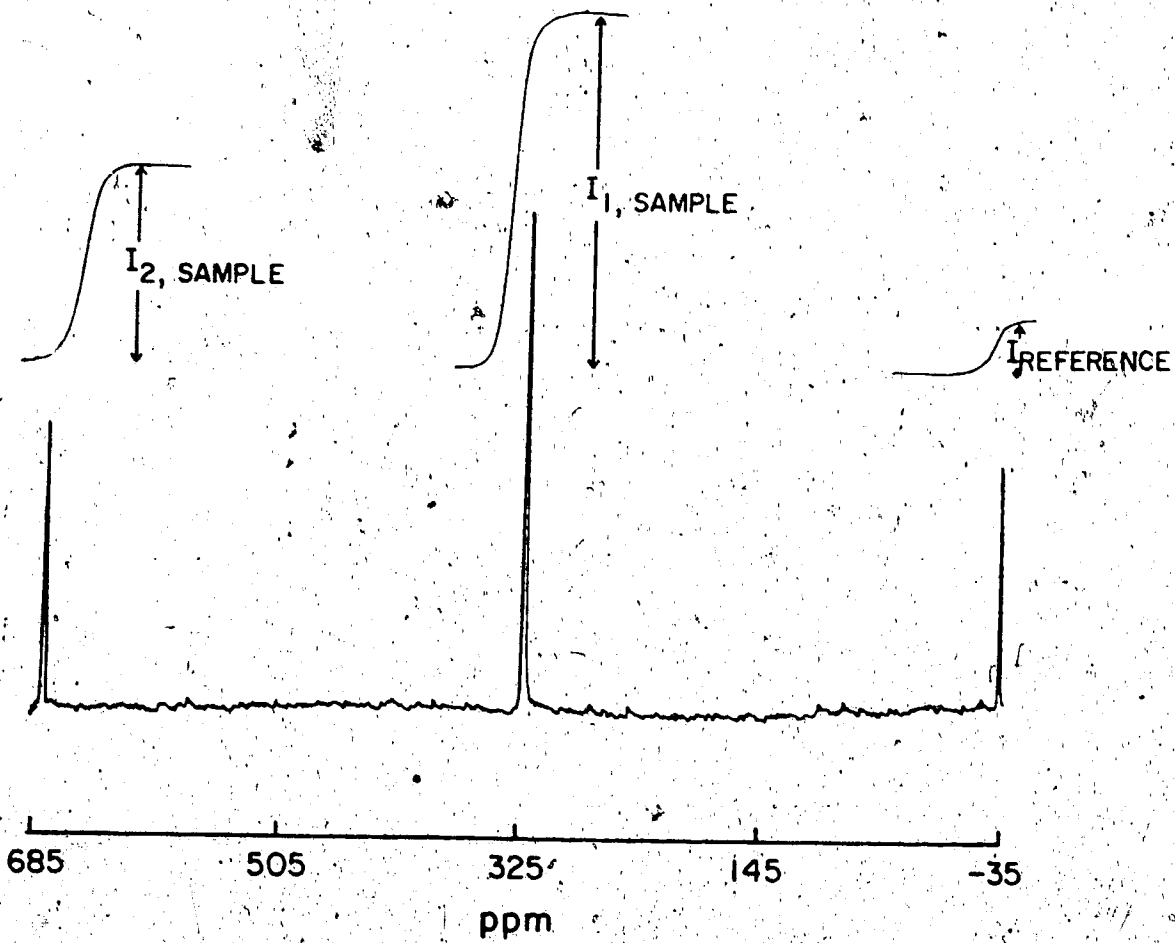


Figure 61. ^{113}Cd NMR spectrum of a 1 to 2 mixture of Cd^{2+} and GSH at pH = 9.5. $[\text{Cd}^{2+}] = 0.1\text{M}$; $[\text{GSH}] = 0.2\text{M}$.

Table 6. Species distribution versus pH of cadmium complexes of glutathione by ^{113}Cd NMR.^a

pH	[Cd] _{tot} (M)	674 ppm resonance			320 ppm resonance		
		$\frac{I_{\text{sample}}}{I_{\text{R}}}$	[Cd] _{measured}	% Cd measured	$\frac{I_{\text{sample}}}{I_{\text{R}}}$	[Cd] _{measured}	% Cd measured
9.5	0.1740	2.85	0.01732	9.95	5.04	0.02885	16.6
9.0	0.1705	2.27	0.01425	8.36	3.92	0.02295	13.5
8.5	0.1603	1.62	0.01083	6.76	2.91	0.01762	11.0

^a[GSH]_{tot} = 2 x [Cd]_{tot}

the linear regression parameters of the calibration curve and the measured ratios. Columns 5 and 8 contain the concentrations measured for the two signals expressed in terms of the percentage of total cadmium in solution.

Only a fraction of the total cadmium is represented in the two signals. The highest percentage of the total cadmium measured is 26.5%, obtained from the sample of pH 9.5. The concentration of species causing the 320 ppm resonance is always higher than that of the species causing the 674 ppm resonance. As the pH decreases, the concentrations of cadmium measured decreases even though no new resonance appears. The species formed at high pH are either being decomposed or transformed. When the pH is decreased between pH 9.5 and 8.5, protons may compete with Cd^{2+} for the binding to the sulfhydryl and amino groups, thus decreasing the concentration of complexed Cd^{2+} .

If the concentrations obtained from the resonances at 320 ppm and 674 ppm are ratioed, the average of the values obtained at the three pH values is 1.63 ± 0.02 . This indicates that the species responsible for the two resonances are part of an equilibrium which is pH dependent. The involvement of the glutamyl amino group in the complexation as the pH is raised above 8 was discussed earlier. The fact that both resonances in the ^{113}Cd NMR spectra lose intensity as the pH is lowered suggests that the species causing at least one of the resonances involves the amino group.

ii. Dependence of the Concentration of Cd²⁺ Species on the Concentration of GSH at pH 9.5

A mole ratio study was conducted at pH 9.5 starting with a ratio $\text{GSH}/\text{Cd}^{2+} = 2$ and increasing the concentration of glutathione. As the ratio of glutathione to cadmium is increased between 2 and 3 the two resonances lose a considerable amount of their intensity until, at a ratio of 3, there appears no resonance in the spectrum. However, at higher ratios (> 4), the resonance at high frequency (~ 674 ppm) is observed. Further increases in the GSH/Cd ratio causes a shift of this resonance to higher frequency and a small increase in its intensity. Quantitative results are summarized in Table 7. Results obtained show that the increase in the concentration of glutathione relative to Cd^{2+} shifts the equilibrium toward the formation of the species giving rise to the resonance at 674 ppm. The disappearance of the resonance at 320 ppm and the increase in concentration of the species causing the resonance at ~ 674 ppm argue in favor of multiligand binding in the latter species. At a ratio of 5.25, 41.8% of the total cadmium is measured as compared to 12.6% measured at the ratio for 2 from the intensity of the 674 ppm resonance. A resonance due to free cadmium is not observed. Free cadmium must be exchanging between different species at rates precluding observation of their resonance(s).

An attempt was made to bring species into the slow

Table 7. Molar ratio study at pH 9.5 of the reaction of Cd²⁺ and GSH by ¹¹³Cd NMR.

[Cd] _{tot} (M)	[GSH] _{tot} (M)	$\frac{[GSH]_{tot}}{[Cd^{2+}]_{tot}}$	Concentration of Cd ²⁺ giving resonances at			
			320 ppm (M)	(M)	-674 ppm (% Cd _{measured})	
0.09637	0.1925	1.99	0.02004	20.8	0.01212	12.6
0.09531	0.2434	2.62	0.00922	9.69	0.00582	6.12
0.09402	0.3018	3.81	a	a	a	a
0.09273	0.3829	4.13	0.00	0.00	0.03670	39.8
0.09093	0.4778	5.25	"	"	0.03805	41.8
0.08923	0.5740	6.43	"	"	0.03868	43.3
0.08701	0.6659	7.65	"	"	0.03727	42.8
0.08484	0.7578	9.17	"	"	0.03517	41.4

aNo ¹¹³Cd resonances were detected.

exchange regime by lowering the temperature. If this could be achieved, new resonances due to the unaccounted for cadmium may be observed. Results shown in Table 8 demonstrate that lowering the temperature to 273°K does not alter the spectrum at the low ratio GSH/Cd²⁺ of 2 or the high ratio of 5 at pH 9.5. At the ratio of 2, the same two resonances are observed being only slightly shifted (674 ppm to ~680 ppm, 320 ppm to ~324 ppm). However, there is an increase in the concentration of measured Cd²⁺ species at 298°K, most noticeable at the ratio 1 to 5 Cd²⁺ to GSH. At 273°K, 30.3% of Cd²⁺ species is measured whereas 41.8% is measured at 298°K. This result indicates that redistribution of species occurs when the temperature is lowered even though new resonances do not appear in the spectrum.

Raising the temperature caused the collapse of the two resonances observed at a ratio of 2. This is depicted in Figure 62, which shows spectra recorded between 0°C and 77°C. As the temperature was increased, the two resonances collapse to a single very broad resonance, which becomes sharper at higher temperatures.

iii. Effect of Dilution on the Distribution of Species

The effect of dilution on the distribution of species was studied to determine the difference between the composition of the complexes which cause the resonances at 320 ppm and 674 ppm. Results are shown in Table 9. The ratio GSH/Cd²⁺ was maintained at 2 and the concentration of Cd²⁺

Table 8. Species distribution of Cd-GSH at 273°K and 298°K by ^{113}Cd NMR.^a

[GSH] (M)	[Cd] _{tot} (M)	Resonance at high frequency		Resonance at low frequency		[Cd] _l /[Cd] _h	δ Cd me
		δ (ppm)	[Cd] _h (M)	δ (ppm)	[Cd] _l (M)		
		<u>273°</u>					
.3692	.1846	679.67	0.01927	323.58	0.03264	1.69	2
.8639	.1728	685.4	0.05239	b	b		3
		<u>298°</u>					
.1925	.09637	674	0.01212	320	0.02004	1.65	3
.4778	.09093	677	0.03805	b	b		4

^apH = 9.5

^bAt the ratio GSH/Cd²⁺ δf 5 the resonance at low frequency is not observed.

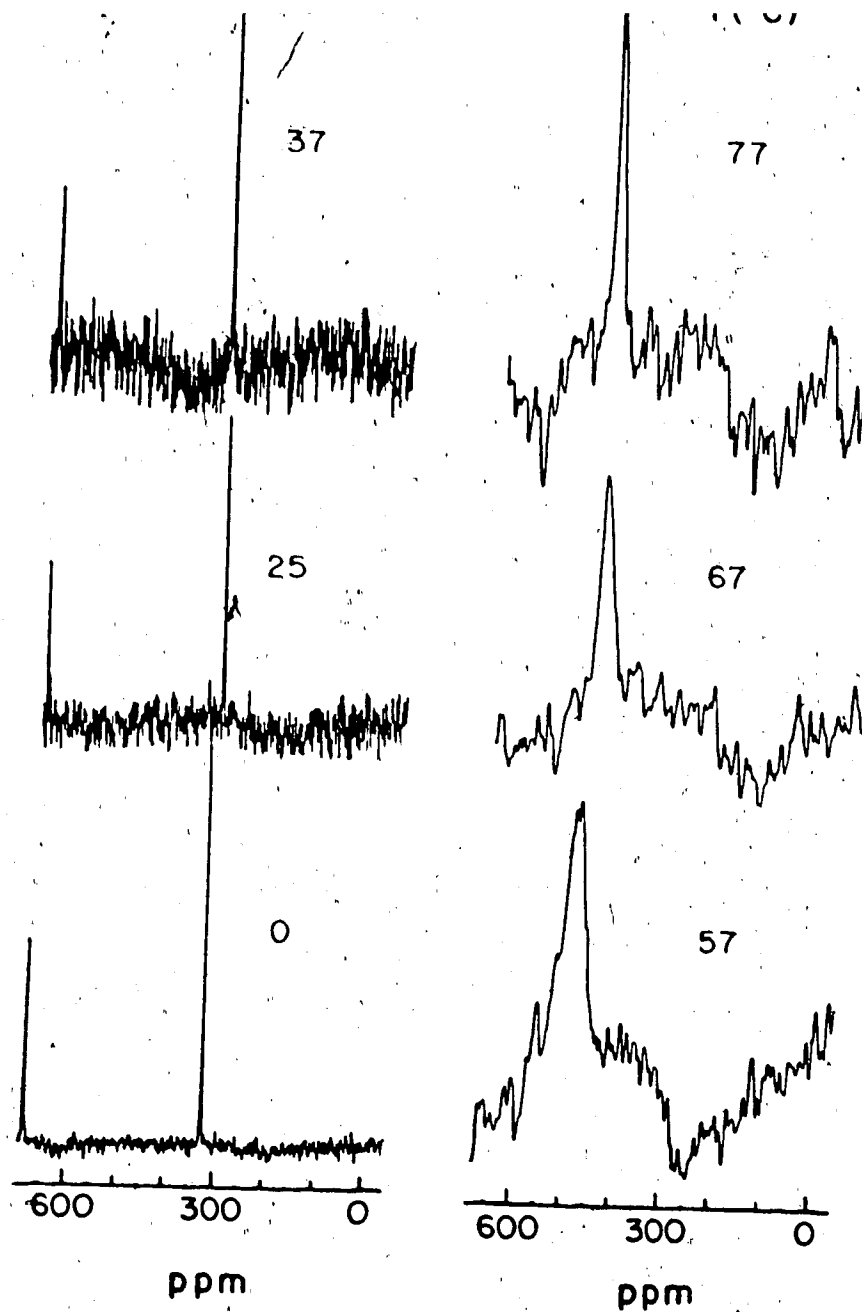


Figure 62. ^{113}Cd NMR spectra of 1 to 2 mixture of Cd^{2+} (0.1M) and GSH (0.2M) at pH = 9.5 from 0°C to 77°C .

Table 9. Dilution experiment at pH 9.5 for a 1:2 mixture of Cd²⁺ and GSH by ¹¹³Cd

[Cd] _{tot}	[Cd] ₃₂₀	[Cd] ₆₇₄	$\frac{[Cd]_{320}}{[Cd]_{674}}$	% Cd total measured	% Cd total measured
0.1805	0.02834	0.01666	1.70	0.0450	24.9
0.1740	0.02885	0.01732	1.66	0.04617	26.5
0.1705	0.03357	0.01896	1.77	0.05255	30.8
0.1497	0.03277	0.02096	1.56	0.05373	35.9
0.09522	0.01668	0.009773	1.71	0.02645	27.8
0.09485	0.01787	0.01105	1.62	0.02892	30.5*

ad20 sample

0.19M and
-0.19M respectively. The concentrations of species under the resonance at low field ([Cd]₆₇₄) and at high field ([Cd]₃₂₀) were determined and their ratios calculated for the different solution concentrations. The ratio [Cd]₃₂₀/[Cd]₆₇₄ is almost constant and an average value of 1.67±0.06 was calculated. This result eliminates the possibility of an unsymmetrical equilibrium (e.g., Cd₂L₃ ⇌ 2CdL + L).

iv. Stoichiometry of Complexes

In order to determine the stoichiometry of the complexes, the concentrations of cadmium species determined from ¹¹³Cd NMR were correlated to concentrations of glutathione species obtained from relative intensities of the resonances in the ¹³C NMR spectrum. The resonances of interest are labelled in Figure 63. On the ¹¹³Cd NMR spectrum (A in Figure 63), the two resonances observed at high pH are labelled 674 and 320. The concentrations of species represented by these resonances are referred to as [Cd]₃₂₀ and [Cd]₆₇₄ in Table 10. An expansion of the methylene region of the ¹³C NMR spectrum is shown in B. For the present purpose, the resonances due to cysteinyl C_α are used because they are free of interference and well resolved as compared to cysteinyl C_β or glutamyl resonances. The resonance labelled 1 was assigned to free glutathione on the basis of its chemical shift of 58.5 ppm. For a solution

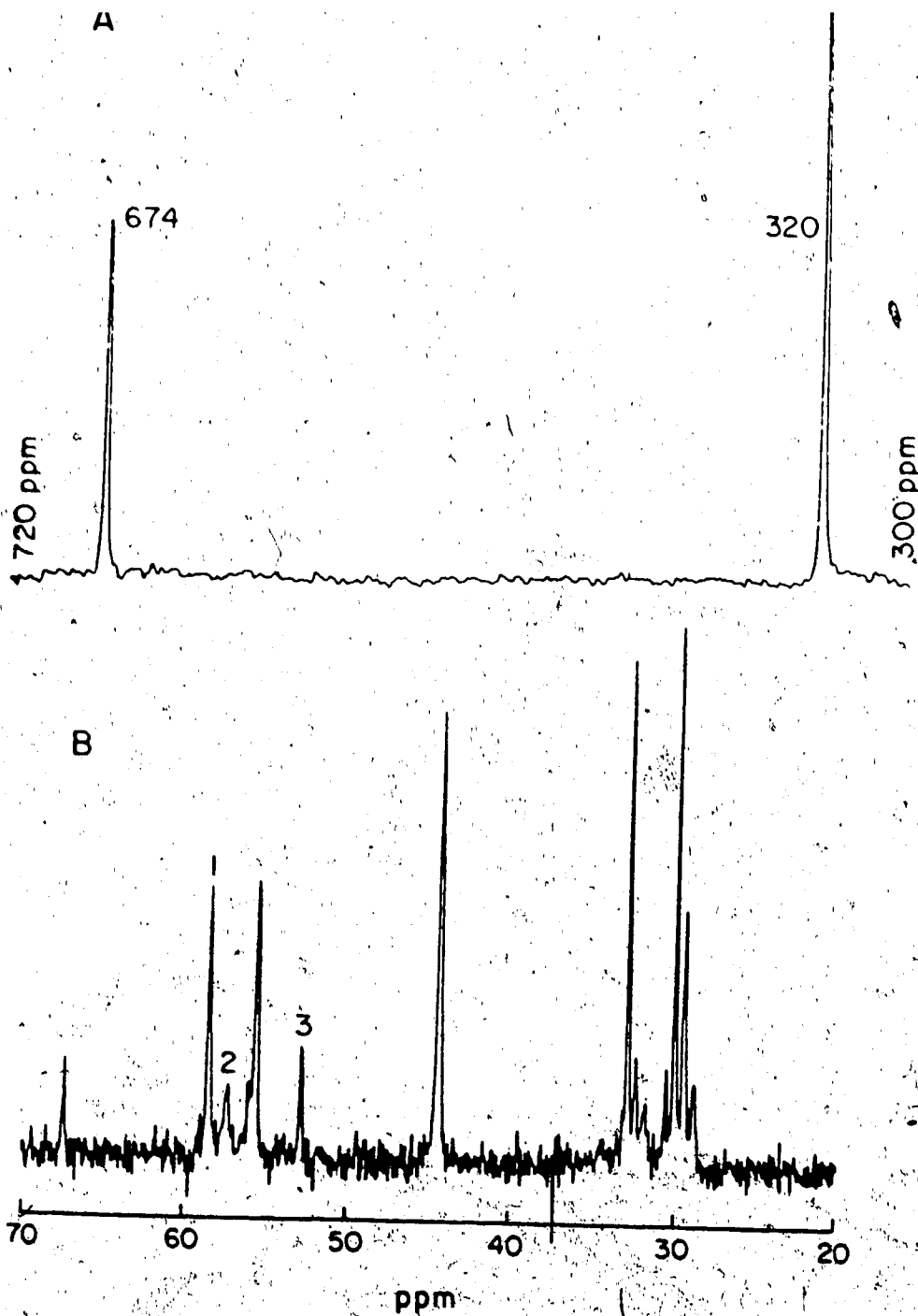


Figure 63. (A) ^{113}Cd NMR and (B) ^{13}C NMR spectra of a 1:2 mixture of Cd^{2+} and GSH at pH 9.5.

Table 10. Determination of the composition of complexes formed by Cd²⁺ and GSH from ¹¹³C NMR and ¹³C NMR intensity measurements (results deduced from spectra in Figure 63).

¹¹³ Cd NMR		¹³ C NMR of cyst Cd		Composition: $\frac{\text{GSH in complex}}{\text{Cd}^{2+} \text{ in comple}}$					
[Cd] ₆₇₄ (M)	$\frac{[\text{Cd}]_{320}}{[\text{Cd}]_{674}}$ (M)	[GSH] ₁ (M)	[GSH] ₂ (M)	[GSH] ₃ (M)	$\frac{[\text{GSH}]_2}{[\text{Cd}]_{674}}$	$\frac{[\text{GSH}]_3}{[\text{Cd}]_{320}}$	$\frac{[\text{GSH}]_3}{[\text{Cd}]_{674}}$	$\frac{[\text{GSH}]_2}{[\text{Cd}]_{32}}$	
0.01212	0.02004	1.65	0.1103	0.03114	0.02004	2.56	2.54	4.21	1.55

PH = 9.5, [Cd]_{tot} = 0.09637M, [GSH]_{tot} = 0.1925M

of glutathione alone at the same pH, the chemical shift measured for this resonance is 58.69 ppm. Resonances 2 and 3 were assigned to cysteinyl C_{α} in complexed glutathione based on the stronger effect of complexation on the chemical shifts of the resonances due to cysteinyl carbons. The intensities of these resonances were measured and fractional concentrations were calculated. Using the known total concentration of GSH in solution, the concentrations of each species were deduced and are given in Table 10 as $[GSH]_1$, $[GSH]_2$ and $[GSH]_3$.

It was first assumed that resonance 2 is due to glutathione in the cadmium species of resonance 674 ppm in the ^{113}Cd NMR spectrum and resonance 3 is due to glutathione in the 320 ppm cadmium species. Ratios $GSH_{\text{complexed}}/Cd_{\text{complexed}}$ of 2.56 and 2.54 are obtained for the 320 ppm and 674 ppm resonances respectively (Table 10) meaning that both species have the same stoichiometry. This result is therefore in agreement with the observation that dilution does not alter the ratio $[Cd]_{320}/[Cd]_{674}$. The closest composition corresponding to the ratio ~2.5 of ligand to metal is $Cd_2(SG)_5$. If assignments of the ^{13}C resonances are reversed, i.e., 2 goes with 320 ppm and 3 goes with 674 ppm resonance, 4.21 and 1.5 are obtained as ratios $GSH_{\text{complexed}}/Cd_{\text{complexed}}$ in the complexes corresponding to the 674 ppm and 320 ppm resonance respectively. The closest composition of the complexes corresponding to those ratios would be

$Cd_3(SG)_{12}$ and $Cd_2(SG)_3$. The latter result indicates a higher ratio of ligand to metal for the cadmium species giving the 674 ppm resonance. This was suggested earlier because only the latter resonance is observed for solutions having high ratios of glutathione to cadmium. Also, a ^{113}Cd NMR spectrum of a mixture containing approximately equimolar amounts of Cd^{2+} and GSH at pH = 10.5 (Figure 64) suggests a lower ratio GSH/Cd in the complex(es) giving the resonance at 320 ppm. In the spectrum, one very intense resonance is observed at 330 ppm and a very weak resonance at 564 ppm. But in a solution containing GSH and Cd^{2+} at a 2:1 ratio, an intense resonance is also observed at 674 ppm besides that at 320 ppm.

Polymeric species of composition $Cd_2(SG)_3$ have been suggested before [83] where the sulfhydryl and glycylic carboxylate groups of a single GSH are bonded simultaneously to different metal ions. Though resonances occurring in the chemical shift region above 600 ppm are generally due to Cd^{2+} bonded to four sulfur donors (CdS_4), some investigators have shown that Cd^{2+} in CdS_3O , CdS_2O_2 and CdO_4 sites may give resonances in this region [90]. Recently Bulman et al. [44], on the basis of resonances observed from a solution of Cd^{2+} and dicysteinoethylenediaminetetraacetic acid (EDTA-Cys₂), have proposed sites made of a combination of nitrogen, sulfur and oxygen donor groups for resonances in the regions 260-270 ppm and 640-670 ppm.

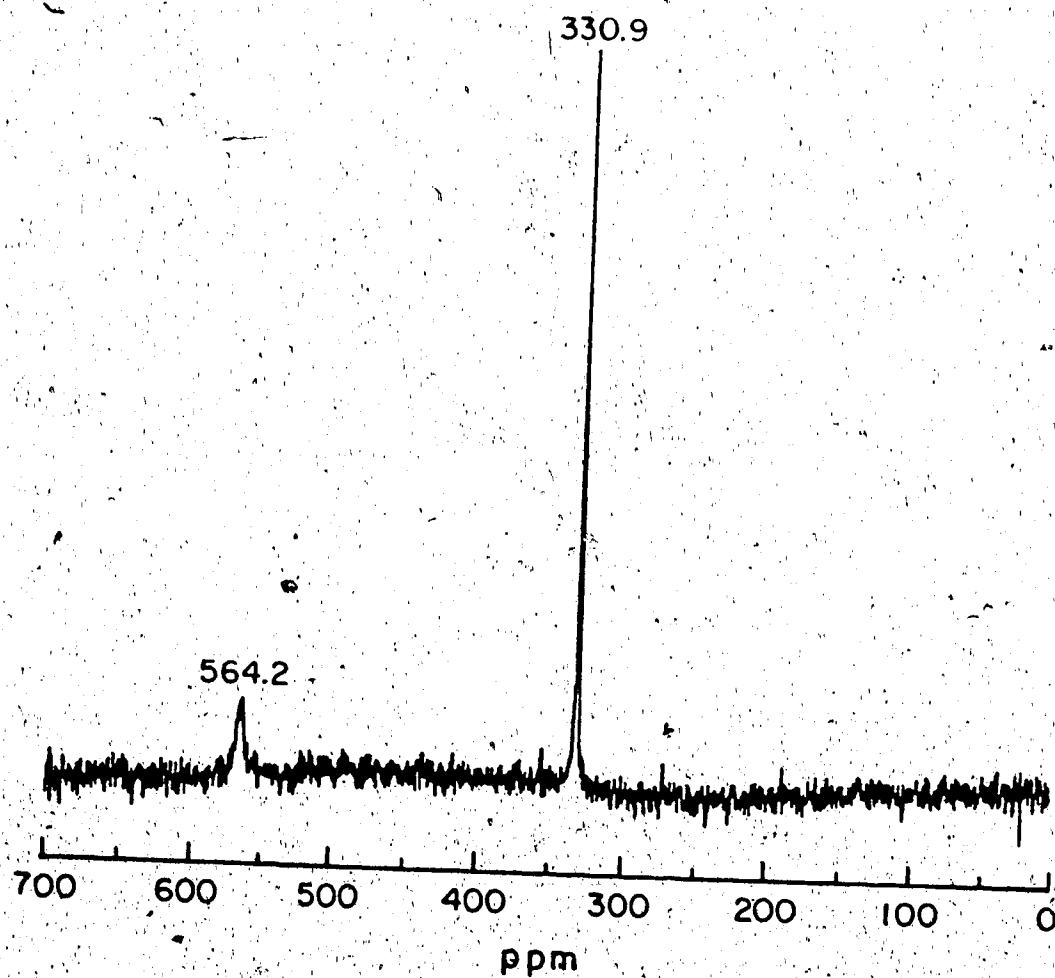
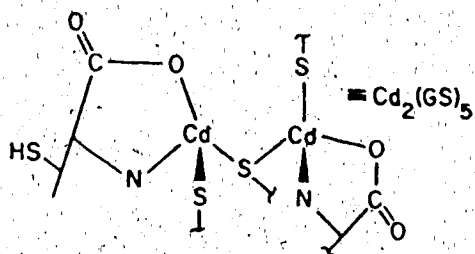


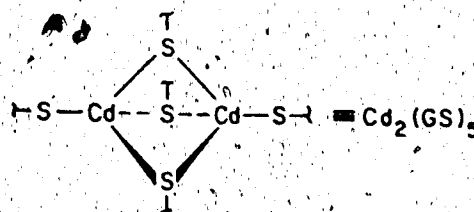
Figure 64. ^{113}Cd NMR spectrum of a 1 to 1 mixture of Cd^{2+} and GSH at pH 10.5.

The structures shown below are proposed based on the stoichiometric ratios calculated. Corresponding to the ratio $\text{GSH}_{\text{complexed}}/\text{Cd}_{\text{complexed}}$ of 2.5 are the structures A and B, for the species giving the resonances at 320 ppm and 674 ppm respectively, in the ^{113}Cd NMR spectrum. Structures C and D were built from the ratios 1.5 and 4.2 for the species represented by the 320 ppm and 674 ppm resonances respectively.



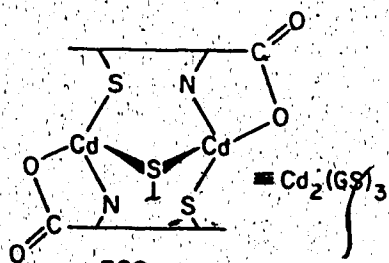
320 ppm

A



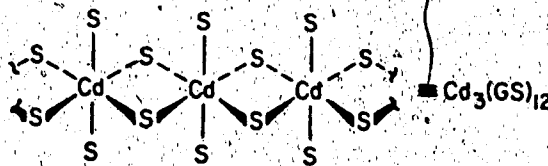
674 ppm

B



320 ppm

C



674 ppm

D

v. Comparative Study with PSH, N-PSH and Cysteine

For comparison, ^{113}Cd NMR measurements were made on solutions containing Cd^{2+} and three other thiols. ^{113}Cd NMR spectra were recorded at different pH values for solutions containing Cd^{2+} and penicillamine, and Cd^{2+} and N-acetylpenicillamine in ratios of 1:2. Contrary to GSH, at high pH only one resonance was observed in the ^{113}Cd NMR spectra at 508.9 ppm and 436 ppm for PSH and N-PSH respectively. These resonances were much broader ($W_{1/2} = 300$ Hz) than those of the glutathione system ($W_{1/2} = 30$ Hz). ($W_{1/2}$ is the width at half height). The corresponding ^{13}C NMR spectra contained a number of resonances equal to the number of carbons in each thiol; additional resonances due to kinetically stable species were not observed as was the case for glutathione. The species formed with these thiols are therefore less stable kinetically as compared to those of glutathione and their exchange is rapid on the NMR time scale. Similar to the Cd^{2+} -glutathione system, no resonance was detectable in the ^{113}Cd NMR spectra of Cd^{2+} -PSH and Cd^{2+} -N-PSH solutions below a pH ~ 6 presumably due to broadening.

The pH was fixed at 9.5 and the concentrations of the ligands increased to determine if the behavior of resonances is similar to that of Cd-GSH resonances. The resonances appeared narrower as the ligand concentration increased and they shifted to larger chemical shifts. In the case of PSH, for example, the resonance was shifted from 508.9 ppm to

564.4 ppm as the ratio of ligand to Cd^{2+} was increased from 2 to 5. This same effect was observed for glutathione complexes.

Quantitation of the resonances was done for solutions containing a 1 to 5 ratio of metal and ligand at pH 9.5, to compare with the glutathione system. Chemical shifts and percentages of cadmium measured are given in Table 11 for PSH, N-PSH, cysteine and glutathione. The percentages calculated decrease in the order N-PSH > PSH > cysteine > GSH, while the order of Cd^{2+} deshielding is reverse, i.e. GSH > cysteine > PSH > N-PSH. Though about 50% of Cd^{2+} is measured for PSH, GSH and cysteine, 100% was measured in the case of N-PSH.

The deshielding order strongly supports the participation of the amino group in the complexes formed with PSH, cysteine and GSH, giving rise to the resonances observed in the region generally assigned to only multisulfur sites. PSH, cysteine and GSH have a free amino group which can coordinate whereas this group is blocked in N-PSH. The lower measured concentration of cadmium for the three thiols PSH, cysteine and GSH might imply exchange is taking place between species of different nature, therefore strongly different resonance frequencies which cause the loss of some signal. On the other hand the fact that 100% of cadmium is measured for the N-PSH system is consistent with the formation of one kind of complex or complexes of very simi-

Table 11. ^{113}Cd chemical shifts and measured % cadmium from mixtures containing Cd^{2+} and thiols in the ratio 1 to 5. pH = 9.5.

Ligand	Chemical shift (ppm)	% Cadmium
N-acetylpenicillamine	545.8	100
Penicillamine	564.4	58.9
Cysteine	626.1	56.3
Glutathione	677	41.8

lar nature having, therefore, small differences in their resonance frequencies so that exchange among them results in the observation of an exchange averaged resonance. This is in agreement with cadmium sites made of only sulfur which is the free coordinating group on N-PSH. Possible participation of the carboxylate group is discussed later.

Though both cysteine and PSH can form five-member chelate rings using their sulfhydryl and amino groups, steric crowding in PSH, which is β -dimethylcysteine, may cause differences in the geometric disposition of the ligand around cadmium. Outer sphere effects of the substitution at the α carbon in a series of related thiolate ligands have been studied [36]. It was found that shifts of the order of 15 to 20 ppm were caused per alkyl group. Two alkyl groups would be expected therefore to cause a shift of the order of 30-40 ppm. However the difference between the resonances due to cadmium in the Cd^{2+} -cysteine and Cd^{2+} -penicillamine complexes is 62 ppm (Table 11). Hence, -22 ppm remains unaccounted for by the substituent effects. Slight geometric modification, as was suggested earlier, may account for this difference. A recent ^{113}Cd NMR study of small dynamically stable Cd^{2+} complexes noted the possibility of a strong influence of the geometry of the complex on the ^{113}Cd chemical shift [46].

The difference of 51 ppm between the ^{113}Cd chemical shifts of cadmium in the glutathione complexes (677 ppm) and

bonding of the donor groups in glutathione to different Cd^{2+} atoms may result in the formation of species with higher rigidity. The carboxylate groups of the glutamyl and glycine residues as well as the peptide linkage between the cysteinyl and glycyI residues have been suggested to be Cd^{2+} binding sites from ^{13}C NMR measurements by Fuhr and Rabenstein [94]. The rigidity of the metalloprotein binding sites has also been considered to be a factor causing the greater shielding in oxygen sites of metalloprotein as compared to oxygen sites of inorganic oxygen ligands [43].

Other factors which cause different shieldings in cadmium thiolate complexes, as well as other cadmium complexes, are the number of coordinating ligands and the geometry of the complex [43]. Chemical shifts of cadmium thiolates increase in the order $\text{CdS} < \text{CdS}_2 < \text{CdS}_3 < \text{CdS}_4$. Cd^{2+} in a tetrahedral coordination geometry appears to be deshielded relative to Cd^{2+} in an octahedral coordination geometry by approximately 50-100 ppm [37]. Though softer ligands such as S donors are known to prefer tetrahedral coordination to Cd^{2+} , octahedral coordination has been proposed in the case of a combination of sulfur with other donor groups [44] (e.g., S and N, S and O, S, N and O). The present data does not allow, however, a discussion of these factors to explain the differences in the observed chemical shifts in the ^{113}Cd

NMR had assigned the resonance at 320 ppm to a 1 to 2 complex $\text{Cd}(\text{SG})_2$ with binding through two cysteinate sulfur atoms [20]. This assignment was based on previous potentiometric [95] and ^1H and ^{13}C NMR measurements [83]. The resonance at 674 ppm was not reported though conditions similar to those of the present study (i.e., pH 9.5, $\text{GSH}/\text{Cd}^{2+} = 2$) were used. Another study of glutathione complexes of cadmium by ^{113}Cd NMR was conducted at a high temperature of 68°C and pH lower than 9 by Birgerson et al. [86]. As GSH was added to a solution of Cd^{2+} a broad resonance was observed and its chemical shift increased with increasing concentrations of GSH. Table 12 reproduces some results of the study. An interesting aspect of these results with relation to those of the present study is that a resonance is observed, even though broad, in the low pH region 8.6 to 1.15. Under the temperature conditions used in the present study (25°C) resonances were not observed below pH 8 when Cd^{2+} and GSH were in the ratio 1:2. No observations were made on low pH samples at higher temperatures. However, at pH 9.5 an increase in temperature caused the collapse of the two resonances at 320 and 674 ppm.

The results of Birgerson et al.'s study agree more with the present study if the temperature effect is considered.

Table 12. ^{113}Cd NMR study of Cd^{2+} -GSH system by Birgersson et al. [86] at 68°C.

$[\text{Cd}]_t$	$\frac{[\text{GSH}]}{[\text{Cd}]_t}$	PD	PPM*
0.3	2	1.15	-18.6
0.3	2	1.95	63.7
0.3	2	2.40	210.8
0.6	2	2.00	211.4
0.6	2	4.90	454.9
0.6	2	5.90	480.0
0.6	2	7.30	516.1
0.6	2	8.60	526.8
0.3	4.1	2.35	333.6
0.3	4.1	4.05	466.9
0.3	4.1	5.10	543.2
0.3	4.1	6.45	590.7
0.3	4.1	7.90	610.3

*Chemical shifts are relative to $0.1\text{M Cd}(\text{ClO}_4)_2$

resonance of chemical shift 526.8 ppm is recorded. Under these conditions of pH and molar ratio and the temperature of 25°C, two resonances were observed simultaneously at 320 ppm and 674 ppm. The higher temperature of 68°C must have caused the collapse of the two resonances. As mentioned already, this effect was confirmed in the present study at pH 9.5 (Figure 62). When the temperature of samples were increased above 37°C, the two resonances first disappeared due to broadening, then a single broad resonance reappeared around 477 ppm in the spectrum recorded at 57°C, which became narrower at higher temperatures.

C. Conclusion

The analysis of ^{113}Cd NMR parameters, with the aim of unravelling the structures of Cd^{2+} complexes and the nature of cadmium binding sites and the dynamics of exchange of cadmium between its complexes in solution, has been concerned mostly with chemical shift, coupling and relaxation information [18-20, 24, 28, 37-41, 43-47, 51, 52, 54, 55, 85-91]. The discussion of the results obtained in the present research on the Cd^{2+} -glutathione system are based largely on this pioneering work. However, the quantitative aspect in the analysis of ^{113}Cd NMR data pertaining to concentrations of species has been largely ignored in the past.

Nevertheless, results reported in this chapter and conclusions drawn therefrom demonstrate the need for considering such an approach. Otherwise unsuspected dynamics were revealed by the quantitation of observed resonances. It is often assumed that ^{113}Cd NMR resonance(s) observed for a given system represent the totality of cadmium species in solution whereas it was shown here that in Cd^{2+} -GSH solutions only a fraction of the Cd^{2+} is observed.

The approach to quantitation used in the present work not only determines the distribution of species but has also the potential to provide information about the stoichiometry of complexes formed. If this potential is realized it will represent an important step towards the determination of solution structures of cadmium complexes by ^{113}Cd NMR.

In analyzing the ^{113}Cd chemical shift data for the Cd^{2+} -thiol complexes, it became obvious that the available information, from which deductions may be made about the effects of coordinating groups, still needs to be expanded, mostly for cases of mixed coordination. Models used in this study were cysteine, penicillamine, glutathione and N-acetylpenicillamine. The first three ligands possess sulfhydryl, amino and carboxylate groups. Glutathione has additionally the nitrogen and oxygen of the peptide linkage. N-acetylpenicillamine has a sulfhydryl and carboxylate group. It was found that the difference in the ^{113}Cd chemical shift of penicillamine complex(es) and N-acetyl-

penicillamine complex(es) could not be totally explained by the inability of the amino group to coordinate in N-acetylpenicillamine. Rather, minor geometric factors were effective in causing shieldings or deshieldings. Also the differences in the chemical shift of cysteine complexes and penicillamine complexes could not be totally accounted for by the substitution of H₂ on C_β of cysteine by (CH₃)₂ on C_β in PSH. Minor modifications in the arrangement of the ligand(s) around cadmium were cited to explain the discrepancies.

Glutathione complexes of cadmium were reexamined with ¹¹³Cd NMR chemical shift data and quantitation of the resonances. Previous studies of the complexation of glutathione by Cd²⁺ in solution have mostly proposed the formation of 1 to 1 and 1 to 2 complexes [19, 83, 86]. The formation of a polymeric species Cd₂(HL)₃ has also been proposed [83]. The extent of deshielding observed in the ¹¹³Cd NMR spectrum of glutathione complexes cannot be accounted for solely by the involvement of sulfur and nitrogen containing groups in the complexation by comparison to the other thiols studied. It is suggested that possible structures of GSH complexes in solution are polymeric similar to those proposed for metallothioneins [37]. Three and four metal clusters bridged by sulfur have been reported to occur in human, calf and rabbit liver metallothionein [37]. Glutathione might be forming similar cluster compounds where Cd²⁺ centers are bound and

bridged by the sulfhydryl group such as those proposed in section iv. of the present chapter.

On several occasions in the discussion of the Cd^{2+} -GSH system, reference has been made to previous studies of the complexation of GSH by Cd^{2+} by ^1H or ^{13}C or ^{113}Cd NMR. The aim of this study was to adopt a more systematic and complete approach using ^1H , ^{13}C and ^{113}Cd NMR. The first obvious consequence was the observation of two resonances where only one has always been observed in the ^{113}Cd NMR spectrum [19, 20, 86]. Secondly, the detailed analysis of a larger body of experimental data from the three probes (^1H , ^{13}C and ^{113}Cd NMR) has shown that some earlier conclusions on the nature of complexes formed were totally or partially false [19, 20, 86]. For example, the resonance at 320 ppm has been attributed to a 1 to 2 complex of Cd-GSH with binding to the sulfhydryl group [18, 19]. It was assumed that this complex was formed in a 1:2 mixture of Cd^{2+} and glutathione after only one resonance was observed in the ^{113}Cd NMR spectra. The present study has proven that only ~15% of Cd^{2+} is represented by the resonance at 320 ppm, the remaining cadmium is distributed between species giving rise to a resonance at 674 ppm and others whose resonances are exchange broadened. Finally, the quantitation of ^{113}Cd resonance intensities indicated hidden dynamics which otherwise could not be detected. As well the amounts of cadmium species measured in a comparative study afforded some

interesting insights on the effects of less drastic
geometric factors in the ^{113}Cd chemical shift.

CHAPTER V

DETERMINATION OF ^{113}Cd CHEMICAL SHIFTS OF Cd^{2+} COMPLEXED BY CARBOXYLATE LIGANDS.

A. Introduction

The assignment of resonances in the ^{113}Cd NMR spectra of biological systems is largely based on comparison with model systems as was exemplified earlier in the case of $\text{Cd}(\text{II})$ metallothionein. Studies have been conducted, placing Cd^{2+} in a variety of ligand environments, to obtain representative chemical shifts for potential biological environments [24, 44, 45, 49, 52, 91]. As stated in the introductory chapter, an important asset of ^{113}Cd NMR lies in the characteristic chemical shifts produced by the donor group of binding ligands. It follows, therefore, that from knowledge of the chemical shift one can determine the chemical environment of cadmium. The need for benchmark chemical shifts of model compounds for the assignments of resonances in more complex biological systems was recognized with the first observations on ^{113}Cd NMR and has been stressed again recently by Armitage [37] and Ellis [43]. The present chapter is a contribution to the cited need.

The ^{113}Cd chemical shifts of Cd^{2+} complexed by a series of carboxylate-containing ligands including acetic acid,

monochloroacetic acid, formic acid, pivalic acid, glycylglycine, histidine and N-acetylhistidine, were determined. These chemical shifts were determined from the pH and concentration dependence of the exchange averaged single ^{113}Cd resonance and known acidity and formation constants.

B. Method

For all the complexes investigated, a single time-averaged resonance is observed in the ^{113}Cd NMR spectra of solutions containing Cd^{2+} and the above cited ligands, indicating rapid exchange of Cd^{2+} among the various complexes formed on the NMR time scale. The chemical shift of such a resonance is the weighted average of the individual chemical shifts of the various cadmium complexes as expressed by equation 102

$$\delta_{\text{obs}} = \delta_f P_f + \delta_1 P_1 + \delta_2 P_2 \dots \quad (102)$$

where δ_f stands for the chemical shift of free cadmium, δ_1 the chemical shift of a given type 1 complex, and δ_2 the chemical shift of a given type 2 complex. P_f , P_1 , and P_2 stand for the fractional concentrations of free cadmium, complex 1 and complex 2 respectively.

Acid-base like titration curves are obtained when δ_{obs} for ^{113}Cd is plotted against the pH of solutions containing Cd^{2+} and the carboxylate ligands. The individual chemical

shifts of the specific complexes were obtained by fitting δ_{obs} versus pH data with known equilibrium models. The models used involved either the formation of both 1 to 1 and 1 to 2 complexes of Cd^{2+} and ligand or the formation of only the 1 to 1 complex of Cd^{2+} and ligand. The stability constants of these complexes may be expressed as follows:

$$K_1 = \frac{[\text{CdL}]}{[\text{Cd}^{2+}][\text{L}]} \quad (103)$$

for the formation of the 1 to 1 complex and

$$\beta_2 = \frac{[\text{CdL}_2]}{[\text{Cd}^{2+}][\text{L}]^2} \quad (104)$$

for the formation of the 1 to 2 complex.

The fractions P_f , P_1 and P_2 can be expressed in terms of the stability constants of the complexes formed and the equilibrium concentration of the ligand. In the case of formation of a 1 to 1 complex only the fractions P_f and P_1 are given by

$$P_f = \frac{[\text{Cd}^{2+}]}{[\text{Cd}^{2+}] + [\text{CdL}]} \quad (105)$$

$$P_1 = \frac{[\text{CdL}]}{[\text{Cd}^{2+}] + [\text{CdL}]} \quad (106)$$

Division of the numerators and denominators of equations 105 and 106 by $[\text{Cd}^{2+}]$ yields the following expressions for P_f and P_1

$$P_f = \frac{1}{1 + [CdL]/[Cd^{2+}]} \quad (107)$$

$$P_1 = \frac{[CdL]/[Cd^{2+}]}{1 + [CdL]/[Cd^{2+}]} \quad (108)$$

the term $[CdL]/[Cd^{2+}]$ is given by $K_1[L]$ from rearrangement of equation 103. Substitution of $[CdL]/[Cd^{2+}]$ by $K_1[L]$ in equations 107 and 108 gives:

$$P_f = \frac{1}{1 + K_1[L]} \quad (109)$$

$$P_1 = \frac{K_1[L]}{1 + K_1[L]} \quad (110)$$

The equation used to fit the data (equation 111) was obtained by substituting P_f and P_1 in equation 102 by equations 109 and 110.

$$\delta_{obs} = \frac{\delta_f + \delta_1 K_1[L]}{1 + K_1[L]} \quad (111)$$

The equilibrium concentration of free ligand $[L]$ is obtained from mass balance equations, pH, and acidity and stability constants as was described in Chapter III. In the case of the formation of a 1 to 1 complex with a ligand having one acidic group the following expression is obtained:

$$[L]^2(K_{a1}K_1 + [H]K_1) + [L](K_{a1} + [H] + K_{a1}K_1Cd_t - K_{a1}K_1L_t)L_tK_{a1} = 0 \quad (112)$$

where K_{a1} is the acidity constant of the ligand, K_1 the formation constant for the 1 to 1 complex, L_t the total concentration of the ligand and Cd_t the total concentration of cadmium. The concentration of L is calculated within the program.

Following the previous reasoning the model involving the formation of both 1 to 1 and 1 to 2 complexes is given by:

$$\delta_{obs} = \frac{\delta_f + \delta_1 K_1 [L] + \delta_2 \beta_2 [L]^2}{1 + K_1 [L] + \beta_2 [L]^2} \quad (113)$$

The method used to calculate the unknown chemical shifts δ_1 and δ_2 is also similar to that described in Chapter III for the determination of acidity constants. Chemical shift vs. pH data obtained at different ratios of cadmium to ligand were fitted to the models described by equations 111 and 113 using the nonlinear least square program KINET.

Generally, three titrations were performed for each ligand with ligand to metal ratios of one, two and four. The first estimate of the chemical shift of the 1 to 1 complex was obtained from data for the titration of a 1 to 1 mixture, assuming only the formation of a 1 to 1 complex. Keeping the chemical shift so calculated constant, titration

data for 1 to 2 or 1 to 4 mixtures were used to determine the first estimate of the chemical shift of the 1 to 2 complex. The latter was then employed to refine the former and so on until the sum of the residuals was brought to a minimum value.

C. Results

1. Carboxylic Acid Complexes

A cadmium nitrate solution was titrated with NaOH and the ^{113}Cd chemical shift measured for solutions between pH 2 and 5. As shown by curve A in Figure 65, the chemical shift of 'free cadmium' is constant between pH 2 and 5. At higher pH, precipitation of $\text{Cd}(\text{OH})_2$ occurred, consequently spectra of samples at higher pH values could not be measured. In the presence of the carboxylic acids listed in Figure 66, the ^{113}Cd resonance is shifted to higher field as the pH of the solution is raised. This shift results from binding of cadmium to the carboxylate group of the carboxylic acids as it is being deprotonated. The shift to higher field was the expected behavior from known effects of donor groups on the ^{113}Cd chemical shift [37, 43]. Figure 65 depicts this effect for the complexation of Cd^{2+} by acetic acid. Curve B, C and D correspond to the titration of mixtures 1:1, 1:2 and 1:4 of Cd^{2+} ; acetic acid respectively. Data points in the middle of the titration curves were left

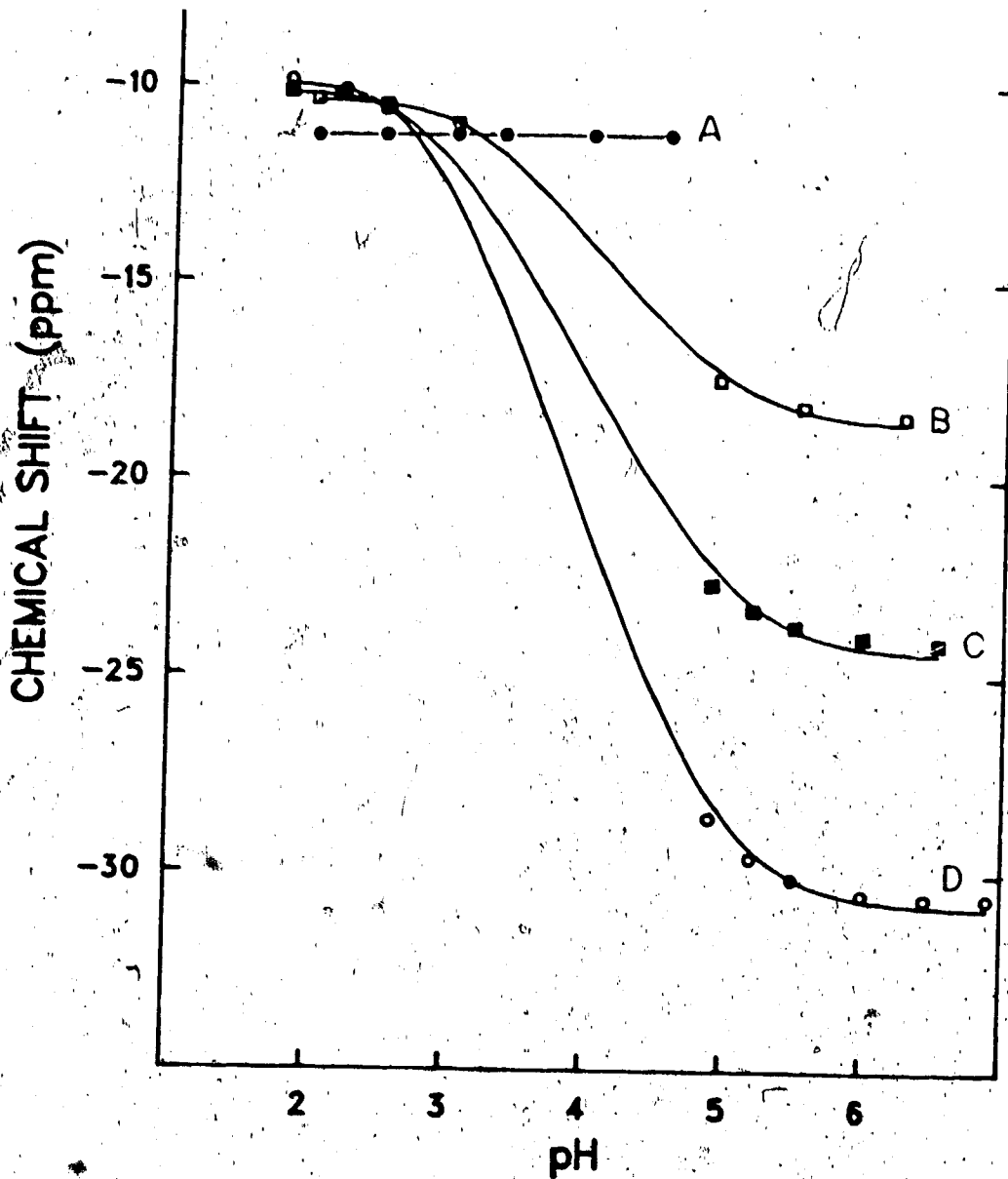


Figure 65. The pH dependence of the ^{113}Cd chemical shift for (A) a $\text{Cd}(\text{NO}_3)_2$ solution and for (B) 1:1, (C) 1:2 and (D) 1:4 mixtures of Cd^{2+} and acetic acid.

ACETIC ACID

X

HCOOH

FORMIC ACID

XI

ClH₂CCOOH

CHLOROACETIC ACID

XII

(H₃C)₃CCOOH

PIVALIC ACID

XIII

Figure 66. Names and structures of carboxylic acids used to determine ¹¹³Cd chemical shifts of cadmium carboxylate complexes.

ments were larger. As the concentration of the ligand increases, increased shieldings are observed indicating more extensive complexation at higher concentrations. Curve B reaches a plateau of ~ -18 ppm, curve C a plateau of ~ -24 ppm and curve D a plateau of ~ -30.5 ppm. The small shift to lower field for the curves of mixtures as compared to that of free cadmium at low pH is due to differences in the ionic strengths. This was verified experimentally. Addition of increasing amounts of sodium acetate to a solution of Cd^{2+} at pH 2, where no binding occurs, caused a shift in ^{113}Cd chemical shift of Cd^{2+} in solution. The points on the figure are experimental whereas the solid curves are calculated curves from the chemical shifts in Table 13 and literature pK_a 's and formation constants.

Figures 67 to 69 depict experimental results and calculated curves for chloroacetic acid, formic acid and pivalic acid. The pK_a values used with KINET were all from the literature [96] and are listed in Table 13 with the chemical shifts of the complexes. Formation constants used were also from the literature for the complexes of acetic acid and formic acid [97]. No literature values were available for the formation constants of Cd-pivalic acid complexes, therefore the formation constants were treated as unknowns when fitting data. The values obtained were $\log K_1 = 1.68 \pm 0.02$

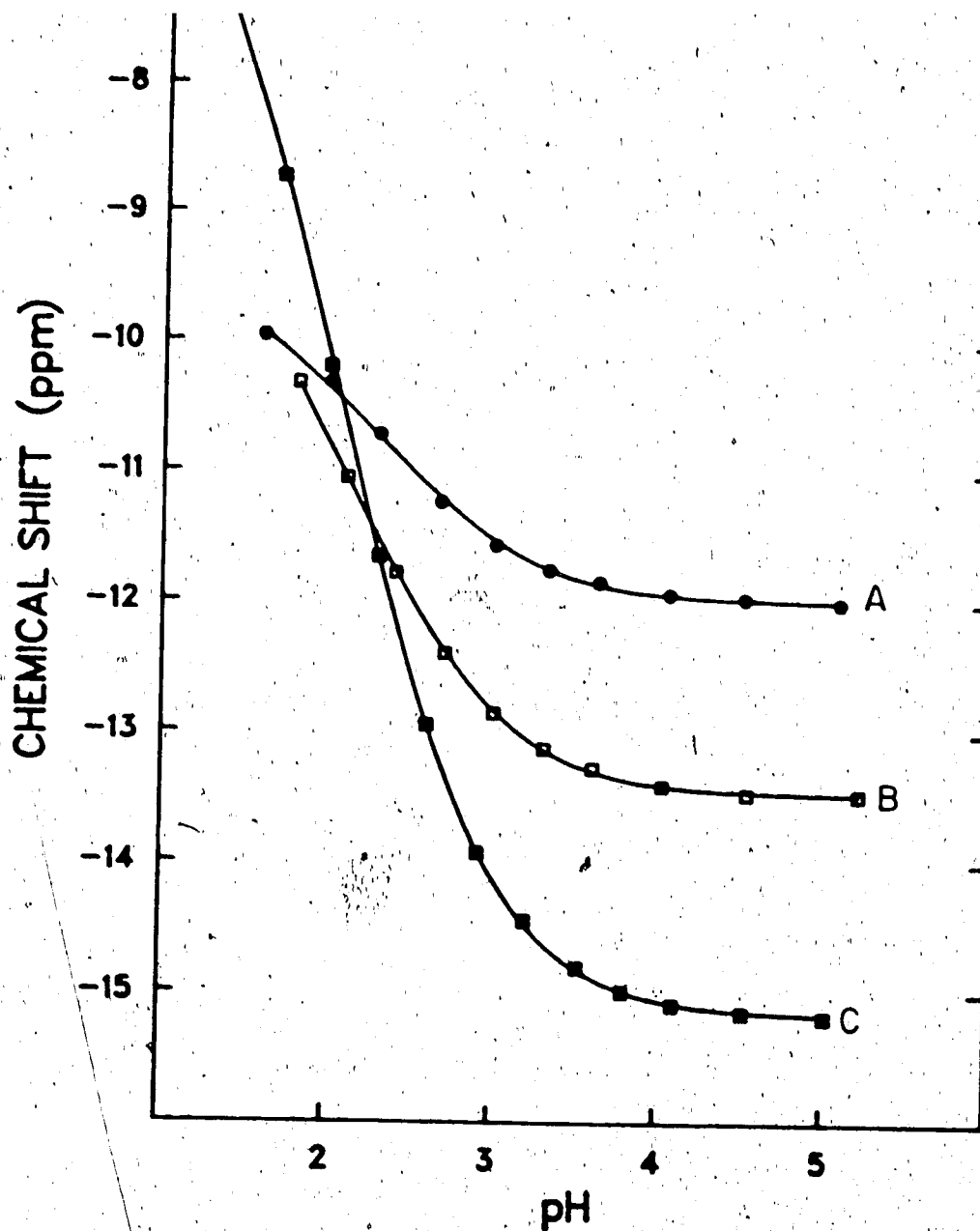


Figure 67. The pH dependence of the ^{113}Cd chemical shift for (A) 1:1, (B) 1:2 and (C) 1:4 mixtures of Cd^{2+} and chloroacetic acid.

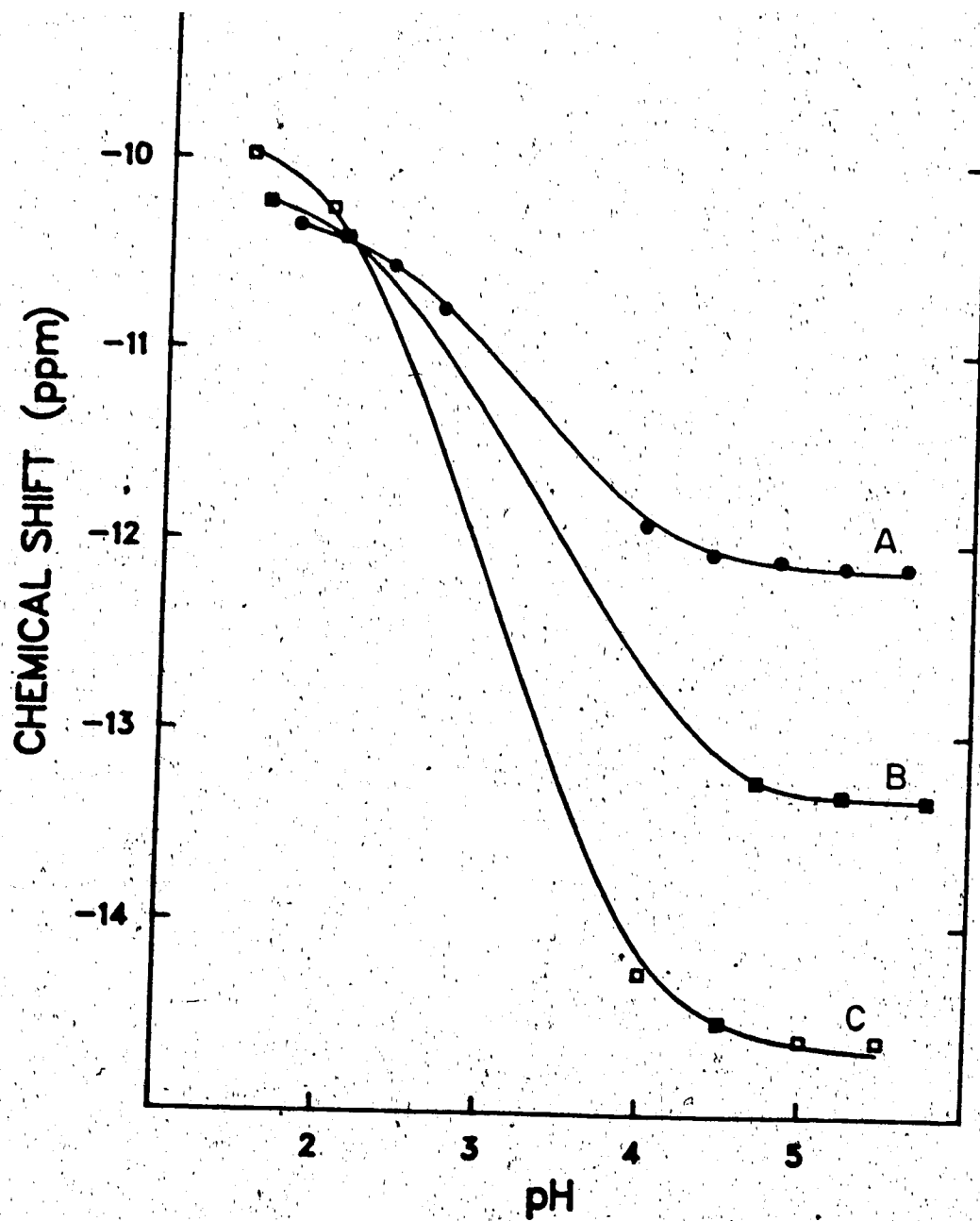


Figure 68. The pH dependence of the ^{113}Cd chemical shift for (A) 1:1, (B) 1:2 and (C) 1:4 mixtures of Cd^{2+} and formic acid.

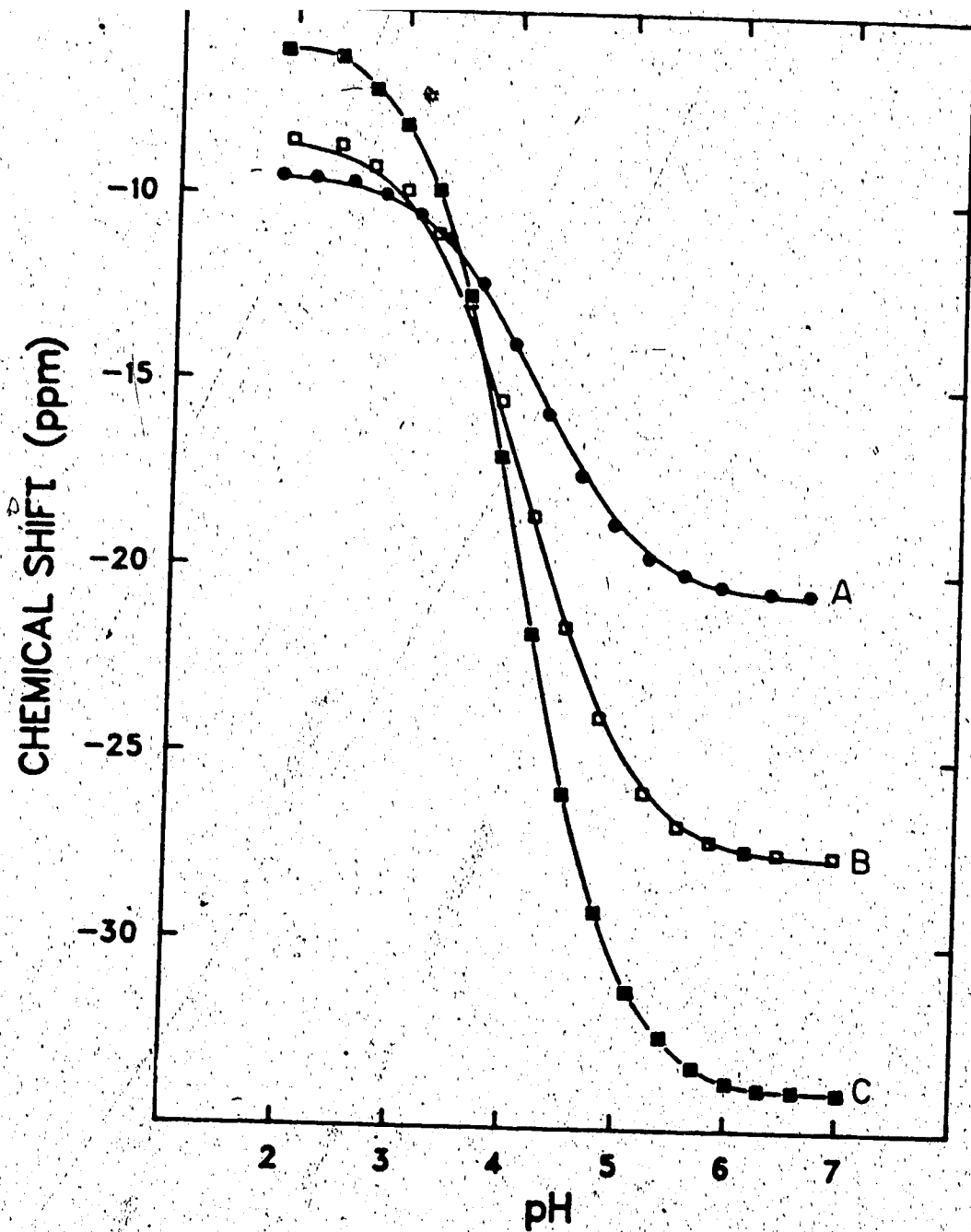


Figure 69. The pH dependence of the ^{113}Cd chemical shift for (A) 1:1, (B) 1:2 and (C) 1:4 mixtures of Cd^{2+} and pivalic acid.

Table 13. ^{113}Cd NMR chemical shifts of complexes of cadmium with selected carboxylic acids.

Ligand	pKa	$\delta_{1:1}$	1:2 titration data	$\delta_{2:1}$	1:4 titration data
Pivalic acid	4.95	-25.1 ± 0.1	-38.0 ± 0.2		
Acetic acid	4.65	-24.4 ± 0.2	-40.2 ± 3.1		-40.0 ± 1.6
Formic acid	3.55	-14.63 ± 0.04	-18.50 ± 0.05		-18.1 ± 0.1
Chloroacetic acid	2.74	-14.28 ± 0.08	-16.38 ± 0.1		-18.5 ± 0.2

and $\log \beta_2 = 2.76 \pm 0.10$. In the case of chloroacetic acid, available literature values [98, 99] yielded erroneous results for the chemical shifts of complexes; therefore, the formation constants in this system were also treated as unknowns. The values obtained were $\log K_1 = 1.15 \pm 0.04$ (evaluated with 1:1 titration data, curve A in Figure 67), $\log \beta_2 = 2.29 \pm 0.04$ (evaluated with 1:2 titration data, curve B in Figure 67) and $\log \beta_2 = 1.86 \pm 0.03$ (evaluated with 1:4 titration data, curve C in Figure 67).

The chemical shifts obtained for cadmium complexes formed with acetic acid and pivalic acid may be considered equal within experimental error (Table 13). Because the pivalate ion is slightly more basic than the acetate ion, the association of Cd^{2+} with pivalate is expected to be somewhat stronger than with acetate. The closer the bond between Cd^{2+} and the binding oxygen donor group, the more shielded is Cd^{2+} and the more ^{113}Cd is shifted to lower frequencies [24]. Pivalic acid, however, has three bulky methyl groups on its α carbon while the same carbon in acetic acid has only three hydrogens. This latter difference explains the lower shielding than expected, on the basis of pK_a 's, when pivalate ions react with Cd^{2+} . The alkyl groups may also have an effect similar to that observed in the case of thiolate ligands [36]. Substitution by an alkyl group on the α carbon of thiolates causes shifts on the order of 15 to 20 ppm per alkyl substituent [36]. Addition of a second

acetate and pivalate ligand shields Cd^{2+} to the same extent; the difference between the ^{113}Cd chemical shift of the 1 to 1 complex and the 1 to 2 complex is about 15 ppm for both acetic acid and pivalic acid.

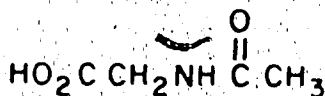
The chemical shifts of Cd^{2+} in its complexes with formate and chloroacetate are shifted to higher frequencies, consistent with the lower basicity of the above cited ligands as compared to acetate and pivalate. The ^{113}Cd chemical shifts of their 1 to 1 complexes is about -14.4 ppm while -24.7 ppm was obtained for the homologue complexes of acetic acid and pivalic acid. However, despite the difference of 0.8 units between the pK_a 's of formic acid and chloroacetic acid, the ^{113}Cd chemical shifts of their complexes are also very similar. This can be explained by the similarity of the formation constants of the formate and chloroacetate complexes of Cd^{2+} even though the formate ion is more basic than the chloroacetate ion. For example the logarithm of the formation constant of the 1 to 1 formate complex is 1.04 [97] and that of the 1 to 1 chloroacetate complex is 0.95 [98], 1.15 [this present study].

Pertaining to the last two ligands discussed, the ^{113}Cd chemical shifts of their 1 to 2 complexes are very close to the ones for their 1 to 1 complex. The stepwise formation constants for the addition of a second ligand on Cd^{2+} is very small for both formate and chloroacetate ions. It is $K_2 = 0.45$ [98] and $K_2 = 1.55$ [97] for the addition of a

second chloroacetate ion and formate ion respectively. Such weak interactions account for the lack of further shielding of Cd^{2+} when the second ligand enters the coordination sphere.

2. Acetylglycine Complexes

The results of ^{113}Cd NMR chemical shift titrations of mixtures of $\text{Cd}(\text{NO}_3)_2$ and acetylglycine (XIV) are depicted in Figure 70. Experimental results are represented by the



N-ACETYLGLYCINE

(XIV)

points on curves A and B for the titration of 1:1 and 1:2 mixtures of Cd^{2+} :acetylglycine respectively. The resonance moves to higher field as the pH is increased, as was the case for carboxylic acids. This behavior is indicative of binding to an oxygen donor group, in this case the carboxylate group of acetylglycine. Data could be fitted only with the model involving the formation of a 1 to 1 complex alone. The solid curves through the 1:1 and 1:2 data show the fit yielded by KINET. A chemical shift of -19.0 ± 0.05 ppm was obtained by fitting the 1:1 titration data and using a pK_a of 3.44 and $\log K_1 = 1.23$ [25]. With the 1:2 titra-

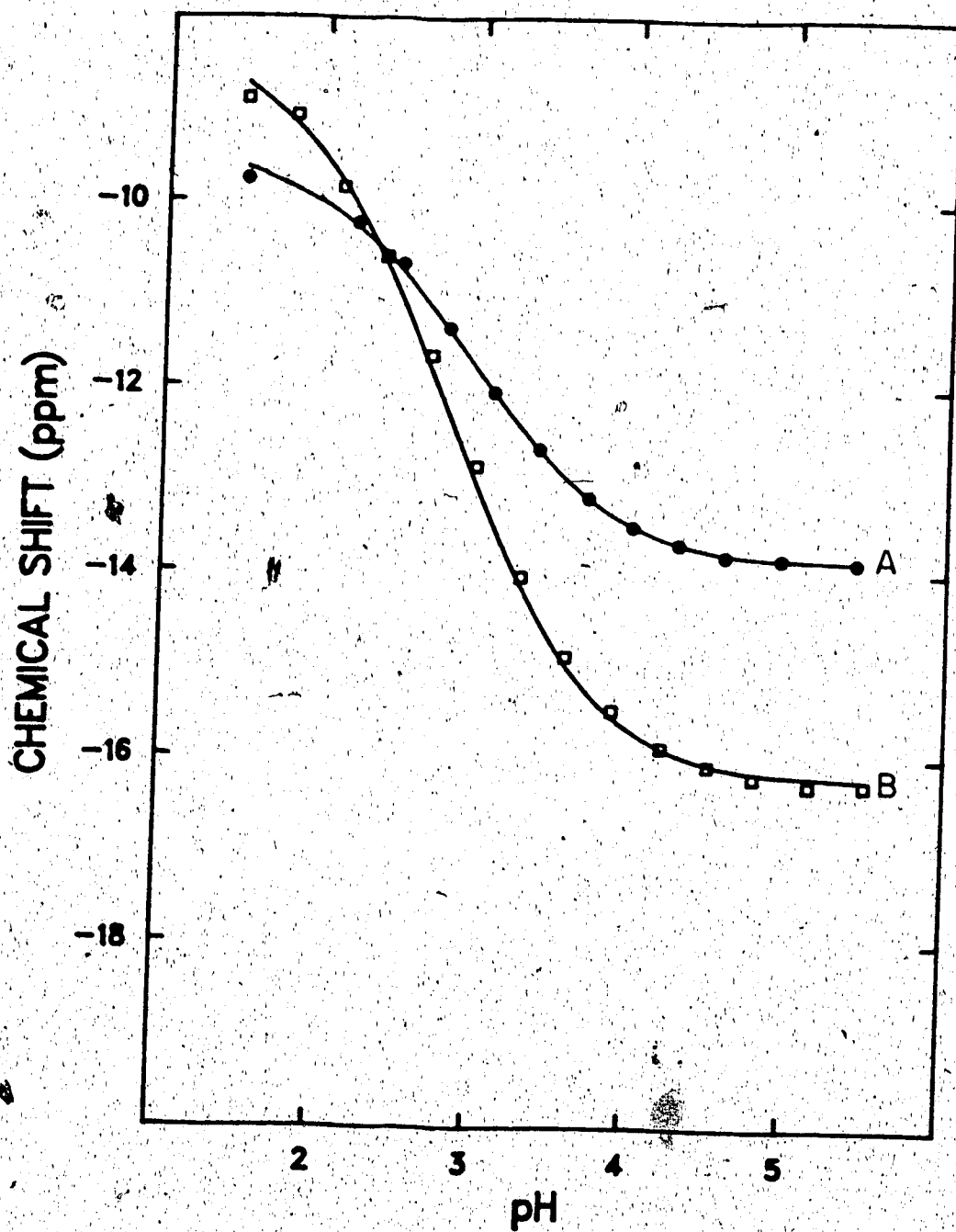
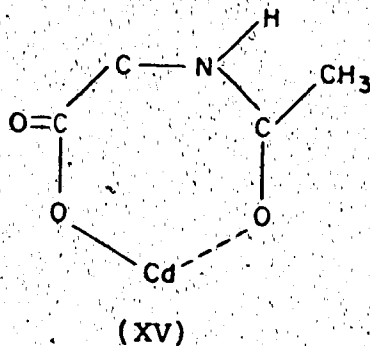


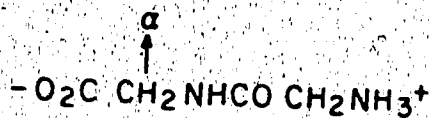
Figure 70. The pH dependence of the ^{113}Cd chemical shift for (A) 1:1 and (B) 1:2 mixtures of Cd^{2+} and acetylglycine.

tion data, the calculated chemical shift was -20.2 ± 0.1 ppm. The value of the chemical shift of the Cd(acetylglycine) complex falls between those calculated for the Cd(acetate) complex (-24.4 ppm) and Cd(formate) complex (-14.6 ppm) even though acetylglycine has a slightly lower pK_a (3.44) than formic acid (3.55). Additional coordination to the oxygen of the peptide link can account for this shift. Hence, results in this study argue in favor of the formation of a chelate ring, which was also proposed on the basis of 1H NMR data [25], having the following structure:



3. Glycylglycine Complexes

The complexation of cadmium by glycylglycine (XVI) has

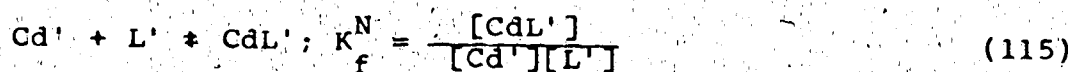
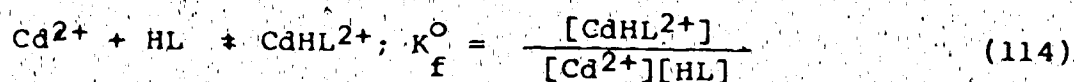


GLYCYLGLYCINE

(XVI)

been previously characterized in aqueous solution by 1H -NMR

[23]. Two reactions were identified from the change in the chemical shift of the methylene protons. The chemical shift of the α -methylene protons indicated that cadmium binds to the C-terminal end of the peptide in the pH range 1-4 while the amino group remains fully protonated. At pH's greater than 4, changes in the chemical shift of the methylene protons adjacent to the amino group pointed to complexation at the amino end also. The reactions described and the appropriate equilibrium constants can be summarized as:



where K_f^{O} is for binding to the carboxylate oxygen and K_f^{N} for binding to the nitrogen. Cd' represents all cadmium that is not bound to the nitrogen group. The values used for the equilibrium constants K_f^{O} and K_f^{N} are 1.04 and 2.76 respectively [23].

In Figure 71 are shown the ^{113}Cd chemical shift titration data for 1 to 1, 1 to 2 and 1 to 4 mixtures of cadmium and glycylglycine. Above pH 4 the three curves are shifted downfield denoting coordination to the amino group. Below pH 4 a smaller upfield shift indicates coordination to the carboxylate group. Given the agreement between our observations and the previously described study, the model

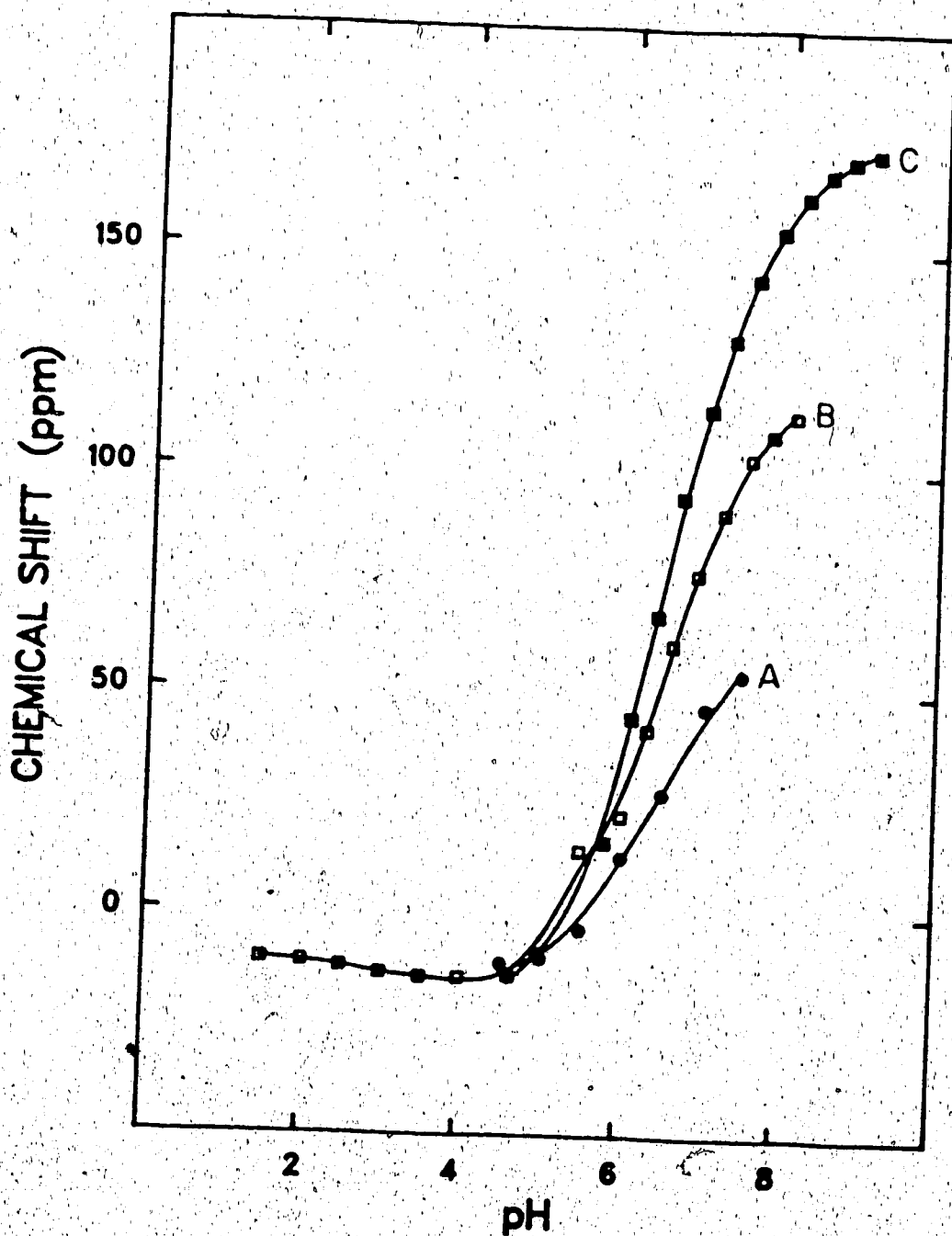
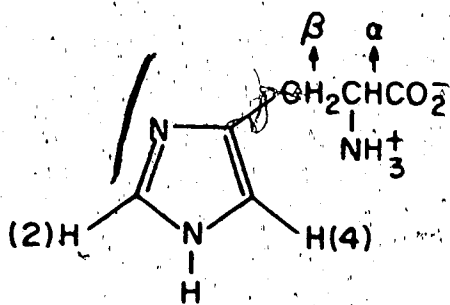


Figure 71. The pH dependence of the ^{113}Cd chemical shift for (A) 1:1, (B) 1:2 and (C) 1:4 mixtures of Cd^{2+} and glycylglycine.

separately. A chemical shift of -18.4 ppm was obtained for the carboxylate complex from the KINET fit of the 1 to 2 titration data shown in Figure 72 at $\text{pH} < 4$. Then 1:1 data at $\text{pH} > 4$ were fitted with KINET (Figure 73) to determine the chemical shift of the amino complex, 82 ± 3 ppm. The latter chemical shift falls in the region of mixed coordination to nitrogen and oxygen donor groups, such as in $\text{Cd}(\text{EDTA})$ (85 ppm) [85]. This possibility was alluded to by Rabenstein and Libich on the basis of $^1\text{H-NMR}$ results [23].

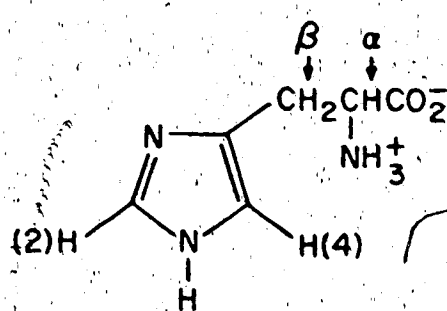
4. Histidine and N-acetylhistidine

The reactions of cadmium with histidine (XVII) and N-acetylhistidine (XVIII) were first investigated by $^1\text{H-NMR}$ in aqueous solution in order to ascertain the nature of the complexes formed and measure their formation constants.



XVII

HISTIDINE



XVIII

N-ACETYLHISTIDINE

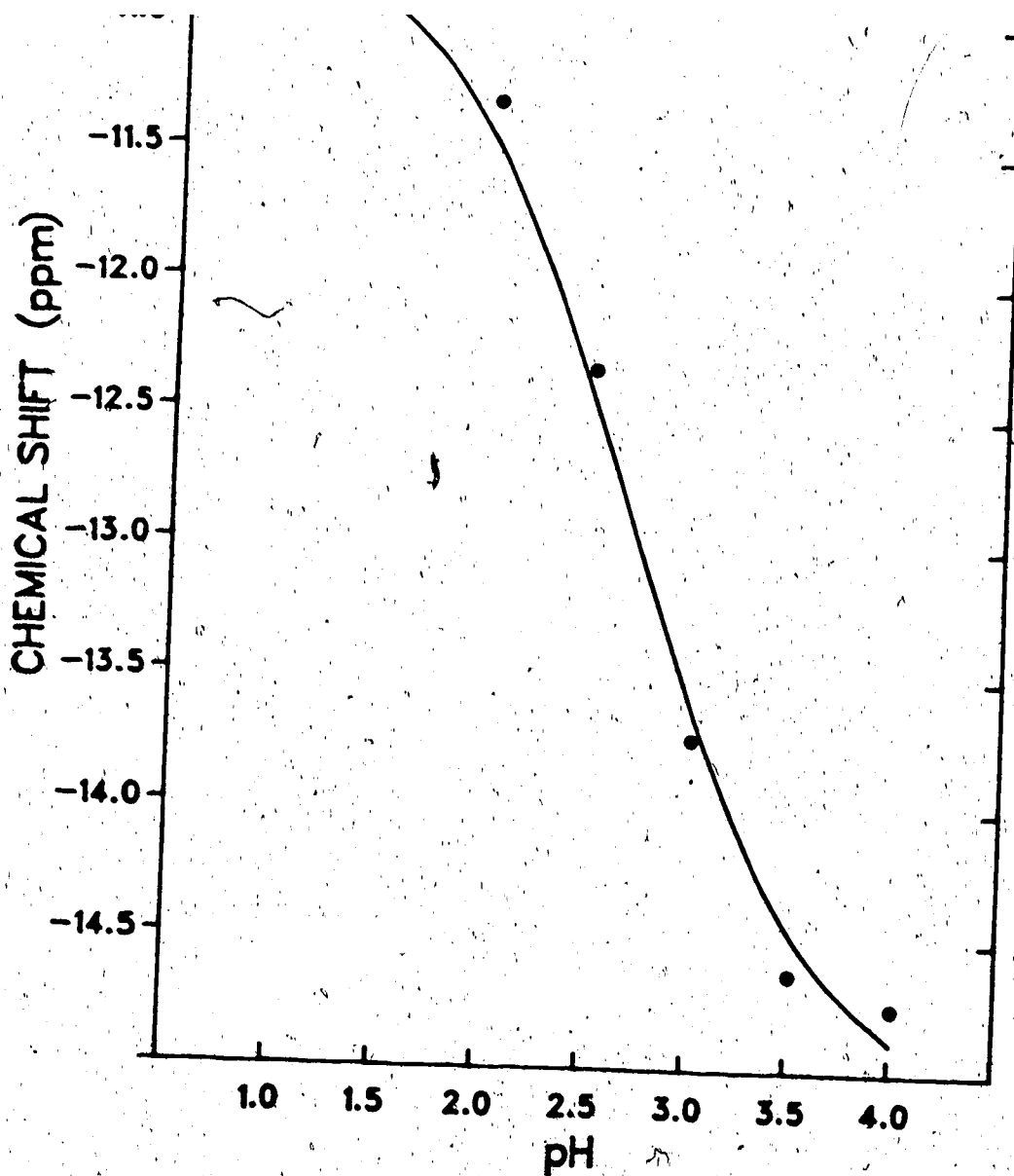


Figure 72. Experimental and calculated curves of ^{113}Cd chemical shift versus pH for the determination of the ^{113}Cd chemical shift of the carboxylate complex of Cd-glycylglycine.

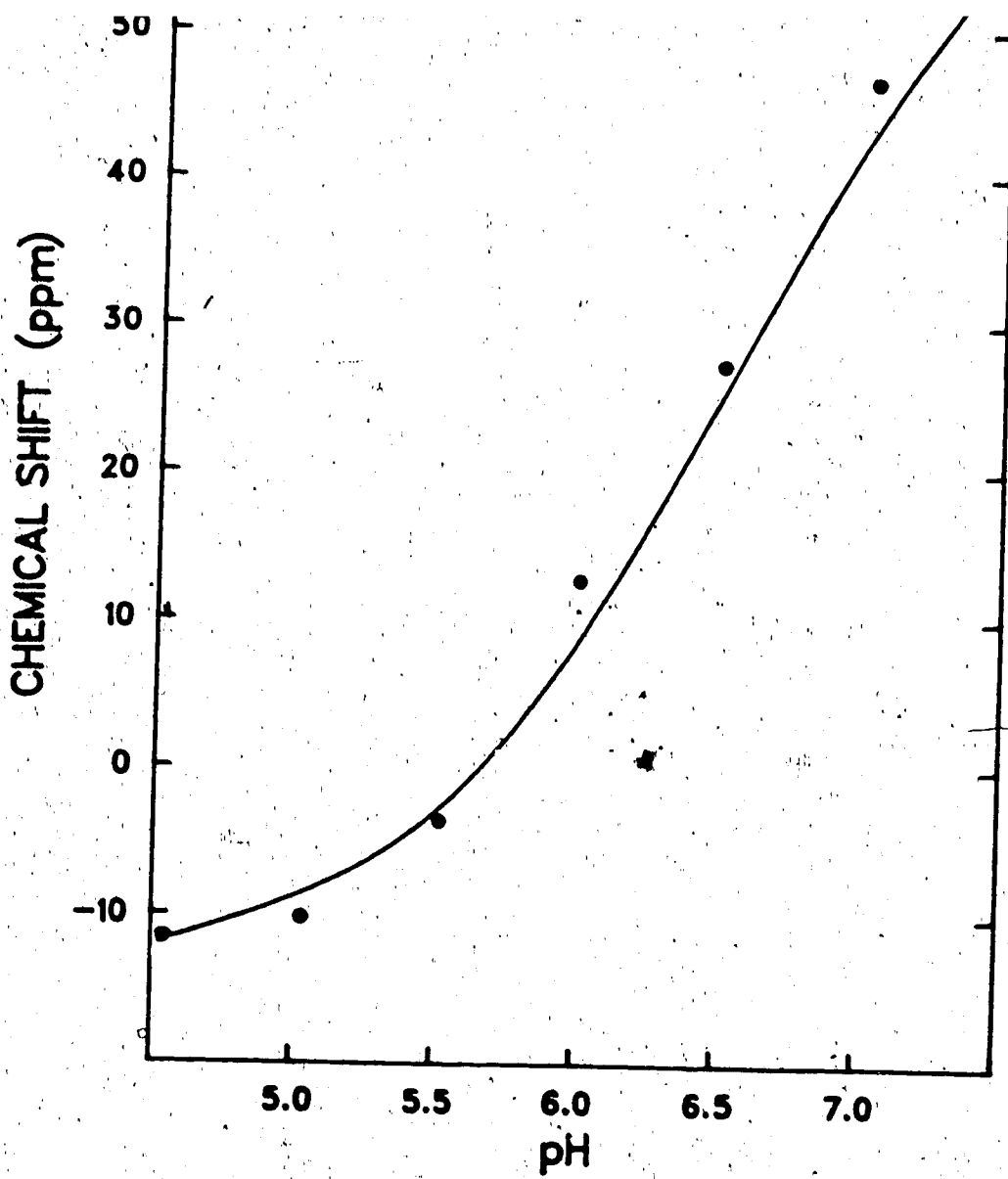


Figure 73. Experimental and calculated curves of ^{113}Cd chemical shift versus pH for the determination of the ^{113}Cd chemical shift of the amino complex of Cd-glycylglycine.

the protons H_a , H_b , H_2 , or H_4 , are the same between pH 1 to pH 4 when the ligand is titrated alone and in the presence of Cd^{2+} , indicating that the carboxylate group does not coordinate. It is shown in Figure 74 for histidine H_2 and H_4 and in Figure 75 for N-acetylhistidine H_4 . From pH 4, the resonances are shifted upfield in the mixture as compared to the ligand. Precipitation occurs before ionization of the amino group in histidine.

Experimental results for both histidine and N-acetylhistidine were best fitted with a reaction model involving the formation of a 1 to 1 complex with the imidazole side chain. In the case of histidine the amino group is protonated. Figures 76 and 77 depict the δ obtained from KINET for the evaluation of pK_a 's and formation constants, which are reported in Table 14. Although the Cd-histidine complex characterized in this study is formed through binding to the imidazole side chain, its formation constant ($\log K_f = 1.40$) is smaller than that of the Cd-imidazole complex ($\log K_f = 2.80$) [42] presumably due to protonation of the amino group in the Cd-histidine complex. The formation constant reported in the literature for the 1 to 1 complex of Cd^{2+} and histidine is also much higher ($\log K_f = 5.65$) [42]. The latter value was obtained from potentiometric titrations data assuming totally deprotonated histidine to be the

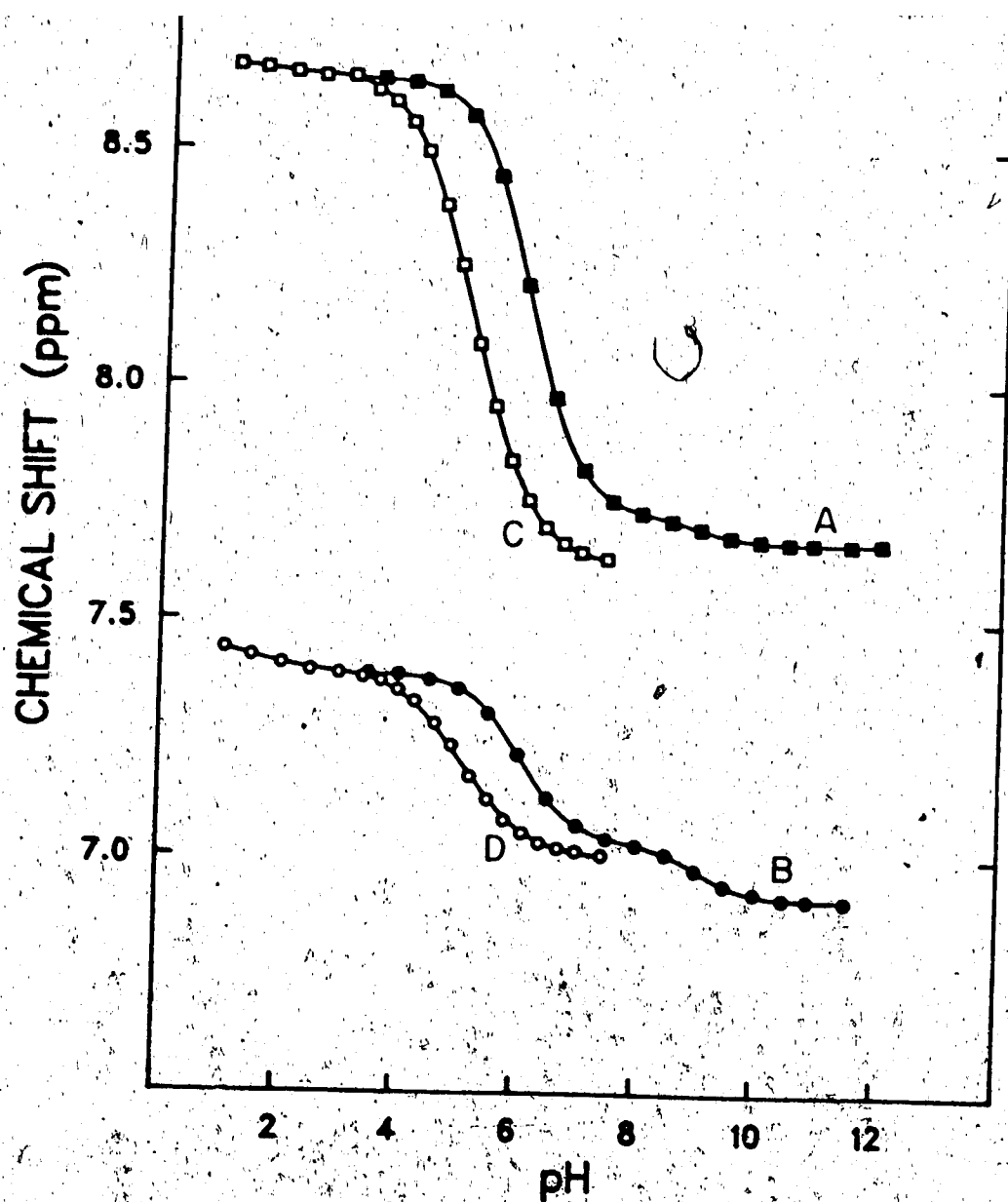


Figure 74. The pH dependence of the chemical shift of (A) H₂ and (B) H₄ protons during titration of histidine and (C) H₂ and (D) H₄ during titration of a 1:1 mixture of Cd²⁺ and histidine.

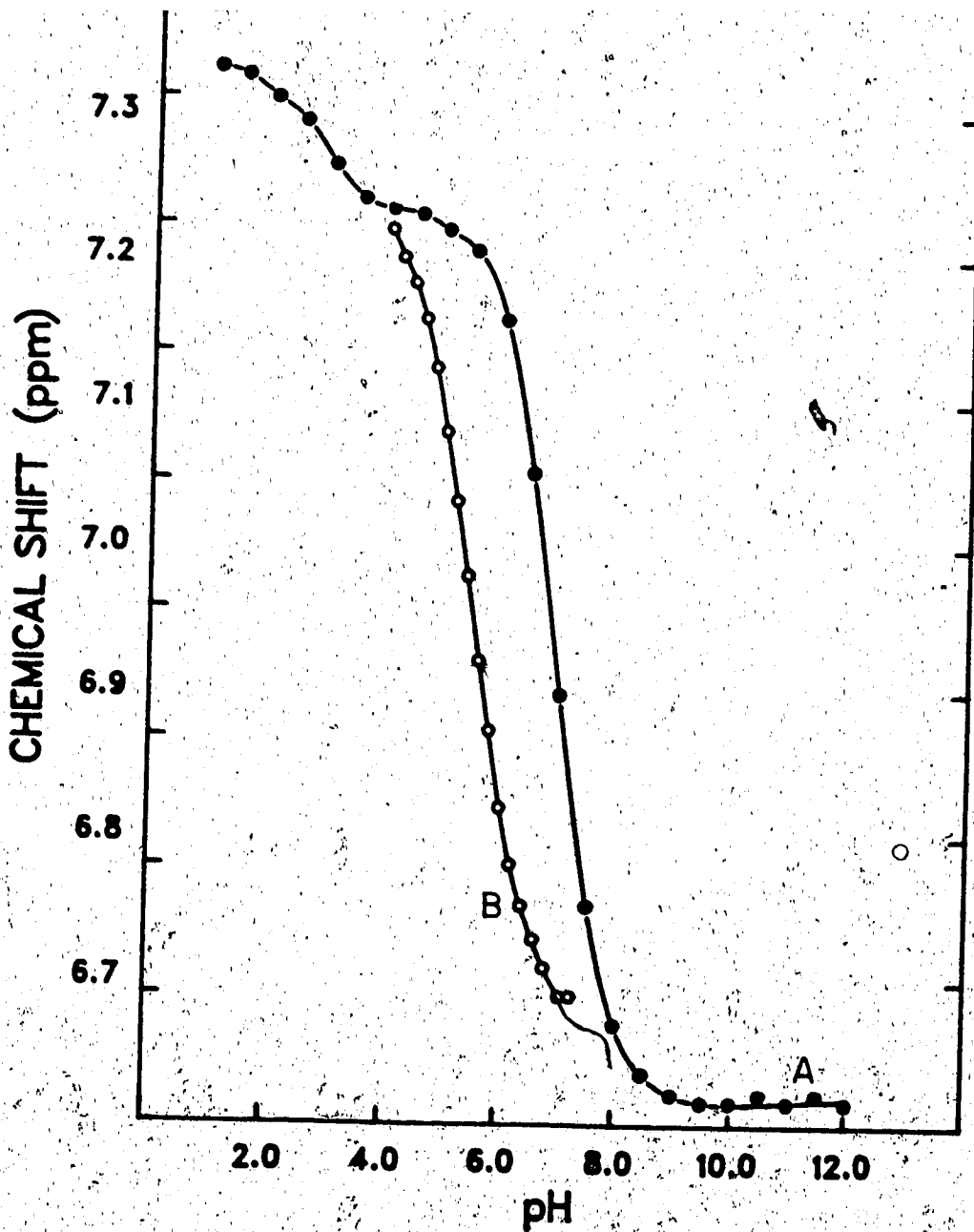


Figure 75. The pH dependence of the chemical shift of H_4 proton (A) during titration of N-acetylhistidine and (B) during titration of a 1:1 mixture of Cd^{2+} and N-acetylhistidine.

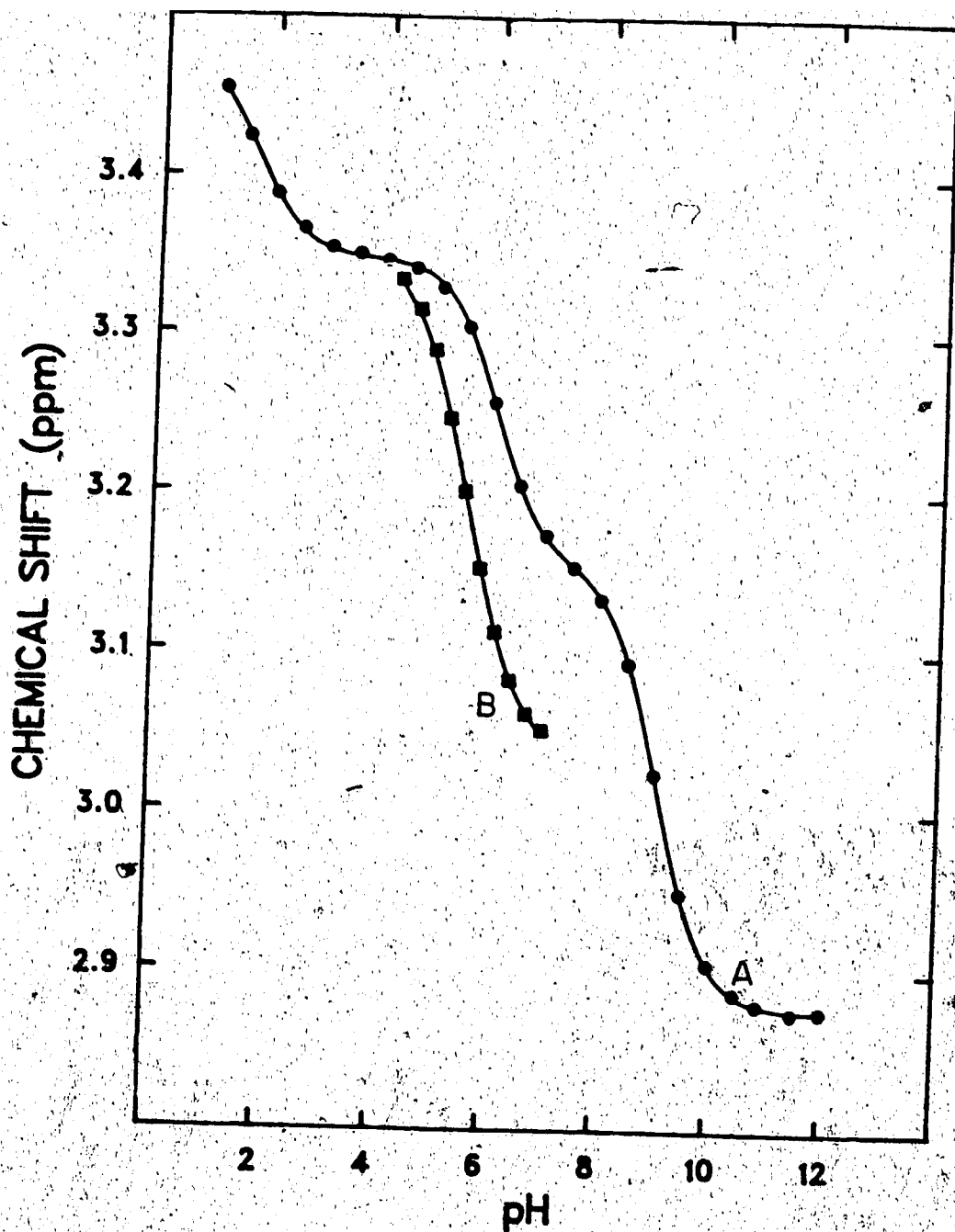


Figure 76. Experimental data and calculated curve of the chemical shift of H_{β} protons versus pH for the determination of (A) histidine's pK_a 's and (B) the formation constant of Cd-histidine complex.

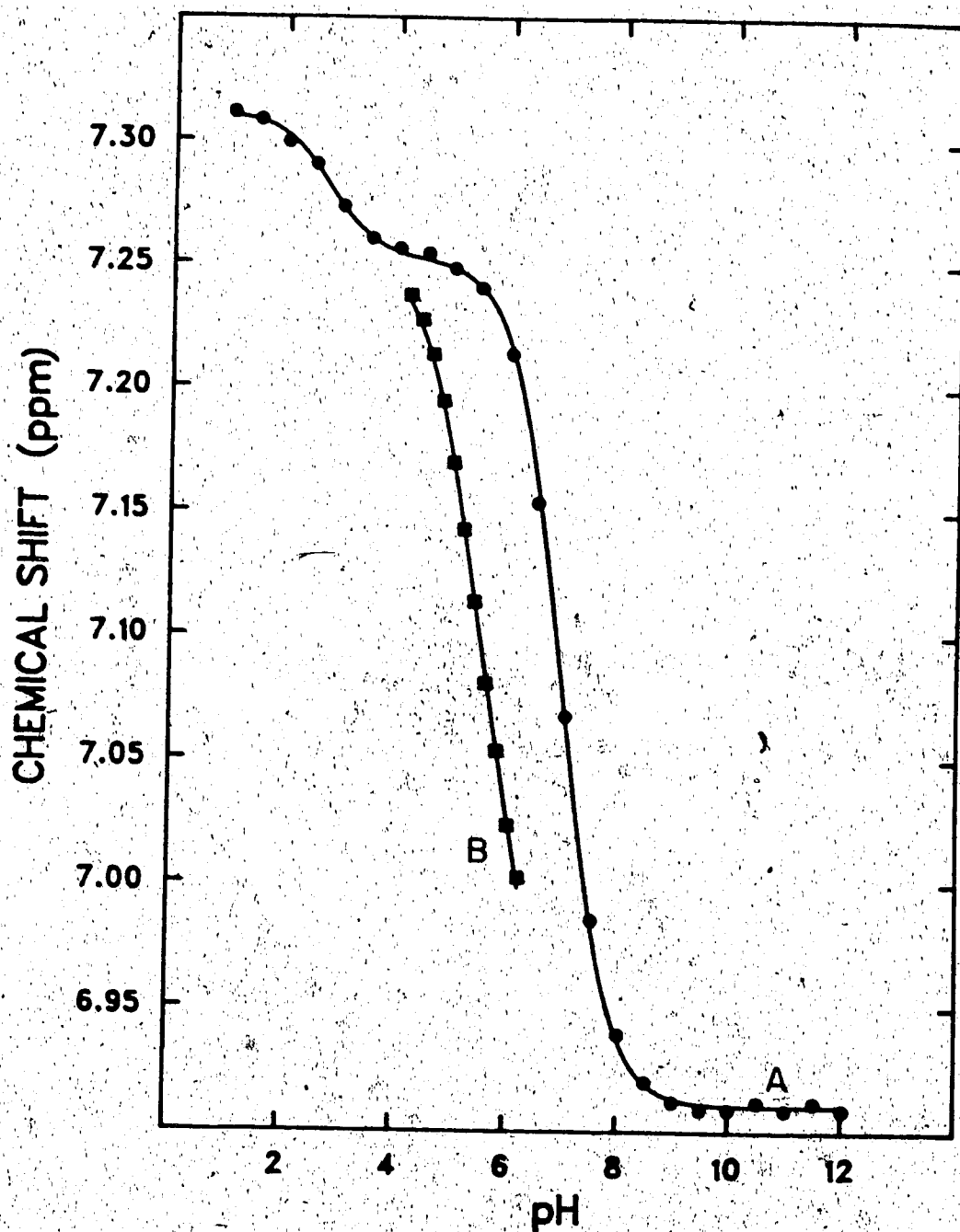


Figure 77. Experimental data and calculated curves of the chemical shift of H_4 proton versus pH for the determination of (A) N-acetylhistidine pK_a 's and (B) the formation constant of Cd-N-acetylhistidine complex.

Table 14. pKa's, Formation constants, ^1H and ^{113}Cd chemical shifts of histidine and N-acetylhistidine species.

Resonance used	pKa1	pKa2	pKa3	log Kf	^1H NMR	^{113}Cd NM
					δ complex ppm	δ complex ppm
<u>Histidine</u>						
H ₂	a	6.04±0.06	8.98±0.06	b	b	
H ₄	a	6.04±0.04	8.95±0.03	b	b	
H _α	1.64±0.01	6.11±0.04	9.06±0.06	b	b	
H _β	1.66±0.03	6.05±0.01	9.05±0.01	1.40±0.02	2.93±0.05	c
<u>N-acetylhistidine</u>						
H ₂		2.83±0.1	6.93±0.01			
H ₄		2.74±0.06	6.92±0.01	2.48±0.02	6.88±0.01	45.6±1.1
H _β		2.71±0.02	6.89±0.01			

- Ionization of the carboxylic group does not affect the chemical shift of H₂ and H₄ resonances.
- Only the H_β resonance was used to determine log Kf because it provided the three pl needed with smallest standard deviations.
- The ^{113}Cd chemical shift of the histidine complex could not be determined because of excessive line broadening.

reacting species. The $\log K_f$ of the Cd-N-acetylhistidine complex determined in the present study, 2.48, compares well with the literature value of 2.70 from potentiometric measurements [42]. The acidity and formation constants so determined were then used with the ^{113}Cd -NMR data to calculate the ^{113}Cd -NMR chemical shift of the complex formed. Figure 78 shows the fit obtained using a value of 45.6 ± 1.1 ppm for the chemical shift of the N-acetylhistidine complex. The experimental data is from the titration of a 1 to 1 mixture of Cd^{2+} and N-acetylhistidine. The titration curves of the 1 to 2 (B) and 1 to 4 (C) mixtures of Cd^{2+} and N-acetylhistidine are given in Figure 79. The limiting chemical shift on curve C is much higher (~ 120 ppm) than the chemical shift obtained for the 1 to 1 complex indicating the formation of higher complex (e.g., 1 to 2 and 1 to 3 Cd^{2+} -N-acetylhistidine complexes). Due to excessive line broadening, no chemical shift data could be recorded for the titration of a 1 to 1 mixture of histidine and Cd^{2+} , thus an estimate of the chemical shift of the 1 to 1 complex could not be obtained. However, experimental results for the higher ratios are shown in Figure 80. The limiting ^{113}Cd chemical shift in histidine solutions is much higher (~ 240 ppm) than in N-acetylhistidine solutions (~ 120 ppm). The additional deshielding observed with histidine suggests the involvement of another deshielding group in the complexation of Cd^{2+} by histidine. The amino group in

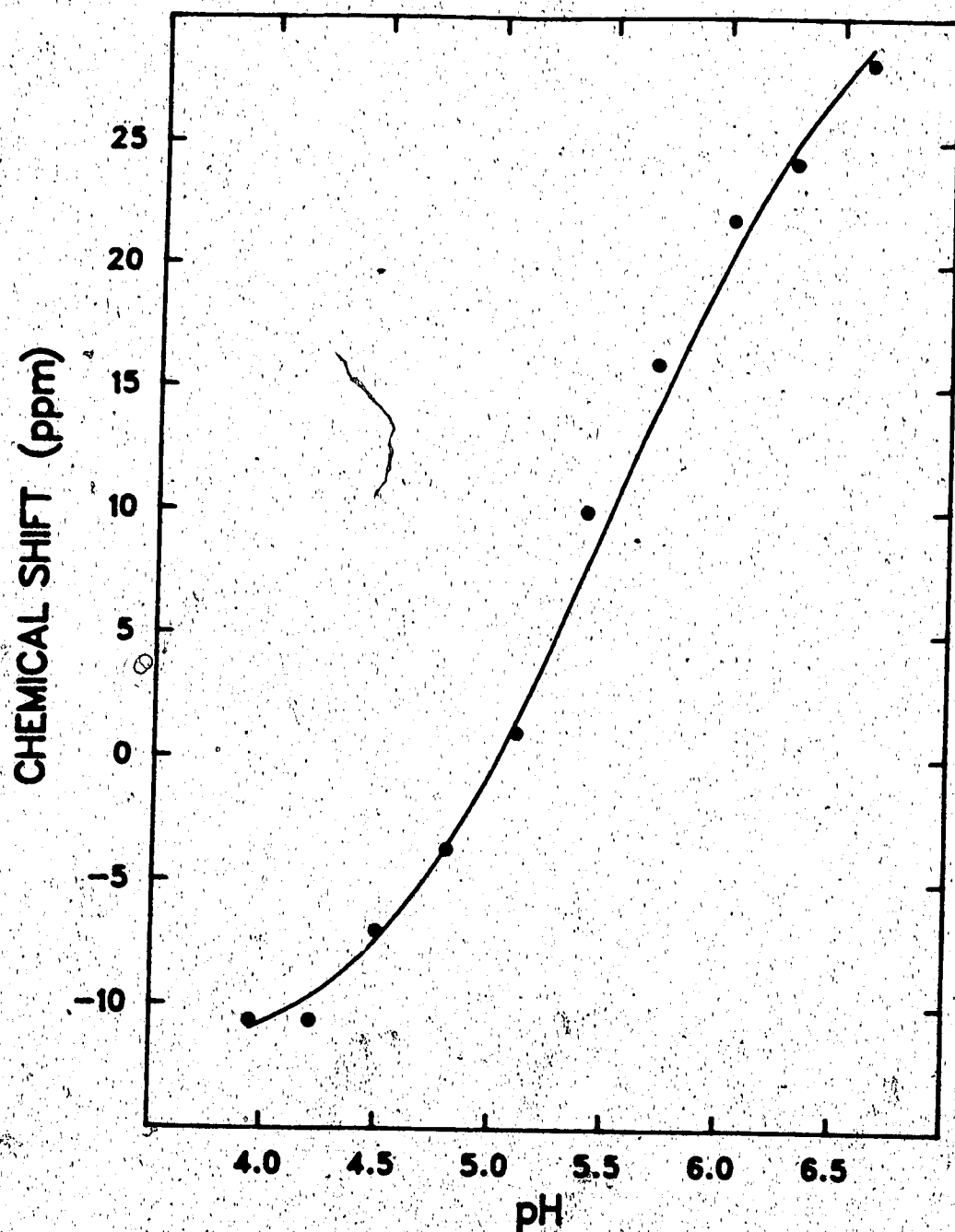


Figure 78. Experimental data and calculated curve of ^{113}Cd chemical shifts versus pH for the determination of the ^{113}Cd chemical shift of Cd-N-acetyl-histidine complex.

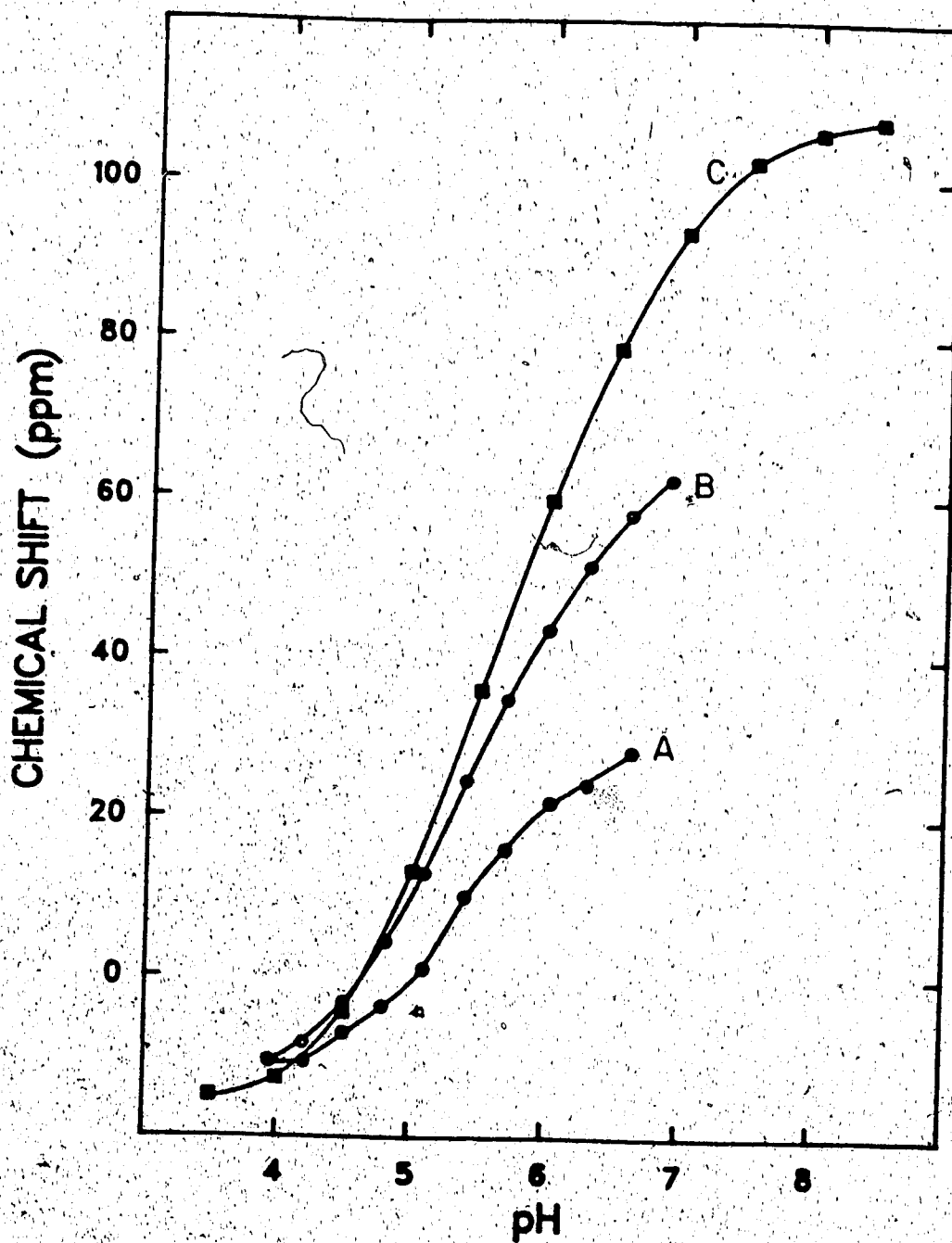


Figure 79. The pH dependence of the ^{113}Cd chemical shift for (A) 1:1, (B) 1:2 and (C) 1:4 mixtures of Cd^{2+} and N-acetylhistidine.

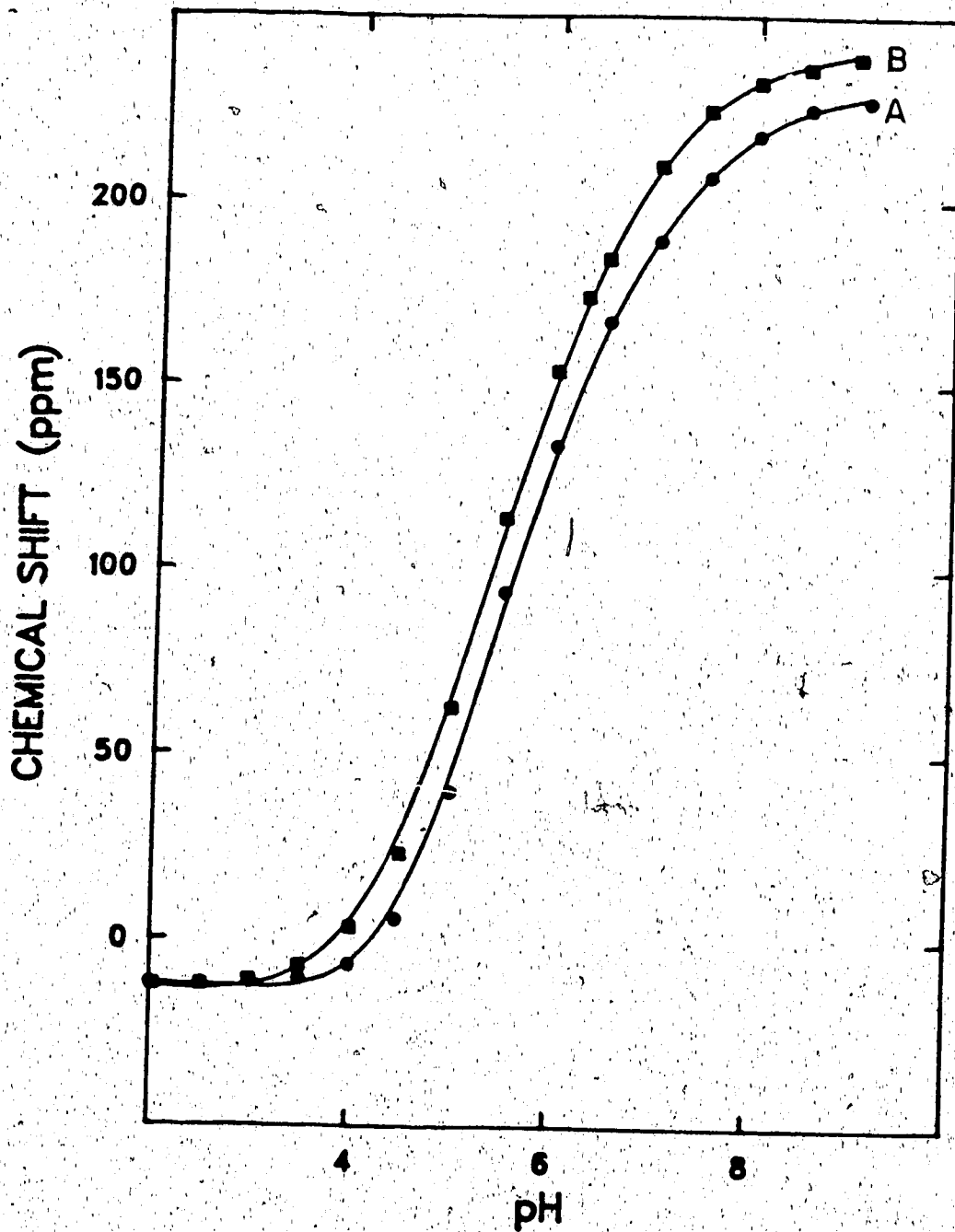


Figure 80. The pH dependence of the ^{113}Cd chemical shift for (A) 1:2 and (B) 1:4 mixtures of Cd^{2+} and histidine.

histidine may therefore be involved in the binding which is not possible with N-acetylhistidine.

D. Discussion

The ^{113}Cd chemical shifts of model complexes which were calculated from exchange averaged chemical shifts are consistent with the known effects of the various coordinating ligands [37, 43]. The complexes of cadmium with carboxylic acids all have chemical shifts between -14 ppm and -40 ppm. The shielding of complexes increases in the order $\text{CdL} < \text{CdL}_2$. The range within which these resonances occur is small due to relatively small formation constants of these complexes. The binding of Cd^{2+} to glycylglycine through the carboxylate group at low pH (< 4) and amino group at high pH (> 4) was confirmed. This binding was studied earlier by ^1H NMR [23]. The ^{113}Cd chemical shift of the carboxylate complex is -18.4 ppm and that of the amino complex 82 ppm. The chemical shift of the amino complex falls in the region of mixed complexation to nitrogen and oxygen donors [52]. Most probably the latter complex involves the carbonyl group of the peptide linkage as well as the amino group. The shielding observed on the chemical shift of the resonance for the Cd^{2+} in the N-acetylhistidine complex (46 ppm) is also a result of the participation of oxygen in the binding. This oxygen may be from the carbonyl

revealed that the carboxylate group does not complex Cd^{2+} below pH 4, it may bind however when another group is bound.

However, the accuracy of the method used in the present study is limited by the accuracy with which the formation constants used in the calculation are known. An even more serious situation is the possibility that some non-identified species occur in solution and are not accounted for in the treatment of data. Given the sensitivity of the ^{113}Cd NMR chemical shift to small changes in the coordination, large errors may result from ignoring a species present even at a low concentration. Benchmark chemical shifts, independently determined on solid complexes of known composition and structure, have been used to evaluate solution data [55]. Unfortunately, such data can not be secured for most systems due to isolation problems and/or the difference between solution and solid state complexes. Also, solvent effects are not reflected by solid state ^{113}Cd NMR data, thus limiting the usefulness of such data.

The use of supercooled solutions has been proposed to obtain ^{113}Cd NMR chemical shifts without use of assumptions regarding species in solution undergoing exchange [54]. By dividing a macroscopic sample into micron size drops through emulsification, it is possible to cool an aqueous solution well below the 0°C freezing point [92, 93]. In so doing,

... state. Using the emulsification method, Ackerman and Ackerman were able to cool aqueous solutions of Cd^{2+} /glycine down to -55°C and observed slow exchange [54]. A total of four resonances were observed between 300 and -100 ppm which initially were thought to be from the complexes $\text{Cd}(\text{gly})^+$, $\text{Cd}(\text{gly})_2$, $\text{Cd}(\text{gly})_3^-$ and $\text{Cd}(\text{gly})_4^{2-}$. However, two of these resonances were also observed in super-cooled aqueous solutions containing varying amounts of $\text{Cd}(\text{II})$ and NO_3^- but in the absence of glycine; these were presumably due to the aquated or ion-pair forms of $\text{Cd}(\text{II})$. Such ambiguities about the assignment of the resonances diminish the viability of this method. Consequently, the approach used in this chapter to determine the cadmium chemical shifts of solution species remains the method of choice in cases of rapid exchange among species leading to the observation of a single weighted average resonance. Caution must be exercised in the selection of the acidity and formation constants used for the computation of ^{113}Cd NMR data; preferably they should be determined under identical conditions of temperature and ionic strength.

QUANTITATIVE STUDY OF CADMIUM COMPLEXATION IN HEMOLYSED
RED BLOOD CELLS

A. Introduction

The main targets in cadmium poisoning are the liver and kidney [1]. Blood, however, participates actively in the toxicology of cadmium through its role as the transport medium. Regardless of the source of cadmium (injection, inhalation or ingestion), it is transported by blood to other tissues in the body where it is ultimately accumulated [100]. As a consequence, studies on the toxicology of cadmium have been in part concerned with the distribution of cadmium in the different compartments of blood and the interactions of cadmium with blood components [100-103].

Cadmium in blood is mainly localized in the erythrocytes and its removal from them is much slower as compared to its removal from the plasma [102, 103]. This slower removal of cadmium from the erythrocytes is an indication that cadmium might be bound tightly by molecules in the erythrocytes. The interactions of Cd^{2+} in red blood cells have been investigated by electrophoresis and gel filtration [102-103]. It was suggested that cadmium is bound to hemoglobin [101], to metallothionein [102], to a high molecular weight fraction,

not hemoglobin and to a low molecular weight fraction of similar molecular weight to hepatic metallothionein but different in other characteristics [100].

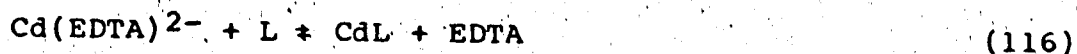
Direct evidence was obtained for the binding of Cd^{2+} to intracellular glutathione and hemoglobin (Hb) from ^1H NMR spin echo experiments [33]. The resonances due to the cysteinyl protons of GSH were most sensitive to Cd^{2+} suggesting that the sulfhydryl group of GSH is a binding site. It was also suggested that a ternary complex involving Cd^{2+} , GSH and hemoglobin may be one of the species formed in erythrocytes.

The aim of the present research was to obtain a semi-quantitative measure of the stability of the complexes formed in red blood cells. A competitive reaction was exploited which involved the use of cadmium in its ethylenediaminetetraacetic acid (EDTA) complex form; $\text{Cd}(\text{EDTA})^{2-}$. A method was developed to deduce concentrations of species from intensity measurements in spin echo ^1H NMR spectra of hemolysed red blood cells (HRBC) to which $\text{Cd}(\text{EDTA})^{2-}$ was added. Results of these studies are presented in this chapter. In addition, results are presented for model systems studied in D_2O solutions by single pulse ^1H NMR.

B. Method

A portion of the spectrum of hemolysed erythrocytes obtained by the spin-echo pulse sequence, $90^\circ\text{-}\tau_2\text{-}180^\circ\text{-}\tau_2\text{-}$ acquisition, with a $\tau_2 = 0.06$ sec is shown in Figure 81. Resonances of interest to the present study are those of glutathione and glycine (g6), and are identified in the Figure. The chemical shifts are reported relative to DSS based on the resonance of glycine which has a chemical shift of 3.54 ppm.

When $\text{Cd}(\text{EDTA})^{2-}$ is added to hemolysed red blood cells, EDTA is displaced from its cadmium complex according to the following competitive equilibrium:



where L stands for ligands in red blood cells. The displacement of EDTA is evidenced by the appearance of resonances due to $\text{Mg}(\text{EDTA})^{2-}$ (Figure 82) in the spectrum of HRBC to which $\text{Cd}(\text{EDTA})^{2-}$ is added. The resonance at 2.69 ppm indicated by an arrow is due to ethylenic protons in $\text{Mg}(\text{EDTA})^{2-}$. Resonances are not observed for the protons of $\text{Cd}(\text{EDTA})^{2-}$ in red blood cells [33]. The $\text{Mg}(\text{EDTA})^{2-}$ is formed from the released EDTA and the magnesium which is present in red blood cells at concentrations around $2.5 \times 10^{-3} \text{M}$ [105]. Hence, the complete reaction when $\text{Cd}(\text{EDTA})^{2-}$ is added to HRBC is:

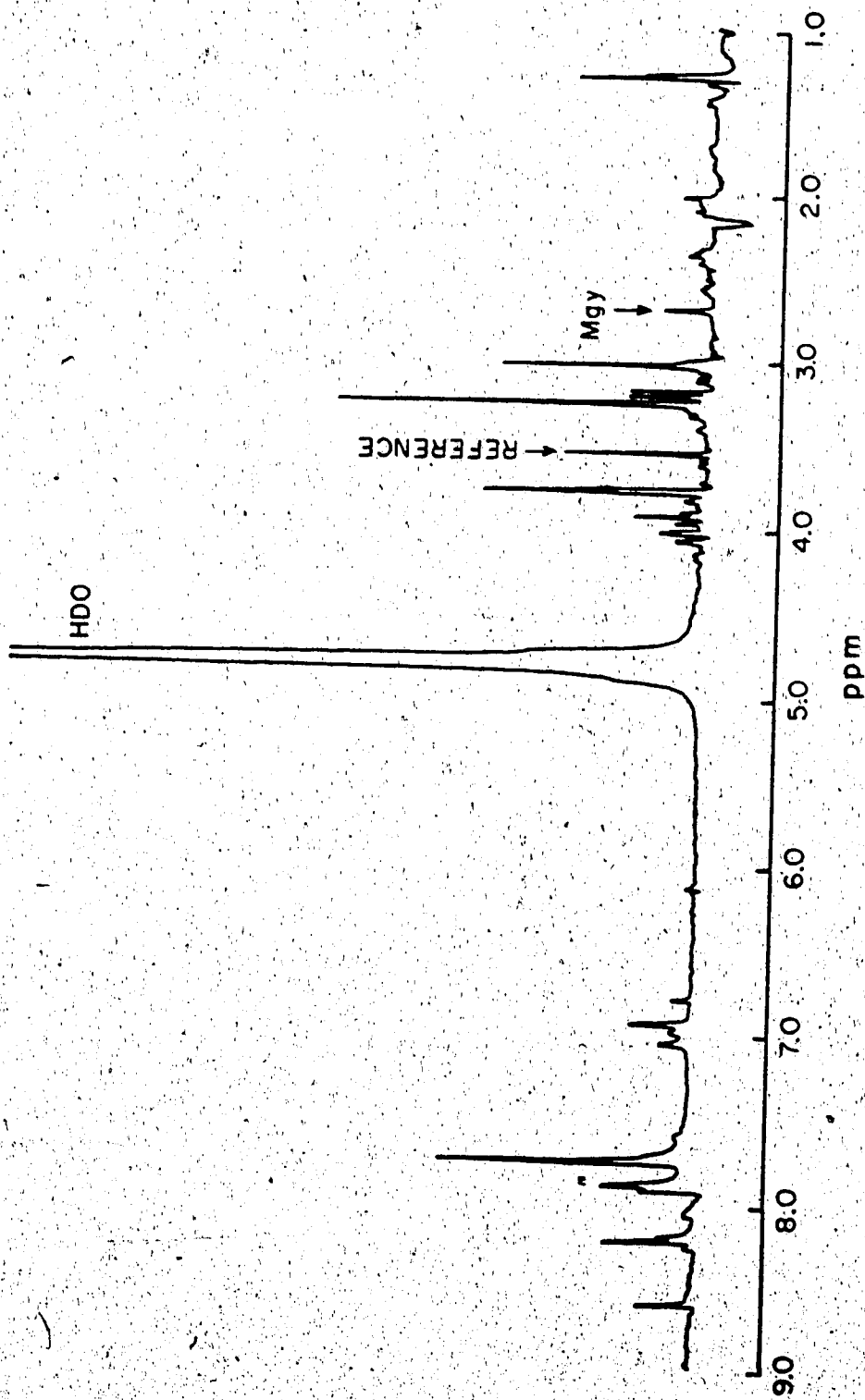
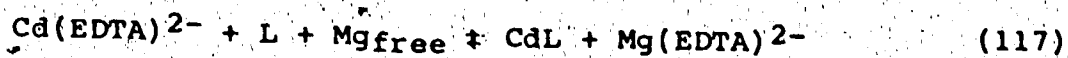


Figure 82. ^1H NMR spin echo spectrum of HRBC to which $\text{Cd}(\text{EDTA})_2^-$ is added.
 $[\text{Cd}(\text{EDTA})_2^-]_{\text{added}} = 2.621 \times 10^{-3}\text{M}$; $[\text{Mg}^{2+}]_{\text{total}} = 4.609 \times 10^{-3}\text{M}$.



for which the following equilibrium constant is defined:

$$K = \frac{[\text{CdL}][\text{Mg(EDTA)}^{2-}]}{[\text{Cd(EDTA)}^{2-}][\text{Mg}]_{\text{free}}[\text{L}]} \quad (118)$$

Though the presence of magnesium drives the reaction described by Equation 117 to the right, it alone can not displace EDTA from Cd(EDTA)^{2-} because the latter has a much higher formation constant ($\log K_{\text{Cd(EDTA)}^{2-}} = 16.5$) than Mg(EDTA)^{2-} ($\log K_{\text{Mg(EDTA)}^{2-}} = 8.7$). To illustrate, the spectrum of an equimolar mixture of Cd^{2+} , Mg^{2+} and EDTA at pH 7 is shown on Figure 83. The spectrum is that of Cd(EDTA)^{2-} , with no evidence of resonances for Mg(EDTA)^{2-} . The outer two lines of the three line pattern at 2.69 ppm are due to the ethylenic protons of Cd(EDTA)^{2-} coupled to ^{113}Cd and ^{111}Cd . The central line is due to the ethylenic protons of the EDTA complexed by all other isotopes of cadmium. The NMR characteristics of cadmium were discussed in Chapter I and Chapter IV. Approximately 25% of naturally occurring cadmium is ^{113}Cd and ^{111}Cd , both of which have a spin $1/2$ wherefore the coupling observed. Acetate protons are also coupled to ^{113}Cd and ^{111}Cd and occur at ~3.1 ppm. The multiplet pattern is an ABX ($\text{H}_A\text{-H}_B\text{-Cd}$) spin system superimposed on an AB system (H_A and H_B). The two protons of each of the acetate arms in the Cd(EDTA)^{2-} complex have similar but not identical chemical shifts, thus they are

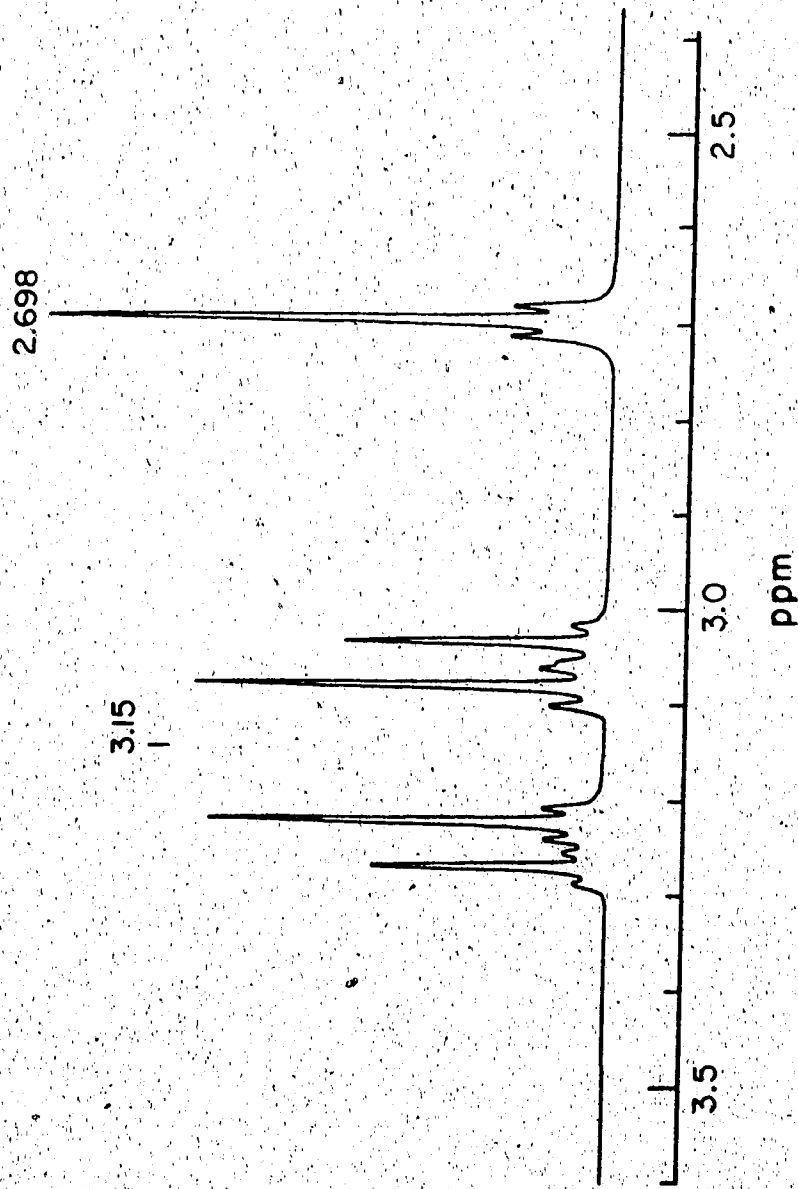


Figure 83. ^1H NMR spectrum of an equimolar mixture of Cd^{2+} , Mg^{2+} and EDTA.

coupled and form an AB system giving rise to four line multiplet pattern. Satellite lines due to coupling to ^{111}Cd and ^{113}Cd flank each of the four lines. The difference between the constants for coupling to ^{113}Cd and ^{111}Cd is very small. Therefore the signals from ^{113}Cd and ^{111}Cd coupling are not resolved and are observed as a doublet only.

The spectrum of $\text{Mg}(\text{EDTA})^{2-}$ is shown in Figure 84. The ethylenic and acetate protons in $\text{Mg}(\text{EDTA})^{2-}$ have a chemical shift of 2.689 ppm and 3.2 ppm respectively.

Assuming that the concentration of reacting species represented by L is high and therefore the changes in their concentrations are negligible when some reacts with Cd^{2+} , the equilibrium constant can be rewritten as:

$$K_{cl} = K \times [L] = \frac{[\text{CdL}][\text{Mg}(\text{EDTA})^{2-}]}{[\text{Cd}(\text{EDTA})^{2-}][\text{Mg}]_{\text{free}}} \quad (119)$$

To determine this equilibrium constant, the concentrations of CdL, $\text{Mg}(\text{EDTA})^{2-}$, $\text{Cd}(\text{EDTA})^{2-}$ and Mg_{free} must be measured.

The total concentration of magnesium in HRBC was first determined by titrating the HRBC with EDTA as described in section C of the present chapter, while monitoring the titration by NMR. A calibration curve for determining the concentration of $\text{Mg}(\text{EDTA})^{2-}$ in HRBC from resonance intensities was established as described in section D and was subsequently used to determine the concentration of $\text{Mg}(\text{EDTA})^{2-}$ when $\text{Cd}(\text{EDTA})^{2-}$ was added to HRBC. The other concentrations in Equation 119 were obtained by difference

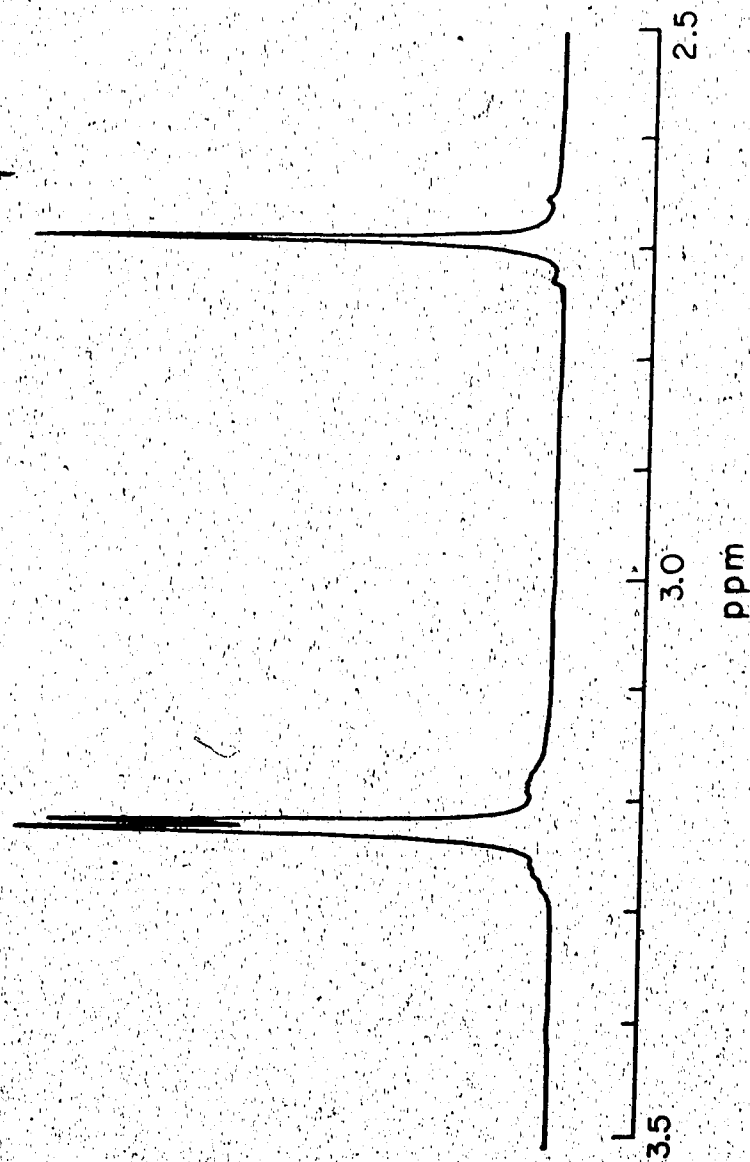


Figure 84. ^1H NMR spectrum of an equimolar mixture of Mg^{2+} and EDTA.

as follows:

$$[\text{Cd}(\text{EDTA})^{2-}] = \text{Cd}_t - [\text{Mg}(\text{EDTA})^{2-}] \quad (120)$$

$$[\text{CdL}] = \text{Cd}_t - [\text{Cd}(\text{EDTA})^{2-}] = [\text{Mg}(\text{EDTA})^{2-}] \quad (121)$$

$$[\text{Mg}]_{\text{free}} = \text{Mg}_t - [\text{Mg}(\text{EDTA})^{2-}] \quad (122)$$

C. Determination of Total Magnesium in Hemolysed Red Blood Cells (HRBC)

Hemolysed erythrocytes, prepared as described in Chapter II, were titrated with EDTA. Five μl increments of a 0.040M EDTA solution in D_2O at $\text{pH} = 7.4$ were added to 0.5 ml of hemolysed cells. When all the magnesium is complexed, resonances from free EDTA start to appear in the spectrum. Shown in Figure 85 are spectra of hemolysed erythrocytes to which 0, 15, 25 and 35 μl of the EDTA solution were added. The resonance due to the ethylenic protons of $\text{Mg}(\text{EDTA})^{2-}$ appears at 2.688 ppm and that due to the ethylene protons of free EDTA at 3.61 ppm. The end point of the titration, i.e., where all magnesium is complexed, was located by following the increase in the intensity of the resonance due to the ethylenic protons in free EDTA. A plot of the ratio of the intensity of the EDTA resonance to that of a reference signal ($I_{\text{EDTA}}/I_{\text{reference}}$) as a function of the volume of EDTA solution added to a HRBC sample is shown in Figure 86. Before the end point, all EDTA added is

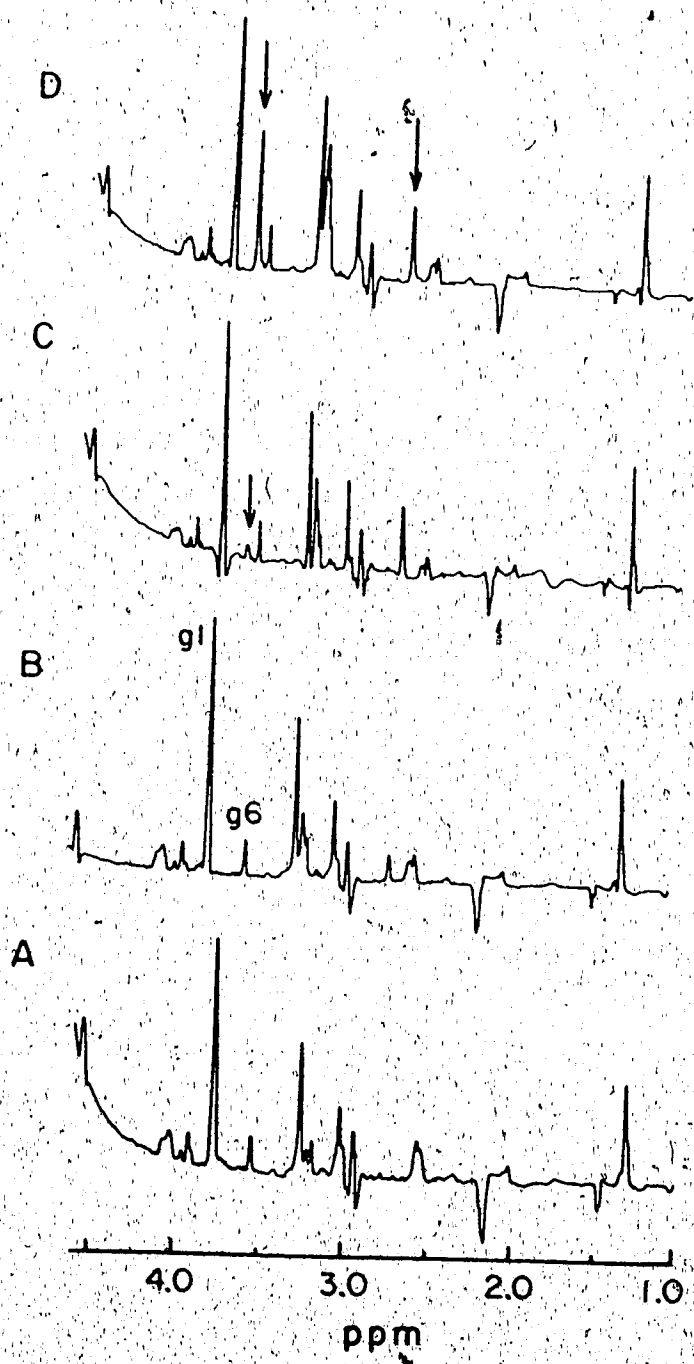


Figure 85. Titration of HRBC with EDTA; ^1H NMR spin echo spectra of HRBC obtained after addition of (A) 0 μl , (B) 15 μl , (C) 25 μl and (D) 35 μl of 0.04M EDTA solution to 0.5 ml of HRBC.

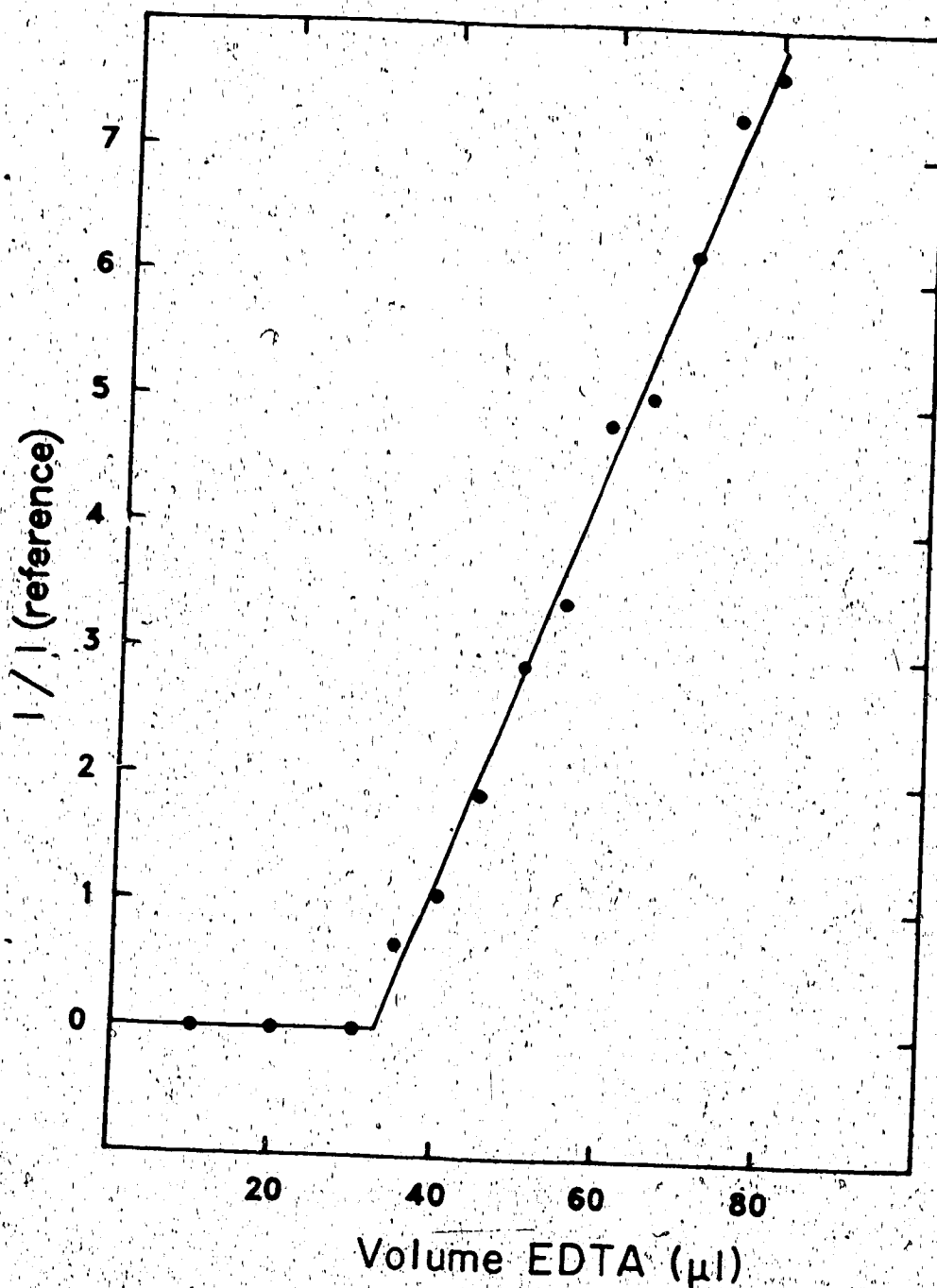


Figure 86. Determination of Mg free in HRBC: $I_{\text{EDTA}}/I_{\text{ref}}$ versus volume of EDTA added. Concentration of EDTA solution is 0.04M.

However, the EDTA added after all the magnesium has been complexed remains free in the HRBC and the intensities of its resonances increase linearly with increasing volumes of EDTA. Hence the second portion of the titration plot is a straight line with a positive slope. The intersection of the two linear portions of the titration curve is the end point. The concentration of magnesium in the aliquot of HRBC was calculated from the volume of EDTA added to the end point and the concentration of the EDTA solution. The resonance due to glycol protons (gl) of glutathione was used as the reference signal for these titrations. This resonance and the other GSH resonances are not affected by the presence of EDTA.

The blood used for all the experiments was from one donor so as to have comparable concentrations of magnesium. The concentration of magnesium in HRBC determined over a period of 40 days for the one donor are given in Table 15. An average value of $2.6 \times 10^{-3} \text{M}$ was obtained for the concentration of magnesium in the red blood cells. This value is comparable to the literature value ($2.5 \times 10^{-3} \text{M}$) given for an average concentration of magnesium in the human erythrocytes [105].

An inherent source of error in this method is the pre-

Dates	06/19/85	07/02/85	07/26/85	07/30/85
Sample 1	2.32×10^{-3}	2.59×10^{-3}	2.66×10^{-3}	2.56×10^{-3}
Sample 2			2.83×10^{-3}	2.66×10^{-3}
Sample 3			2.75×10^{-3}	
Average	2.32×10^{-3}	2.59×10^{-3}	2.75×10^{-3}	2.61×10^{-3}

... include other metal ions besides Mg^{2+} . The most abundant divalent metal after Mg^{2+} is Ca^{2+} present in red blood cells at an average concentration of $0.06 \times 10^{-3} M$ [108] which is about forty times lower than the concentration of magnesium.

D. Calibration Curve for $Mg(EDTA)^{2-}$ in HRBC

Intensity measurements on the resonance due to the ethylenic protons of the $Mg(EDTA)^{2-}$ complex and on a reference signal were used to calibrate $Mg(EDTA)^{2-}$ in HRBC. The approach used consisted of first titrating a sample (0.5 ml) of HRBC with EDTA, as described in the previous section, to determine the concentration of magnesium in the HRBC. An excess of EDTA (about three times the end point concentration) was then added, followed by increments of Mg^{2+} ions from a 0.5M solution of $MgCl_2$ in D_2O . As magnesium was added, the intensity of the resonance due to $Mg(EDTA)^{2-}$ increased while that of the free EDTA resonance decreased as shown in Figure 87. The magnesium added reacts with EDTA to form $Mg(EDTA)^{2-}$ thus causing the increase and decrease in the intensity of resonances due to $Mg(EDTA)^{2-}$ and EDTA respectively. The intensity of the 2.69 ppm resonance of $Mg(EDTA)^{2-}$ and that of a reference signal were measured and

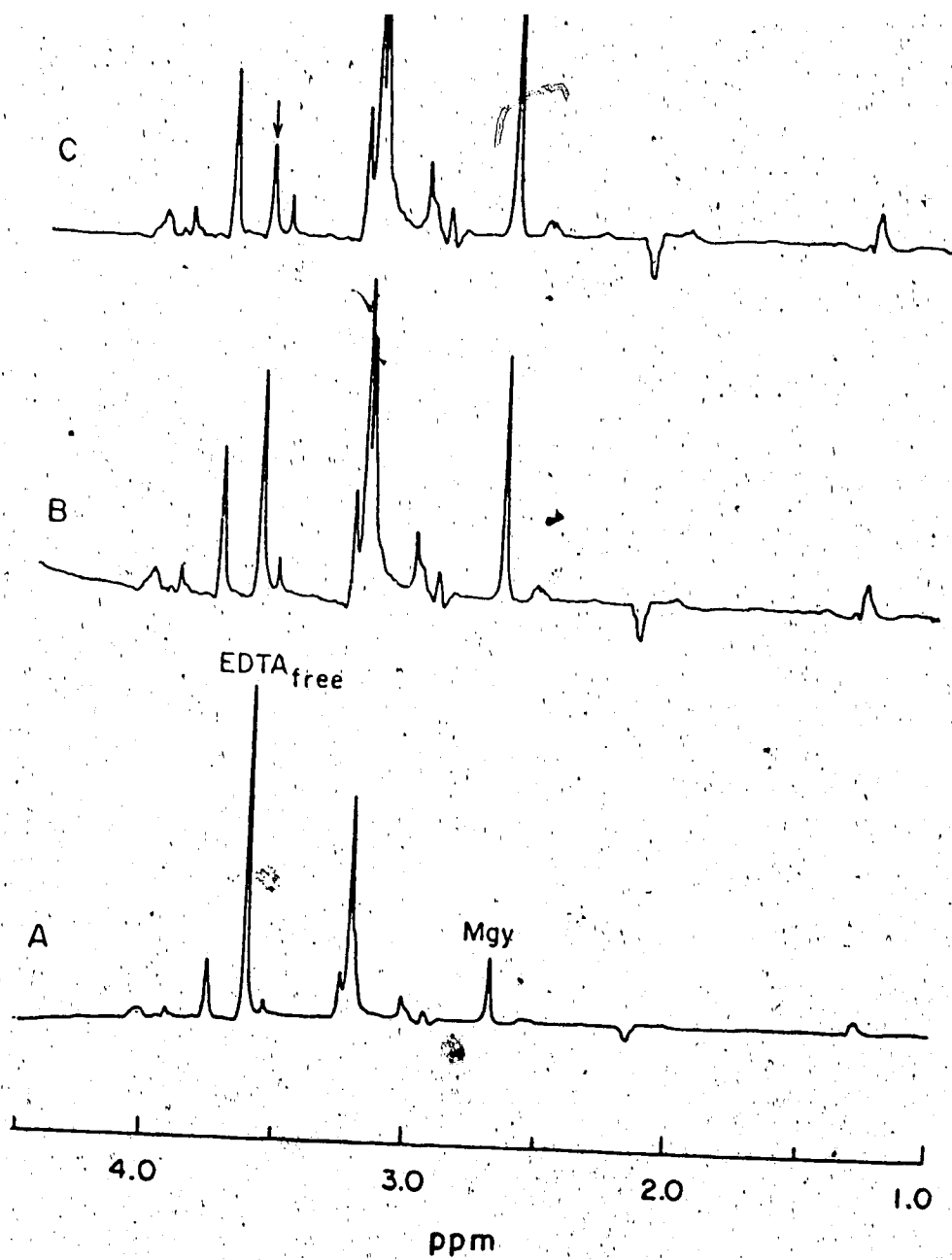


Figure 87. Representative spectra used for the calibration of $\text{Mg}(\text{EDTA})_2^-$ in HRBC. $[\text{Mg}]_t =$ (A) $4.65 \cdot 10^{-3}\text{M}$, (B) $6.09 \cdot 10^{-3}\text{M}$ and (C) $6.78 \cdot 10^{-3}\text{M}$.

is the sum of the concentration of magnesium in the HRBC as determined by EDTA titration and that of added $MgCl_2$. The reference signal used was the resonance at 3.54 ppm which is due to the CH_2 protons of free glycine. The reference resonance used had to be from a molecule which is indifferent to the presence of $Cd(EDTA)^{2-}$ because the calibration curve is used to determine $Mg(EDTA)^{2-}$ in samples of HRBC to which $Cd(EDTA)^{2-}$ is added. The calibration curve obtained is shown in Figure 88. The points on the figure are experimental results and the solid line is the linear regression curve calculated from experimental data.

E. Determination of the Equilibrium Constant K_{C1} in HRBC

Samples of hemolysed erythrocytes (0.5 ml) were prepared as described in Chapter II. At least two aliquots of HRBC's were titrated with EDTA to determine the concentration of magnesium in the HRBC that were being used. Another aliquot of HRBC was then titrated with a $Cd(EDTA)^{2-}$ solution prepared as described in Chapter II. Titrations were performed on HRBC's with its natural magnesium concentration and in the presence of added magnesium. Addition of Mg^{2+} shifts the equilibrium described by Equation 115 to the right, i.e., toward the formation of $Mg(EDTA)^{2-}$ and con-

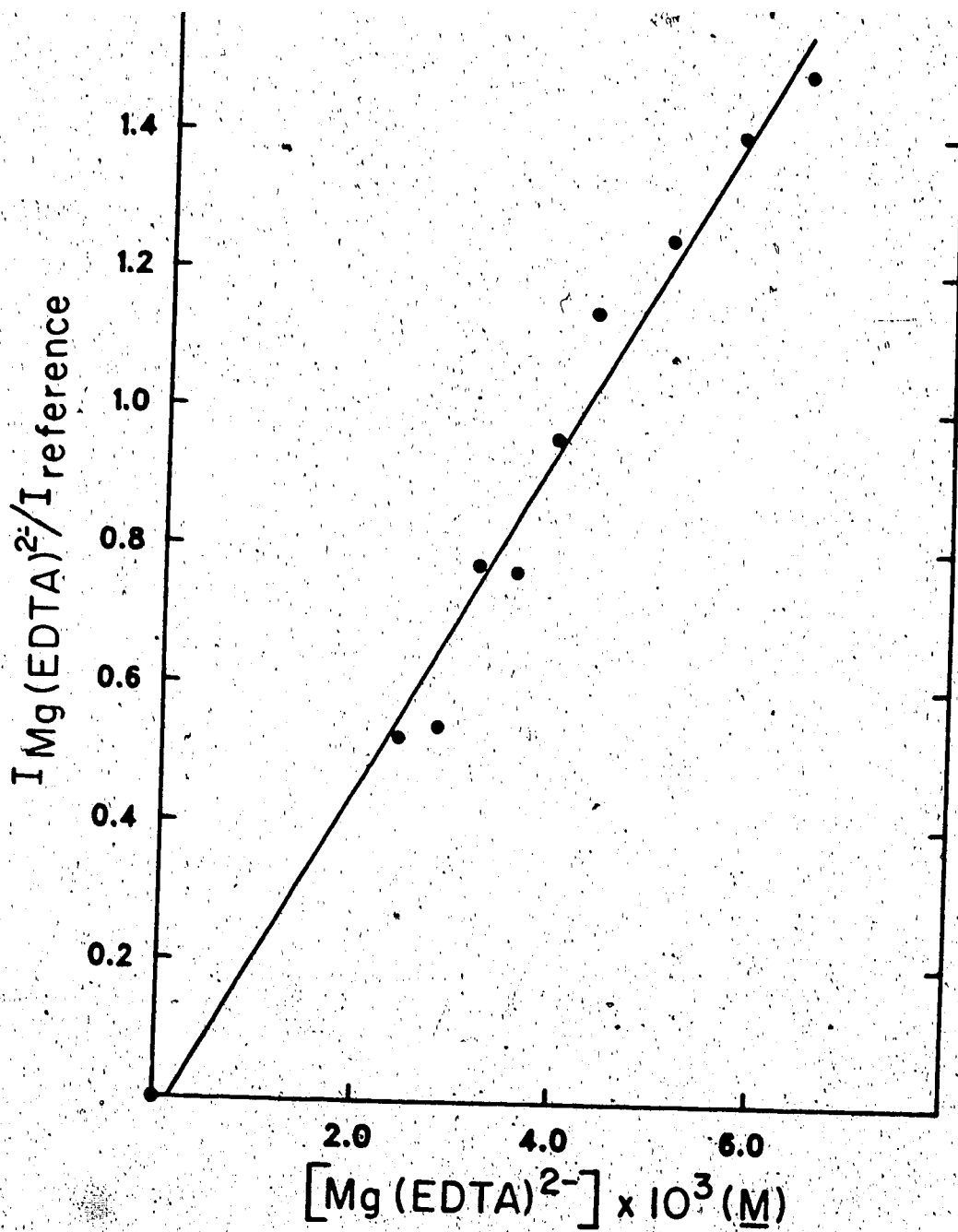


Figure 88. Calibration curve for Mg(EDTA)^{2-} in HRBC.

Figure 89 depicts representative spectra from a typical experiment. As expected, addition of $\text{Cd}(\text{EDTA})^{2-}$ affects the glutathione resonances. At a concentration of $\sim 1.8 \times 10^{-3} \text{M}$, the intensities of resonances g5 and g2 have decreased due to the binding of glutathione with Cd^{2+} . At an added $\text{Cd}(\text{EDTA})^{2-}$ concentration of $2.6 \times 10^{-3} \text{M}$, resonances g5 and g2 are not detected and the intensities of the glutamyl resonances g3 and g4 have also decreased. Simultaneously, resonances due to $\text{Mg}(\text{EDTA})^{2-}$ appear in the spectrum and their intensities increase with increasing concentrations of $\text{Cd}(\text{EDTA})^{2-}$. The arrow in Figure 89 indicates the resonance due to the ethylenic protons of $\text{Mg}(\text{EDTA})^{2-}$; the free glycine resonance is labelled reference on the figure. The intensities of the $\text{Mg}(\text{EDTA})^{2-}$ and the glycine resonances were measured and ratioed. The concentration of $\text{Mg}(\text{EDTA})^{2-}$ was determined from the ratios $I(\text{Mg}(\text{EDTA})^{2-})/I(\text{reference})$ by using the calibration curve prepared in Section D. The concentrations of the other species: Mg_{free} , CdL and $\text{Cd}(\text{EDTA})^{2-}$ were determined as described in Section B and then the equilibrium constant K_{Cl} was calculated.

Two sets of results are reported for this study. The hemolysed erythrocytes used for each set were obtained from fresh blood drawn from the same donor on different days. Within a set, results are reported for a titration of HRBC with and without added magnesium. The first set of results

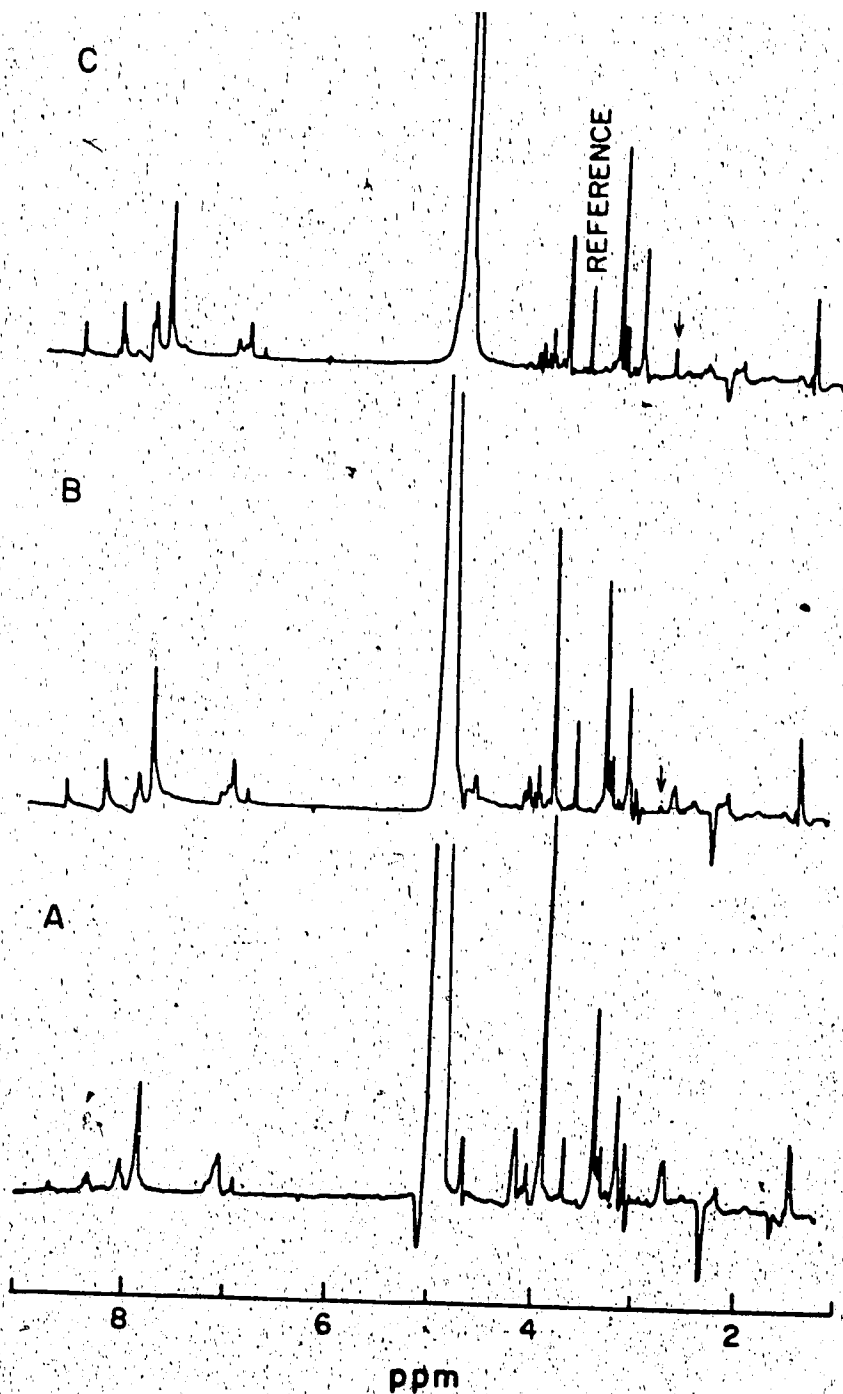


Figure 89. Spectra of the titration of HRBC with $\text{Cd}(\text{EDTA})_2^-$.
 $[\text{Mg}]_{\text{tot}} = 4.6 \times 10^{-3} \text{M}$; $[\text{Cd}(\text{EDTA})]_{\text{added}} =$ (A) 0,
 (B) $1.778 \times 10^{-3} \text{M}$, and (C) $2.621 \times 10^{-3} \text{M}$.

are given in Tables 16 and 17 and the second set in Tables 16 and 18. Tables 16 and 17 are results obtained in the absence of added magnesium and Tables 17 and 19 in the presence of added magnesium. The values obtained for the equilibrium constant K_{C1} as defined in equation 119 vary between 13.6×10^{-2} and 6.9×10^{-2} . Considering each titration separately, the equilibrium constants seem to be independent of the concentration of $\text{Cd}(\text{EDTA})^{2-}$ added. Thus the assumption that $[\text{L}]$ is essentially constant is verified. The values calculated from data obtained from the titrations performed in the presence of added magnesium are slightly lower (8.1×10^{-2} and 9.7×10^{-2}) than those from titrations on HRBC containing only naturally occurring magnesium (11.6×10^{-2} and 11.9×10^{-2}). However, this trend may not be real considering the variation observed in values for K_{C1} within a titration. For example in Table 16, K_{C1} values vary between 13.0×10^{-2} and 9.3×10^{-2} , in Table 17 they vary between 13.6×10^{-2} and 8.3×10^{-2} , and in Table 18 they vary between 12.9×10^{-2} and 7.3×10^{-2} . The two sets of results agree well within experimental error. The change of K_{C1} between experiments is 17% which is well in the range of deviations observed within an experimental set (11% to 23%).

If magnesium in red blood cells is complexed by some red blood cell components, the reaction in equation 117 will experience a smaller driving force than in the presence of free Mg^{2+} ions. The red cell ligands will be competing with

Table 16. Results of the titration of HRBC with Cd(EDTA)²⁻.

[Mg(EDTA) ²⁻]	[Mg] ^{Ta}	[Mg] _{free}	[Cd(EDTA) ²⁻] added	[Cd(EDTA) ²⁻]	K _{cl} ^b
7.473x10 ⁻⁴	2.368x10 ⁻³	1.622x10 ⁻³	3.390x10 ⁻³	2.643x10 ⁻³	13.03x10 ⁻²
7.652x10 ⁻⁴	2.329x10 ⁻³	1.564x10 ⁻³	3.749x10 ⁻³	2.984x10 ⁻³	12.55x10 ⁻²
7.681x10 ⁻⁴	2.290x10 ⁻³	1.522x10 ⁻³	4.097x10 ⁻³	3.328x10 ⁻³	11.64x10 ⁻²
7.420x10 ⁻⁴	2.216x10 ⁻³	1.474x10 ⁻³	4.757x10 ⁻³	4.015x10 ⁻³	9.30x10 ⁻²

^a[Mg]_{HRBC} = (2.75 ± 0.08) x 10⁻³ M Average of 3 determinations 2.664 x 10⁻³ M

2.832 x 10⁻³ M

2.747 x 10⁻³ M

^bK_{cl} avg = (11.6 ± 1.6) x 10⁻²

Table 17. Results of the titration of (HRBC + Mg²⁺) with Cd(EDTA)²⁻.

[Mg(EDTA) ²⁻]	[Mg] _T	[Mg] free	[(Cd(EDTA) ²⁻) added]	[Cd(EDTA) ²⁻]	K _{cl}
6.114x10 ⁻⁴	4.648x10 ⁻³	4.037x10 ⁻³	1.740x10 ⁻³	1.129x10 ⁻³	8.203x10 ⁻²
6.642x10 ⁻⁴	4.568x10 ⁻³	3.904x10 ⁻³	2.137x10 ⁻³	1.473x10 ⁻³	7.672x10 ⁻²
7.569x10 ⁻⁴	4.489x10 ⁻³	3.733x10 ⁻³	2.521x10 ⁻³	1.764x10 ⁻³	8.702x10 ⁻²
8.262x10 ⁻⁴	4.414x10 ⁻³	3.588x10 ⁻³	2.892x10 ⁻³	2.066x10 ⁻³	9.208x10 ⁻²
7.783x10 ⁻⁴	4.341x10 ⁻³	3.563x10 ⁻³	3.250x10 ⁻³	2.472x10 ⁻³	6.877x10 ⁻²

$K_{cl} \text{ avg} = (8.13 \pm 0.90) \times 10^{-2}$

$[Mg]_{HRBC} = 2.748 \times 10^{-3} M$

Table 18. Results of the titration of HRBC with Cd(EDTA)²⁻.

[Mg(EDTA) ²⁻]	[Mg] _{free}	[Mg] _{added}	[Cd(EDTA) ²⁻]	K _{cl}
7.654x10 ⁻⁴	2.418x10 ⁻³	1.652x10 ⁻³	2.826x10 ⁻³	12.55x10 ⁻²
8.235x10 ⁻⁴	2.395x10 ⁻³	1.572x10 ⁻³	3.180x10 ⁻³	13.56x10 ⁻²
7.307x10 ⁻⁴	2.374x10 ⁻³	1.643x10 ⁻³	3.677x10 ⁻³	8.34x10 ⁻²
8.673x10 ⁻⁴	2.353x10 ⁻³	1.484x10 ⁻³	3.937x10 ⁻³	12.89x10 ⁻²
8.632x10 ⁻⁴	2.331x10 ⁻³	1.468x10 ⁻³	4.332x10 ⁻³	11.72x10 ⁻²

$K_{cl} \text{ avg} = (11.8 \pm 2.0) \times 10^{-2}$

$[Mg]_{HRBC} = (2.61 \pm 0.07) \times 10^{-3} M$

Average of 2 determinations $2.561 \times 10^{-3} M$

$2.662 \times 10^{-3} M$

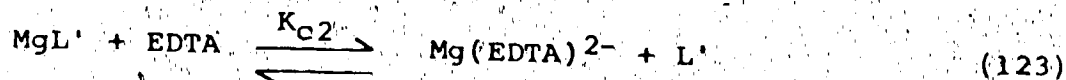
Table 19. Results of the titration of (HRBC + Mg²⁺) with Cd(EDTA)²⁻.

[Mg(EDTA) ²⁻]	[Mg] _T	[Mg] _{free}	[(Cd(EDTA) ²⁻)] added	[Cd(EDTA) ²⁻]	K _{cl}
6.374x10 ⁻⁴	4.693x10 ⁻³	4.056x10 ⁻³	1.779x10 ⁻³	1.142x10 ⁻³	8.77x10 ⁻²
8.245x10 ⁻⁴	4.651x10 ⁻³	3.826x10 ⁻³	2.204x10 ⁻³	1.379x10 ⁻³	12.88x10 ⁻²
8.605x10 ⁻⁴	4.609x10 ⁻³	3.748x10 ⁻³	2.621x10 ⁻³	1.760x10 ⁻³	11.22x10 ⁻²
8.366x10 ⁻⁴	4.568x10 ⁻³	3.731x10 ⁻³	3.030x10 ⁻³	2.194x10 ⁻³	8.55x10 ⁻²
8.347x10 ⁻⁴	4.527x10 ⁻³	3.693x10 ⁻³	3.433x10 ⁻³	2.598x10 ⁻³	7.26x10 ⁻²

$$K_{cl} \text{ avg} = (9.7 \pm 2.3) \times 10^{-2}$$

$$[Mg]_{HRBC} = 2.611 \times 10^{-3} M$$

EDTA for the Mg^{2+} according to the following reaction:

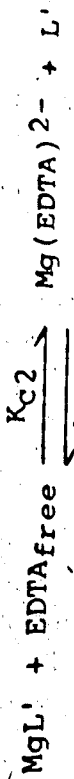


where L' represents the red cell ligands which bind magnesium. To verify the existence of this reaction, data from an experiment done to determine the concentration of magnesium were reexamined. Equation 123 describes the equilibrium before the end point if magnesium is in the form MgL' . In the presence of a large excess of EDTA this reaction will be totally shifted to the right given the high formation constant of $Mg(EDTA)^{2-}$ ($10^{8.7}$). Therefore data obtained before the end point were used to determine the following equilibrium constant, assuming $[L']$ is constant.

$$K_{c2} = \frac{[Mg(EDTA)^{2-}]}{[MgL'][EDTA]_{free}} \quad (124)$$

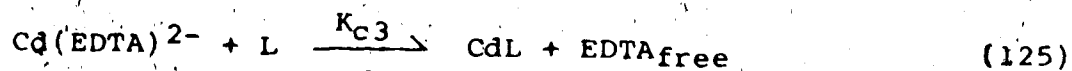
The concentration of $Mg(EDTA)^{2-}$ was determined from intensity measurements on the resonance due to the ethylenic protons of $Mg(EDTA)^{2-}$ as described earlier. The concentrations of MgL' and $EDTA_{free}$ were obtained by difference using total concentrations of magnesium and EDTA. Results obtained are given in Table 20, which indicate indeed, that all the EDTA added is not bound by magnesium. An average value of $5.5 \pm 1.6 \times 10^3 M^{-1}$ was obtained for K_{c2} from three determinations. The equilibrium constants K_{c1} and K_{c2} can be used to determine the equilibrium constant for the competitive

Table 20. Determination of the equilibrium constant for the reaction:



$[\text{Mg}(\text{EDTA})^{2-}]$ (M)	$[\text{Mg}]_{\text{T}}$ (M)	$[\text{Mg}]_{\text{free}} = [\text{Mg}^{2+}]$ (M)	$[\text{EDTA}]_{\text{tot}}$ (M)	$[\text{EDTA}]_{\text{free}}$ (M)	K_{C2} (M ⁻¹)
1.048×10^{-3}	2.584×10^{-3}	1.536×10^{-3}	1.153×10^{-3}	1.051×10^{-4}	6.492×10^3
1.229×10^{-3}	2.559×10^{-3}	1.331×10^{-3}	1.523×10^{-3}	2.937×10^{-4}	3.145×10^3
1.623×10^{-3}	2.535×10^{-3}	0.912×10^{-3}	1.885×10^{-3}	2.622×10^{-4}	6.784×10^3

reaction



as follows:

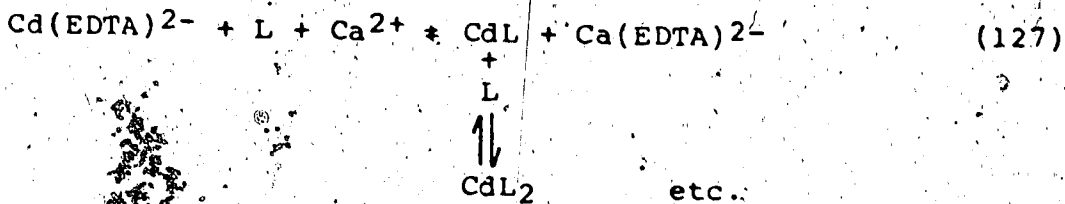
$$K_{C3} = \frac{[\text{CdL}][\text{EDTA}]_{\text{free}}}{[\text{Cd}(\text{EDTA})^{2-}]} = \frac{K_{C1}}{K_{C2}} \quad (126)$$

The values calculated for K_{C3} from the values for K_{C1} in Tables 16 to 19 and the average value of 5.5×10^3 for K_{C2} ranged from 1.2×10^{-5} to $2.2 \times 10^{-5} \text{M}$. These values indicate that equilibrium 125 is strongly shifted to the left; this is not surprising considering the stability of the $\text{Cd}(\text{EDTA})^{2-}$ complex.

F. Comparative Study of the Reaction of $\text{Cd}(\text{EDTA})^{2-}$ with Selected Ligands in D_2O

The displacement of EDTA from its cadmium complex by a competitive reaction similar to that in hemolysed erythrocytes was studied in D_2O solutions for selected ligands by single pulse ^1H NMR. The thiols GSH, N-acetylpenicillamine, cysteine and S-methylglutathione were selected to mimic the reaction in red blood cells. The objective was to determine equilibrium constants for model systems which would provide a guide to validate the results obtained for the hemolysed red blood cells. Due to the interference of the $\text{Mg}(\text{EDTA})^{2-}$

resonances with resonances of some of the ligands, calcium was used instead to bind the EDTA released from $\text{Cd}(\text{EDTA})^{2-}$. Calcium is also suitable because the formation constant of its EDTA complex ($\log K_{f, \text{Ca}(\text{EDTA})^{2-}} = 10.7$) is smaller than that of the $\text{Cd}(\text{EDTA})^{2-}$ complex ($\log K_{f, \text{Cd}(\text{EDTA})^{2-}} = 16.5$) but similar to that of the $\text{Mg}(\text{EDTA})^{2-}$ complex ($\log K_{f, \text{Mg}(\text{EDTA})^{2-}} = 8.7$). Therefore the following reaction scheme is applicable.



By analogy to the competitive reaction in HRBC, the equilibrium constant for this reaction can be defined as in equation 128, if the concentration of L is much higher than that of the other species and thus remains essentially constant.

$$K_{fc} = \frac{[\text{CdL}]_t [\text{Ca}(\text{EDTA})^{2-}]}{[\text{Cd}(\text{EDTA})^{2-}] [\text{Ca}^{2+}]} \quad (128)$$

$[\text{CdL}]_t$ stands for the total concentration of the various CdL species, CdL , CdL_2 , CdL_3 , etc.

The displacement of EDTA from cadmium is caused by the reaction of Cd^{2+} with the thiols. Because $\text{Ca}(\text{EDTA})^{2-}$ has a smaller stability constant ($\log K_f = 10.7$) as compared to $\text{Cd}(\text{EDTA})$ ($\log K_f = 16.5$), Ca^{2+} does not on its own displace

EDTA as was the case also with Mg^{2+} . The two sample spectra in Figure 90 are from a pH titration of an equimolar mixture of Ca^{2+} , Cd^{2+} and EDTA. They show that only $Cd(EDTA)^{2-}$ is formed along all the pH range. There are no detectable resonances from $Ca(EDTA)^{2-}$, whose spectrum is shown in Figure 91 for comparison. If the concentration of either $Ca(EDTA)^{2-}$ or $Cd(EDTA)^{2-}$ can be determined, the other equilibrium concentrations may be deduced by difference from knowledge of total concentrations of reacting species.

A possible side reaction is the binding of Ca^{2+} to the thiol ligand. If it occurs, it must be accounted for in order to have accurate values of K_{fc} . All reactions were conducted under conditions where Ca^{2+} does not react with the ligand molecules in order to simplify computation of experimental results. Evidence is presented for each of the ligands studied to indicate that this is the case.

For direct comparisons with the results obtained with the hemolysed red blood cells an equilibrium constant equivalent to K_{cl} was deduced from values of K_{fc} and K as defined in equation 128 and 129, as follows:

$$K = \frac{K_{fCa}(EDTA)^{2-}}{K_{fMg}(EDTA)^{2-}} \quad (128)$$

$$K_{cl} = \frac{[CdL]_t \times [Mg(EDTA)^{2-}]}{[Cd(EDTA)^{2-}] \times [Mg^{2+}]} = \frac{K_{fc}}{K} \quad (129)$$

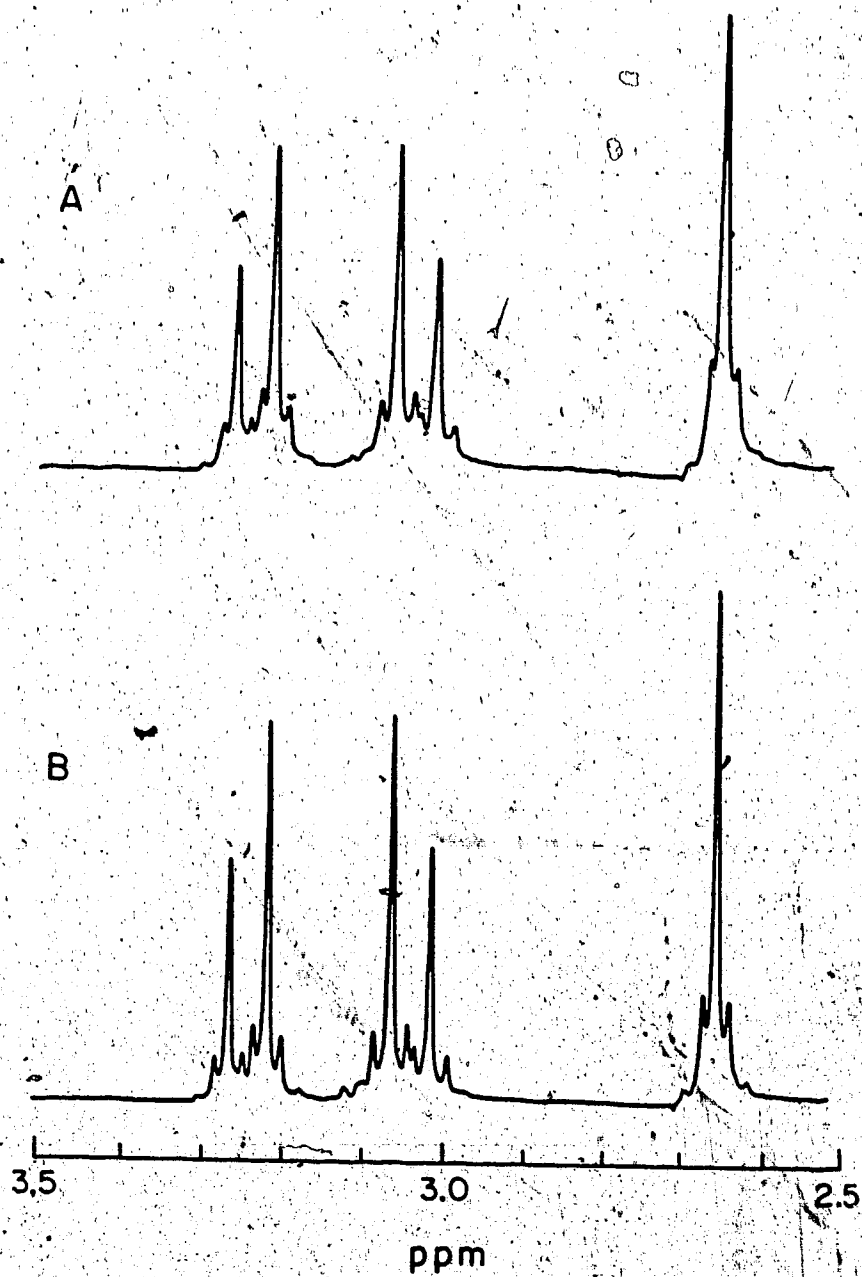


Figure 90. ^1H NMR spectra of equimolar solutions of Cd^{2+} , Ca^{2+} and EDTA at pH (A) 7.02 and (B) 9.10.

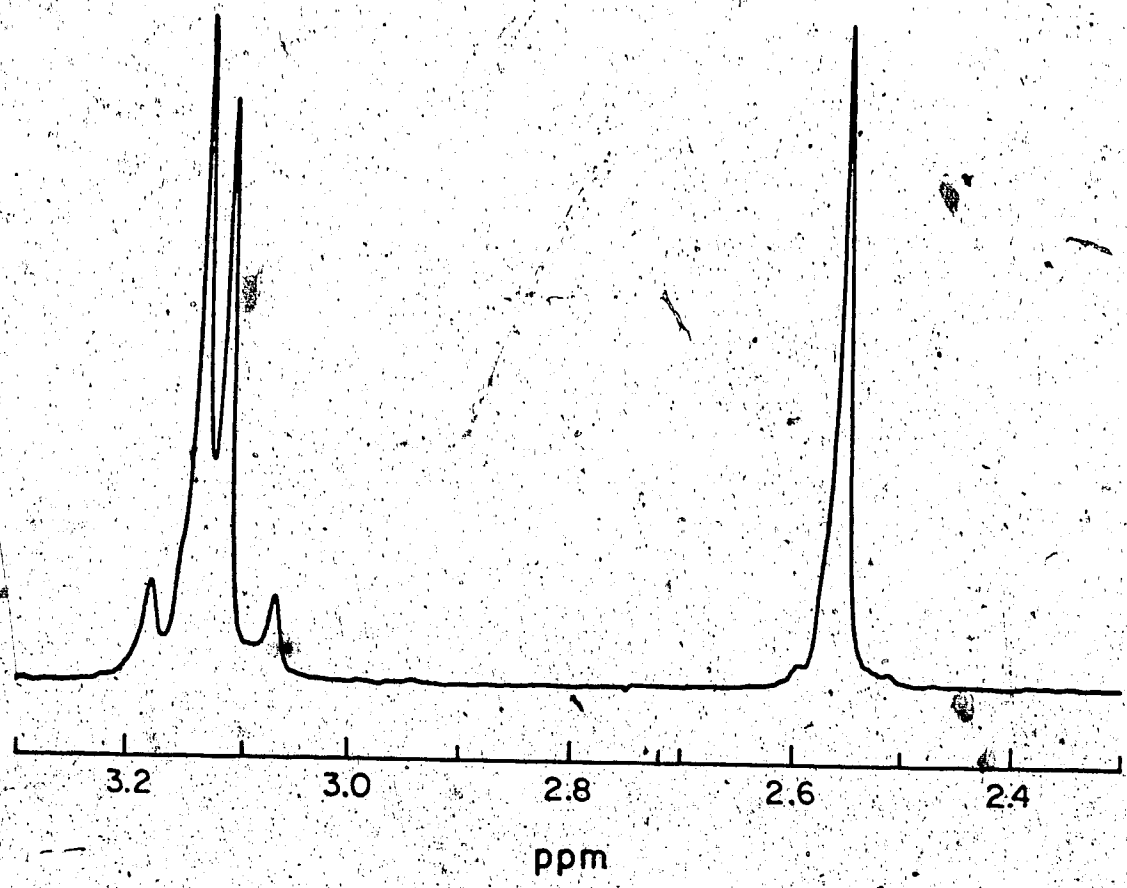


Figure 91. ¹H NMR spectra of Ca(EDTA)²⁻ (equimolar solution of Ca²⁺ and EDTA at pH 6.9).

1. Reaction of Cd(EDTA)²⁻ with Glutathione

The behavior of the chemical shifts of the resonances of glutathione protons in the presence of Ca²⁺ was first investigated to determine if cadmium binds glutathione. Glutathione (0.02M) was titrated with NaOD in the presence of Ca(NO₃)₂ (0.01M) and samples were withdrawn in the pH range 2.9 to 12.1 for the NMR experiments. The chemical shifts of all GSH resonances in the presence of Ca²⁺ are superimposable on those of GSH alone, as shown in Figure 92 indicating that Ca²⁺ is not complexed by GSH in the pH range ~2.9 to 12. Hence, the equilibrium established when Ca²⁺ and Cd(EDTA)²⁻ are added to a solution is as described by equation 127.

The displacement of EDTA from Cd(EDTA)²⁻ in solutions containing Ca²⁺ and GSH is demonstrated by spectra in Figure 93. The bottom spectrum on the figure (A) was obtained for an equimolar solution of Cd²⁺, Ca²⁺ and EDTA at pH 6. It contains resonances only for Cd(EDTA)²⁻. The triplet due to the ethylenic protons appears at 2.69 ppm (1 on spectrum A) and the quartet of triplets due to acetate protons is centered at ~3.15 ppm (2 on spectrum A). As increasing amounts of GSH are added to the solution, the intensity of the Cd(EDTA)²⁻ resonances decreases. Simultaneously there appear resonances at 2.55 ppm (3 on spectra B, C and D) and at ~3.12 ppm (4 on spectra B, C and D) due to ethylenic and acetate protons respectively of Ca(EDTA)²⁻. Resonance 3

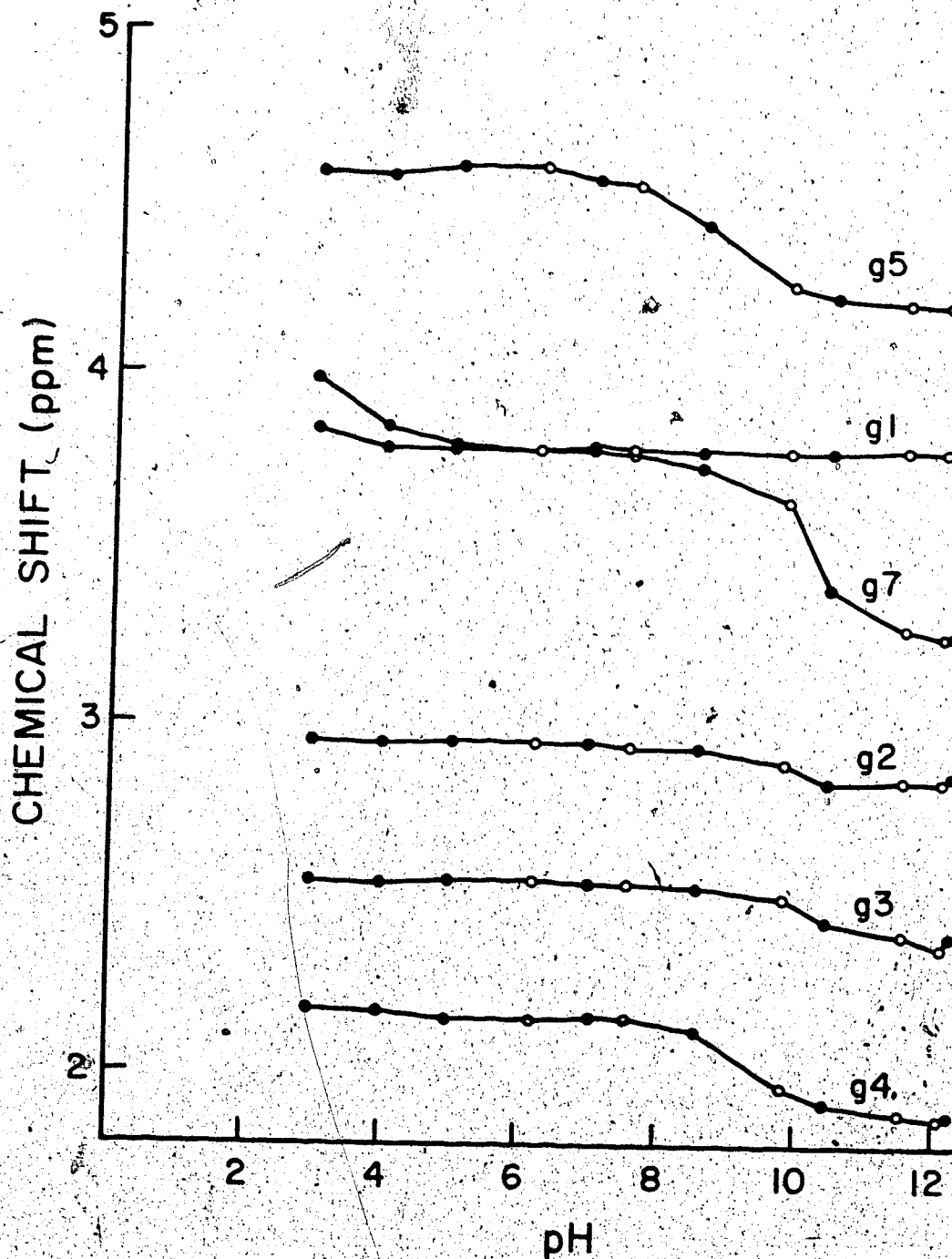


Figure 92. pH Dependence of the chemical shift of g5, g1, g7, g2, g3, g4 during titration of GSH (darkened circles) and during titration of a 1:2 mixture of Ca²⁺ and GSH (open circles).

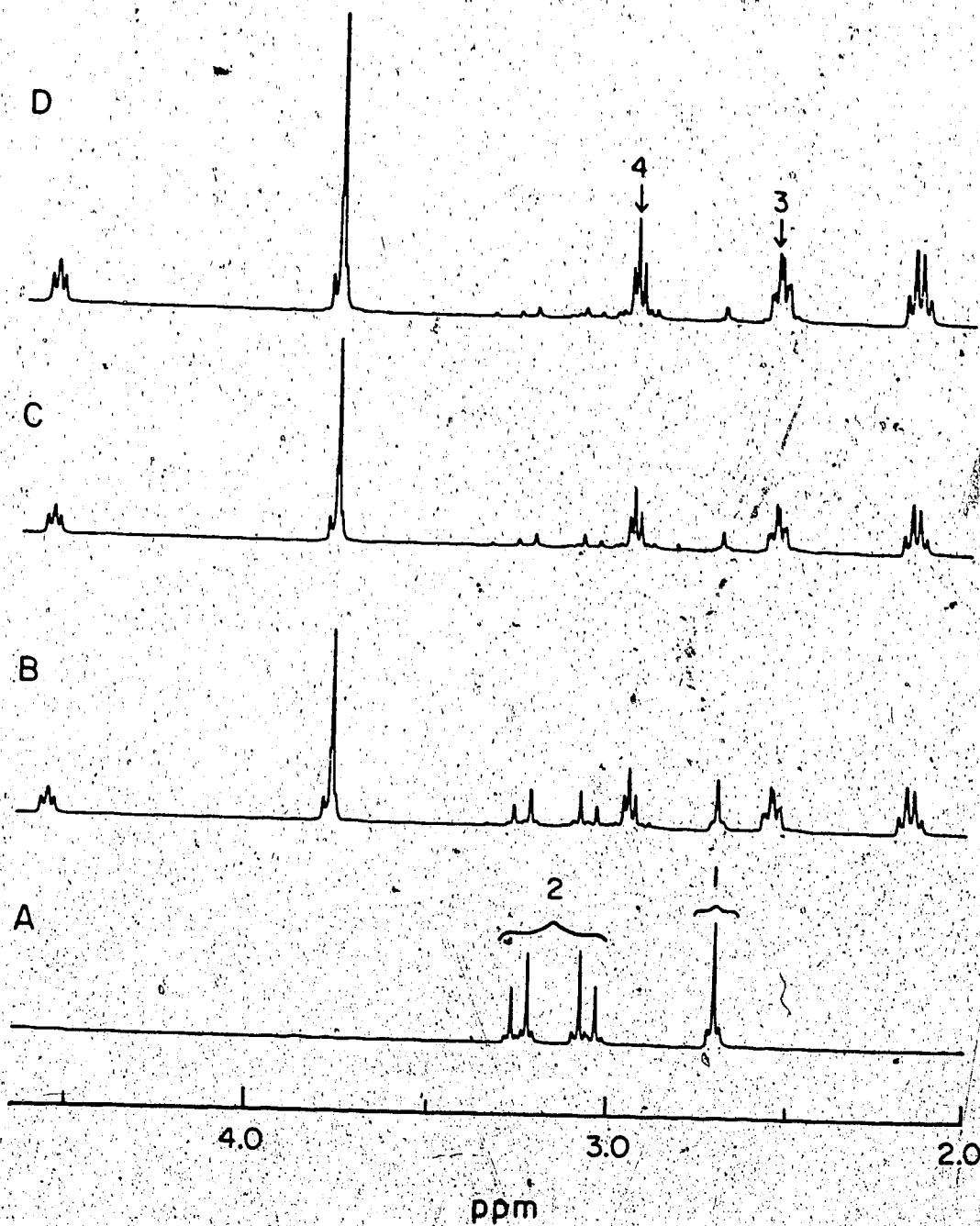
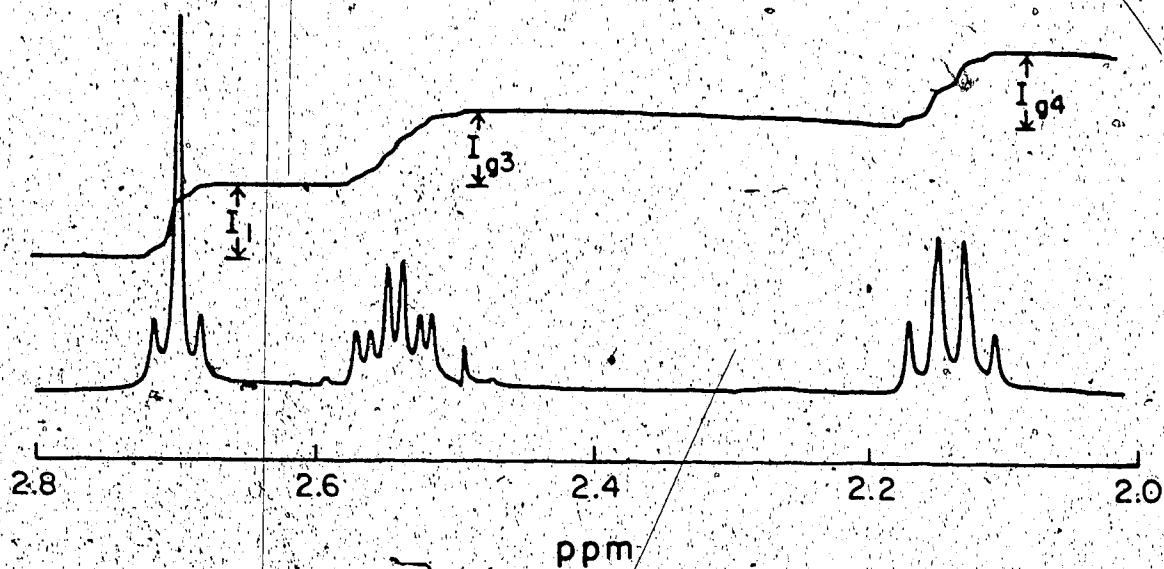


Figure 93. Effect of the addition of GSH on the ¹H NMR spectrum of an equimolar solution (0.005M) of Cd(EDTA)²⁻ and Ca²⁺ at pH 6 (Spectrum A).
 (A) [GSH] = 0 M, (B) [GSH] = 1.84 × 10⁻² M,
 (C) [GSH] = 3.77 × 10⁻² M, (D) [GSH] = 5.68 × 10⁻² M.

falls under resonance g3 of GSH and is detected as an increase of intensity of one of the quartet lines of g3. Resonance 4 falls under resonance g2 of glutathione and resonance 2 of $\text{Cd}(\text{EDTA})^{2-}$. Another interference which is not obvious in the spectra is the satellite signals of resonance g3 due to ^{13}C - ^1H coupling. The part of the satellites on the left side of resonance g3 falls under resonance 1 of $\text{Cd}(\text{EDTA})^{2-}$. However, its contribution to the intensity of resonance 1 of $\text{Cd}(\text{EDTA})^{2-}$ can be obtained easily as will be shown later. The change in the intensity of resonance 1 of $\text{Cd}(\text{EDTA})^{2-}$ was therefore used to determine the concentration of $\text{Cd}(\text{EDTA})^{2-}$ first and then the concentrations of the other species ($\text{Ca}(\text{EDTA})^{2-}$, CdL_t , Ca^{2+}) were obtained by difference from total concentrations. The intensity of resonance 1 was compared to that of resonance g4 of glutathione to deduce the concentration of $\text{Cd}(\text{EDTA})^{2-}$ from the concentration of GSH. Illustration of the procedure used is given in Figure 94 which shows only the portion of the spectrum, for the mixture Cd^{2+} , EDTA, Ca^{2+} , and GSH, of interest for the determination of the concentration of $\text{Cd}(\text{EDTA})^{2-}$. The intensity of resonance 1 is initially corrected for the contribution of the satellites due to coupling of ^{13}C and g3 protons. The intensity of the resonance due to g4 protons was used as this resonance is free of interference and its intensity is equal to that of resonance g3. From the natural abundance of ^{13}C (1.108%) the following equation was



$$[\text{Cd}(\text{EDTA})^{2-}] = \frac{(I_1 - 0.00554 I_4) \times [\text{GSH}]}{2 \times I_4}$$

Figure 94. Determination of $\text{Cd}(\text{EDTA})^{2-}$ from intensity measurements on g_4 resonance of GSH and resonance of ethylenic protons of $\text{Cd}(\text{EDTA})^{2-}$.

used to subtract the contribution of the ^{13}C - ^1H satellites to the intensity of resonance 1 of $\text{Cd}(\text{EDTA})^{2-}$:

$$I_1 \text{ corrected} = I_1 - 0.00554 I_{g4} \quad (131)$$

The value 0.00554, half of the 1.108%, is used because only one of the pair of satellites falls under resonance 1 of $\text{Cd}(\text{EDTA})^{2-}$. Correlating the corrected intensity to the intensity of g_4 and the concentration of glutathione, the concentration of $\text{Cd}(\text{EDTA})^{2-}$ is deduced as shown in the equation:

$$[\text{Cd}(\text{EDTA})^{2-}] = \frac{I_1 \text{ corrected} \times [\text{GSH}]_t}{2 I_{g4}} \quad (132)$$

The 2 in the denominator accounts for the fact that resonance 1 of $\text{Cd}(\text{EDTA})^{2-}$ is due to four protons while resonance g_4 is due to two protons.

Having obtained the concentration of $\text{Cd}(\text{EDTA})^{2-}$, the concentrations of the other species were calculated from equations 133-135.

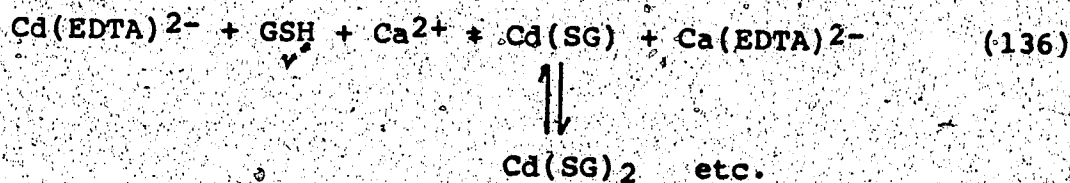
$$[\text{CdL}]_t = [\text{Cd}]_t - [\text{Cd}(\text{EDTA})^{2-}] \quad (133)$$

$$[\text{Ca}(\text{EDTA})] = [\text{Cd}]_t - [\text{Cd}(\text{EDTA})^{2-}] \quad (134)$$

$$[\text{Ca}^{2+}] = [\text{Ca}]_t - [\text{Ca}(\text{EDTA})^{2-}] \quad (135)$$

The experiments were always conducted under conditions of equimolar amounts of Cd^{2+} , Ca^{2+} and EDTA so that $[\text{Cd}(\text{EDTA})^{2-}] = [\text{Ca}^{2+}]$ and $[\text{Ca}(\text{EDTA})^{2-}] = [\text{CdL}]_t$.

The dependence of the concentration of $\text{Cd}(\text{EDTA})^{2-}$ on the pH of a mixture of 1:1:1:10 Cd^{2+} ; EDTA; Ca^{2+} ; GSH is shown in Figure 95. At pH 5 glutathione has already displaced about 25% of EDTA. The percentage of $\text{Cd}(\text{EDTA})^{2-}$ in solution decreases as the pH increases. Only ~10% of $\text{Cd}(\text{EDTA})^{2-}$ remains in solution at pH 7. In this pH region, Cd^{2+} is mainly binding to the sulfhydryl group. This is demonstrated in Figure 96 showing the pH dependence of the ^{13}C chemical shifts of the cysteinyl C_β and glutamyl C_β of glutathione in a solution of GSH (curve A and C) and a mixture of $\text{Cd}(\text{EDTA})^{2-}$, Ca^{2+} and GSH (curve B and D). Curves C and D, which are due to glutamyl C_β in GSH and in the mixture respectively, are superimposed meaning that the glutamyl residue in GSH is not complexing with Cd^{2+} through binding to its amino or carboxylate group. However, curve C for cysteinyl C_β of GSH in the mixture is shifted downfield up to a maximum of about 3.1 ppm relative to curve A of cysteinyl C_β in GSH from pH > 4, indicating binding to the sulfhydryl group. Up to pH 6, curve C indicates that the amino group is protonated. The reaction occurring in the mixture up to pH ~6 can therefore be represented by:



and the equilibrium constant by

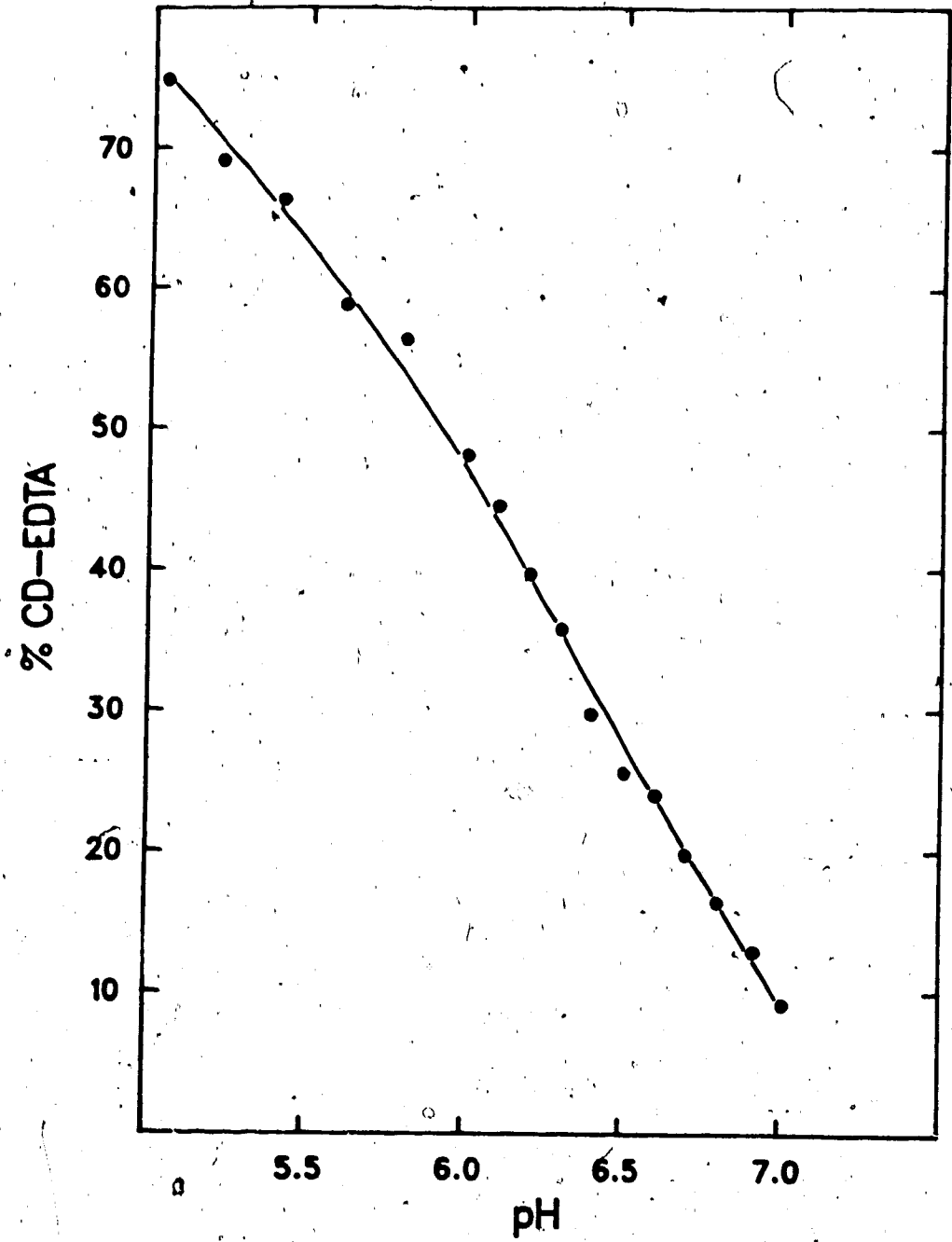


Figure 95. % Cd(EDTA) versus pH during titration of a 1:1:1:10 mixture of Cd²⁺, Ca²⁺, EDTA and GSH.

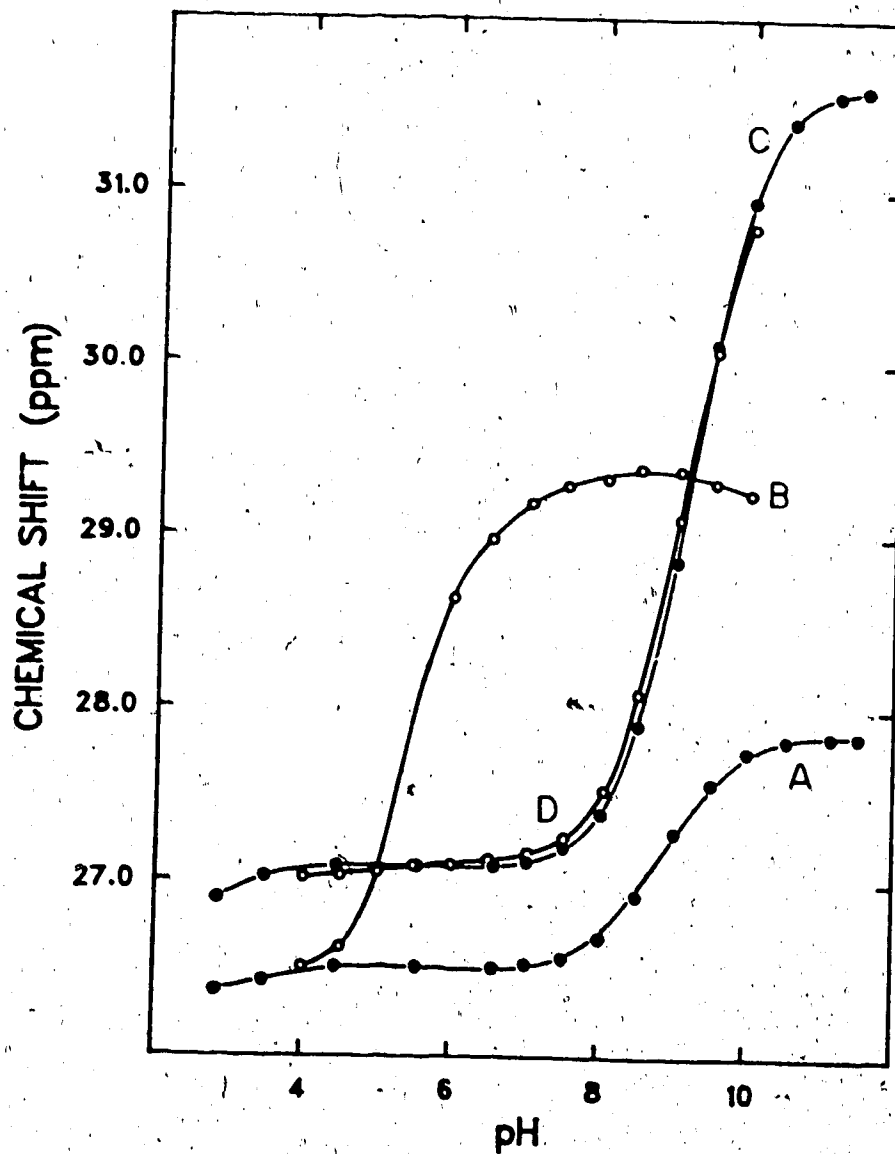


Figure 96. pH dependence of the ^{13}C chemical shifts of (A) cysteinyl C_β and (C) glutamyl C_β during titration of GSH and (B) cysteinyl C_β and (D) glutamyl C_β during titration of a 10:1:1 mixture of GSH, $\text{Cd}(\text{EDTA})^{2-}$ and Ca^{2+} .

$$K_{eq} = \frac{[Cd(SG)]_t [Ca(EDTA)^{2-}]}{[Cd(EDTA)^{2-}] [Ca^{2+}] [GSH]} \quad (137)$$

If it is assumed that the concentration of the GSH is large and does not vary much as the reaction proceeds, the following expression is obtained:

$$K_{fc} = \frac{[Cd(SG)]_t [Ca(EDTA)^{2-}]}{[Cd(EDTA)^{2-}] [Ca^{2+}]} \quad (138)$$

An equilibrium constant similar to that calculated with the hemolysed red cells:

$$K_{c1} = \frac{[Cd(SG)]_t [Mg(EDTA)^{2-}]}{[Cd(EDTA)^{2-}] [Mg^{2+}]} \quad (139)$$

can be obtained from K_{fc} and K as described by equation 129.

Results obtained for K_{fc} and K_{c1} as a function of pH, at $[GSH]_t = 0.05M$ and $[Cd]_t = [Ca]_t = [EDTA]_t = 0.005M$, are given in Table 21. K_{fc} and K_{c1} increase as the pH is increased. This is due to the pH dependence of the concentration of Cd(SG) species according to the following reaction:



A pH increase means a decrease in the concentration of H^+ ions. The latter decrease shifts the equilibrium to the right towards the production of more H^+ ions.

The highest pH at which K_{fc} and K_{c1} were evaluated for the present system was 6.6. Above this pH the intensity of

Table 21. Equilibrium constants for the reaction $\text{Cd}(\text{EDTA})^{2-} + \text{Ca}^{2+} + \text{GSH}$.

PH	$[\text{GSH}]_t$ (M)	$[\text{Cd}]_t$ (M)	K_{fc}^a	K_{cl}^b	% $\text{Cd}(\text{EDTA})^{2-}$
5.040	4.980×10^{-2}	4.980×10^{-3}	5.144×10^{-3}	5.144×10^{-5}	74.84
5.221	4.917×10^{-2}	4.917×10^{-3}	6.505×10^{-3}	6.505×10^{-5}	69.06
5.415	4.915×10^{-2}	4.915×10^{-3}	1.643×10^{-2}	1.643×10^{-4}	66.28
5.616	4.914×10^{-2}	4.914×10^{-3}	3.741×10^{-2}	3.741×10^{-4}	58.74
5.805	4.912×10^{-2}	4.912×10^{-3}	7.814×10^{-2}	7.814×10^{-4}	56.26
6.002	4.910×10^{-2}	4.910×10^{-3}	1.893×10^{-1}	1.833×10^{-3}	48.08
6.102	4.909×10^{-2}	4.909×10^{-3}	3.693×10^{-1}	3.693×10^{-3}	44.47
6.204	4.908×10^{-2}	4.908×10^{-3}	6.623×10^{-1}	6.623×10^{-3}	39.67
6.303	4.907×10^{-2}	4.907×10^{-3}	1.027	1.027×10^{-2}	35.76
6.402	4.905×10^{-2}	4.905×10^{-3}	1.732	1.732×10^{-2}	29.74
6.508	4.903×10^{-2}	4.903×10^{-3}	3.579	3.579×10^{-2}	25.60
6.605	4.902×10^{-2}	4.902×10^{-3}	5.141	5.141×10^{-2}	24.00

^a K_{fc} as defined by equation 138.

^b K_{cl} as defined by equation 139 for the reaction $\text{Cd}(\text{EDTA})^{2-} + \text{Mg}^{2+} + \text{GSH}$.

the resonance due to the ethylenic protons of $\text{Cd}(\text{EDTA})^{2-}$ becomes too low to afford accurate measurements. For comparison with the results of the study on hemolysed red blood cells, $\log K_{\text{Cl}}$'s were calculated and plotted against the pH. Extrapolation to pH 7 yielded a K_{Cl} value of 26×10^{-2} which is comparable to the average value of K_{Cl} in hemolysed red blood cells 10.4×10^{-2} . This result is interesting because in red blood cells, glutathione binds Cd^{2+} [33].

2. Reaction of $\text{Cd}(\text{EDTA})^{2-}$ with N-acetylpenicillamine (N-PSH)

The pH dependence of the chemical shift of the resonance due to the H_α proton is depicted in Figure 97 for N-PSH in the absence (curve A) and presence (curve B) of Ca^{2+} . As shown in Figure 97, curves A and B are superimposed from pH 4 to pH 8 indicating that Ca^{2+} does not complex N-PSH in this pH range. Above pH 8, the two curves are slightly shifted one from another suggesting that complexation occurs between Ca^{2+} and N-PSH above pH 8. Hence, only experimental data below pH 8 were used to evaluate equilibrium constants K_{fc} and K_{Cl} , as defined in equations 128 and 130 respectively, for the reaction of $\text{Cd}(\text{EDTA})^{2-}$ with N-PSH in the presence of Ca^{2+} . A spectrum of the mixture $\text{Cd}(\text{EDTA})^{2-}$, Ca^{2+} and N-PSH (1:1:1:10) at pH 6 is shown in Figure 98. Resonances due to the ethylene protons of $\text{Cd}(\text{EDTA})^{2-}$ and $\text{Ca}(\text{EDTA})^{2-}$ are free of interferences. Figure 99 shows portions of the spectra

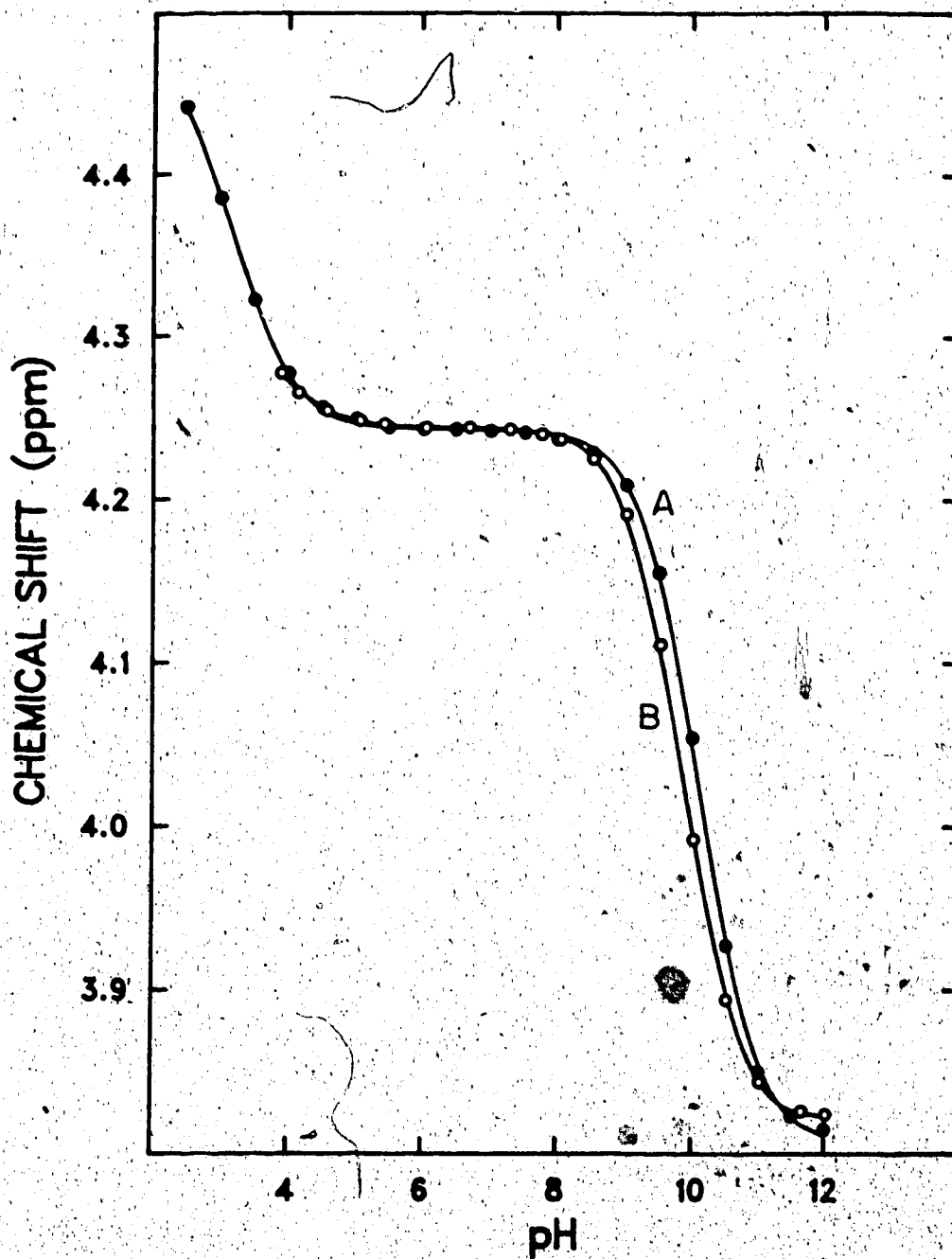


Figure 97. pH dependence of the chemical shift of H_{α} protons (A) during titration of N-PSH (0.02M) and (B) during titration of an equimolar solution of N-PSH and Ca^{2+} (0.02M).

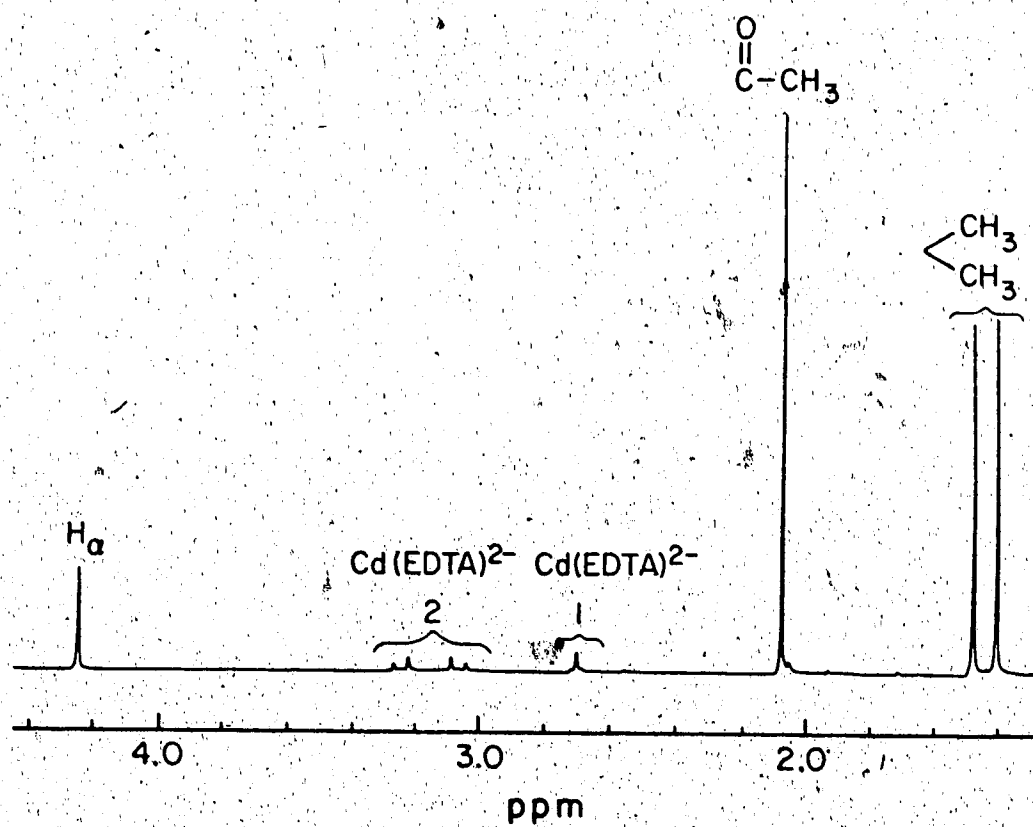


Figure 98. ^1H NMR spectrum of a 1 to 1 to 10 mixture of Cd(EDTA)^{2-} , Ca^{2+} and N-PSH at pH 6. $[\text{Cd}]_t = 0.005\text{M}$.

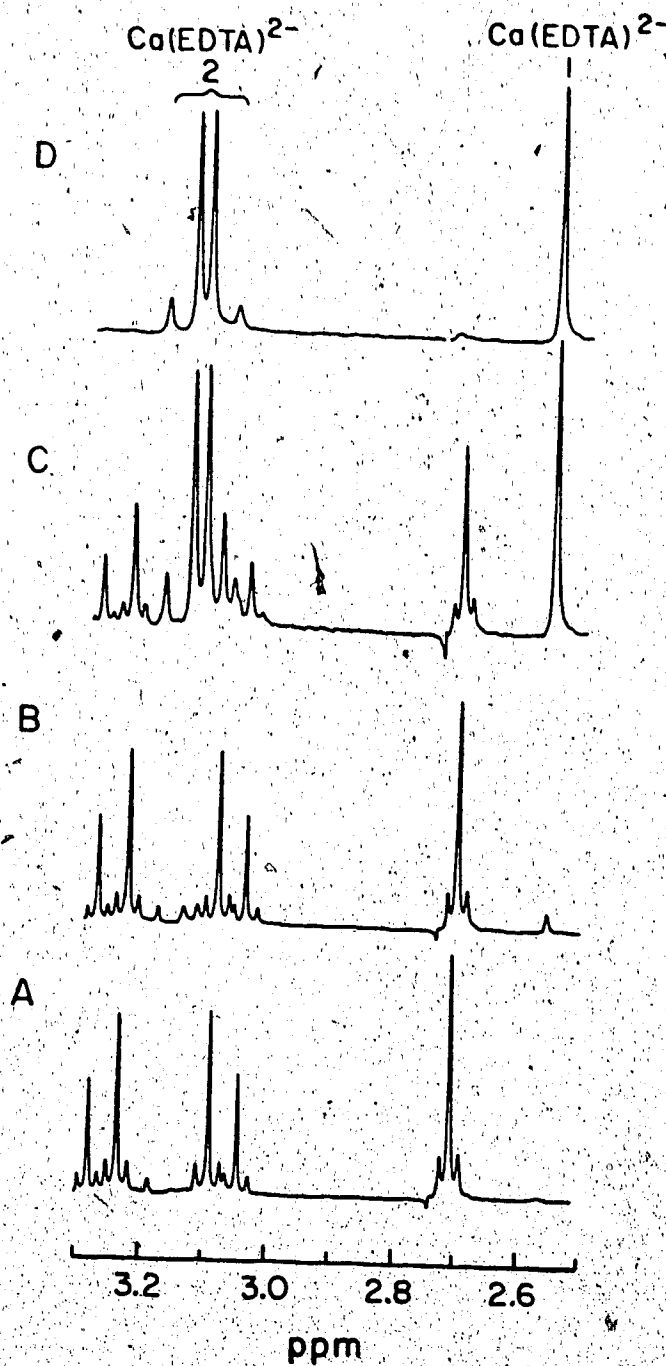


Figure 99. Portions of ^1H NMR spectra of Figure 98 mixture at pH (A) 5.4, (B) 5.9, (C) 7.1, and (D) 8.2.

which contain the resonances from protons of $\text{Cd}(\text{EDTA})^{2-}$ and $\text{Ca}(\text{EDTA})^{2-}$ as a function of pH. As the pH is increased, the intensity of the resonances due to $\text{Cd}(\text{EDTA})^{2-}$ decrease and that of the $\text{Ca}(\text{EDTA})^{2-}$ resonances increase as a result of $\text{Cd}(\text{EDTA})^{2-}$ reaction with N-PSH. The concentrations of the species were determined from the intensities of the resonances due to ethylenic protons in $\text{Cd}(\text{EDTA})^{2-}$ and $\text{Ca}(\text{EDTA})^{2-}$. First the fractional concentrations of $\text{Cd}(\text{EDTA})^{2-}$ and $\text{Ca}(\text{EDTA})^{2-}$ were obtained from the relative intensities of their resonances with the following relations:

$$I_t = I_{\text{Cd}(\text{EDTA})^{2-}} + I_{\text{Ca}(\text{EDTA})^{2-}} \quad (141)$$

$$f_{\text{Cd}(\text{EDTA})^{2-}} = \frac{I_{\text{Cd}(\text{EDTA})^{2-}}}{I_t} \quad (142)$$

$$f_{\text{Ca}(\text{EDTA})^{2-}} = \frac{I_{\text{Ca}(\text{EDTA})^{2-}}}{I_t} \quad (143)$$

where I_t stands for total integrated intensity, $I_{\text{Cd}(\text{EDTA})^{2-}}$ the integrated intensity of the resonance due to the ethylenic protons of $\text{Cd}(\text{EDTA})^{2-}$, $I_{\text{Ca}(\text{EDTA})^{2-}}$ the integrated intensity of the resonance due to the ethylenic protons of $\text{Ca}(\text{EDTA})^{2-}$ and f the fractional concentration of the complex indicated. Then, concentrations were obtained with equations 144 to 147.

$$[\text{Cd}(\text{EDTA})^{2-}] = f_{\text{Cd}(\text{EDTA})^{2-}} \times [\text{Cd}]_t \quad (144)$$

$$[\text{Ca}(\text{EDTA})^{2-}] = f_{\text{Ca}(\text{EDTA})^{2-}} \times [\text{Ca}]_t \quad (145)$$

$$[\text{Cd}]_t = [\text{Cd}]_t - [\text{Cd}(\text{EDTA})^{2-}] \quad (146)$$

$$[\text{Ca}^{2+}] = [\text{Ca}]_t - [\text{Ca}(\text{EDTA})^{2-}] \quad (147)$$

The concentration of $\text{Cd}(\text{EDTA})^{2-}$ decreases as the pH increases, as shown in Figure 100, which shows the pH dependence of the concentration of $\text{Cd}(\text{EDTA})^{2-}$ (expressed as percent of total cadmium in solution). This decrease is shifted to slightly higher pH values as compared to the glutathione system. The equilibrium constants K_{fc} and K_{c1} were calculated from data between pH 5.37 and 7.45; the results are given in Table 22. As was the case for the reaction with glutathione, the values of the two equilibrium constants increase as the pH increases. As more ligand is titrated, the concentration of $\text{Cd}(\text{N-PS})$ increases. At pH 7.45, a value of 5.74×10^{-2} was obtained for K_{c1} which compares well with the value 10.4×10^{-2} calculated for the reaction of $\text{Cd}(\text{EDTA})^{2-}$ with the HRBC's. This result indicates that it is the presence of the sulfhydryl which determines the value of the equilibrium constant.

3. Reaction of $\text{Cd}(\text{EDTA})^{2-}$ with Cysteine

Cysteine reacts with Ca^{2+} above pH 7 as demonstrated in Figure 101. The chemical shift of the H_α proton of cysteine in the mixture of Ca^{2+} and cysteine becomes slightly shifted from that in a solution of cysteine alone above pH 7. Hence the reaction of cysteine with $\text{Cd}(\text{EDTA})^{2-}$ in presence of Ca^{2+}

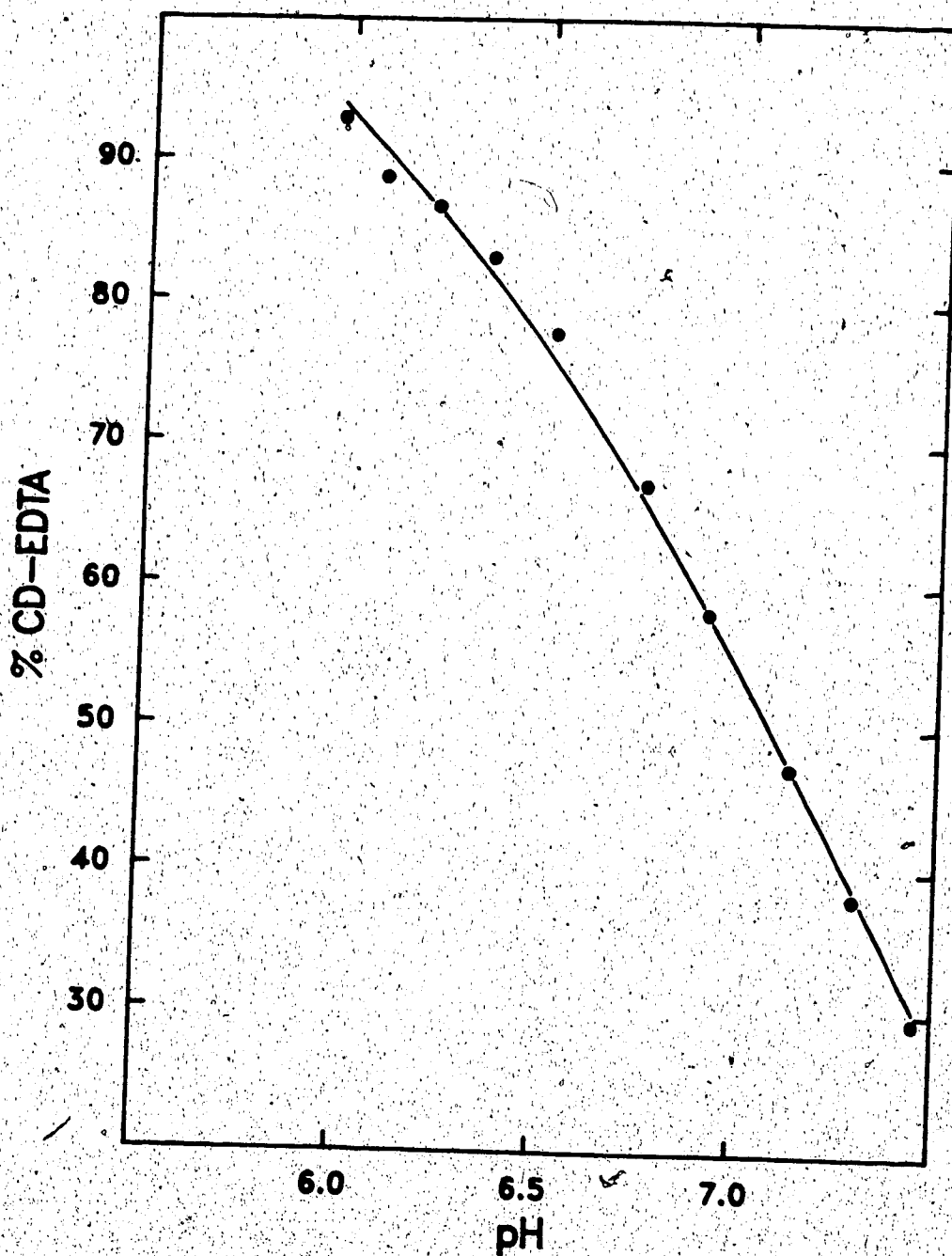


Figure 100. % Cd(EDTA)²⁻ vs. pH during titration of a 1:1:10 mixture of Cd(EDTA)²⁻, Ca²⁺ and N-PSH.

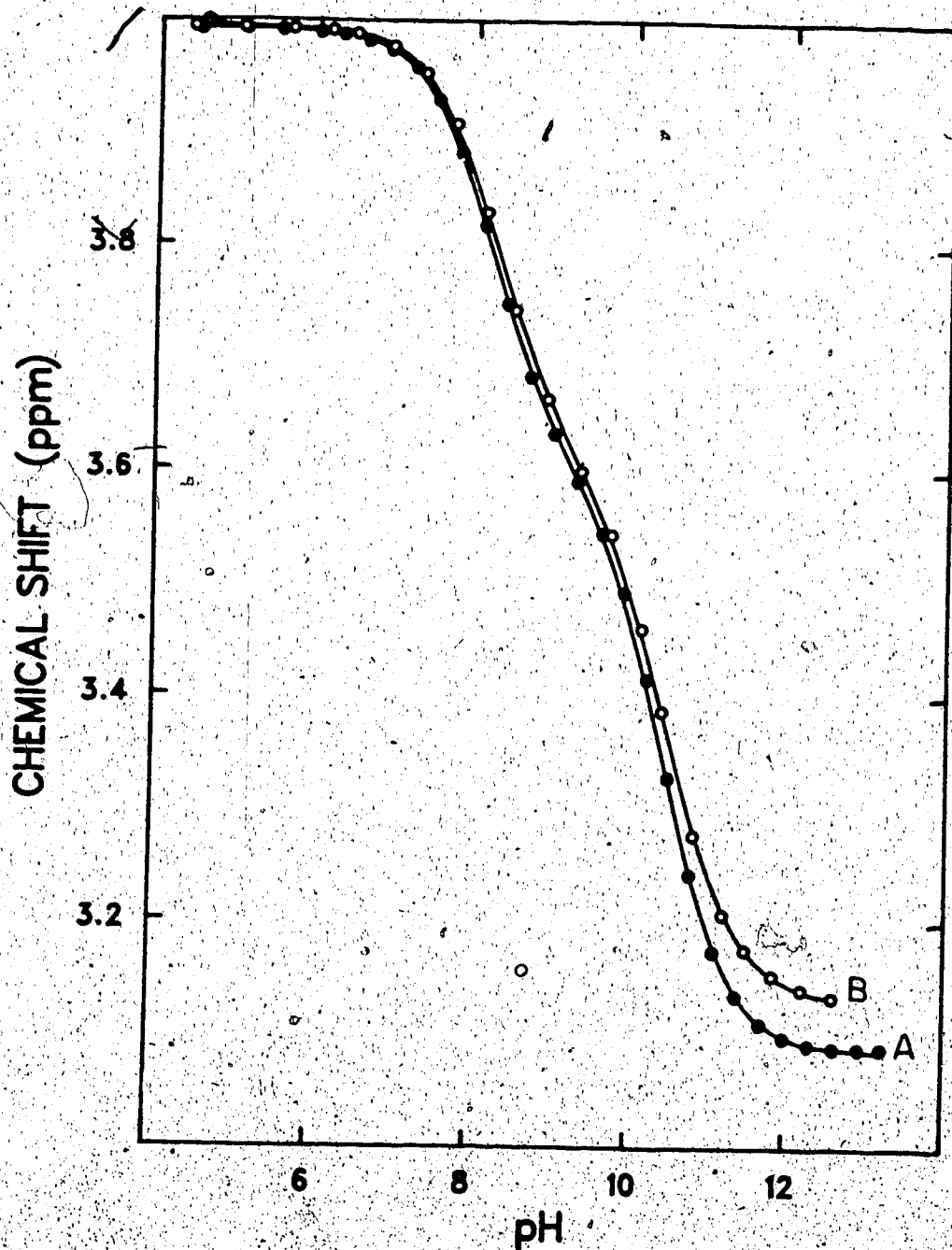


Figure 101. pH dependence of the chemical shift of H_{α} during titration of (A) cysteine (0.02M) and (B) an equimolar solution of Ca^{2+} and cysteine (0.02M).

Table 22. Equilibrium constants for the reaction $\text{Cd}(\text{EDTA})^{2-} + \text{Ca}^{2+} + \text{NAC-PSH}$.

PH	$[\text{NAC-PSH}]_t$ (M)	$[\text{Cd}]_t$ (M)	K_{Fc}	K_{Cl}	$\% \text{ Cd}(\text{EDTA})^{2-}$
5.373	4.916×10^{-2}	4.496×10^{-3}	5.879×10^{-3}	5.879×10^{-5}	92.88
6.084	"	"	1.631×10^{-2}	1.631×10^{-4}	88.67
6.216	"	"	2.378×10^{-2}	2.378×10^{-4}	86.64
6.358	"	"	4.178×10^{-2}	4.178×10^{-4}	83.03
6.523	"	"	8.232×10^{-2}	8.232×10^{-4}	77.70
6.760	"	"	2.417×10^{-1}	2.417×10^{-3}	67.03
6.924	"	"	5.237×10^{-1}	5.237×10^{-2}	58.01
7.133	"	"	1.253	1.253×10^{-2}	47.17
7.296	"	"	2.642	2.642×10^{-2}	38.08
7.454	"	"	5.744	5.744×10^{-2}	29.43

was investigated at a fixed pH 6.5. Cysteine was added to an equimolar mixture of Cd^{2+} , Ca^{2+} and EDTA at pH 6.5. Representative spectra from this experiment are shown in Figure 102. Similarly to GSH and N-PSH, addition of cysteine causes the displacement of EDTA from $\text{Cd}(\text{EDTA})^{2-}$ as indicated by the appearance of resonances for $\text{Ca}(\text{EDTA})^{2-}$. The resonances of the ethylenic protons of $\text{Cd}(\text{EDTA})^{2-}$ and $\text{Ca}(\text{EDTA})^{2-}$ are free of interference as in the case of N-PSH. Therefore the concentrations of species $\text{Cd}(\text{EDTA})^{2-}$, $\text{Ca}(\text{EDTA})^{2-}$, CdL and Ca^{2+} were determined following the procedure used previously with the N-PSH system. The decrease of the concentration of $\text{Cd}(\text{EDTA})^{2-}$ (expressed as % of total cadmium) is depicted in Figure 103 as a function of the concentration of cysteine. Results obtained for K_{fc} and K_{cl} for this system are given in Table 23. Both K_{fc} and K_{cl} increase with increasing concentrations of cysteine, presumably due to the change in the nature of the complex(es) formed as the ratio $\text{Cd}^{2+}/\text{cysteine}$ increases ($\text{Cd}(\text{cys}) + \text{Cd}(\text{cys})_2$ etc. ...). The value of the equilibrium constant: K_{fc} depends on the stability constant of the complex formed as described in equation 148 where β stands for the stability constant.

$$K_{fc} = \frac{\beta[\text{Cys}]K_{f\text{Ca}(\text{EDTA})^{2-}}}{K_{f\text{Cd}(\text{EDTA})^{2-}}} \quad (148)$$

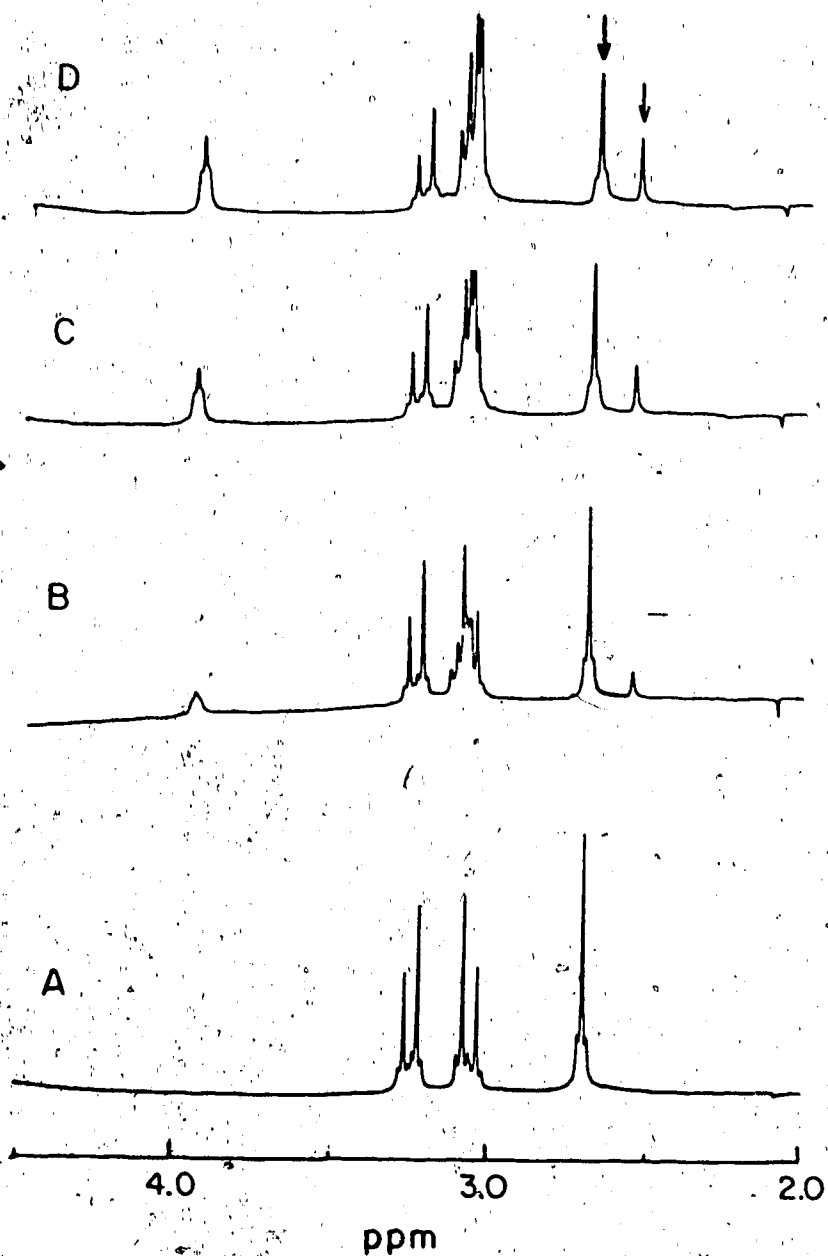


Figure 102. Effect of addition of cysteine on the ^1H NMR spectrum of an equimolar mixture of $\text{Cd}(\text{EDTA})^{2-}$ and Ca^{2+} at pH 6.5. $[\text{Cd}(\text{EDTA})^{2-}] = [\text{Ca}^{2+}] = 0.005\text{M}$, $[\text{Cysteine}] =$ (A) 0, (B) $5.97 \cdot 10^{-3}\text{M}$, (C) $1.19 \cdot 10^{-2}\text{M}$ and (D) $1.59 \cdot 10^{-2}\text{M}$.

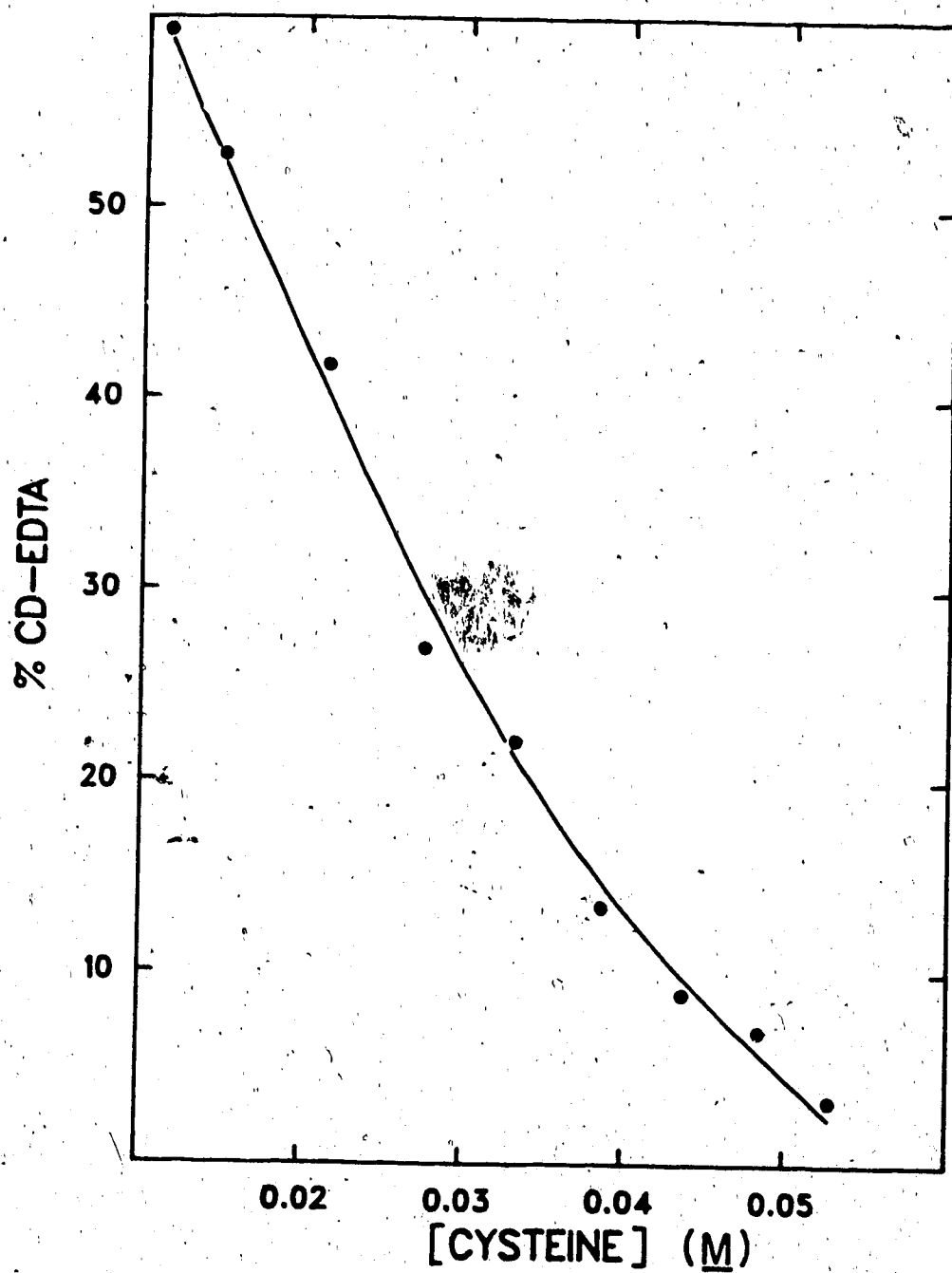


Figure 103. % Cd(EDTA)²⁻ versus concentration of cysteine at pH 6.5.

Table 23. Equilibrium constants of the reaction $\text{Cd}(\text{EDTA})^{2-} + \text{Ca}^{2+} + \text{cysteine}$ at $\text{pH} = 6.5$.

[Cysteine] _t (M)	[Cd] _t (M)	K _{fc}	K _{c1}	% Cd(EDTA) ²⁻
1.128x10 ⁻²	4.702x10 ⁻³	2.043x10 ⁻²	2.043x10 ⁻⁴	59.29
1.476x10 ⁻²	4.615x10 ⁻³	4.191x10 ⁻²	4.191x10 ⁻⁴	52.74
2.135x10 ⁻²	4.449x10 ⁻³	1.735x10 ⁻¹	1.735x10 ⁻³	41.67
2.750x10 ⁻²	4.297x10 ⁻³	8.313x10 ⁻¹	8.313x10 ⁻³	36.90
3.323x10 ⁻²	4.154x10 ⁻³	1.798	1.798x10 ⁻²	22.04
3.853x10 ⁻²	4.020x10 ⁻³	7.105	7.105x10 ⁻²	13.41
4.363x10 ⁻²	3.895x10 ⁻³	2.041x10 ¹	2.042x10 ⁻¹	8.86
4.835x10 ⁻²	3.778x10 ⁻³	3.481x10 ¹	3.481x10 ⁻¹	6.93
5.280x10 ⁻²	3.667x10 ⁻³	1.863x10 ²	1.863	3.32

2

4. Reaction of $\text{Cd}(\text{EDTA})^{2-}$ with S-methylglutathione

The S-methylated derivative of glutathione displaces EDTA from its $\text{Cd}(\text{EDTA})^{2-}$ complex only at fairly high pH as shown in Figure 104. Also, this displacement is not extensive as indicated by the relative intensity of $\text{Cd}(\text{EDTA})^{2-}$ and $\text{Ca}(\text{EDTA})^{2-}$ resonances. Even at a pH as high as 12.0, the intensity of the resonance due to the ethylenic protons of $\text{Cd}(\text{EDTA})^{2-}$ is clearly much higher than the intensity of the resonance of ethylenic protons in $\text{Ca}(\text{EDTA})^{2-}$. Above pH 9.2 both resonances are free of interference and their intensities were used to deduce equilibrium concentrations of species as detailed in section F.2 for the case of N-PSH. Figure 105 depicts the decrease of the percentage of $\text{Cd}(\text{EDTA})^{2-}$ in solution as a function of pH. At pH 12, only 18% of $\text{Cd}(\text{EDTA})^{2-}$ is dissociated. The values of the equilibrium constants K_{fc} and K_{cl} obtained for this system, given in Table 24, are about 100 times lower than those obtained with the GSH, N-PSH and cysteine systems.

G. Discussion and Conclusions

The exact nature of the complexes of Cd^{2+} formed in red blood cells is not known although ternary complexes of the nature $(\text{GS})\text{Cd}(\text{Hb})$ have been suggested [33]. Two studies cited earlier on the distribution of cadmium among blood components [100] and on the interaction of cadmium with red

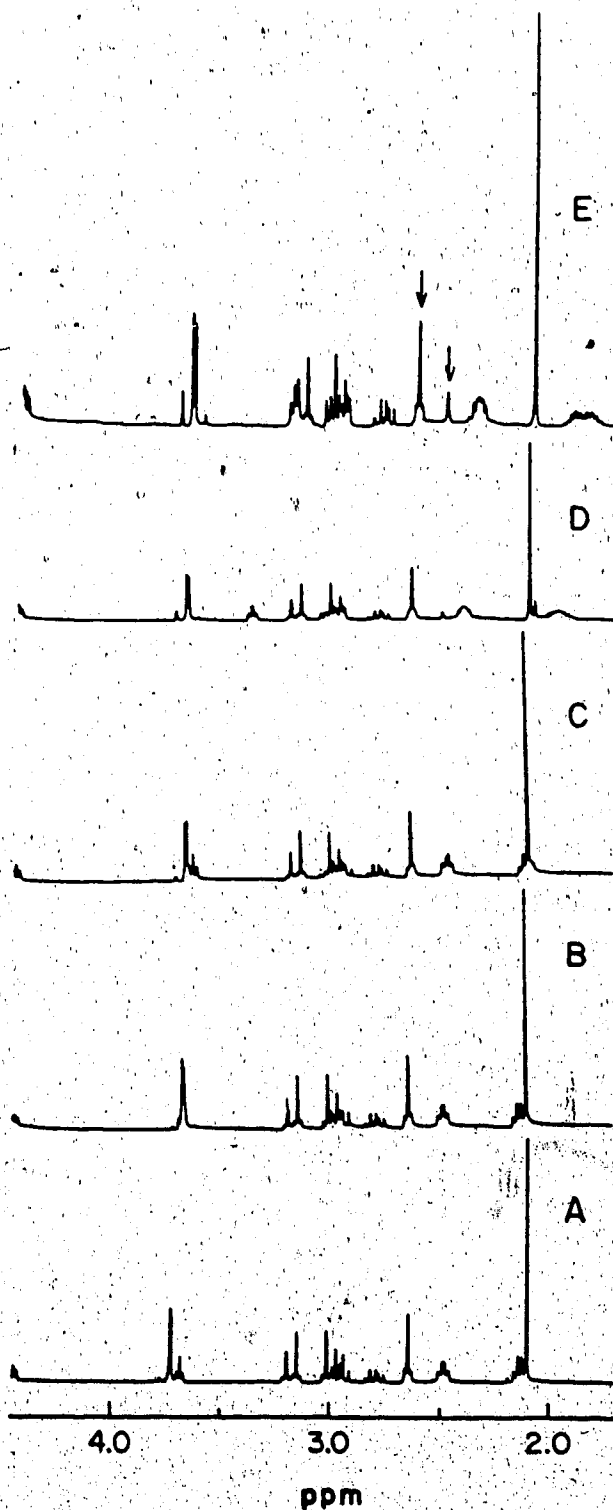


Figure 104. ^1H NMR spectra of 1:1:2 mixture of $\text{Cd}(\text{EDTA})_2^{2-}$, Ca^{2+} and CH_3SG at (A) 4.04, (B) 6.48, (C) 8.43, (D) 9.82 and (E) 12.00. $[\text{Cd}]_t = 0.01\text{M}$.

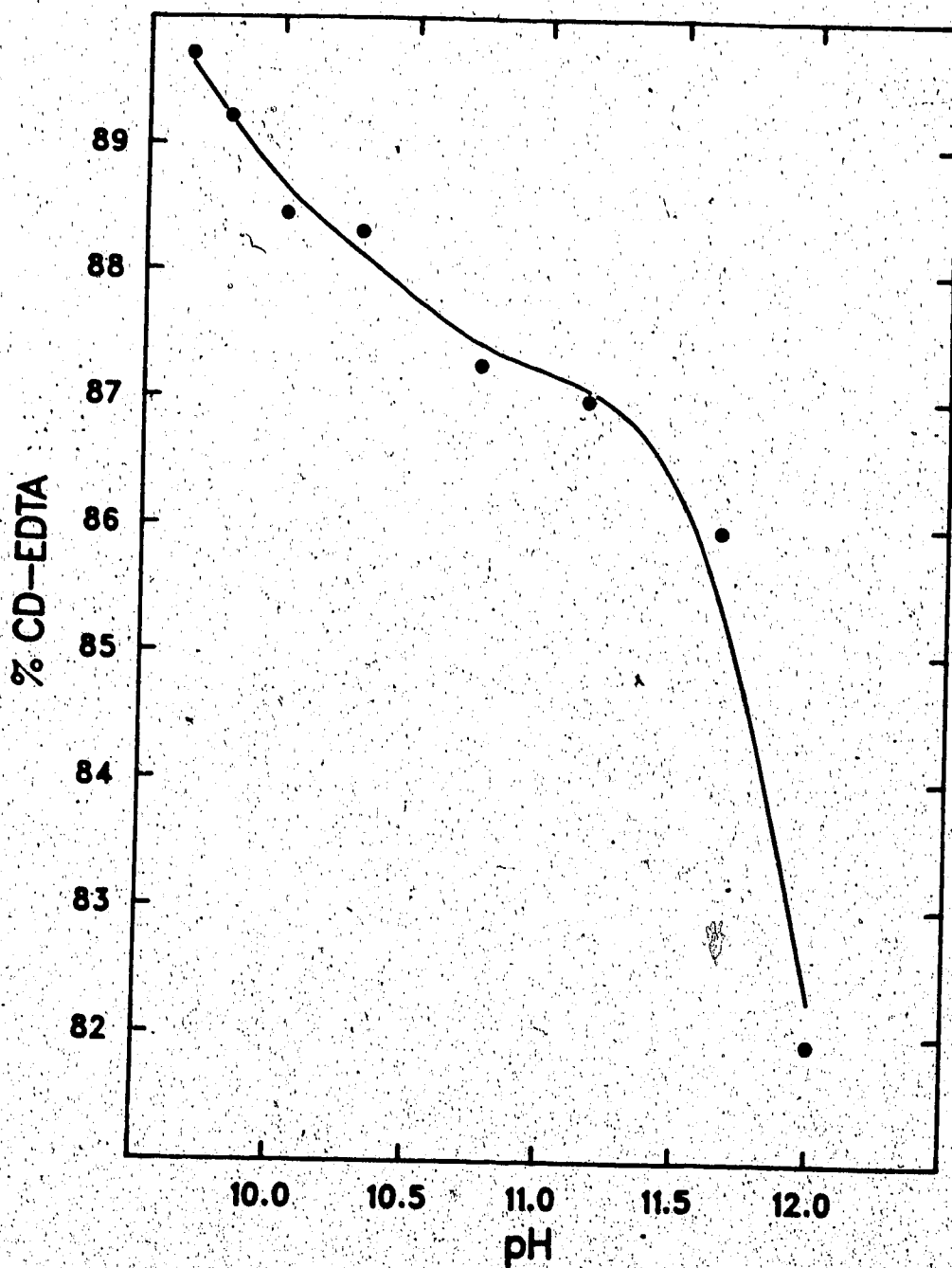


Figure 105. % $\text{Cd}(\text{EDTA})^{2-}$ versus pH during titration of a 1:1:2 mixture of $\text{Cd}(\text{EDTA})^{2-}$, Ca^{2+} and CH_3SG .

Table 24. Equilibrium constants for the reaction $\text{Cd}(\text{EDTA})^{2-} + \text{Ca}^{2+} + \text{CH}_3\text{SG}$.

PH	$[\text{CH}_3\text{SH}]_t$ (M)	$[\text{Cd}]_t$ (M)	K _{fc}	$\frac{\text{KCl}}{\text{fc}}$	$\frac{8}{\text{Cd}(\text{EDTA})^{2-}}$
9.660	1.965×10^{-2}	9.827×10^{-3}	1.315×10^{-2}	1.315×10^{-4}	89.71
9.806	1.964×10^{-2}	9.822×10^{-3}	1.461×10^{-2}	1.461×10^{-4}	89.21
10.020	1.963×10^{-2}	9.816×10^{-3}	1.703×10^{-2}	1.703×10^{-4}	88.44
10.300	1.962×10^{-2}	9.808×10^{-3}	1.757×10^{-2}	1.757×10^{-4}	88.30
10.754	1.959×10^{-2}	9.797×10^{-3}	2.135×10^{-2}	2.135×10^{-4}	87.25
11.151	1.958×10^{-2}	9.792×10^{-3}	2.241×10^{-2}	2.241×10^{-4}	86.98
11.654	1.957×10^{-2}	9.783×10^{-3}	2.666×10^{-2}	2.666×10^{-4}	85.96
12.005	1.954×10^{-2}	9.772×10^{-3}	4.866×10^{-2}	4.866×10^{-4}	81.93

blood cell molecules are of interest to the present discussion and are reviewed here.

Klassen et al. [100] investigated the redistribution of Cd^{2+} to the blood of rats after a number of studies had each identified a different blood component binding cadmium [101-103]. The results of gel chromatography measurements on the cytosol of red blood cells obtained from rats sixty hours after injection of CdCl_2 suggested cadmium was bound to the following entities: i) a high molecular weight fraction; ii) hemoglobin; iii) a protein of molecular weight similar to hepatic metallothionein and (iv) a low molecular weight fraction. The binding of Cd^{2+} to human red blood cells was studied at the molecular level by spin echo ^1H NMR [33]. In this study, a τ_2 of 0.06 sec was initially used in the spin echo pulse sequence to observe mainly resonances from small molecules in the erythrocytes. Among the small molecules, glutathione was found to bind Cd^{2+} . No significant changes were observed in the resonances due to other small molecules (e.g., glycine, creatine, alanine, ergothioneine) meaning little if any binding to these molecules. A shorter delay time of 0.015 sec was used to observe resonances from the imidazole side-chains of hemoglobin. Changes in the resonances due to the c-4 and c-2 hydrogens of the imidazole side-chains indicated that Cd^{2+} was also strongly binding to hemoglobin in agreement with the study of Klassen et al. [100]. It was suggested

that Cd^{2+} was binding to at least one histidine residue of hemoglobin. Suggestion of the ternary complex implicating GSH and hemoglobin ($(\text{GS})\text{Cd}(\text{Hb})$) was inferred from observed increased sensitivity of GSH resonances to Cd^{2+} in red cells as compared to GSH in aqueous solutions of Cd^{2+} . It was proposed on the basis of these results that the possible Cd^{2+} -containing species in red blood cells are single ligand complexes with GSH or hemoglobin of the type $\text{Cd}(\text{SG})_n$, $\text{Cd}(\text{Hb})_n$, and the ternary complex $(\text{GS})\text{Cd}(\text{Hb})$. Based on the latter assumption the equilibrium constant K_{c1} evaluated in the present study may be expressed as:

$$K_{c1} = \frac{[\text{Cd}(\text{SG})_t + \text{Cd}(\text{Hb})_t + (\text{GS})\text{Cd}(\text{Hb})][\text{Mg}(\text{EDTA})^{2-}]}{[\text{Cd}(\text{EDTA})^{2-}][\text{Mg}]_{\text{free}}} \quad (149)$$

where $\text{Cd}(\text{SG})_t$ represents the total concentration of all species of the type $\text{Cd}(\text{SG})_n$ and $\text{Cd}(\text{Hb})_t$ the total concentration of all species of the type $\text{Cd}(\text{Hb})_n$.

The equilibrium constant K_{c1} gives an indirect measurement of the stability of the complexes formed. The displacement of EDTA from $\text{Cd}(\text{EDTA})^{2-}$ depends on the strength of the bond(s) formed between Cd^{2+} and the molecules of the red blood cells. From K_{c1} a type of conditional stability constant can be deduced as follows:

$$K(\text{CdL}) = \frac{[\text{CdL}]_t}{[\text{Cd}^{2+}][\text{L}]_{\text{free}}} = \frac{K_{c1}}{[\text{L}]_{\text{free}}} \times \frac{K_{f\text{Cd}(\text{EDTA})^{2-}}}{K_{f\text{Mg}(\text{EDTA})^{2-}}} \quad (150)$$

With the average K_{c1} of 10.4×10^{-2} , a value of $\frac{6.5 \times 10^6}{[L]_{free}}$ is obtained for $K(CdL)$. The average concentrations of GSH and hemoglobin in red cells are 2.2 mM and 5.2 mM respectively [106], from which $[L]_{free}$ may be assumed to be at the millimolar level. With the latter assumption an estimated value of $\sim 6.5 \times 10^9$ is obtained for $K(CdL)$, which agrees with the suggestion of strong binding by Rabenstein et al [33]. Such a value also points more to complexation through the sulfhydryl groups. Cadmium complexes in aqueous solution with binding to thiolate groups are reported to have stability constants of this order and higher (29, 81, 82), whereas complexes with binding to amino or carboxylate groups have much lower stability constants [107] with the exception of stable chelates formed with ligands such as EDTA and nitrilotriacetic acid. Predominant binding through sulfhydryl groups is further supported by the values obtained for K_{c1} from the reaction of $Cd(EDTA)^{2-}$ with thiols in the present study. The values calculated of K_{c1} 26×10^{-2} , 5.74×10^{-2} , 7.10×10^{-2} for the reaction of $Cd(EDTA)^{2-}$ with GSH, N-PSH and cysteine respectively are comparable to the average value of K_{c1} 10.4×10^{-2} for the reaction of $Cd(EDTA)^{2-}$ with hemolysed red blood cells. The values obtained for K_{c1} with the derivative of GSH having its sulfhydryl group blocked with a methyl group were about 100 times smaller than those obtained with the three above cited thiols.

The previous ^1H NMR study on the binding of Cd^{2+} in red blood cells and the present study could not provide evidence for the binding of Cd^{2+} to the sulfhydryl groups of the hemoglobin residues. With the evidence collected so far, the most abundant species formed in the erythrocytes would be complexes of the type $\text{Cd}(\text{SG})_n$ and $(\text{Hb})\text{Cd}(\text{SG})$. The predominance of glutathione complexes over hemoglobin complexes has been ascertained in the case of the binding of methylmercury ($\text{CH}_3\text{Hg}(\text{II})$) in human erythrocytes from ^1H NMR chemical shift measurements using the saturation transfer method [107]. The effective formation constant of the $\text{CH}_3\text{Hg}(\text{II})$ complexes of glutathione was estimated to be approximately six times that of $\text{CH}_3\text{Hg}(\text{II})$ complexes of hemoglobin.

The estimated conditional stability constant of complex(es) formed in red blood cells ($\log K_f \sim 9$) is higher than the formation constant of the $\text{Cd}(\text{SG})$ complex ($\log K_f = 6.64$) formed in aqueous solution. This constant was obtained from the study of mixed $\text{Cd}(\text{NTA})_L$ complexes reported in Chapter III. The high stability of the complex(es) formed in red cells explains the known slow removal of Cd^{2+} from the red blood cells as compared to the plasma [102, 103]. The ultimate accumulation of cadmium in the liver and kidney [11, 13] means that even more stable complexes are formed therein. Metallothionein formed in liver and kidney upon accumulation of cadmium were discussed earlier in the thesis (Chapters I and IV). The complexes

consisting of 3 and 4 metal clusters, as inferred from ^{113}Cd NMR measurements [28, 88, 89], form a rigid and very stable system. The complexes of Cd-GSH exhibit a resonance in the region where those of cadmium-metallothionein occur. This resonance, however, was observed only at high pH values (pH \geq 8.5). At physiological pH, no resonance was detectable in the ^{113}Cd NMR spectrum of Cd-GSH systems. The complexes formed with GSH at physiological pH are therefore very labile. In fact, toxicological studies have shown that three hours after injection of Cd^{2+} the concentration of cadmium decreased almost two orders of magnitude [100]. This relatively rapid displacement of Cd^{2+} from blood implies that much more stable complexes are formed in tissues where cadmium is ultimately accumulated.

The study of mixed complexes $\text{Cd}(\text{NTA})\text{L}$ demonstrates that only thiols displaced NTA from its cadmium complex forming mixed as well as single ligand complexes. Ordinary amino acids possessing only the amino and carboxylate groups as potential donor groups, did not displace NTA and formed only mixed complexes with $\text{Cd}(\text{NTA})^-$. The complex $\text{Cd}(\text{EDTA})^{2-}$ used in the red blood cell study has a higher formation constant ($\log K_f = 16.5$) than the $\text{Cd}(\text{NTA})^-$ complex ($\log K_f = 9.43$) making EDTA even more difficult to displace. Thus, the Cd^{2+} complexes which form in red cells when EDTA is displaced from its Cd^{2+} complex must involve a sulfhydryl donor group. It was not possible to demonstrate experimentally that the

cysteinyl residues in hemoglobin do not react with cadmium when $\text{Cd}(\text{EDTA})^{2-}$ is added to HRBC. Given the size of the $\text{Cd}(\text{EDTA})^{2-}$ complex it will preferably react on the sulfhydryl group of glutathione which is more readily exposed and much less hindered than the sulfhydryl group of hemoglobin. Also the previous ^1H NMR study and the present study on the interactions of Cd^{2+} in red blood cells have indicated a pronounced effect of Cd^{2+} on the resonances due to the cysteinyl protons of glutathione. It is thus suggested that GSH displaces EDTA in a first step and hemoglobin reacts subsequently with the Cd-GSH complex initially formed. The fact that the measured displacement of EDTA from $\text{Cd}(\text{EDTA})^{2-}$ in aqueous solution of GSH is comparable to its displacement in red cells also supports an initial reaction of $\text{Cd}(\text{EDTA})^{2-}$ with GSH in the red cells.

Once the Cd-GSH complex is formed in the red cells, restrictions are imposed on further reactions by the nature of this complex. The complexation of Cd^{2+} in red blood cells [33] was found to affect the resonances due to protons of some of the imidazole side-chains of hemoglobin. It is possible that these particular sites were the ones which accommodated best the Cd-GSH complex.

REFERENCES

1. D.F. Flick, H.F. Kraybill and J.M. Dimitroff, *Environ. Res.*, 4, 71 (1971).
2. P.E. Carroll, *J. Amer. Med. Assoc.*, 198, 267 (1966).
3. S.A. Gunn, T.C. Gould and W.A.D. Anderson, *Bull. Pathol.*, 8, 42 (1967).
4. H.S. Schroeder and J.J. Balassa, *Am. J. Physiol.*, 209, 433 (1965).
5. S.A. Gunn, T.C. Gould and W.A.D. Anderson, *Bull. Pathol.*, 8, 68 (1967).
6. Le Baron R. Briggs, *Bull. Environ. Contam. Toxicol.*, 22, 840 (1979).
7. C. Sugawara and N. Sugawara, *Bull. Environ. Contam. Toxicol.*, 14(2), 159 (1975).
8. S.A. Dressing, R.P. Maas and C.M. Weiss, *Bull. Environ. Contam. Toxicol.*, 28, 172 (1982).
9. J.A. Titus and R.M. Pfister, *Bull. Environ. Contam. Toxicol.*, 28, 703 (1982).
10. Yen-Wan Hung, *Bull. Environ. Contam. Toxicol.*, 28, 546 (1982).
11. M. Margoshes and B.L. Vallee, *J. Amer. Chem. Soc.*, 79, 4813 (1957).
12. J.H.R. Kagi and B.L. Vallee, *J. Biol. Chem.*, 236, 2433 (1961).

13. R.U. Byerrum, R.A. Anwar and C.A. Hoppert, J. Amer. Water Works Assoc., 52, 651 (1960).
14. J.M. Epstein, J.C. Dewar, D.L. Kepert and A.H. White, J.C.S. Dalton, 1949 (1974).
15. M. Cannas, G. Carta, A. Cristini and G. Marongui, J.C.S. Dalton, 210 (1976).
16. S.M. Nelson et al., Chem. Comm., 167 (1977).
17. R.J. Flook, H.C. Freeman, C.J. Moore and M.L. Scudder, Chem. Comm., 753 (1973).
18. G.E. Maciel and M. Borzo, Chem. Comm., 394 (1973).
19. R.J. Kostelnik and A.A. Bothner-By, J. Mag. Res., 14, 141 (1974).
20. R.A. Haberkorn, L. Que, Jr., W.O. Gillum, R.H. Holm, C.S. Liu and R.C. Lord, Inorg. Chem., 15, 2408 (1976).
21. M.J.A. Rainier and B.M. Rode, Inorg. Chim. Acta, 58, 59 (1982).
22. G.B. Gavioli, L. Benedetti, G. Grandi, G. Marcotrigian, G.C. Pellacani and M. Tonelli, Inorg. Chim. Acta, 37, 5 (1979).
23. D.L. Rabenstein and S. Libich, Inorg. Chem., 11(12), 2960 (1972).
24. S.M. Wang and R.K. Gilpin, Anal. Chem., 55, 493 (1983).
25. D.L. Rabenstein, Can. J. Chem., 50, 1036 (1972).
26. K.S. Squibb and R.J. Cousins, Environ. Physiol. Biochem., 4, 24 (1974).

27. I. Bremner and B.W. Young, *Biochem. J.*, 157, 517 (1976).
28. Y. Boulanger and I.M. Armitage, *J. Inorg. Biochem.*, 17, 147 (1982).
29. E.J. Kuchinskas and Y. Rosen, *Arch. Biochem. Biophys.*, 97, 370 (1962).
30. A. Avdeef and D.L. Kearney, *J. Am. Chem. Soc.*, 104, 7212 (1982).
31. H.C. Freeman, F. Hug, G.N. Stevens, *J. Chem. Soc. Chem. Commun.*, 90 (1976).
32. A.J. Carty, N.J. Taylor, *Inorg. Chem.*, 16, 177 (1977).
33. D.L. Rabenstein, A.A. Isab, W. Kadima and P. Mohanakrishnan, *Biochim. Biophys. Acta*, 762, 531 (1983).
34. P.A.W. Dean, *Can. J. Chem.*, 59, 3221 (1981).
35. P.F. Rodesiler and E.L. Amma, *J. Chem. Soc. Chem. Commun.*, 182 (1982).
36. G.K. Carson, P.A.W. Dean and M.J. Stillman, *Inorg. Chim. Acta*, 56, 59 (1981).
37. I.M. Armitage and Y. Boulanger, "Cadmium-113 NMR" in *NMR of Newly Accessible Nuclei*, Vol. 2, Academic Press, Inc., (1983).
38. I.M. Armitage, R.T. Pajfer, A.J.M. Schoot Uiterkamp, J.F. Chebesowki and J.E. Coleman, *J. Am. Chem. Soc.*, 98, 5710 (1976).

39. J.L. Sudmeier and S.J. Bell, *J. Am. Chem. Soc.*, 99, 4499 (1977).
40. T. Drakenberg, B. Lindman, A. Cavé and J. Parello, *FEBS Lett.*, 92, 346 (1978).
41. B.R. Bobsein and R.J. Myers, *J. Am. Chem. Soc.*, 102, 2454 (1980).
42. L.G. Sillén and A.E. Martell, Stability Constants of Metal-Ion Complexes, Special Publication No. 17 of the Chemical Society: London (1964).
43. P.D. Ellis in The Multinuclear Approach to NMR Spectroscopy, (J.B. Lambert and F.G. Riddell, eds.), D. Reidel Publishing Co., (1983), Chap. 22.
44. R.A. Bullman, J.K. Nicholson, D.P. Higham and P.J. Sadler, *J. Am. Chem. Soc.*, 106, 1118 (1984).
45. I.G. Dance and J.K. Saunders, *Inorg. Chim. Acta*, 96, L71 (1985).
46. A.D. Keller, T. Drakenberg, R.W. Briggs and I.M. Armitage, *Inorg. Chem.*, 24, 1170 (1985).
47. R.S. Honkanen and P.D. Ellis, *J. Am. Chem. Soc.*, 106, 5488 (1984).
48. S. Forsén, E. Thulin and H. Lilja, *FEBS Lett.*, 104, 123 (1979).
49. S. Forsén, E. Thulin, T. Drakenberg, J. Krebs and K. Seamon, *FEBS Lett.*, 117, 189 (1980).

50. J.L. Sudmeier, S.J. Bell, M.C. Storm and M.P. Dunn, *Science* (Washington, D.C.), 212, 560 (1980).
51. D.B. Bailey, P.D. Ellis, A.D. Cardin and W.D. Behnke, *J. Am. Chem. Soc.*, 100, 5236 (1978).
52. C.F. Jensen, S. Deshmukh, H.J. Jakobsen, R.R. Inners, and P.D. Ellis, *J. Am. Chem. Soc.*, 103, 3659 (1981).
53. S. Harada, Y. Funaki and T. Yasunaga, *J. Am. Chem. Soc.*, 102, 136 (1980).
54. M.J.B. Ackerman and J.J.H. Ackerman, *J. Phys. Chem.*, 84, 3151 (1980).
55. J.J.H. Ackerman, T.V. Orr, V.J. Bartuska and G.E. Maciel, *J. Am. Chem. Soc.*, 101(2), 341 (1978).
56. D.L. Rabenstein and R.J. Kula, *J. Am. Chem. Soc.*, 91, 2492 (1969).
57. R.B. Martin and J.T. Edsall, *Bull. Soc. Chim. Biol.*, 40(12), 1770 (1958).
58. A.I. Vogel, Textbook for Quantitative Inorganic Analysis, 3rd Ed., pp. 437, 443 and 444.
59. R.G. Bates, Determination of pH, Theory and Practice, 2nd Ed., John Wiley & Sons, Inc., (1973), pp. 97 and 101.
60. R.L. Vold, J.S. Waugh, M.P. Klein and D.E. Phelp, *J. Chem. Phys.*, 48, 3831 (1968).
61. D.L. Rabenstein, A.A. Isab and D.W. Brown, *J. Mag. Res.*, 41, 361 (1980).

62. F.F. Brown, I.D. Campbell, P.W. Kuchel, D.L. Rabenstein, *FEBS Lett.*, 82, 12-16 (1977).
63. I.D. Campbell, C.M. Dobson, R.J.P. Williams and P.E. Wright, *FEBS Lett.*, 57, 96 (1975).
64. D.L. Rabenstein, *Anal. Chem.*, 50, 1265A (1978).
65. D.L. Rabenstein and T.T. Nakashima, *Anal. Chem.*, 51, 1465A (1979).
66. R. Freeman and H.D.W. Hill in *Dynamic Nuclear Magnetic Resonance Spectroscopy* (L.M. Jackman and F.A. Cotton, eds.), Academic Press, New York (1975), pp. 131-162.
67. J.L. Dye and V.A. Nicely, *J. Chem. Ed.*, 48(7), 443 (1971).
68. D. Reddy, B. Sethuram and T.N. Rao, *Ind. J. Chem.*, 20A, 150 (1981).
69. H. Matsui and H. Ohtaki, *Bull. Chem. Soc. Japan*, 55, 461 (1982).
70. H. Matsui and H. Ohtaki, *Bull. Chem. Soc. Japan*, 55, 2131 (1982).
71. D.L. Rabenstein and G. Blakney, *Inorg. Chem.*, 12(1), 129 (1973).
72. B.A. Abd-El-Nabey and M.S. El-Ezaby, *J. Inorg. Nucl. Chem.*, 40, 739 (1978).
73. G. Schwarzenbach and R. Gut, *Helv. Chim. Acta*, 39, 1589 (1956).

74. H.F. Hellwege and G.K. Schweitzer, *J. Inorg. Nucl. Chem.*, 27, 99 (1965).
75. G. Schwarzenbach and E. Freitag, *Helv. Chim. Acta*, 34, 1492 (1951).
76. G. Anderegg, *Helv. Chim. Acta*, 43, 825 (1960).
77. F. Debreczni and I. Nagypál, *Inorg. Chim. Acta*, 72, 61 (1982).
78. G.S. Sharma, J.P. Tandon, *Talanta*, 18, 1163 (1971).
79. J. Israeli and J.R. Cayotte, *Can. J. Chem.*, 49, 199 (1971).
80. Y. Sugiura, A. Yokoyama and H. Tanaka, *Chem. Pharm. Bull.*, 18(4), 693 (1970).
81. A.M. Corrie, M.D. Walker and D.R. Williams, *J.C.S. Dalton*, 1012 (1976).
82. R. Strand, W. Lund, J. Aaseth, *J. Inorg. Biochem.*, 19, 301 (1983).
83. D.L. Rabenstein, R. Guevremont and C.A. Evans, "Glutathione and Its Metal Complexes" in Metal Ions in Biological Systems, vol. 9, Helmut Sigel, Ed., Marcel Dekker, Inc., New York, 1979.
84. D.L. Rabenstein, *J. Am. Chem. Soc.*, 95(9), 2797 (1973).
85. A.D. Cardin, P.D. Ellis, J.D. Odom and J.W. Howard, *J. Am. Chem. Soc.*, 97(7), 1672 (1975).

86. B. Birgersson, R.E. Carter, T. Drakenberg, J. Mag. Res., 28, 299 (1977).
87. J.L. Evelhoch, D.F. Bocian and J.L. Sudmeier, Biochem., 20(17), 4951 (1981).
88. J.D. Otvos and I.M. Armitage, Proc. Natl. Acad. Sci. USA, 77, 7094 (1980).
89. R.W. Briggs and I.M. Armitage, J. Biol. Chem., 257, 1259 (1982).
90. P.D. Murphy, W.C. Stevens, T.T.P. Cheung, S. Lacelle, B.C. Gerstein and D.M. Kurtz, Jr., J. Am. Chem. Soc., 103, 4400 (1981).
91. N.G. Charles, E.A.H. Griffith, P.F. Rodesiler and E.L. Anna, Inorg. Chem., 22, 2717 (1983).
92. D.J. Turnbull, Appl. Phys., 21, 1022 (1950).
93. D.H. Rasmussen, A.P. Mackenzie, Water Structure at the Water Polymer Interface, H.H.G. Jellinek, Ed., Plenum Press, New York, 1972, p. 126.
94. B.J. Fuhr and D.L. Rabenstein, J. Am. Chem. Soc., 95(21), 6944 (1973).
95. D.D. Perrin and A.E. Watt, Biochim. Biophys. Acta, 230, 96 (1971).
96. S. Libich and D.L. Rabenstein, Anal. Chem., 45, 118 (1973).

97. I. Filipov, I. Piljac, A. Medved, S. Savic, A. Bujack, B. Bach-Dragutinovic and B. Mayer, *Croat. Chem. Acta*, 40, 131 (1968).
98. I. Filipovic, A. Bujack and V. Vukicevic, *Croat. Chem. Acta*, 42, 493 (1970).
99. J.W. Bunting and K.M. Thong, *Can. J. Chem.*, 48, 1654 (1970).
100. M. Garty, K.L. Wong and C.D. Klaassen, *Toxicol. Appl. Pharmacol.*, 59, 548 (1981).
101. J.A. Carlson, L. Friberg, *Scand. J. Clin. Lab. Invest.*, 9, 67 (1957).
102. C.F. Nordberg, M. Piscator, M. Nordberg, *Acta Pharmacol.*, 30, 289 (1971).
103. C.E. Hildebrand and L.S. Gram, *Proc. Exp. Biol. Med.*, 161, 438 (1979).
104. C.D. Klaassen and F.N. Kotsonis, *Toxicol. Appl. Pharmacol.*, 41, 101 (1977).
105. C.A. Keele and E. Neil, Samson Wright's Applied Physiology, Oxford University Press, 12th Ed., (1971), p. 521.
106. D.L. Rabenstein, A.A. Isab and R. Stephen Reid, *Biochim et Biophys. Acta*, 696, 53 (1982).
107. D.G. Dhuley and V.G. Dongre, *Indian J. Chem.*, 20A, 208 (1981).
108. L.S. Valberg et al., *J. Clin. Invest.*, 44, 379 (1965).

APPENDIX 1

Microprogram of Pulse Sequence Used to Obtain Totally Decoupled ^{13}C -NMR Spectra

1. Ze Zero data and reset scan counter
2. D1 BB S1 Apply BB during D1 with Power S1
3. D2 S2 Switch BB during D2 to Power S2
4. GO = 2 Acquire the FID with BB on S2
5. D2 S1 Switch BB back to S1
6. Exit Exit with decoupler to S1

BB is the broad band decoupler pulse, delays D1 and D2 were kept at 1.0 and 0.01 seconds respectively. S1 and S2 are 0.4 and 2 watts.

APPENDIX 2

Microprogram of the Pulse Sequence Used to Measure ^1H -NMR Spectra in H_2O

1. Ze Zero data and reset scan counter
2. D1 HG Apply selective saturation during $D1 = 2\text{s}$
3. D0 Turn off the decoupler
4. D2 Wait $D2 = 0.002\text{s}$
5. GO = 2 Acquire FID
6. Exit Exit with decoupler off